FOREST PATHOLOGY IN CHANGING CLIMATE

EDITED BY: Denita Hadziabdic, Jane E. Stewart, Caterina Villari, Richard Hamelin and Matt Kasson

PUBLISHED IN: Frontiers in Forests and Global Change

frontiers Research Topics

ISSN 1664-8714
ISBN 978-2-83250-500-7
DOI 10.3389/978-2-83250-500-7

About Frontiers

Frontiers is more than just an open-access publisher of scholarly articles: it is a pioneering approach to the world of academia, radically improving the way scholarly research is managed. The grand vision of Frontiers is a world where all people have an equal opportunity to seek, share and generate knowledge. Frontiers provides immediate and permanent online open access to all its publications, but this alone is not enough to realize our grand goals.

Frontiers Journal Series

The Frontiers Journal Series is a multi-tier and interdisciplinary set of open-access, online journals, promising a paradigm shift from the current review, selection and dissemination processes in academic publishing. All Frontiers journals are driven by researchers for researchers; therefore, they constitute a service to the scholarly community. At the same time, the Frontiers Journal Series operates on a revolutionary invention, the tiered publishing system, initially addressing specific communities of scholars, and gradually climbing up to broader public understanding, thus serving the interests of the lay society, too.

Dedication to Quality

Each Frontiers article is a landmark of the highest quality, thanks to genuinely collaborative interactions between authors and review editors, who include some of the world's best academicians. Research must be certified by peers before entering a stream of knowledge that may eventually reach the public - and shape society; therefore, Frontiers only applies the most rigorous and unbiased reviews.
Frontiers revolutionizes research publishing by freely delivering the most outstanding research, evaluated with no bias from both the academic and social point of view. By applying the most advanced information technologies, Frontiers is catapulting scholarly publishing into a new generation.

What are Frontiers Research Topics?

Frontiers Research Topics are very popular trademarks of the Frontiers Journals Series: they are collections of at least ten articles, all centered on a particular subject. With their unique mix of varied contributions from Original Research to Review Articles, Frontiers Research Topics unify the most influential researchers, the latest key findings and historical advances in a hot research area! Find out more on how to host your own Frontiers Research Topic or contribute to one as an author by contacting the Frontiers Editorial Office: frontiersin.org/about/contact

FOREST PATHOLOGY IN CHANGING CLIMATE

Topic Editors:
Denita Hadziabdic, The University of Tennessee, Knoxville, United States
Jane E. Stewart, Colorado State University, United States
Caterina Villari, University of Georgia, United States
Richard Hamelin, University of British Columbia, Canada
Matt Kasson, West Virginia University, United States

Citation: Hadziabdic, D., Stewart, J. E., Villari, C., Hamelin, R., Kasson, M., eds. (2022). Forest Pathology in Changing Climate. Lausanne: Frontiers Media SA. doi: 10.3389/978-2-83250-500-7

Table of Contents

frontiers | Frontiers in Forests and Global Change

TYPE Editorial
PUBLISHED 30 September 2022
DOI 10.3389/ffgc.2022.1032035

OPEN ACCESS

EDITED AND REVIEWED BY
Kimberly Wallin,
North Dakota State University,
United States

*CORRESPONDENCE
Denita Hadziabdic
dhadziab@utk.edu

SPECIALTY SECTION
This article was submitted to Pests, Pathogens and Invasions, a section of the journal Frontiers in Forests and Global Change

RECEIVED 30 August 2022
ACCEPTED 06 September 2022
PUBLISHED 30 September 2022

CITATION
Hadziabdic D, Hamelin RC, Stewart JE and Villari C (2022) Editorial: Forest pathology in changing climate. *Front. For. Glob. Change* 5:1032035. doi: 10.3389/ffgc.2022.1032035

Editorial: Forest pathology in changing climate

Denita Hadziabdic[1]*, Richard C. Hamelin[2], Jane E. Stewart[3] and Caterina Villari[4]

[1]Department of Entomology and Plant Pathology, University of Tennessee, Knoxville, Knoxville, TN, United States, [2]Department of Forest and Conservation Sciences, The University of British Columbia, Vancouver, BC, Canada, [3]Department of Agricultural Biology, Colorado State University, Fort Collins, CO, United States, [4]Warnell School of Forestry and Natural Resources, University of Georgia, Athens, GA, United States

KEYWORDS

forest pathology, climate change, ecosystem services, forest health, forests, pathogens and climate change, pests and diseases

Editorial on the Research Topic
Forest pathology in changing climate

Forests cover over 31% of the earth's surface and are vital to our existence. They provide essential ecosystem services by reducing society's carbon footprint and fostering biodiversity. They also provide important societal and economic benefits: the economic value of forest ecosystem services is estimated to contribute between $125 and 145 trillion per year (Costanza et al., 2014). Currently, forests and forest health are in global decline from natural pressures and human-induced threats. Healthy forests are not necessarily pristine and disease-free, but stable and resilient ecosystems that are ecologically dynamic with evolutionary adaptive responses to different stressors (Hadziabdic et al.). However, with globalization and changes in climate patterns, both natural and planted forests are at risk from invasive exotic insect pests and pathogens, climate-induced wildfires, wind disturbance, extended drought cycles or extreme precipitation events, and air pollution. In this special issue of *Forest pathology in changing climate*, nine articles discuss current major forest diseases affecting different tree species, modeling to predict their epidemics, and the current state of forest pathology and related careers in North America.

The first manuscript is a review article focusing on the future of forest pathology in North America. Hadziabdic et al. are a group of researchers, scientists, academics, and administrators from across the United States (U.S.) and Canada working in the field of Forest Health and Forest Pathology. The authors discuss how the Anthropocene is disrupting the current, natural balance and the effect of globalization on invasive exotic insect pests and pathogens that affect historically, culturally, and economically significant tree species. Climate change will have a compounding effect on forest health by changing rainfall patterns, prolonging and intensifying periods of drought or rainfall, increasing temperatures, and shifting seasonal weather patterns that will increase abiotic stressors, making tree hosts more vulnerable to both insect pests and

pathogens. Combined, these effects could result in economic losses between $4.3 and 20.2 trillion per year in ecosystem services (Costanza et al., 2014). The authors offer solutions and suggestions, including establishing forest pathology research consortia with multidisciplinary training, approaches, and resources to illuminate society's path forward to protecting and managing our natural resources.

A research area that is still fairly unexplored, but gaining growing attention, involves the role of the host-associated microbiome in tree diseases. Tree endophytes might display diverging roles that span from modulating resistance to exacerbating disease outcomes and could also be affected by climate. Morrison et al. propose the need for considering species composition within pathogen complexes, as well as the broader endophytic community when assessing disease progression and its outcome. In the beech bark disease pathosystem, two different pathogens, *Neonectria faginata* and *N. ditissima*, are broadly co-occurring, but have opposite climate adaptations and are likely associated with different stages of tree decline. The authors indicate that other fungal taxa associated with the system may have a contributing role in driving disease outcomes.

With a similar focus on the role of the microbiome in plant-microbe interactions, but with an emphasis on their beneficial effects, Blumenstein et al. screen Scots pine endophytes for their potential use as control agents against *Diplodia* tip blight disease caused by the fungus *Sphaeropsis sapinea*. They find some promising candidate species that do not change their behavior toward the host plant during drought conditions, which notoriously can trigger a lifestyle switch from endophytes to pathogens in opportunistic species.

Chahal et al.'s study focuses on Thousand Cankers Disease (TCD) in black walnut trees. The TCD complex involves the walnut twig beetle (*Pityophthorus juglandis*) and the fungal pathogen *Geosmithia morbida*. TCD symptoms, incidence, and severity differ between eastern and western U.S. outbreak localities, resulting in high host mortality rates, mainly in the western U.S. The authors report differential virulence among genetic clusters of *G. morbida* isolates and reject the hypothesis that *G. morbida* is less virulent in its native region, the eastern U.S. The authors indicate that both eastern and western isolates can induce cankers, given favorable conditions.

Within the TCD pathosystem, Williams and Ginzel demonstrate how wood moisture content influences the fungal competition of *G. morbida* and model predictions regarding pathogen survival and potential future outbreaks. The authors indicate that the process of fungal competition and distribution involves not only a combination of different abiotic conditions that limit competitive success, sporulation, and dispersal of the fungus, but that the host microbiome plays a crucial role in lowering the severity of TCD in the native range of black walnut. The authors predict that the survival of *G. morbida* was highest in historical epicenters of TCD in the western U.S., which is expected as *G. morbida* is evolutionarily adapted to drier climatic conditions. Future climate scenarios indicate that TCD will expand into the native range of black walnut, threatening their long-term sustainability.

Ash dieback caused by the invasive fungus *Hymenoscyphus fraxineus* has been causing massive mortality of European ash (*Fraxinus excelsior*) populations across Europe. Klesse et al. provide a comprehensive overview of the landscape features that determine ash mortality rates in Switzerland over a 10-year period. Using data from long-term forest monitoring programs in Switzerland, the authors indicate that ash mortality increased significantly since the first discovery of *H. fraxineus* in 2008, especially among the smaller diameter, or slower growing, trees and stands with increased humidity. Climate-change-induced warming may reduce the virulence of the pathogen and, combined with host-induced resistance and different elevation gradients, could improve the long-term conservation of ash in Europe.

Characterizing changes in root pathogens as western forests become drier is vital to making future management decisions. Using Maximum Entropy (MaxEnt) analyses, Kim et al. use contemporary climate space of the root pathogen *Armillaria solidipes* and a common host, Douglas-fir (*Pseudotsuga menziezii*), to predict how the pathogen will move in association to this host based on two future climate scenarios. The authors predict that the range of *A. solidipes* will increase in more northern areas of western North America. These movements follow the trends of the predicted geographic movement of Douglas-fir and suggest that *A. solidipes* could become more prevalent where Douglas-fir becomes maladapted on sites. Using MaxEnt to extrapolate new host and pathogen geographic ranges can be used as an important tool to help manage future forests, giving insights into how our forest will change in future climate scenarios.

Genomic approaches are providing novel ways to understand the impact climate change will have on tree-pathogen interactions and possibly help improve predictions under future climates. Variability within species is generally not considered in prediction models. This may be significant as lineages and genetic variants sometimes exhibit different environmental tolerance ranges which may impact disease severity and climate adaptation. Herpin-Saunier et al. discover that this is the case for the lineages of the Swiss needle cast pathogen, *Nothophaeocryptopus gaeumannii*. The authors use PCR assays to identify two lineages of *N. gaeumannii* in Douglas-fir and included lineage identification in prediction models. Results predict the expansion of one lineage that has a broader environmental tolerance range, which could potentially increase its spread.

Ghosh et al. utilize genomics for a different approach as the novelty of their work disentangles the metabolic host response to pathogens of variable virulence. They experimentally simulate drought and high-temperature conditions and perform inoculations using the aggressive pine pathogen *Diplodia sapinea* and the less virulent *D. scrobiculata*. Their results confirm that under warmer and drier conditions, Austrian pines are hindered by weaker host defense systems that increase susceptibility to less aggressive pathogens. Transcriptome analyses reveal that the climate-change-simulated environment result in a critical change in the expression of genes in the host carbon and nitrogen metabolism and host-defense-associated pathways. These studies indicate that not only pathogen lineages could gain fitness benefits from climate change, but also those host defense reactions could become compromised, which could open the door to even weak pathogen infections.

This special issue highlights the importance of considering climate change in forest disease outbreaks. It also shows that common approaches, such as genomics and modeling, can be applied to different forest pathosystems. We forecast a need in understanding how climate change will affect forest health issues that should be an essential part of future research on forest health.

Author contributions

All authors listed have made a substantial, direct, and intellectual contribution to the work and approved it for publication.

Conflict of interest

The authors declare that the research was conducted in the absence of any commercial or financial relationships that could be construed as a potential conflict of interest.

Publisher's note

All claims expressed in this article are solely those of the authors and do not necessarily represent those of their affiliated organizations, or those of the publisher, the editors and the reviewers. Any product that may be evaluated in this article, or claim that may be made by its manufacturer, is not guaranteed or endorsed by the publisher.

References

Costanza, R., de Groot, R., Sutton, P., van der Ploeg, S., Anderson, S., Kubiszewski, I., et al. (2014). Changes in the global value of ecosystem services. *Glob. Environ. Change* 26, 152–158. doi: 10.1016/j.gloenvcha.2014.04.002

frontiers in Forests and Global Change

ORIGINAL RESEARCH
published: 22 March 2021
doi: 10.3389/ffgc.2021.645920

Spread and Severity of Ash Dieback in Switzerland – Tree Characteristics and Landscape Features Explain Varying Mortality Probability

Stefan Klesse[1,2], Meinrad Abegg[2], Sven E. Hopf[3], Martin M. Gossner[1,4], Andreas Rigling[4,5] and Valentin Queloz[1]*

[1] Forest Health and Biotic Interactions, Swiss Federal Research Institute for Forest, Snow, and Landscape Research WSL, Birmensdorf, Switzerland, [2] Forest Resources and Management, Swiss Federal Research Institute for Forest, Snow, and Landscape Research WSL, Birmensdorf, Switzerland, [3] Institute for Applied Plant Biology, Witterswil, Switzerland, [4] Department of Environmental Systems Science, Institute of Terrestrial Ecosystems, ETH Zürich, Zurich, Switzerland, [5] Forest Dynamics, Swiss Federal Research Institute for Forest, Snow, and Landscape Research WSL, Birmensdorf, Switzerland

OPEN ACCESS

Edited by:
Richard Hamelin, University of British Columbia, Canada

Reviewed by:
Giorgio Maresi, Fondazione Edmund Mach, Italy
Kayla I. Perry, The Ohio State University, United States

***Correspondence:**
Stefan Klesse
Stefan.klesse@wsl.ch

Specialty section:
This article was submitted to Pests, Pathogens and Invasions, a section of the journal Frontiers in Forests and Global Change

Received: *24 December 2020*
Accepted: *01 March 2021*
Published: *22 March 2021*

Citation:
Klesse S, Abegg M, Hopf SE, Gossner MM, Rigling A and Queloz V (2021) Spread and Severity of Ash Dieback in Switzerland – Tree Characteristics and Landscape Features Explain Varying Mortality Probability. Front. For. Glob. Change 4:645920. doi: 10.3389/ffgc.2021.645920

Since the 1990s the invasive fungus *Hymenoscyphus fraxineus* has been threatening European ash (*Fraxinus excelsior*), a tree species with high ecological and economic importance. This pathogen is causing severe crown dieback, leading to high mortality rates across Europe and is present in Switzerland since 2008. In this study, we provide a comprehensive overview of the temporal evolution of crown damage and mortality rates in Switzerland over the 2009–2019 period. Harnessing the power of the annualized design of the Swiss national forest inventory (NFI), we show that annual mortality rates (*AMR*s) of ash increased significantly since the arrival of the fungus, with stronger effects in small trees [<26 cm diameter at breast height (DBH)]. Mortality modeling confirmed a size and growth-rate dependent mortality probability (MP). It also revealed that stands with higher humidity – either through higher mean annual precipitation or more humid soil conditions – showed also increased MP. Decreasing host abundance with increasing elevation was also associated with lower MP. Special ash surveys performed over the last 10 years still show a large percentage of ash trees with very low defoliation. This gives hope to finding possible tolerant or resistant trees for (inter-)national breeding programs. In the mean-time our results reinforce previously published management guidelines to promote not only healthy big trees, but also healthy and fast-growing young trees in more open stands for long-term conservation of ash in Europe.

Keywords: *Hymenoscyphus fraxineus*, mortality, defoliation, national forest inventory, mortality model, tree health assessment, invasive pathogen, European ash

INTRODUCTION

Invasive species represent an increasing challenge for forest and tree health globally (Holmes et al., 2009; Moser et al., 2009; Pyšek and Richardson, 2010; Trumbore et al., 2015). Moreover, some invasive pathogens can lead to near extinction of tree species and threaten whole ecosystems and their functioning (Pautasso et al., 2015). A prominent example is Ash dieback (ADB) in Europe.

ADB is caused by the ascomycete *Hymenoscyphus fraxineus* (Baral et al., 2014) native to Eastern Asia (NE China, Korea, and Japan). First symptoms resembling late frost were observed in the early 1990s in north-eastern Poland and Lithuania (Kowalski and Łukomska, 2005; Cleary et al., 2016; Gil et al., 2017). Since then the disease has spread fast (around 75 km/year) and is now threatening European ash (*Fraxinus excelsior*) populations throughout Europe (Gross et al., 2014). The wind-dispersed pathogen spreads through ascospores, formed on old rachises of ash in the litter, that infect leaves in summer and cause necrotic lesions that lead to early leaf wilting (Gross et al., 2014). The fungus may further spread to the xylem through the petiole–shoot junction leading to dieback of shoots and twigs (Hanáčková et al., 2017). Repeated annual infections disrupt nutrient and water transport and lead to gradual crown dieback and ultimately the tree's death.

Besides its high cultural and economic values (Boshier et al., 2005; Pautasso et al., 2013) ash also is considered a keystone species for biodiversity providing critical habitat for many species (Mitchell et al., 2014; Rigling et al., 2016). Ash is a tree species phylogenetically distinct from most central European tree genera and thus characterized by a distinct and highly specialized community of associated organisms [30% of all phytophagous insect and mite species are host specialists (Brändle and Brandl, 2001)]. As a consequence many associated species face a high risk of extinction when ash trees disappear from the European landscape (McKinney et al., 2012; Hultberg et al., 2020).

It has become evident that small trees and slow-growing trees are more vulnerable to crown dieback and subsequent mortality than big and fast-growing trees (Marçais et al., 2017; Enderle et al., 2018; Enderle, 2019; Klesse et al., 2020). Recent research has also shown that low host abundance and less-humid microclimatic conditions negatively influence the spread and severity of the disease (Grosdidier et al., 2020). Indeed, ash trees in hedges or in forests with open canopies tend to have a microclimate with higher crown temperatures and lower humidity unfavorable to fungal spore germination and growth (Bakys et al., 2013; Hauptman et al., 2013; Marçais et al., 2016; Grosdidier et al., 2018, 2020). This is in line with findings that dieback symptoms are less severe in drier and warmer compared to more humid and cooler forest stands (Chira et al., 2017; Davydenko and Meshkova, 2017; Ghelardini et al., 2017; Heinze et al., 2017). Despite the general high impact of the pathogen on ash trees, several studies have shown that a small percentage of trees without or with only low levels of crown dieback exist even in the neighborhood of highly affected trees (Lenz et al., 2016; Hopf, 2019; Klesse et al., 2020; Menkis et al., 2020).

In Switzerland, *F. excelsior* is the third most abundant broadleaf tree species (4.4% of total stem number) and constitutes 3.8% of standing tree volume [second highest volume among broadleaf tree species, Brändli et al. (2020)]. Young trees and saplings [<12 cm diameter at breast height (DBH)] even account for 22.5% of the stem count in forest regeneration plots. However, the percentage of damaged ash regeneration area has increased from 1% (2004–2006) to 14% (2009–2017) and is even higher in the tree class with >1.3 m height (30%; Brändli et al., 2020). This increase in damaged regeneration is mainly attributed to *H. fraxineus*, first observed in 2008 (Engesser et al., 2009) in the northern regions of Switzerland and ubiquitous since 2015. Several systematic and targeted forest monitoring programs have additionally tracked the disease development over time and space, also under the aspect of finding ash trees tolerant or even resistant to the fungus for future reforestation purposes (Hopf, 2019; Queloz and Gossner, 2019). In this study we harness the power of the systematic and continuous inventory design of the Swiss national forest inventory (NFI) to make an unbiased and representative assessment of the current situation of ADB in Switzerland. A continuous or rotating NFI enables a cost-effective and more frequent production of representative reports on the state of forests (Schreuder et al., 1999; Fischer and Traub, 2019). In a continuous inventory data of permanent plots are not collected periodically every 10 years but each year a sub-grid covering the entire country is visited, completing the inventory after n years, where $1/n$ is the size of the sub-grid. We supplement the NFI dataset with data from specific and non-specific (ash) monitoring programs in Switzerland. Specifically, we were interested in answering the following questions: (1) How did the annual mortality rates develop since 2008? (2) Which tree characteristics and landscape features determine the probability of mortality? (3) Do the data reveal possibilities for the *F. excelsior* population to overcome or recover from ADB?

MATERIALS AND METHODS

Monitoring Data

We used data from four different long-term monitoring programs: (1) The Swiss NFI, (2) targeted regional ash surveys of the Institute for Applied Plant Biology (IAP), (3) the targeted ash survey of the Swiss Federal Research Institute WSL, and (4) the Swiss long-term forest ecosystem research program LWF.

1. The NFI is conducted on a regular sampling grid in Switzerland (Fischer and Traub, 2019). It started in 1983 with a periodical design and changed in 2009 to a continuous forest inventory in which sampling takes place on a sub-grid each year, completing the full grid within 9 years. The permanent sample plots consist of two concentric circles covering an area of 200 and 500 m^2, respectively, in which each tally tree with a minimum DBH of ≥12 cm (>36 cm in the outer circle) is measured. This allows reconstructing each tally tree's history since its first measurement. The fourth NFI was conducted from 2009 to 2017, directly followed by the first 2 years of the fifth inventory in 2018 and 2019, revisiting plots from 2009 and 2010. Since 2009, 661 unique plots had at least one ash tree tallied (median: 2, maximum: 13). Examined plots with ash per year ranged from 43 to 103, and surveyed ash trees ranged from 88 to 257, totaling 1,583 unique trees. The median DBH of surveyed ash trees in the third NFI before the arrival of the fungus (2004–2006) was 26 cm. The observed forest types predominantly belong to the rather wet *Alno-Fraxinion* group (Keller et al., 1998) in the lower elevations of Switzerland (**Supplementary Figure 1**) with mean annual temperatures around 8.9°C

[interquartile range (IQR): 7.9–9.5°C] and mean annual precipitation sums of 1,240 mm (IQR: 1,140–1,420 mm). True to the concept of the annualized inventory design, we did not detect systematic differences in tree size, elevation, or forest type between the individual years the inventories were conducted.

2. In 2013 and 2014, 22 European ash dominated stands in north-west Switzerland (across an area of ∼2,500 km^2) were selected for observation from the IAP (Queloz et al., 2017; Hopf, 2019). At the time of selection, the disease was fully established throughout the region. In these stands, between six and ten apparently healthy trees belonging to (co-) dominant social classes were selected and visually inspected for crown transparency and disease intensity each year at the end of August. Altogether, the IAP monitored 205 trees. The median DBH at the beginning of the survey was 40 cm. Due to the low number of trees per plot this survey – covering a rather homogeneous geographic region – was analyzed as one population in the subsequent analysis.
3. In 2011, the Swiss Federal Research Institute WSL installed three monitoring plots with varying sizes south of Zürich in ash dominated stands surveying each year 60, 104, and 40 trees, respectively (Klesse et al., 2020). Median DBH of the annually monitored trees in 2011 were 18, 20, and 43 cm, respectively.
4. We further included one site belonging to the Swiss long-term forest ecosystem research program LWF (Etzold et al., 2014; Eichhorn et al., 2016), which is also part of the European long-term ecosystem research (LTER) and ICP-forests monitoring programs. Switzerland maintains 19 sites that are regularly monitored, but only one site (site name: Schänis, size: 2 ha), located in north-eastern Switzerland, had enough ash trees (n = 83, median DBH in 2010: 53 cm) to be included in this analysis.

Observed Mortality and Crown Damage

Based on individual tree data, annual mortality rate (*AMR*) was calculated for each of the four data sources and each inventory end year as:

$$AMR = \left(1 - \left(\left(\frac{N_{\Delta t}}{N_0}\right)^{\frac{1}{\Delta t}}\right)\right) * 100,$$

where N_0 and $N_{\Delta t}$ are the numbers of living trees at the beginning and end of the interval, respectively, and Δt is the inventory interval length in years (Sheil and May, 1996). Due to the switch from periodic to annualized inventory design in the NFI, subsets with different N_0 and thus different lengths Δt were first calculated separately and then combined with a weighted average according to the abundance of observations in each subset. To detect whether mortality rates since the arrival of the pathogen are different from before, we established a baseline *AMR* with the periodic NFI inventories ending before 2008. Therefore, and because each inventory year 2009–2017 consists of different trees, bootstrap resampling with 1,000 iterations and 133 draws with replacement (representing the lowest number of individuals in the inventory of 2009) was applied to estimate uncertainties (IQR and 2.5th and 97.5th percentile) of the mortality estimates. We also calculated *AMR* and associated uncertainties for all non-ash trees in the investigated NFI plots and repeated this analysis for small (<26 cm DBH) and big trees, separately. In these instances, resampling was performed with 72 and 61 samples, respectively. We did not resample the data of the other three data sources, because they consist of the same trees in each inventory year. Please note that mortality rate values for a given year in the NFI and LWF relate not to actual mortality rate in that year, but to integrated *AMR* of the entire inventory interval. Whereas, *AMR* in the targeted surveys (IAP and WSL plots) can be readily interpreted as trees that died in the survey year.

Concerning crown damage, we investigated the percentage of trees with considerable crown loss (>50% defoliation) in the inventory year. For the NFI data we applied the same uncertainty analysis as above. We also subdivided the actual targeted annually monitored trees into those with crown defoliation greater than 50% to enable comparison with the pseudo-annual NFI crown loss time series. Additionally, for the non-NFI surveys we also calculated the percentage of trees that showed little crown dieback symptoms, i.e., <25% defoliation. This information is unavailable for the NFI plots.

Modeled Mortality Probability

We applied generalized logistic regression (Hosmer et al., 2013) to model mortality probability (MP) based on the NFI data collected from 2009 to 2019, i.e., including only observations since the arrival of the fungus in Switzerland. The MP p of tree i in plot j at time k was defined as:

$$logit\left(p_{i,j,\mathrm{k}}\right) = log\left(\frac{p_{i,j,\mathrm{k}}}{1 - p_{i,j,\mathrm{k}}}\right) = \boldsymbol{\beta}\mathbf{X} + \log(\triangle\mathbf{t})$$

where $\boldsymbol{\beta}$ $\mathbf{X}$ represents a linear combination of parameters $\boldsymbol{\beta}$ to be estimated and explanatory variables $\mathbf{X}$ and $\Delta\mathbf{t}$ is a vector with the inventory interval lengths $t_{i,j,k} - t_{i,j,k-1}$. This parameter is included as an offset, i.e., an independent variable whose parameter is fixed to 1, acting as a composite interest rate upon the annual MP (Fortin et al., 2008). Because the number of observations per plot j at time k is very small (≤2 in 64% of all plots), we did not apply a mixed-effects model.

We used tree-, stand-, and forest district-specific variables to model MP. Tree-specific variables included DBH at the beginning of the inventory period (DBH, log-transformed) and relative annual basal area increment (relBAI). relBAI (Bigler and Bugmann, 2004) was calculated for the inventory period preceding the period of interest as

$$relBAI_{i,j,k} = \left(\frac{BA_{i,j,k-1}}{BA_{i,j,k-2}}\right)^{\frac{1}{\Delta t}}$$

with $BA_{i,j}$ being the basal area of tree i in plot j and Δt denoting the number of vegetation periods between observations, i.e., the inventory interval length between time $k-1$ and $k-2$. Negative increments were reset to zero. We applied a modified log10

transformation based on the common logarithm that is applicable even to the few observations where relBAI = 0 (Stahel, 2019).

Stand-specific variables (as provided by the NFI) included elevation, slope steepness, slope curvature, stand density related variables such as standing basal area and basal area of larger trees, number of growing season periods between two consecutive inventories, forest type, and climate. We created a binary variable based on the forest type classification of Keller et al. (1998) to distinguish between wet and not-wet forest types. Mean annual precipitation totals and mean annual temperature were extracted from gridded and downscaled meteorological data from MeteoSwiss with a resolution of 1 km (MeteoSwiss, 2021).

Based on feedback of country-wide surveys and laboratory confirmed cases we determined the first year of observation of the fungus within a given forest district. For each forest district this year of first observation was subtracted from the year of the actual inventory to create a variable of fungal presence time (TIMESINCE). If the inventory pre-dated the first observation of the fungus, this variable was set to −1.

Model selection based on the Bayesian information criterion (BIC) was performed in R (R Core Team, 2018, R Version 3.5.2) using the dredge function in the *MuMIn* package (Bartoń, 2018), and included all possible two-way interactions. The final model structure was then applied to NFI data prior to 2008 to compare how factors influencing MP have changed with the new disease.

RESULTS

Observed Crown Defoliation

We found a significant step increase in the percentage of NFI ash trees with >50% crown loss in 2014 from near 0–8% and another step increase to 22% in 2019 ($p < 0.001$, **Figure 1**). Because the different inventories 2009–2017 do not consist of the same trees, and the response variable is binary (>50% crown loss, yes or no) and does not account for previous crown defoliation (e.g., 5, 25, or 45%), we caution against over-interpreting these step changes. No increase in crown damage was observed in non-ash trees at the same plots, staying <1% in all eleven inventory years. We did not find such a step increase in the other surveys, where the percentage of alive trees with >50% crown defoliation increased only slightly over time (**Figure 2A**). However, we found large differences in absolute values between surveys, ranging from 1% in 2019 in the IAP survey, specifically targeting initially resistant trees, to 17 and 33% in the two WSL plots with the smallest average DBH (RAM and LW1) in more vulnerable stands. In both the LWF and IAP survey more than 80% of the trees in 2019 (n_{total} = 75 and 189, respectively) had still very healthy crowns with less equal or less than 25% defoliation (**Figure 2B**).

Observed Mortality

We found a strong increase in *AMR* since 2009 (**Figure 3A**) in the NFI data. In the beginning of the investigated period *AMR* averaged at 0.3% and was indistinguishable from *AMR* before the arrival of the fungus. Since 2014, *AMR* was significantly higher than observed background mortality rates and reached 1.4% in the 2019 survey. *AMR* for small ash trees started around 0.4% and reached 2.0% in 2019 and was notably higher than those of big ash trees (0.2–0.9%, **Figures 3B,C**). No trend was observed in *AMR* of non-ash trees, which stayed rather constant at 0.7%. A constant *AMR* was also observed for the four most abundant co-occurring species *Picea abies*, *Fagus sylvatica*, *Abies alba*, and *Acer pseudoplatanus*, separately (**Supplementary Figure 2**).

Annual mortality rate was very low in the IAP survey and averaged 0.9% (range 0–2.6%, **Figure 2C**). Putting this number (which is based on the 2013–2019 period) into context of 9 years (NFI 2010–2019) would return an *AMR* of 0.6% (by adding 3 years with zero mortality in the beginning). The 11 trees that died in the IAP survey also had a much smaller DBH (median: 27 cm; range: 12–45 cm) compared to the population average of 40 cm. Only in 2019 the first two trees belonging to the lowest quartile in DBH died in the LW2 plot. In contrast, *AMR* in RAM and LW1 were considerably higher, resulting in very high cumulative mortality in 2019 of 72 and 35%, respectively (**Figure 2D**).

Modeled MP in Relation to Environmental Factors and Time of Pathogen Arrival

We found a clear size and growth rate-dependent MP in both investigated periods (pre-ADB, with ADB) with very similar log-odds ratios (**Table 1** and **Figure 4**). Small trees and relatively slow-growing trees had a much higher MP. In both periods, steeper slopes had a significant positive effect on MP. However, in wet forest types slope steepness did not influence MP. Since the arrival of the invasive fungus MP was 85% higher in wet forest types compared to normal and dry forest types. In areas with higher mean annual precipitation MP also increased, whereas in higher elevation stands MP was reduced. Both factors did not influence MP before the arrival of the fungus. Time since first observation had a significant positive effect on MP.

Compared to the time before the arrival of the fungus MP for small (<20 cm DBH) and slow-growing trees (relBAI < 2%) has drastically increased and was up to 55% higher in 2019, whereas MP was relatively unchanged (+4%) for big (>50 cm DBH) and fast-growing trees (>3% relBAI, **Figure 3**).

DISCUSSION

In this study, we provided a comprehensive overview of crown damage and mortality rates of ash trees in Switzerland over the past 11 years. For the first time we provide a national-wide and geographically unbiased assessment of mortality rates before and after the arrival of *H. fraxineus* harnessing the power of the annualized design of the Swiss NFI. We showed that *AMR*s of *F. excelsior* are at unprecedented levels compared to observations before the arrival of the pathogen and have disproportionally increased in small and slow-growing trees. Further, our analyses confirm previous observations that mortality elevated in stands with humid microclimatic conditions and high abundance of ash trees. At the same time, we showed that in many stands there are still healthy trees seemingly tolerant to the disease. In the following, we discuss our results in the context of

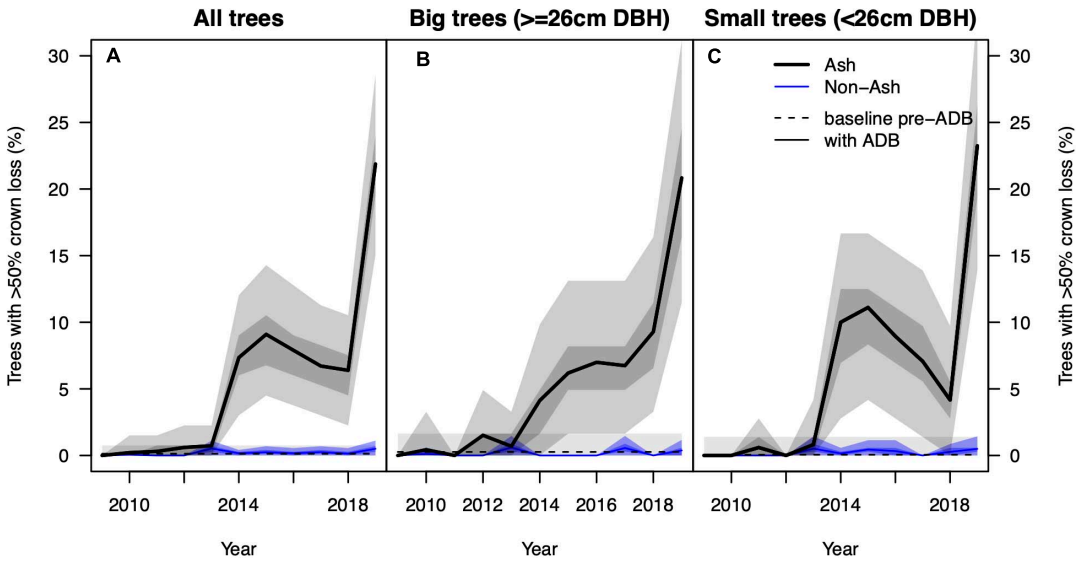

FIGURE 1 | (A) Observed percentage of ash (solid black line) and non-ash trees (blue line) with >50% crown loss based on data from the National Forest Inventory. The dashed black line denotes the "background" percentage of *Fraxinus excelsior* with >50% crown loss before the arrival of the fungus. The shadings around the solid lines show the interquartile range (dark) and 95% confidence interval (light) after 1,000 iterations of resampling with replacement. Panels **(B,C)** show the same information for big (≥26 cm DBH) and small trees (<26 cm DBH), respectively. Please note only the data pairs 2009/2018 and 2010/2019 comprise the same trees (excluding ingrowth and mortality).

other systematic (non-targeted) forest inventory and targeted monitoring literature and provide an outlook for *F. excelsior* conservation in Europe.

Modeled and Observed MP

The growth rate and size-dependent MP of *F. excelsior* found in the NFI (**Figure 3**) matches that of *F. excelsior* in forest reserves in Switzerland (Wunder et al., 2008; Hülsmann et al., 2017), Poland (Wunder et al., 2008), and Denmark (Wolf et al., 2004). For Swiss forest reserves, Hülsmann et al. (2016) reported a 2.2% background mortality. The higher value in the forest reserves compared to our reported background mortality of 0.3% in the NFI plots can be explained by the much smaller DBH threshold (4 cm compared to 12 cm in the NFI) and the smaller mean DBH (18.7 cm compared to 26.6 cm in the NFI). A size-dependent (reverse-J shaped) mortality pattern of ash was also observed in Germany (Holzwarth et al., 2013), Norway (Díaz-Yáñez et al., 2020), and Lithuania (Ozolincius et al., 2005).

Similar to our findings ash mortality dramatically increased over time in the Norwegian NFI (Díaz-Yáñez et al., 2020), where mortality almost tripled in trees with the smallest diameters (5–15 cm) since the arrival of *H. fraxineus*. However, given that the Swiss NFI's sampling threshold is 12 cm, the five-fold increase (0.4–2%) in small trees in Switzerland appears even more severe. Our targeted surveys support the mortality model showing strongest increases in mortality in the plots with the smallest trees. Other ash surveys in Europe also revealed increases in ash mortality with increased time since exposure to the fungus, with strongest effects in small trees and saplings, posing challenges for natural forest regeneration (Marçais et al., 2017; Vasaitis and Enderle, 2017; Coker et al., 2019). The disproportional increase in MP of small and slow-growing trees since the arrival of the fungus was hypothesized to be caused by a lack of non-structural carbohydrates (NSC) in these trees (Klesse et al., 2020). A lack of NSCs would lead to lower turgor pressure and smaller earlywood vessels responsible for efficient water transport, reducing photosynthetic rates, the production of defenses, and tree vigor. Nevertheless, our model also showed that MP is still comparatively low in fast-growing small trees (**Figure 4**). This suggests that not only large healthy trees, but also smaller trees that do not yet show large crown damages should be promoted (Chandelier et al., 2017).

By comparing *AMR*s and crown damage of ash to that of non-ash trees in the same plots we could show how unusual the increase in mortality and crown damage of ash is. Because of the wide ecological amplitude of *F. excelsior* (Schlüter, 1967; Keller et al., 1998), its ability to grow on very dry to wet soils, its high drought tolerance (Scherrer et al., 2011; Brinkmann et al., 2016), its climate-growth responses similar to co-occurring species (Čufar et al., 2008; Roibu et al., 2020), and its general wind resistant build-up, we can rule out abiotic factors (such as climate and storm damage) as main factor driving increased mortality. These factors would have likely affected other tree species as well (**Figures 1**, **3**). A similar comparative approach was used in Díaz-Yáñez et al. (2020) using the Norwegian forest inventory. They also showed that the most common co-occurring species spruce, alder, and birch had the same size-dependent mortality rates in the latest inventory interval compared to the two intervals before. Thus, the observed increases in crown damage and mortality rate since 2008 in Switzerland can be most certainly exclusively attributed to the presence of *H. fraxineus*.

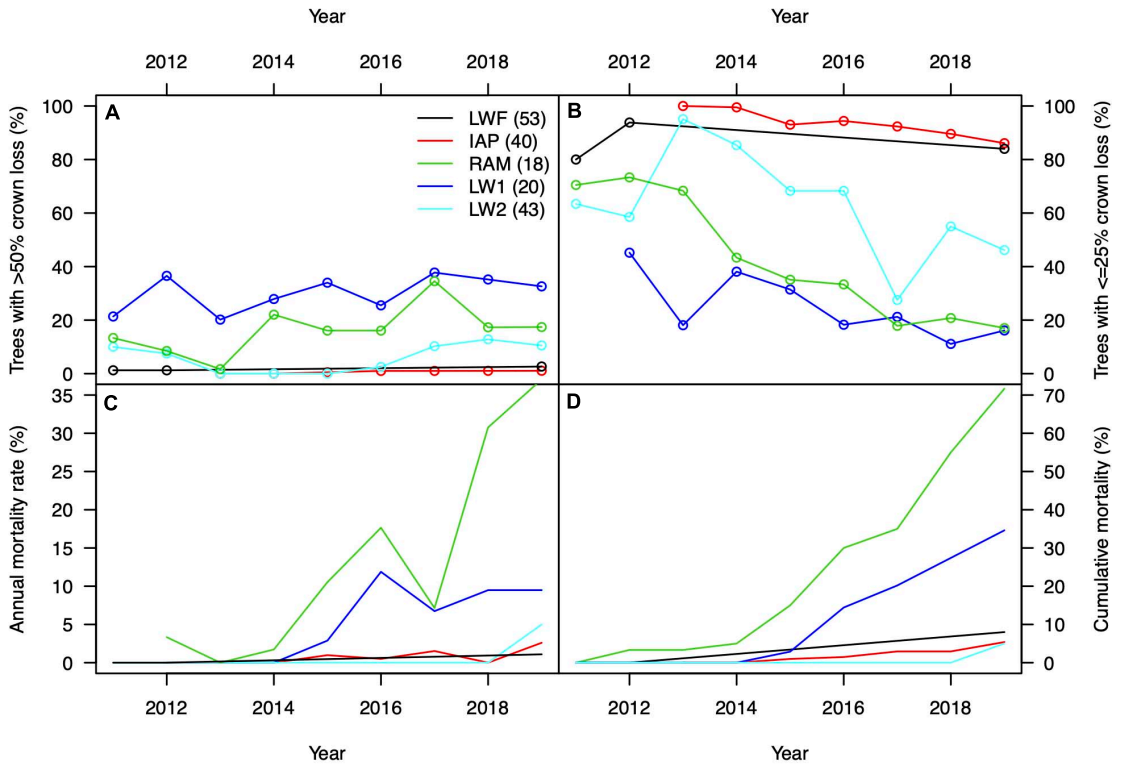

FIGURE 2 | (A) Observed percentage of ash trees with >50% crown loss and **(B)** ≤25% crown loss in the targeted monitoring plots. Numbers in brackets denote the median DBH of monitored trees in the first year of the respective survey. Panel **(C)** shows annual mortality rate and **(D)** the cumulative mortality of the monitored trees. In panel **(C)** data from LWF was excluded, because the monitoring interval was not annual [see circles in panel **(A)** for actual years of survey]. RAM, LW1, and LW2 are the monitoring plots of the WSL survey.

One of the strongest predictors for MP was the time since the arrival of the fungus in the respective forest district. Even though this variable is a rather coarse estimate for the actual arrival within the permanent sample plot, the significance of the predictor that varied in values from −1 to 11 showed the importance of exposure time in disease severity affecting mortality. The absence of significance of a negative quadratic term of exposure time (TIMESINCE) shows that the disease has not yet reached peak mortality rates, i.e., there is no statistical support for a flattening or even decrease in mortality rates after 10 years of exposure. The continuous design of the Swiss NFI is well positioned to keep track of mortality rates and as such disease severity of ADB (but also any other species-specific damaging agent) on a national level. It would thus be interesting to compare ash mortality rates of the Swiss NFI with other systematic European national forest inventories. Yet, to our knowledge, no such data have been published so far (but see Díaz-Yáñez et al., 2020, for Norway).

Landscape Features Influencing MP

Our mortality model identified three distinct landscape characteristics positively affecting ADB that have been previously identified in other parts in Europe (**Table 1**). We found elevated MP in places with higher mean annual precipitation and in wet forest types predominantly belonging to the *Alno-Fraxinion* group (Keller et al., 1998). These two factors underscore the effect of humid microclimatic conditions favoring fungal sporulation and infection success (Marçais et al., 2016; Enderle et al., 2018). Despite its large ecological amplitude ash only dominates forests of the *Alno-Fraxinion* group that are considered too wet for *F. sylvatica*, its main competitor (Professur für Waldbau und Professur für Forstschutz and Dendrologie der ETH Zürich, 1995). This supports previous findings that ash abundance plays also a critical role in the manifestation of disease severity, through increased pathogen infection pressure (Grosdidier et al., 2020). Elevation was found to negatively affect MP, which seems counter-intuitive if elevation is interpreted as a climate proxy. Elevation positively correlates with mean annual precipitation ($r = 0.47$, $p < 0.001$) thereby increasing humidity. Warmer maximum summer temperatures at lower elevation have been shown to be unfavorable or even lethal for the fungus (Hauptman et al., 2013; Grosdidier et al., 2018). We also would rule out elevation effects due to the cold tolerance of *H. fraxineus*, because it has been found to be very resistant to frost (Gross et al., 2014). Therefore, we interpret the negative effect of elevation on MP primarily as the consequence of lower ash abundance and as such lower pathogen infection pressure in higher regions (**Supplementary Figure 1**). The positive effect of slope steepness on MP in non-wet forest types – already observed before the arrival of

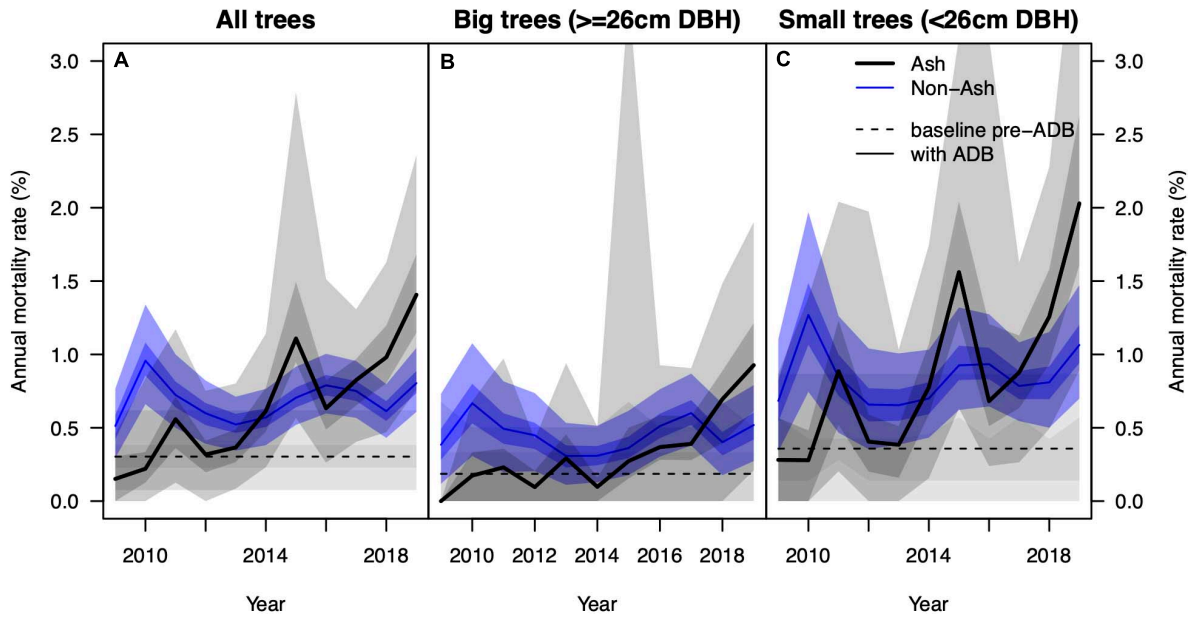

FIGURE 3 | (A) Observed annual mortality rate of ash (solid black line) and non-ash trees (blue line) based on data from the National Forest Inventory. The dashed black line denotes the annual "background" mortality rate before the arrival of the fungus. The shading around the solid lines shows the interquartile range and 95% confidence interval after 1,000 iterations of resampling with replacement. Panels **(B,C)** show the same information for big (≥26 cm DBH) and small trees (< 26 cm DBH), respectively.

TABLE 1 | Parameters of generalized linear model of mortality probability (MP) based on data of the NFI.

	2009–2019			<2008		
Predictors	**Log-odds**	**SE**	***p***	**Log-odds**	**SE**	***p***
Intercept	−6.70	0.29	**<0.001**	−6.13	0.25	**<0.001**
Log(DBH)	−0.65	0.11	**<0.001**	−0.60	0.17	**0.001**
Log(relBAI)	−0.75	0.09	**<0.001**	−0.76	0.13	**<0.001**
Slope	0.62	0.13	**<0.001**	0.45	0.18	**0.020**
Wetness	0.62	0.27	**0.023**	0.20	0.39	0.604
MAP	0.50	0.12	**<0.001**	−0.05	0.17	0.936
Elevation	−0.64	0.13	**<0.001**	−0.18	0.17	0.218
TIMESINCE	0.20	0.04	**<0.001**			
Slope × wetness	−0.67	0.23	**0.004**	−0.24	0.34	0.522
Observations	1,885			1,323		

In both models all variables except TIMESINCE (time of arrival = 0, time step = 1) were normalized using mean and variance of the 2009–2018 model. DBH = diameter at breast height, MAP = mean annual precipitation, relBAI = relative annual basal area increment, TIMESINCE = observation year minus year of first fungal presence in forest district. Mean DBH is 30.3 cm, and mean relBAI is 2.97%. Bold-faced numbers indicate significance at p < 0.05.

H. fraxineus – could be interpreted as generally increased ash mortality at very dry sites.

Probability of Ash Tolerance Against the Pathogen

Besides the increased mortality rates over the last 2009–2019 period, our analysis also revealed a medium to high proportion of trees with low crown dieback symptoms at the targeted monitoring plots (**Figure 2B**). Whereas the IAP plots (where 82% of the trees showed ≤25% crown defoliation in 2019) were specifically chosen to only include trees that were still without symptoms in 2013 and 2014, the abundance of healthy trees in the LWF and LW1 plots (83 and 45%, respectively) – stands that were not targeted for their healthy trees – is encouraging. This is supported by another national survey in 2018 that revealed widespread occurrence of seemingly tolerant trees across northern Switzerland, with 35% of trees ($N_{treetotal}$ = 2,990, N_{plot} = 144) showing less than 25% crown defoliation (Queloz, unpublished data).

Landscape features and tree competition are dominant drivers modulating MP, yet, there are clear signs that genetic variability also plays a role in susceptibility to the fungus (Cleary et al., 2017; Kjær et al., 2017). Several studies have now described certain genetic markers associated with higher tolerance against ADB (McKinney et al., 2014; Harper et al., 2016; Havrdová et al., 2016; Sollars et al., 2017; Stocks et al., 2019; Chaudhary et al., 2020; Menkis et al., 2020; Sahraei et al., 2020). Other studies have identified chemical defenses linked to increased fungal resistance, such as leaf (Sambles et al., 2017) or bark metabolites (Villari et al., 2018; Nemesio-Gorriz et al., 2020) that certainly will be associated to genetic variation in the future. Earlier flushing, and earlier leaf-shedding phenotypes also have been found to be more tolerant to the disease (Bakys et al., 2013; Muñoz et al., 2016; Nielsen et al., 2017). Early flushing could desynchronize leaf maturation and fungal sporulation, impeding fungal penetration of a thicker leaf cuticula. However, a drawback of early flushing for ash trees is the increased vulnerability to late frost events (Muñoz et al., 2016).

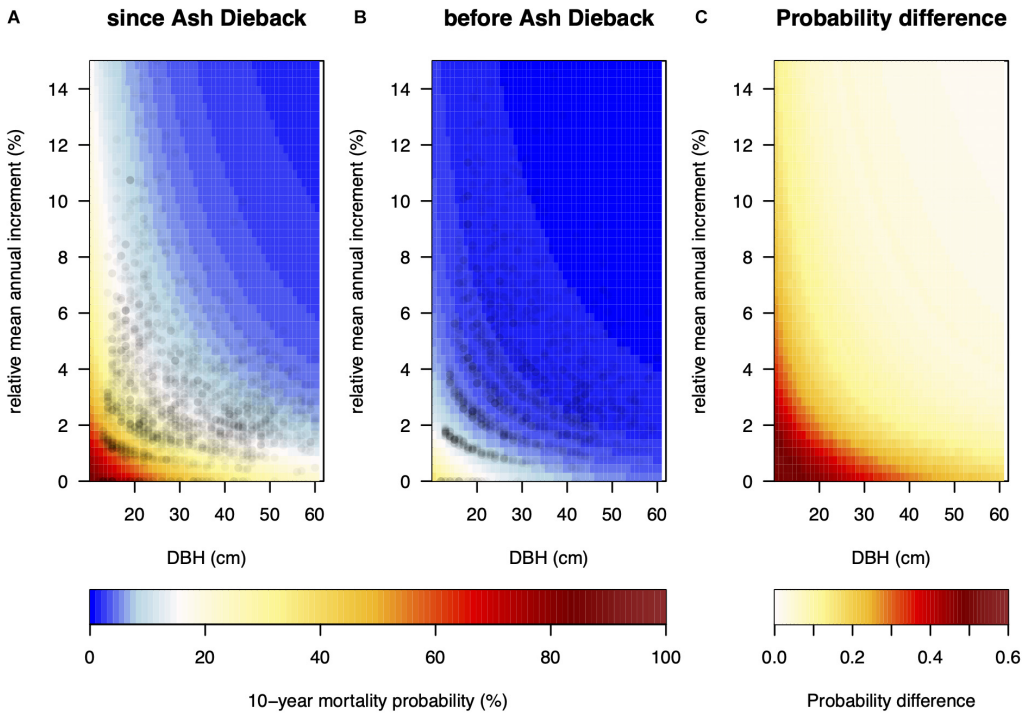

FIGURE 4 | (A) Size and growth-dependent predicted 10-year mortality probability. Fixed variables were set as if the model tree was surveyed in 2019 in a wet forest type, at an elevation of 700 m, slope inclination of 38%, 1,300 mm mean annual precipitation, and first occurrence of Ash dieback in 2008 (i.e., TIMESINCE = 11). Panel **(B)** shows the same prediction without year of survey and year of first detection of fungal presence with the model preceding the arrival of the fungus in Switzerland. Panel **(C)** displays the difference between panels **(A,B)**. Points in panels **(A,B)** show observed pairs of relative annual basal area increment (relBAI) and diameter at breast height (DBH).

Susceptibility to ADB was found to be strongly negatively correlated to reproductive success under controlled conditions in a clonal field trial (Semizer-Cuming et al., 2019). In contrast, Wohlmuth et al. (2018) did not find a significant relationship between crown damage of adult trees and their saplings in a natural setting, suggesting a complex interaction between environmental conditions and genotypes in controlling ADB tolerance. Nevertheless, the identification and continuous monitoring of healthy *F. excelsior* seems a simple and straightforward approach for the selection of potentially ADB-tolerant trees to be tested in common garden trials (Menkis et al., 2020). The combined effort of monitoring programs with progeny trials and the ever-improving knowledge about genetic and biogeochemical markers related to higher tolerance against the fungus should warrant the long-term survival of *F. excelsior* in Europe.

CONCLUSION

In this study, we showed that *AMR*s of *F. excelsior* have drastically increased since the arrival of *H. fraxineus* in Switzerland, and that the increase was disproportionally strong in small and slow-growing trees. For the first time on a national level we quantified which landscape features influence MP, confirming previous research highlighting ash abundance and humidity as primary variables modulating mortality risk. Mortality rates of *F. excelsior* will likely stay high over the coming years in Switzerland. However, on the one hand climate change-induced warming including more frequent heat waves might disproportionally reduce the vigor of the fungus compared to ash trees. On the other hand, the wide-spread abundance of still healthy trees, especially in northern Switzerland where the fungus has been first reported, gives hope to finding genotypes resistant to the fungus. In the mean-time, promoting healthy ash trees, independent of their size, and reducing air humidity for example through thinning, should be paramount for forestry practitioners to sustain a high population diversity of ash in Europe preserving its reproductive potential for coming decades.

DATA AVAILABILITY STATEMENT

The data analyzed in this study is subject to the following licenses/restrictions: Swiss NFI data are accessible upon contractual agreement. Pre-processed NFI data (e.g., data for **Supplementary Figure 2**) can be accessed via www.lfi.ch. For Raw data please contact christoph.fischer@wsl.ch. Non-NFI data will be made available via envidat.ch.

AUTHOR CONTRIBUTIONS

SK designed the study with input of MG, AR, and VQ. SK performed the analysis and wrote the first draft of the manuscript. SH provided the IAP data. MA provided the NFI data. All authors commented critically on the manuscript.

FUNDING

SK was supported by the SwissForestLab (Research Grant SFL-17 P3), and by the Federal Office for the Environment FOEN.

ACKNOWLEDGMENTS

The authors thank Christian Hug, Vivanne Dubach, Sophie Strohecker, and the numerous other people involved in the monitoring programs of LWF, NFI, WSL, and IAP, and Jeanne Portier and Eckehard Brockerhoff for discussion.

SUPPLEMENTARY MATERIAL

The Supplementary Material for this article can be found online at: https://www.frontiersin.org/articles/10.3389/ffgc.2021.645920/full#supplementary-material

REFERENCES

Bakys, R., Vasaitis, R., and Skovsgaard, J. P. (2013). Patterns and severity of crown dieback in young even-aged stands of european ash (*Fraxinus excelsior* L.) in relation to stand density, bud flushing phenotype, and season. *Plant Protect. Sci.* 49, 120–126. doi: 10.17221/70/2012-PPS

Baral, H.-O., Queloz, V., and Hosoya, T. (2014). Hymenoscyphus fraxineus, the correct scientific name for the fungus causing ash dieback in Europe. *IMA Fungus* 5, 79–80. doi: 10.5598/imafungus.2014.05.01.09

Bartoń, K. (2018). *MuMIn: Multi-Model Inference. R package version 1.42.1.*

Bigler, C., and Bugmann, H. (2004). Predicting the time of tree death using dendrochronological data. *Ecol. Appl.* 14, 902–914. doi: 10.1890/03-5011

Boshier, D., Cordero, J., Harris, S., Pannell, J., Rendell, S., Savill, P., et al. (2005). *Ash Species in Europe: Biological Characteristics and Practical Guidelines for Sustainable Use*. Oxford: University of Oxford.

Brändle, M., and Brandl, R. (2001). Species richness of insects and mites on trees: expanding Southwood. *J. Anim. Ecol.* 70, 491–504. doi: 10.1046/j.1365-2656.2001.00506.x

Brändli, U.-B., Abegg, M., and Allgaier Leuch, B. (2020). *Schweizerisches Landesforstinventar. Ergebnisse der vierten Erhebung 2009–2017. Birmensdorf, Eidgenössische Forschungsanstalt für Wald, Schnee und Landschaft. Bern, Bundesamt für Umwelt*. Available online at: https://www.envidat.ch/#/metadata/schweizerisches-landesforstinventar-2009-2017 (accessed October 12, 2020)

Brinkmann, N., Eugster, W., Zweifel, R., Buchmann, N., and Kahmen, A. (2016). Temperate tree species show identical response in tree water deficit but different sensitivities in sap flow to summer soil drying. *Tree Physiol.* 36, 1508–1519. doi: 10.1093/treephys/tpw062

Chandelier, A., Delahaye, L., Claessens, H., and Lassois, L. (2017). "Ash dieback in Wallonia, southern Belgium: research on disease development, resistance and management options," in *Dieback of European Ash (Fraxinus spp.) – Consequences and Guidelines for Sustainable Management*, eds R. Vasaitis and R. Enderle (Uppsala: Swedish University of Agricultural Sciences), 53–60.

Chaudhary, R., Rönneburg, T., Stein Åslund, M., Lundén, K., Durling, M. B., Ihrmark, K., et al. (2020). Marker-trait associations for tolerance to Ash Dieback in Common Ash (*Fraxinus excelsior* L.). *Forests* 11:1083. doi: 10.3390/f11101083

Chira, D., Chira, F., Tăut, I., Popovici, O., Blada, I., Doniță, N., et al. (2017). "Evolution of ash dieback in Romania," in *Dieback of European Ash (Fraxinus spp.) – Consequences and Guidelines for Sustainable Management*, eds R. Vasaitis and R. Enderle (Uppsala: Swedish University of Agricultural Sciences), 185–194.

Cleary, M., Nguyen, D., Marčiulynienė, D., Berlin, A., Vasaitis, R., and Stenlid, J. (2016). Friend or foe? Biological and ecological traits of the European ash dieback pathogen *Hymenoscyphus fraxineus* in its native environment. *Sci. Rep.* 6, 1–11. doi: 10.1038/srep21895

Cleary, M., Nguyen, D., Stener, L. G., Stenlid, J., and Skovsgaard, J. P. (2017). "Ash and ash dieback in Sweden: a review of disease history, current status, pathogen and host dynamics, host tolerance and management options in forests and landscapes," in *Dieback of European Ash (Fraxinus spp.) – Consequences and Guidelines for Sustainable Management*, eds R. Vasaitis and R. Enderle (Uppsala: Swedish University of Agricultural Sciences), 195–208.

Coker, T. L. R., Rozsypálek, J., Edwards, A., Harwood, T. P., Butfoy, L., and Buggs, R. J. A. (2019). Estimating mortality rates of European ash (*Fraxinus excelsior*) under the ash dieback (*Hymenoscyphus fraxineus*) epidemic. *Plants People Planet* 1, 48–58. doi: 10.1002/ppp3.11

Čufar, K., Luis, M. D., Zupančič, M., and Eckstein, D. (2008). A 548-year tree-ring chronology of oak (*Quercus* spp.) for Southeast Slovenia and its significance as a dating tool and climate archive. *Tree Ring Res.* 64, 3–15. doi: 10.3959/2007-12.1

Davydenko, K., and Meshkova, V. (2017). "The current situation concerning severity and causes of ash dieback in Ukraine caused by Hymenoscyphus fraxineus," in *Dieback of European Ash (Fraxinus spp.) – Consequences and Guidelines for Sustainable Management*, eds R. Vasaitis and R. Enderle (Uppsala: Swedish University of Agricultural Sciences), 220–227.

Díaz-Yáñez, O., Mola-Yudego, B., Timmermann, V., Tollefsrud, M. M., Hietala, A. M., and Oliva, J. (2020). The invasive forest pathogen *Hymenoscyphus fraxineus* boosts mortality and triggers niche replacement of European ash (*Fraxinus excelsior*). *Sci. Rep.* 10:5310. doi: 10.1038/s41598-020-61990-4

Eichhorn, J., Roskams, P., Potocic, N., Timmermann, V., Ferretti, M., Mues, V., et al. (2016). "Part IV: visual assessment of crown condition and damaging agents," in *Manual on Methods and Criteria for Harmonized Sampling, Assessment, Monitoring, and Analysis of the Effects of Air Pollution on Forests*, ed. UNECE ICP Forests Programme Co-ordinating Centre (Eberswalde: Thünen Institute of Forest Ecosystems). Available online at: https://www.icp-forests.org/pdf/manual/2016/ICP_Manual_2017_02_part04.pdf (accessed March 8, 2021).

Enderle, R. (2019). An overview of ash (*Fraxinus* spp.) and the ash dieback disease in Europe. *CAB Rev.* 14, 1–12. doi: 10.1079/PAVSNNR201914025

Enderle, R., Metzler, B., Riemer, U., and Kändler, G. (2018). Ash Dieback on sample points of the national forest inventory in South-Western Germany. *Forests* 9:25. doi: 10.3390/f9010025

Engesser, R., Queloz, V., Meier, F., Kowalski, T., and Holdenrieder, O. (2009). Das Triebsterben der Esche in der Schweiz. *Wald und Holz* 90, 24–27.

Etzold, S., Waldner, P., Thimonier, A., Schmitt, M., and Dobbertin, M. (2014). Tree growth in Swiss forests between 1995 and 2010 in relation to climate and stand conditions: recent disturbances matter. *Forest Ecol. Manag.* 311, 41–55. doi: 10.1016/j.foreco.2013.05.040

Fischer, C., and Traub, B. (2019). *Swiss National Forest Inventory-Methods and Models of the Fourth Assessment*. Cham: Springer International Publishing.

Fortin, M., Bédard, S., DeBlois, J., and Meunier, S. (2008). Predicting individual tree mortality in northern hardwood stands under uneven-aged management in southern Québec, Canada. *Ann. Forest Sci.* 65, 205–205. doi: 10.1051/forest:2007088

Ghelardini, L., Migliorini, D., Santini, A., Pepori, A. L., Maresi, G., Vai, N., et al. (2017). "From the alps to the apennines: possible spread of ash dieback in Mediterranean areas," in *Dieback of European Ash (Fraxinus spp.) – Consequences and Guidelines for Sustainable Management*, eds R. Vasaitis and R. Enderle (Uppsala: Swedish University of Agricultural Sciences), 140–149.

Gil, W., Kowalski, T., Kraj, W., Zachara, T., Łukaszewicz, J., Paluch, R., et al. (2017). "Ash dieback in Poland – history of the phenomenon and possibilities of its limitation," in *Dieback of European Ash (Fraxinus spp.) – Consequences and*

Guidelines for Sustainable Management, eds R. Vasaitis and R. Enderle (Uppsala: Swedish University of Agricultural Sciences), 176–184.

Grosdidier, M., Ioos, R., and Marçais, B. (2018). Do higher summer temperatures restrict the dissemination of *Hymenoscyphus fraxineus* in France? *Forest Pathol.* 48:e12426. doi: 10.1111/efp.12426

Grosdidier, M., Scordia, T., Ioos, R., and Marçais, B. (2020). Landscape epidemiology of ash dieback. *J. Ecol.* 108, 1789–1799. doi: 10.1111/1365-2745.13383

Gross, A., Holdenrieder, O., Pautasso, M., Queloz, V., and Sieber, T. N. (2014). *Hymenoscyphus pseudoalbidus*, the causal agent of European ash dieback. *Mol. Plant Pathol.* 15, 5–21. doi: 10.1111/mpp.12073

Hanáčková, Z., Havrdová, L., Černy, K., Zahradník, D., and Koukol, O. (2017). Fungal endophytes in ash shoots – diversity and inhibition of *Hymenoscyphus fraxineus*. *Balt. Forestry* 23:19.

Harper, A. L., McKinney, L. V., Nielsen, L. R., Havlickova, L., Li, Y., Trick, M., et al. (2016). Molecular markers for tolerance of European ash (*Fraxinus excelsior*) to dieback disease identified using Associative Transcriptomics. *Sci. Rep.* 6:19335. doi: 10.1038/srep19335

Hauptman, T., Piškur, B., de Groot, M., Ogris, N., Ferlan, M., and Jurc, D. (2013). Temperature effect on *Chalara fraxinea*: heat treatment of saplings as a possible disease control method. *Forest Pathol.* 43, 360–370. doi: 10.1111/efp.12038

Havrdová, L., Novotná, K., Zahradník, D., Buriánek, V., Pešková, V., Šrůtka, P., et al. (2016). Differences in susceptibility to ash dieback in Czech provenances of *Fraxinus excelsior*. *Forest Pathol.* 46, 281–288. doi: 10.1111/efp.12265

Heinze, B., Tiefenbacher, H., Litschauer, R., and Kirisits, T. (2017). "Ash dieback in Austria – history, current situation and outlook," in *Dieback of European Ash (Fraxinus spp.) – Consequences and Guidelines for Sustainable Management*, eds R. Vasaitis and R. Enderle (Uppsala: Swedish University of Agricultural Sciences), 33–52.

Holmes, T. P., Aukema, J. E., Holle, B. V., Liebhold, A., and Sills, E. (2009). Economic impacts of invasive species in forest past, present, and future. *Ann. N. Y. Acad. Sci.* 1162, 18–38.

Holzwarth, F., Kahl, A., Bauhus, J., and Wirth, C. (2013). Many ways to die – partitioning tree mortality dynamics in a near-natural mixed deciduous forest. *J. Ecol.* 101, 220–230. doi: 10.1111/1365-2745.12015

Hopf, S. (2019). *Eschenmonitoring Zustandsbericht 2019*. Witterswil: Institut für angewandte Pflanzenbiologie.

Hosmer, D. W. Jr., Lemeshow, S., and Sturdivant, R. X. (2013). *Applied Logistic Regression*. Hoboken, NJ: John Wiley & Sons.

Hülsmann, L., Bugmann, H., and Brang, P. (2017). How to predict tree death from inventory data — lessons from a systematic assessment of European tree mortality models. *Can. J. Forest Res.* 47, 890–900. doi: 10.1139/cjfr-2016-0224

Hülsmann, L., Bugmann, H. K. M., Commarmot, B., Meyer, P., Zimmermann, S., and Brang, P. (2016). Does one model fit all? Patterns of beech mortality in natural forests of three European regions. *Ecol. Appl.* 26, 2465–2479. doi: 10.1002/eap.1388

Hultberg, T., Sandström, J., Felton, A., Öhman, K., Rönnberg, J., Witzell, J., et al. (2020). Ash dieback risks an extinction cascade. *Biol. Conserv.* 244:108516. doi: 10.1016/j.biocon.2020.108516

Keller, W., Wohlgemuth, T., Kuhn, N., Schütz, M., and Wildi, O. (1998). *Waldgesellschaften der Schweiz auf floristischer Grundlage. Mitteilungen der Eidgenössischen Forschunganstalt für Wald, Schnee und Landschaft*, Vol. 73. Birmensdorf: Eidgenössische Forschungsanstalt für Wald, 269.

Kjær, E. D., McKinney, L. V., Hansen, L. N., Olrik, D. C., Lobo, A., Thomsen, I. M., et al. (2017). "Genetics of ash dieback resistance in a restoration context – experiences from Denmark," in *Dieback of European Ash (Fraxinus spp.) – Consequences and Guidelines for Sustainable Management*, eds R. Vasaitis and R. Enderle (Uppsala: Swedish University of Agricultural Sciences), 106–114.

Klesse, S., von Arx, G., Gossner, M. M., Hug, C., Rigling, A., and Queloz, V. (2020). Amplifying feedback loop between growth and wood anatomical characteristics of *Fraxinus excelsior* explains size-related susceptibility to ash dieback. *Tree Physiol.* doi: 10.1093/treephys/tpaa091 [Epub ahead of print].

Kowalski, T., and Łukomska, A. (2005). *The Studies on Ash Dying (Fraxinus excelsior L.) in the Włoszczowa Forest Unit stands*. Available online at: https://pubag.nal.usda.gov/catalog/5239646 (accessed February 3, 2020).

Lenz, H. D., Bartha, B., Straßer, L., and Lemme, H. (2016). Development of Ash Dieback in South-Eastern Germany and the increasing occurrence of secondary pathogens. *Forests* 7:41. doi: 10.3390/f7020041

Marçais, B., Husson, C., Caël, O., Dowkiw, A., Delahaye, L., Collet, C., et al. (2017). Estimation of ash mortality induced by *Hymenoscyphus fraxineus* in France and Belgium. *Baltic Forestry* 23, 159–167.

Marçais, B., Husson, C., Godart, L., and Caël, O. (2016). Influence of site and stand factors on *Hymenoscyphus fraxineus*-induced basal lesions. *Plant Pathol.* 65, 1452–1461. doi: 10.1111/ppa.12542

McKinney, L. V., Nielsen, L. R., Collinge, D. B., Thomsen, I. M., Hansen, J. K., and Kjær, E. D. (2014). The ash dieback crisis: genetic variation in resistance can prove a long-term solution. *Plant Pathol.* 63, 485–499. doi: 10.1111/ppa.12196

McKinney, L. V., Thomsen, I. M., Kjær, E. D., Bengtsson, S. B. K., and Nielsen, L. R. (2012). Rapid invasion by an aggressive pathogenic fungus (*Hymenoscyphus pseudoalbidus*) replaces a native decomposer (*Hymenoscyphus albidus*): a case of local cryptic extinction? *Fungal Ecol.* 5, 663–669. doi: 10.1016/j.funeco.2012.05.004

Menkis, A., Bakys, R., Stein Åslund, M., Davydenko, K., Elfstrand, M., Stenlid, J., et al. (2020). Identifying *Fraxinus excelsior* tolerant to ash dieback: visual field monitoring versus a molecular marker. *Forest Pathol.* 50:e12572. doi: 10.1111/efp.12572

MeteoSwiss (2021). *Spatial Climate Analyses*. Available online at: https://www.meteoswiss.admin.ch/home/climate/swiss-climate-in-detail/raeumliche-klimaanalysen.html (accessed February 15, 2021)

Mitchell, R. J., Beaton, J. K., Bellamy, P. E., Broome, A., Chetcuti, J., Eaton, S., et al. (2014). Ash dieback in the UK: a review of the ecological and conservation implications and potential management options. *Biol. Conserv.* 175, 95–109. doi: 10.1016/j.biocon.2014.04.019

Moser, W. K., Barnard, E. L., Billings, R. F., Crocker, S. J., Dix, M. E., Gray, A. N., et al. (2009). Impacts of nonnative invasive species on US forests and recommendations for policy and management. *J. Forestry* 107, 320–327.

Muñoz, F., Marçais, B., Dufour, J., and Dowkiw, A. (2016). Rising out of the ashes: additive genetic variation for crown and collar resistance to *Hymenoscyphus fraxineus* in *Fraxinus excelsior*. *Phytopathology* 106, 1535–1543. doi: 10.1094/PHYTO-11-15-0284-R

Nemesio-Gorriz, M., Menezes, R. C., Paetz, C., Hammerbacher, A., Steenackers, M., Schamp, K., et al. (2020). Canditate metabolites for ash dieback tolerance in *Fraxinus excelsior*. *J. Exp. Bot.* 71, 6074–6083. doi: 10.1093/jxb/eraa306

Nielsen, L. R., Mckinney, L. V., and Kjær, E. D. (2017). Host phenological stage potentially affects dieback severity after *Hymenoscyphus fraxineus* infection in *Fraxinus excelsior* seedlings. *Baltic Forestry* 23, 229–232.

Ozolincius, R., Miksys, V., and Stakenas, V. (2005). Growth-independent mortality of Lithuanian forest tree species. *Scand. J. Forest Res.* 20, 153–160. doi: 10.1080/14004080510042164

Pautasso, M., Aas, G., Queloz, V., and Holdenrieder, O. (2013). European ash (*Fraxinus excelsior*) dieback – A conservation biology challenge. *Biol. Conserv.* 158, 37–49. doi: 10.1016/j.biocon.2012.08.026

Pautasso, M., Schlegel, M., and Holdenrieder, O. (2015). Forest health in a changing world. *Microb. Ecol.* 69, 826–842. doi: 10.1007/s00248-014-0545-8

Professur für Waldbau und Professur für Forstschutz and Dendrologie der ETH Zürich (1995). *Mitteleuropäische Waldbaumarten. Artbeschreibung und Ökologie unter besonderer Berücksichtigung der Schweiz. Zürich*. Available online at: https://ethz.ch/content/dam/ethz/special-interest/usys/ites/waldmgmt-waldbau-dam/documents/Lehrmaterialien/Skripte/Baumartenbeschreibungen/ME-Waldbaumarten (accessed October 29, 2020).

Pyšek, P., and Richardson, D. M. (2010). Invasive species, environmental change and management, and health. *Annu. Rev. Environ. Resour.* 35, 25–55. doi: 10.1146/annurev-environ-033009-095548

Queloz, V., and Gossner, M. M. (2019). *Zukunft der Esche – zwei neue Projekte an der WSL. Waldschutz aktuell 3*. Available online at: https://www.dora.lib4ri.ch/wsl/islandora/object/wsl%3A21870/datastream/PDF/Queloz-2019-Zukunft_der_Esche_%E2%80%93_zwei-%28published_version%29.pdf (accessed October 7, 2020)

Queloz, V., Hopf, S., Schoebel, C. N., Rigling, D., and Gross, A. (2017). "Ash dieback in Switzerland: history and scientific achievements," in *Dieback of European Ash (Fraxinus spp.) – Consequences and Guidelines for Sustainable Management*, eds R. Vasaitis and R. Enderle (Uppsala: Swedish University of Agricultural Sciences), 68–78.

R Core Team (2018). *R: A Language and Environment for Statistical Computing*. Vienna: R Foundation for Statistical Computing.

Rigling, D., Hilfiker, S., Schöbel, C., Meier, F., Engesser, R., Scheidegger, C., et al. (2016). *Das Eschentriebsterben. Biologie, Krankheitssymptome und Handlungsempfehlungen*. Birmensdorf: Eidg. Forschungsanstalt WSL.

Roibu, C.-C., Sfeclă, V., Mursa, A., Ionita, M., Nagavciuc, V., Chiriloaei, F., et al. (2020). The climatic response of tree ring width components of ash (*Fraxinus excelsior* L.) and common oak (*Quercus robur* L.) from Eastern Europe. *Forests* 11:600. doi: 10.3390/f11050600

Sahraei, S. E., Cleary, M., Stenlid, J., Brandström Durling, M., and Elfstrand, M. (2020). Transcriptional responses in developing lesions of European common ash (*Fraxinus excelsior*) reveal genes responding to infection by *Hymenoscyphus fraxineus*. *BMC Plant Biol.* 20:455. doi: 10.1186/s12870-020-02656-1

Sambles, C. M., Salmon, D. L., Florance, H., Howard, T. P., Smirnoff, N., Nielsen, L. R., et al. (2017). Ash leaf metabolomes reveal differences between trees tolerant and susceptible to ash dieback disease. *Sci. Data* 4:170190. doi: 10.1038/sdata.2017.190

Scherrer, D., Bader, M. K.-F., and Körner, C. (2011). Drought-sensitivity ranking of deciduous tree species based on thermal imaging of forest canopies. *Agric. Forest Meteorol.* 151, 1632–1640. doi: 10.1016/j.agrformet.2011.06.019

Schlüter, H. (1967). Buntlaubhölzer in kollinen Waldgesellschaften Mittelthüringens. *Die Kulturpflanze* 15, 115–138. doi: 10.1007/BF02095708

Schreuder, H. T., Hansen, M., and Kohl, M. (1999). Relative costs and benefits of a continuous and a periodic forest inventory in Minnesota. *Environ. Monit. Assess.* 59, 135–144. doi: 10.1023/A:1006137914405

Semizer-Cuming, D., Finkeldey, R., Nielsen, L. R., and Kjær, E. D. (2019). Negative correlation between ash dieback susceptibility and reproductive success: good news for European ash forests. *Ann. Forest Sci.* 76:16. doi: 10.1007/s13595-019-0799-x

Sheil, D., and May, R. M. (1996). Mortality and recruitment rate evaluations in heterogeneous tropical forests. *J. Ecol.* 84, 91–100. doi: 10.2307/2261703

Sollars, E. S. A., Harper, A. L., Kelly, L. J., Sambles, C. M., Ramirez-Gonzalez, R. H., Swarbreck, D., et al. (2017). Genome sequence and genetic diversity of European ash trees. *Nature* 541, 212–216. doi: 10.1038/nature20786

Stahel, W. (2019). *regr0: Building Regression Models*. Available online at: https://R-Forge.R-project.org/projects/regdevelop/ (accessed July 10, 2020).

Stocks, J. J., Metheringham, C. L., Plumb, W., Lee, S. J., Kelly, L. J., Nichols, R. A., et al. (2019). Genomic basis of European ash tree resistance to ash dieback fungus. *bioRxiv [Preprint]* doi: 10.1101/626234

Trumbore, S., Brando, P., and Hartmann, H. (2015). Forest health and global change. *Science* 349, 814–818. doi: 10.1126/science.aac6759

Vasaitis, R., and Enderle, R. (2017). "Dieback of European ash (*Fraxinus* spp.) – consequences and guidelines for sustainable management," in *Dieback of European ash (Fraxinus spp.) – Consequences and Guidelines for Sustainable Management*, eds R. Vasaitis and R. Enderle (Uppsala: Swedish University of Agricultural Sciences).

Villari, C., Dowkiw, A., Enderle, R., Ghasemkhani, M., Kirisits, T., Kjær, E. D., et al. (2018). Advanced spectroscopy-based phenotyping offers a potential solution to the ash dieback epidemic. *Sci. Rep.* 8:17448. doi: 10.1038/s41598-018-35770-0

Wohlmuth, A., Essl, F., and Heinze, B. (2018). Genetic analysis of inherited reduced susceptibility of *Fraxinus excelsior* L. seedlings in Austria to ash dieback. *Forestry (Lond.)* 91, 514–525. doi: 10.1093/forestry/cpy012

Wolf, A., Møller, P. F., Bradshaw, R. H. W., and Bigler, J. (2004). Storm damage and long-term mortality in a semi-natural, temperate deciduous forest. *Forest Ecol. Manag.* 188, 197–210. doi: 10.1016/j.foreco.2003.07.009

Wunder, J., Brzeziecki, B., Żybura, H., Reineking, B., Bigler, C., and Bugmann, H. (2008). Growth–mortality relationships as indicators of life-history strategies: a comparison of nine tree species in unmanaged European forests. *Oikos* 117, 815–828. doi: 10.1111/j.0030-1299.2008.16371.x

Conflict of Interest: The authors declare that the research was conducted in the absence of any commercial or financial relationships that could be construed as a potential conflict of interest.

frontiers in Forests and Global Change

ORIGINAL RESEARCH
published: 24 May 2021
doi: 10.3389/ffgc.2021.655769

Sphaeropsis sapinea and Associated Endophytes in Scots Pine: Interactions and Effect on the Host Under Variable Water Content

*Kathrin Blumenstein[1], Johanna Bußkamp[2], Gitta Jutta Langer[2], Rebekka Schlößer[1,2], Natalia Marion Parra Rojas[1] and Eeva Terhonen[1]**

[1] Forest Pathology Research Group, Department of Forest Botany and Tree Physiology, Faculty of Forest Sciences and Forest Ecology, University of Göttingen, Göttingen, Germany, [2] Section Mycology and Complex Diseases, Department of Forest Protection, Northwest German Forest Research Institute (NW-FVA), Göttingen, Germany

OPEN ACCESS

Edited by:
Caterina Villari, University of Georgia, United States

Reviewed by:
Treena Burgess, Murdoch University, Australia
Benoit Marçais, INRA Centre Nancy-Lorraine, France

***Correspondence:**
Eeva Terhonen
terhonen@uni-goettingen.de

Specialty section:
This article was submitted to Pests, Pathogens and Invasions, a section of the journal Frontiers in Forests and Global Change

Received: *19 January 2021*
Accepted: *26 April 2021*
Published: *24 May 2021*

Citation:
Blumenstein K, Bußkamp J, Langer GJ, Schlößer R, Parra Rojas NM and Terhonen E (2021) Sphaeropsis sapinea and Associated Endophytes in Scots Pine: Interactions and Effect on the Host Under Variable Water Content. Front. For. Glob. Change 4:655769. doi: 10.3389/ffgc.2021.655769

The ascomycete *Sphaeropsis sapinea* is the causal agent of the Diplodia Tip Blight disease on pines and other conifer species. This fungus has a symptomless endophytic life stage. Disease symptoms become visible when trees have been weakened by abiotic stress, usually related to warmer temperatures and drought. Currently, this disease is observed regularly in Scots pine (*Pinus sylvestris*) sites in parts of Europe, such as Germany, increasing dramatically in the last decade. Changes in climatic conditions will gradually increase the damage caused by this fungus, because it is favored by elevated temperature. Thus, host trees with reduced vitality due to climate change-related environmental stress are expected to be more susceptible to an outbreak of Diplodia Tip Blight disease. There is currently no established and effective method to control *S. sapinea*. This project aims to reveal the nature of the endophyte community of Scots pine. Utilizing the antagonistic core community of endophytes could serve as a novel tool for disease control. Results from this study provide a starting point for new solutions to improve forest health and counter *S. sapinea* disease outbreaks. We screened potential antagonistic endophytes against *S. sapinea* and infected Scots pine seedlings with the most common endophytes and *S. sapinea* alone and combination. The host was stressed by limiting access to water. The antagonism study revealed 13 possible fungi with the ability to inhibit the growth of *S. sapinea in vitro*, for example *Sydowia polyspora*. None of the tested co-infected fungi (*Desmazierella acicola, Didymellaceae* sp., *Microsphaeropsis olivacea, Sydowia polyspora, and Truncatella conorum-piceae*) showed strong necrosis development *in vivo*, even when host stress increased due to drought. However, the infection experiment demonstrated that drought conditions enhance the effect of the disease outbreak, triggering *S. sapinea* to cause more necrosis in the infected twigs.

Keywords: Diplodia tip blight, climate change, antagonism, infection, drought, *Sphaeropsis sapinea, Sydowia polyspora*

INTRODUCTION

Climate change is a potential driver of adverse effects on forest health. With climate change, there is an increase in drought-associated stress, rendering trees more susceptible to threats such as pests and pathogens which can compromise their overall health (Bußkamp, 2018; Brodde et al., 2019; Terhonen et al., 2019b). Scots pine (*Pinus sylvestris* L.) is one of the most economically important forestry tree species in Europe. Changes in the environment, especially those related to drought, will affect Scots pine pathosystems. The ascomycete fungus *Sphaeropsis sapinea* (Fr.) Dyko & B. Sutton (≡ *Diplodia sapinea* (Fr.) Fuckel, *Diplodia pinea* (Desm.) J. Kickx f.) is recognized as the most widespread necrotrophic pathogen responsible for dramatic losses of *Pinus* species across the continents, causing a disease called Diplodia tip blight (Smith et al., 1996; Fabre et al., 2011; Bußkamp, 2018; Paez and Smith, 2018; Brodde et al., 2019). The correct name of this anamorphic Botryosphaeriaceae is in discussion and it is epityped (de Wet et al., 2003; Phillips et al., 2013), but the current name after Index Fungorum is still *S. sapinea.* The preferred name after the EPPO Global Database, however, is *Diplodia sapinea*[1].

Recently, the disease Diplodia tip blight has been increasing in Germany, especially after the hot and dry years of 2018 and 2019 (Blumenstein et al., 2020). *Sphaeropsis sapinea* has a latent endophytic stage (Burgess et al., 2004; Flowers et al., 2006; CABI, 2019; Bußkamp et al., 2020; Terhonen et al., 2021) and disease symptoms become visible when trees have been weakened by stress, usually related to temperature and drought, allowing *S. sapinea* to switch its lifestyle from endophytic to pathogenic (Blodgett et al., 1997a; Stanosz et al., 2001; Blumenstein et al., 2020). The production of reactive oxygen species (e.g., hydrogen peroxide, H_2O_2) and the accumulation of free amino acids are common plant responses to drought (Sherwood et al., 2015). Because these drought-induced perturbations in metabolism also often occur during pathogenic attack, they may be partly responsible for an enhanced susceptibility to fungal pathogens (Desprez-Loustau et al., 2006; Sturrock et al., 2011; Sherwood et al., 2015) or lifestyle-switch. Nevertheless, it is not known in detail which fungal or host genetic factors are responsible in the lifestyle-switch of *S. sapinea*.

The term "endophyte" is used to describe microbes that live asymptotically inside plant tissues for the entire or at least a significant part of their life cycle without causing any clear negative harm to the host (Petrini, 1991; Saikkonen et al., 1998). Although endophytes in conifers have been studied intensively (e.g. Bußkamp, 2018; Bußkamp et al., 2020; e.g., Saikkonen et al., 1998; Sieber, 2007; Terhonen et al., 2019b), generally the interaction between different endophytes and their host remains poorly understood (Sieber and Grünig, 2013; Witzell et al., 2014; Compant et al., 2016; Terhonen et al., 2018; Witzell and Martín, 2018). Several endophytes are regarded as parasites tolerated by their host or as opportunistic or latent pathogens (Sanz-Ros et al., 2015). Endophytes can also act as primary colonizers and may remain in a physiological resting phase in their host. For example *S. sapinea* is a typical member of the fungal community of natural pruning of branches defined by Butin and Kowalski (1990). Growing inside their hosts' tissues, they can form fruiting bodies and spores (Chapela and Boddy, 1988; Griffith and Boddy, 1988; Kehr, 1998; Osono, 2006; Oses et al., 2008; Sanz-Ros et al., 2015). The question is, how do endophytes overcome a host's defenses and colonize them? This could either be due to the secretion of metabolites by the endophyte (Peters et al., 1998; Schulz et al., 2015, 2002) or by changing the phytohormone balance in the tree (Navarro-Meléndez and Heil, 2014). It is also conceivable that the endophyte defeats the metabolism of the tree by secreting lyzing enzymes (Schulz et al., 1998; Suryanarayanan et al., 2012). Sherwood et al. (2015) proposed a new model of fungal infection of plants based on interactions of the metabolisms of the free amino acid proline and H_2O_2 with drought. The authors showed that droughted Austrian pine (*Pinus nigra* Arnold) accumulated hydrogen peroxide in shoots. Hydrogen peroxide is toxic to *S. sapinea*, but the infection of the droughted Austrian pine with this pathogen led to a reduction in the H_2O_2-concentration in the host plants. *S. sapinea* is able to produce catalase and peroxidase in response to the oxidative stress by H_2O_2. Proline is a preferred nitrogen source for *S. sapinea in vitro* and it increased in the plant as well in response to drought as and in response to infection with *S. sapinea*. Sherwood et al. (2015) conclude from their results that the proline precursor, glutamate, protects *S. sapinea* from hydrogen peroxide damage.

In vitro, endophytes produce a variety of secondary metabolites such as herbicides, fungicides and antibiotics (Schulz et al., 2002; Kusari et al., 2012). The metabolites may serve the plant to maintain numerous balances: between endophytes and host, but also between other endophytic fungi and bacteria. The endophytic stage represents a balanced interaction between the fungus and its host. However, endophytic fungal species can become pathogens when this balance is disturbed or saprotrophs if the host dies (Müller and Krauss, 2005; Rodriguez et al., 2009; Bußkamp, 2018; Terhonen et al., 2016, 2019a).

Fungal endophytes are known to contribute to the health of plants, acting as growth promotors that synthesize phytohormones; in addition, they can potentially protect plants from pathogenic fungi by their anti-fungal activity (Witzell et al., 2014; Terhonen et al., 2018, 2019b). In conifer trees, it has been shown that inoculations with fungal endophytes protect the host from natural infection by *Dothistroma septosporum* (Dorogin) M. Morelet (Ridout and Newcombe, 2015). Consequently, several metabolites with antifungal properties have been isolated from foliar endophytes of *Picea rubens* Sarg. and *Picea mariana* (Mill.) Britt., E.E. Sterns & Poggenburg (McMullin et al., 2017). These results support the hypothesis that fungal endophytes may enhance the tolerance of the host tree to fungal pathogens (Sumarah et al., 2011, 2015; Richardson et al., 2014; Tanney et al., 2016; Oliva et al., 2021). Some endophytes can also be used as antagonists against potential pathogens (Arnold et al., 2003; Ganley et al., 2008; Rungjindamai et al., 2008; Martín et al., 2015). Whether an endophyte acts

[1]https://gd.eppo.int/taxon/DIPDPI

as an antagonist or competes with a particular pathogen, can be studied *in vitro* using so-called antagonism assays (Santamaría et al., 2012; Blumenstein, 2015; Romeralo et al., 2015; Bußkamp, 2018; Rigerte et al., 2019). These findings are extremely important as, in the future, the use of beneficial endophytes that can act as biocontrol agents against pathogens, in this case against *S. sapinea*, may be a valuable approach to disease control. Potential antagonistic fungi, such as *Sydowia polyspora* (Bref. & Tavel) E. Müll., *Alternaria* sp. and *Epicoccum nigrum* Link, were recently discussed in a study by Oliva et al. (2021).

Climate change could transform *S. sapinea* into a global threat to forest health, as the growth rate will be favored by climate warming (Fabre et al., 2011). Indirect effects (temperature, drought) are important because susceptibility of pines to *S. sapinea* is strongly enhanced by water stress (Blodgett et al., 1997a,b; Stanosz et al., 2001; Desprez-Loustau et al., 2006; Bußkamp, 2018). Hence, understanding how the lifestyle of fungi switches due to environmental stress is critical for deciphering the evolution of host–microbe interactions (Kuo et al., 2014). Fungal lifestyles are not in that sense stable but dynamic, and are likely to be influenced by the genetics of the fungal species, host factors and changing environments (Kuo et al., 2014). Endophytes may have evolved to switch their lifestyles to adapt different environmental conditions (Kuo et al., 2014). *S. sapinea* can be considered a very good model to test the direct effects of environmental changes on a fungal pathogen (lifestyle-switch), as well as indirect effects on the host susceptibility (stress). The high levels of Diplodia tip blight symptoms in forest stands are not due to a high abundance but rather depend on environmental conditions (Feci et al., 2002; Bußkamp, 2018; Blumenstein et al., 2020). The impact of climate change could shift the endophyte communities and will probably also affect the nature of fungal pathogens. Increased temperature may mean that host resistance to disease may be overcome more quickly as a result of rapid disease cycles. For *S. sapinea*, warmer temperatures will be suitable for accelerated growth and reproduction. To mitigate the impacts of climate change, understanding the factors that trigger development of forest tree disease epidemics will be essential.

The aims of this study on the pathosystem of *S. sapinea* and *P. sylvestris* were (1) to identify fungal Scots pine endophytes which may have the ability to antagonize the pathogen *S. sapinea in vitro*, (2) to test how the strength of drought-induced stress due to different levels of water availability effects potential disease symptoms, measured by necrosis length, in inoculation tests performed with *S. sapinea* and selected Scots pine endophytes *in planta*, and (3) to investigate whether there are potential remote influences between Scots pine endophytes and *S. sapinea* in an *in vivo* experiment. Aims 2 and 3 were tested in a greenhouse experiment. We infected Scots pine saplings with *S. sapinea* and selected endophytes from pine that are either reported to be latent pine pathogens or putative antagonistic endophytes. The host plants were inoculated with a single test strain or combined with different fungal strains on a separate twigs.

MATERIALS AND METHODS

Test for Antagonistic Endophytes Against *S. sapinea*

Fungal Material: Isolates From Scots Pine Tips

In this study, 30 fungal isolates (two *Sphaeropsis sapinea* strains and 28 endophytes) were used for either the antagonism assay or inoculations (**Table 1**). The fungal strains chosen are regularly isolated from Scots pine tips in German forests according to Bußkamp et al. (2020). Origin and locations of the strains are described in Blumenstein et al. (2020). One strain (*Didymellaceae* sp., NW-FVA ID 5756) originated from a sample of the nursery pine plants (see section "Pre-experiment Detection of Endophytes Including *Sphaeropsis sapinea* in Plant Material") that were used in this study for the antagonism assay.

In vitro Study: Antagonism Assay

In order to identify endophytic fungal isolates that may have the ability to antagonize the pathogen *S. sapinea* inside the pine trees' tissue (*in planta)*, the interactions of 27 isolated pine endophytes (Blumenstein et al., 2020) against two different *S. sapinea* strains were investigated by means of a paired-growth assay (antagonism assay *in vitro*) as described in Rigerte et al. (2019). The ability of an endophyte to antagonize the pathogen was determined based on the inhibition level (defined as pathogen growth with and without the endophyte) over a given period of time. This was achieved by assessing and measuring the concurrent growth of the pathogens on 1.5% Malt-Yeast-Peptone (MYP-agar, after Langer (1994)) nutrient medium (pH = 6) and the assessment by eye of the growth behavior of the paired fungal strains. The latter observations were categorized as follows: (1) Inhibition of *S. sapinea* growth (**Figure 1A**), (2) endophyte superior = the endophyte has overgrown and inhibited the mycelium of *S. sapinea* (**Figure 1B**), (3) Equal growth capability = the tested endophyte and *S. sapinea* did not overgrow or obviously inhibit each other (**Figure 1C**), and (4) *S. sapinea* superior = *S. sapinea* inhibited and may also have overgrown the tested endophyte strain (**Figure 1D**). The endophyte and pathogen were placed opposite each other on the surface of MYP agar plates within 2.1 cm of the perimeter of the petri dish (**Figure 2**; Rigerte et al., 2019). Such pairings were prepared in triplicate. Control plates containing only the pathogen (located identically on the plate as in the paired setup) were also prepared. All these plates were then incubated under the same conditions: room temperature (ca. 22°C) and diffuse daylight. Growth was assessed 3, 7, and 10 days after inoculation. Measurements were performed with a ruler for both the endophytes and the pathogens in the antagonism test plate. For analysis of the data and to determine whether the presence of an endophyte had an effect to the pathogen, a *t*-test to compare the pathogens' growth (alpha direction, **Figure 2**) after 10 days with the growth of the control was performed with SPSS version 26.0 (IBM Corporation, New York, United States).

Greenhouse-Study

Four endophytes, *Desmazierella acicola* Lib., *Microsphaeropsis olivacea* (Bonord.) Höhn., *Sydowia polyspora*, *Truncatella*

TABLE 1 | All isolates used in antagonist study or/and inoculation study, their accession numbers and observations against *S. sapinea*.

			Antagonist test results		
Isolate ID (NW-FVA)	**Gene Bank Accession No.**	**Species name**	**Visual observation**	**Paired *t*-test based on measured growth along two axes**	
5756	MW365344	*Didymellaceae* sp.	NA	Endophyte versus *S. sapinea*	
4739	MT790326	*Sphaeropsis sapinea*	NA	*S. sapinea*, strain 4739	*S. sapinea* strain 4740
4740	MT790327	*Sphaeropsis sapinea*	NA	*p*-Value	*p*-Value
4741	MT790316	*Diaporthe sp.* 1	Equal growth capability	0.008	0.004
4742	MT790328	*Sydowia polyspora*	Inhibition of pathogen growth	0.010	0.005
4743	MT790320	*Microsphaeropsis olivacea*	Equal growth capability	0.014	0.002
4744	MT790317	*Epicoccum nigrum*	Equal growth capability	0.011	0.005
4745	MT790329	*Truncatella conorum-piceae*	Pathogen superior	0.018	0.000
4746	MT790311	*Alternaria alternata*	Inhibition of pathogen growth	0.019	0.006
4747	MT790325	*Rosellinia* sp.	Endophyte superior	0.017	0.003
4748	MT821234	*Xylaria polymorpha*	Endophyte superior	0.016	0.005
4749	MT821235	*Fusarium* sp.	Equal growth capability	0.015	0.005
4750	MT821236	*Nemania diffusa*	Inhibition of pathogen growth	0.019	0.007
4751	MT790315	*Desmazierella acicola*	Equal growth capability	0.016	0.005
4753	MT821237	*Diaporthe* sp. 2	Inhibition of pathogen growth	0.013	0.004
4754	MT790312	*Biscogniauxia mediterranea*	Endophyte superior	0.016	0.008
4755	MT790318	*Hypoxylon fragiforme*	Equal growth capability	0.021	0.005
4756	MT790313	*Biscogniauxia nummularia*	Equal growth capability	0.036	0.008
4757	MT790324	*Pyronema domesticum*	Endophyte superior	0.011	0.004
4758	MT790314	*Botrytis cinerea*	Equal growth capability	0.013	0.004
4759	MT790323	*Pseudocamarosporium brabeji*	Equal growth capability	0.025	0.003
4760	MT790321	*Nemania serpens*	Pathogen superior	0.029	0.006
4761	MW365343	*Pezicula eucrita*	Inhibition of pathogen growth	0.024	0.005
4762	MT790322	*Preussia funiculata*	Inhibition of pathogen growth	0.032	0.009
4763	MT821238	*Mollisia sp.*	Pathogen superior	0.037	0.006
4764	MT821239	*Preussia sp.*	Inhibition of pathogen growth	0.011	0.002
4765	MT790319	*Jugulospora rotula*	Endophyte superior	0.010	0.003
4766	MT821240	*Daldinia sp.*	Endophyte superior	0.011	0.003
4767	MT790330	*Therrya fuckelii (*strain 6)	Pathogen superior	0.019	0.006
4768	MT821241	*Therrya fuckelii* (strain 7)	Pathogen superior	0.126	0.005

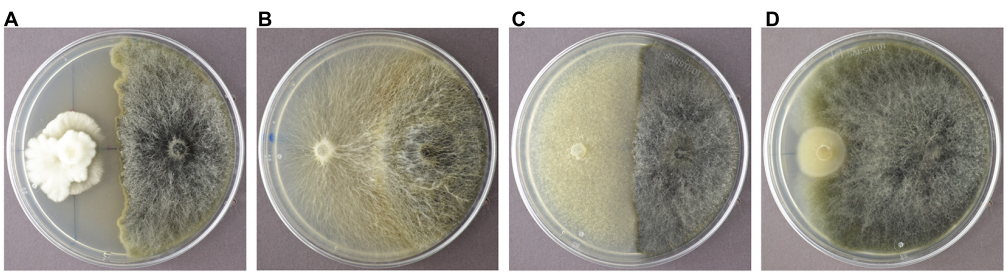

FIGURE 1 | Examples of the different reactions of the endophyte (white mycelium in examples A-D) during the antagonism assays growing in dual culture with *S. sapinea* (brownish-gray morphology). **(A)** *Nemania diffusa* (4750) vs. *S. sapinea*: inhibition of *S. sapinea* growth; **(B)** *Biscogniauxia mediterranea* (4754) vs. *S. sapinea*: endophyte superior; **(C)** *Botrytis cinerea* (4758) vs. *S. sapinea*: equal growth; **(D)** *Mollisia* sp. (4763) vs. *S. sapinea*: *S. sapinea* superior.

conorum-piceae (Tubeuf) Steyaert, and *S. sapinea* were chosen for the greenhouse inoculation experiment. We compared the infection capacity of these fungi under variable water content on infected pine trees both alone and in combination. Combined infections were set up so that different twigs of the plants were infected with different fungi, to test for possible remote synergistic effects of the endophytic fungi on *S. sapinea*. Additionally, one endophyte (*Didymellaceae* sp.) was included in the study that was isolated with the highest frequency in pre-experiment detection of endophytes (section "Pre-experiment

Detection of *Endophytes Includ*ing Sphaeropsis sapinea in Plant Material").

Plant Material

The plant material consisted of 1008 2-year-old, apparently healthy and vital, Scots pine (*P. sylvestris*) seedlings purchased from Niedersächsische Landesforsten Services GmbH (seeds originated from the collin Black Forest area, Germany) and LIECO GmbH & Co KG. Seedlings were potted into plastic containers arranged in trays with six containers / tray. These were filled with fertilized peat (Flora gard, TKS®2 Instant Plus and PERLIGRAN® Extra 2-6mm, Hermann Meyer KG, Rellingen, Germany). Containers were placed on tables covered with plastic sheets where excess water could accumulate and be absorbed later. The seedlings were acclimatized to the greenhouse conditions for 30-days prior to receiving water according to their treatment group (section "Experimental Design of the Green-House Study"), during the initial period they received tap water as required to maintain moist soil. No additional fertilization was given during the experiment.

Pre-experiment Detection of Endophytes Including *Sphaeropsis sapinea* in Plant Material

Six seedlings were examined for pre-colonization of the internal woody tissues by *S. sapinea* and to reveal the endophyte community. The methodology followed the procedures described in Bußkamp et al. (2020). The complete stem and all shoots of each plant were investigated by culture-based isolation of endophytes. Needles were removed and the tips und stem were surface sterilized (1 min in 70% ethanol/5 min 4% sodium hypochlorite/1 min 70% ethanol) and cut into segments (0.5 cm). Three segments were plated on a petri dish filled with 1.5% MYP-agar. In total, 457 woody plant segments were plated (Ø 76 segments, min. 50, max. 122). Additionally, discolored or dead needles that were found occasionally were checked for infection with *S. sapinea*. Discolored needles (n = 6 needles, =62 plated tissue segments) were treated according to the same procedure as the woody plant part, except with a shorter 1 min sterilization in 4% sodium hypochlorite. Dead needles were incubated in a moist chamber for potential formation of pycnidia by *S. sapinea*. After 7 and 14 days all petri dishes were checked for the presence of *S. sapinea* and other outgrowing endophytes.

DNA Extraction, PCR, and Sequencing

Before inoculations, the DNA was extracted from 150 mg of the homogenized mycelium sample as described in Keriö et al. (2020). 1000 µl of PVP extraction buffer (1 M NaCl, 100 mM Tris-Hcl, 10 mM EDTA, 2% PVP (w/v)) was added to a 1.5 ml Eppendorf tube with 0.3 g of ground mycelium sample. After incubation at 65°C for 15 min, the sample was centrifuged 5000 rpm for 10 min. The supernatant was transferred into a 1.5 ml tube (ca. 500 µl). One volume of SDS (1% SDS (w/v), 0.5 M KCl) was added. The sample was vortexed for 20 s and centrifuged at 15 000 rpm for 10 min. The supernatant (ca.700 µl) was transferred into a 1.5 ml tube. 0.85 volume of isopropanol was added and mixed by inversion for 20 s, followed by centrifuging for 10 min at 15 000 rpm. The supernatant was removed by pouring it away and the pellet was washed with 200 µl of cold 70% ethanol. After centrifuging at 15 000 rpm for 5 min, ethanol was removed and the pellet dried for 15 min at 65°C. The pellet was re-suspended in nuclease free water (50 µl).

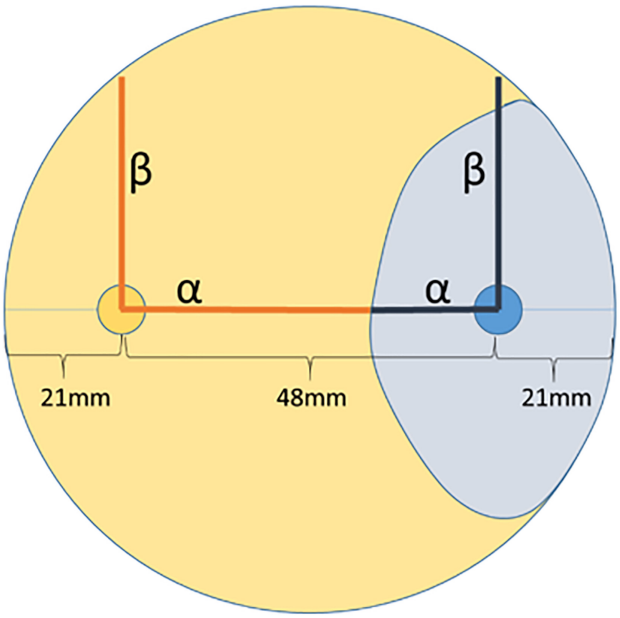

FIGURE 2 | Arrangement of the two-paired culture assay of one fungus (e.g., endophyte) in orange and the other fungus (e.g., pathogen) in blue. Measurement was along the alpha and beta axes. The light orange and blue areas suggest possible growth areas of the fungi and how their growth could be measured.

Taq DNA polymerase (Qiagen) was used for PCR amplification of ITS regions with the primer pair ITS1-F and ITS4 (White et al., 1990; Gardes and Bruns, 1993). Briefly, the PCR protocol was as follows: 1X PCR Buffer, 200 µM dNTP, 0.5 µM primer 1, 0.5 µM primer 2, 100 ng template DNA, 0.2 U/µL DNA polymerase; the reaction was adjusted to 25 µL with autoclaved MQ H_2O. The PCR conditions used were 94°C for 3 min; 30 cycles of 94°C for 30 s, 55°C for 1 min, 72°C for 1 min, and 72°C for 10 min. Possible contaminants were determined with a negative control using sterile water as a template in both PCR protocols. StainIN RED™ Nucleic Acid Stain was used to confirm DNA amplicons on a 1.5% agarose gel and the visual detection was undertaken with ultraviolet transillumination. ITS region PCR products were purified and sequenced using the ITS4 primer at Microsynth SEQLAB (Göttingen, Germany).

The ITS sequences were extracted with the open source software ITSx to separate the ITS1 and ITS2 subregions from the fungal ITS sequences (Bengtsson-Palme et al., 2013). The ITS1 and ITS2 sequences were used for BLASTN (Zhang et al., 2000) searches against GenBank/NCBI (Sayers et al., 2011) to provide taxonomic identification. The sequences with ≥98% similarity and a query coverage ≥97% were set to constrict species level (Arnold and Lutzoni, 2007; Koukol et al., 2012) and confirmed the morphological identification (**Table 1**).

Experimental Design of the Green-House Study

The experiment was conducted at the University of Göttingen, Germany (51°33′28.4″ N 9°57′30.5″ E) from mid-March until August 2019. The 1008 seedlings were randomly block-assigned to waterproof tables in four water treatment groups: the optimal water content (100%) and addition of water equivalent to 75%, 50%, and 25% of the optimal amount (Linnakoski et al., 2019; Terhonen et al., 2019b). The optimal amount of water was considered to be sufficient to maintain moist soil (not soaked), which was measured regularly with a soil moisture meter. Fungal isolates were plated on 2% Malt Extract Agar (MEA) and grown at 21°C for 2 weeks prior to the experimental inoculations. Three months after the planting and two months after the start of water availability treatments, the trees were inoculated (**Table 2**): 768 trees were infected with one species (= one tip per tree, I): *S. sapinea* (25 per water treatment group), *T. conorum-piceae* (25 per treatment group), *M. olivacea* (25 per treatment group), *Didymellaceae* sp. (25 per treatment group), *Sy. polyspora* (25 per treatment group), *D. acicola* (25 per treatment group), mock-inoculated controls with an agar plug (20 per treatment group), and 22 per water treatment group were left entirely untreated. A total of 240 trees were inoculated with four fungi, one on each tip (**Table 2**):

- treatment group II; mock-control, *S. sapinea*, *T. conorum-piceae*, *S. polyspora* (20 per treatment group);
- treatment group III; mock-control, *S. sapinea*, *M. olivacea*, *D. acicola* (20 per treatment group) and
- treatment group IV; mock-control, *Didymellaceae* sp., *T. conorum-piceae*, *Sy. polyspora* (20 per treatment group).

Inoculations were on a first-year shoot. A sterile Ø 3 mm cork-borer was used to punch through hyphae (fungi or control, 2% MEA) in order to get a round-shaped plug. One 1 cm tip of a side shoot per seedling or four tips of four side-shoots (combination-infections), were cut off with a scissor. The agar plug was placed onto the exposed surface, with the mycelium facing the cut, and sealed with Parafilm® (**Figure 3**).

The inoculation experiment ran for 66 days. Since seedling water intake varied with the ambient temperature, we continuously monitored the amounts of water applied, in order to maintain the essential level in the 100% watering treatment group, considered to be the optimal amount. The moisture for each treatment was measured with a soil moisture meter for the same seedlings throughout the experiment. The water amounts needed to be adjusted to the increasing temperatures during the growing season in 2019. At the beginning of the experiment, each seedling in the optimum (100%) water treatment group was given 60 ml of water three times per week, and each seedling in the drought stress water treatment group (25%) was given 15 ml of water three times per week. After 2 weeks, the watering regimes were modified to 120 ml for the 100% water treatment group, and 30 ml × 3 for the 25% water treatment groups. After 5 weeks, the water level was modified again to 180 ml × 3 and 45 ml × 3, respectively. The 75% and 50% water treatment groups received the corresponding amounts per seedling relative to the optimal. Water quantities were increased in July and maintained at that level until August.

Data Collection and Post-experiment Detection of Fungal Species

The lesion lengths (nearest 0.001 mm) were measured with a stereomicroscope (Stemi 508, Carl Zeiss Microscopy GmbH, Jena, Germany) with an attached camera (Axiocam ERc5s, Carl Zeiss Microscopy GmbH, Jena, Germany) using the freely available software Labscope (Carl Zeiss Microscopy GmbH, Jena, Germany). First, the bark was gently peeled to expose the necrosis in the phloem and then measured. The lesion length was measured only in the vertical direction. Dead twigs were removed from necrosis length analysis and analyzed separately. After measurements, five randomly chosen seedlings (in total 35 seedlings) were selected from each fungal or control treatment, to confirm the infection and to guarantee the fulfillment of Koch's postulates. Pieces from the interface of necrosis and healthy tissue were surface sterilized (as described above) and plated onto a 1.5% MYP plate. The fungi were first identified by morphology, followed by DNA extraction and ITS region sequencing to confirm identity (as described above). The sequences obtained were aligned with BLASTN (Zhang et al., 2000) to confirm that the isolate was the same as used in infections (**Table 3**).

Data Analysis

Data (water content and necrosis length) were analyzed using SPSS version 26.0 (IBM Corporation, New York, United States). A generalized linear model (GLM) was constructed to evaluate the fixed effects of inoculation method (control/fungal species) and combination (single or combined infection) under different water treatments (25%, 50%, 75%, and 100%) on necrosis length in tips. Initial fixed explanatory variables in the necrosis length model included inoculation method (categorical value), water treatment (categorical value), and combination (categorical value). Tray (categorical) was set as random factor in the model. The necrosis lengths in statistically different treatments were further assessed by Tukey HSD test for two-samples assuming equal variances. Differences were considered statistically significant if the p-value was below the threshold of 0.01. Similarly, the water content during different time points (each week) between water treatments was assessed by ONE-WAY-ANOVA and Tukey HSD test for two-samples.

The generalized linear model (glm) in R version 3.5.1 (R Core Team, 2019) was run for twig mortality as with the results of the water treatment / fungal inoculation. Further one-way-ANOVA (aov) was conducted and Tukey's HSD test was used to examine the differences between groups (in water/fungal treatment).

RESULTS

In vitro Study: Antagonism Assay

Four different kinds of interaction between the Scots pine endophytes and *S. sapinea* strains were observed (**Figure 1**

TABLE 2 | Total amount of seedlings and the number of the infections of Scots pine seedlings in different water treatments.

Treatment group (running No. of the treatment)	Method	Fungal species	Strain No.	25% water	50% water	75% water	100% water	SUM (total number of seedlings)
			NW-FVA	Low water (number of seedlings)		High water (number of seedlings)		
I (1)	Single infected	Mock-inoculated control	-	20	20	20	20	80
I (2)		*Sphaeropsis sapinea*	4740	25	25	25	25	100
I (3)		*Sydowia polyspora*	4742	25	25	25	25	100
I (4)		*Truncatella conorum-piceae*	4745	25	25	25	25	100
I (5)		*Microsphaeropsis olivacea*	4743	25	25	25	25	100
I (6)		*Desmazierella acicola*	4751	25	25	25	25	100
I (7)		*Didymellaceae* sp.	5756	25	25	25	25	100
I (8)		Untreated	-	22	22	22	22	88
II (1, 2, 3, 4)	Combination infected	Mock-control, *S. sapinea*, *S. polyspora*, *T. conorum-piceae*	x, 4740, 4745, 4742	20	20	20	20	80
III (1, 2, 5, 6)		Mock-control, *S. sapinea*, *M. olivacea*, *D. acicola*	x, 4740, 4743, 4751	20	20	20	20	80
IV (1, 3, 4, 7)		Mock-control, *S. polyspora, T. conorum-piceae, Didymellaceae sp.*	x, 4745, 4742, 5756	20	20	20	20	80
Total amount of seedlings								1008

and **Table 1**). About a quarter of the tested endophytes (26%, *Alternaria* alternata (Fr.) Keissl., *Diaporthe* sp. 2, *Nemania diffusa* (Sowerby) Gray, *Pezicula eucrita* (P. Karst.) P. Karst., *Preussia* sp., *Preussia funiculate* (Preuss) Fuckel, and *S. polyspora*, **Figure 1A**) inhibited the growth of *S. sapinea.* Twenty-two percent of all tested endophytes were superior in growth *v*ersus *S. sapinea* (**Figure 1B**, *Biscogniauxia mediterranea* (De Not.) Kuntze, *Jugulospora rotula* (Cooke) N. Lundq., *Daldinia* sp. *Pyronema domesticum* (Sowerby) Sacc., *Rosellinia* sp., and *Xylaria polymorpha* (Pers.) Grev.). A third of the tested strains (33%, *Biscogniauxia nummularia* (Bull.) Kuntz*, Botrytis cinerea* Pers.*, D. acicola, Diaporthe* sp. 1*, E. nigrum, Fusarium* sp., *Hypoxylon fragiforme* (Pers.) J. Kickx f., and *M. olivacea*) showed equal growth capability (**Figure 1C** and **Table 1**). Nineteen percent of endophytes tested against *S. sapinea* were inferior (= *S. sapinea* was superior; **Figure 1D**, *Mollisia* sp., *Nemania serpens* (Pers.) Gray, *T. conorum-piceae*, and *Therrya fuckelii* (Rehm) Kujala). All of the endophytes had statistical effect with respect at least to one of the *S. sapinea* strains after ten days (**Table 1**).

Sphaeropsis sapinea, strain 4740, had higher *p*-Values (presence of endophytes had stronger effect). If stricter rules for the *p*-value had been applied and only lower *p*-values accepted ($p < 0.01$), only two endophytes would have exhibited statistically significant inhibition (*Sydowia polyspora* and *Diaporthe* sp. 2). *Sy. polyspora* (**Figure 4A**), *M. olivacea* (**Figure 4B**), *T. conorum-piceae* (**Figure 4C**), and *D. acicola* (**Figure 4D**) were chosen for inoculation studies because of their frequent endophytic occurrence in *P. sylvestris*.

In planta Study: Greenhouse Inoculations

Pre-experiment Detection of *Sphaeropsis sapinea* and the Fungal Isolates

Eighteen different endophytic fungal species were isolated from stems and shoots of the six studied nursery pine trees (**Table 4**); these included *Alternaria* spp., *Diaporthe* spp., *E. nigrum, M. olivacea, Sy. polyspora,* and *T. conorum-piceae*. The most frequently isolated species was identified as *Didymellaceae* sp. (NW-FVA ID 5756) and it occurred in all tested trees and 30.9% of all analyzed shoot segments. *S. sapinea* was not isolated from asymptomatic woody tissues of those pines nor detected in any discolored or dead needles that were attached to the plants.

Soil Water Content

At week 3, the soil moisture in the 25% water content treatment was statistically lower than in the 50% ($p = 0.008$) and 100% ($p = 0.010$) treatments (**Figure 5**). After 4 weeks the soil moisture in the 100% treatment was statistically higher than in the 25%, 50%, and 75% treatments. Similarly, the soil moisture in the 25% treatment was lower than the soil moisture of the other

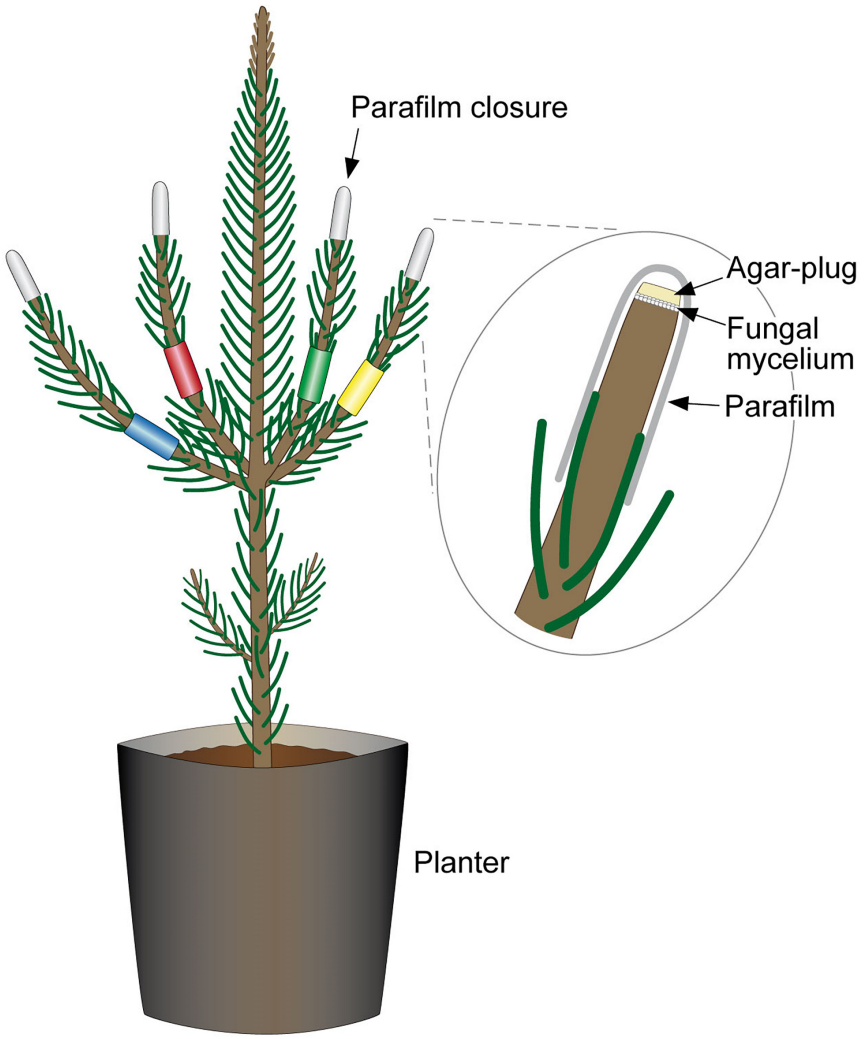

FIGURE 3 | Combined-infection of pine seedlings. Each of the side-shoots is color-labeled to indicate the different fungal strains with which pine was infected. The labeling allowed differentiation during necrosis measurements and re-isolations. Excised tips were replaced with a mycelium-covered agar plug and were sealed with Parafilm®.

treatment groups (all p-Values 0.00, except for 100% versus 50% $p = 0.003$). The soil moisture in the 50% and 75% treatments was, overall, the same throughout the study. In the middle of the experiment (week 5), the soil moisture in the 25% treatment was statistically lower than in the 100% ($p = 0.00$), 75% ($p = 0.003$) and 50% ($p = 0.035$) treatments. The same results were obtained for week 6. At week 7, the soil moisture in the 25% treatment was statistically lower than in the 100% $p = 0.00$ and 75% ($p = 0.001$) treatments and the soil moisture in the 75% treatment was statistically lower than in the 100% treatment ($p = 0.013$). Similarly, the soil moisture in the 50% treatment was lower than in the 100% treatment ($p = 0.035$). At week 8, the soil moisture in the 75% treatment was still statistically lower than in the 100% treatment ($p = 0.019$), and the soil moisture in the 25% treatment was lower than in all other groups: 100% $p = 0.000$, 75% $p = 0.04$, 50% $p = 0.028$. At week 9 the soil moisture in the 25% group was again lower than in the other groups (100% $p = 0.000$, 75% $p = 0.009$, 50% $p = 0.024$), the soil moisture in the 50% ($p = 0.017$) and 75% ($p = 0.011$) treatments was lower than in the 100% treatment. At the end of the study (week 10), the soil moisture in the 25% treatment was statistically lower ($p = 0.042$, 0.001, and 0.00) than the 50%, 75%, and 100% treatments.

Necrosis Length and Dead Twigs

The untreated control plants stayed healthy during the experiment and no dead twigs were observed. In the mock-inoculated control 7.1% of the twigs died. The inoculation with *S. sapinea* led to the highest shoot mortality of inoculated Scots pine twigs in the greenhouse study (**Figure 6**; **Table 3**). Over all treatment groups these necroses caused complete die-off of 18% of all inoculated twigs ($n = 260$) compared to 1.2-8.3% for individual inoculated endophyte and 7.1% for twigs inoculated with the mock community. *S. sapinea* killed 31.9% of inoculated

TABLE 3 | Greenhouse-experiment: Mean necrosis length in mm, percentage of dead twigs, and results of re-isolation.

No.	Treatment method*	Water treatment	I				II				III				IV				All treatments				Percentage of dead twigs in the treated twigs	Re-isolation of inoculated strains	Re-isolation of non-inoculated *S. sapinea*
			25%	50%	75%	100%	25%	50%	75%	100%	25%	50%	75%	100%	25%	50%	75%	100%	25%	50%	75%	100%			
1	Mock-inoculated control		2.0	1.1	1.8	0.6	0.9	0.8	0.9	0.5	1.4	0.9	0.9	0.9	1.1	0.8	0.8	0.7	1.3	0.9	0.9	0.7	7.1	No	No
2	*Sphaeropsis sapinea*		7.6	6.0	8.8	5.1	5.8	6.8	7.4	6.0	4.3	4.7	9.3	6.2	0	0	0	0	5.8	6.0	8.3	5.7	18.1	Yes	NA
3	*Sydowia polyspora*		1.2	1.1	2.0	1.3	0.7	1.1	0.7	0.6	0	0	0	0	1.4	1.5	1.4	0.7	1.0	1.1	1.1	0.8	4.2	Yes	No
4	*Truncatella conorum-piceae*		2.3	1.2	1.7	0.9	0.8	0.7	1.1	0.9	0	0	0	0	1.0	0.6	2.3	0.4	0.9	0.7	1.5	0.6	7.3	Yes	No
5	*Microsphaeropsis olivacea*		2.4	1.6	1.7	1.8	00	0	0	0	2.0	1.5	2.1	1.2	0	0	0	0	1.8	1.4	1.8	1.4	8.3	Yes	No
6	*Desmazierella acicola*		1.3	1.9	1.5	0.9	0	0	0	0	1.6	1.4	2.1	1.2	1.5	2	1.8	1.8	1.4	1.5	1.5	1.2	7.8	Yes	No
7	*Didymellaceae* sp.		2.2	1.6	2.3	2.0	0	0	0	0	0	0	0	0	0	0	0	0	1.7	1.7	1.8	1.9	2.2	Yes	No

**I = single infection of fungi/control; II = combination of No. 1, 2, 3, 4; III = combination of No. 1, 2, 5, 6; IV = combination of No. 1, 3, 4, 7.*

twigs in the 25% water treatment, 27.7% in both the 50% and the 75% water treatments and only 13% in the 100% water treatment (**Supplementary Table 1**). After *M. olivacea* inoculation, 8.3% of the twigs were dead, followed by *D. acicola* (7.8%), *T. conorum-piceae* (7.3%), mock-inoculated control (7.1%), *Sy. polyspora* (4.2%), and *Didymellaceae sp.* (2.2%).

The necrosis length model for endophytes and pathogen (GLM) showed that necrosis size (length) was statistically affected by treatment (fungal species) and water availability but not by the combination used (single infection or several in one plant) (**Table 5**). Statistical differences are listed only in **Table 6** and omitted from **Figure 7**. Statistical differences were found between *S. sapinea* (**Figure 7** and **Table 6**) and all other inoculation treatments in all water treatments. Similarly, necrosis caused by *Didymellaceae* sp. was statistically higher than the mock-control and *T. conorum-piceae* in the 100% water treatment. Necrosis length was statistically higher (mock-control) in the 25% water treatment than in the 100% treatment (**Figure 7** and **Table 6**). The necrosis was greatest statistically in the 75% water treatment compared to the 100% (for *S. sapinea* and *T. conorum-piceae*) (**Figure 7** and **Table 6**). Similarly, for *S. sapinea* inoculation, the necrosis was statistically higher in the 75% compared to the 25% water treatment (**Figure 7** and **Table 6**).

The generalized linear model showed that the number of dead twigs was affected by fungal inoculation due to *S. sapinea* (p = 0.0079, **Supplementary Figure 1A**). The water treatment also affected twig mortality (p = 0.05). The Tukey HSD test showed that the mortality of the twigs was statistically higher in the 25% (p = 0.03) and 50% (p = 0.03) water treatments compared to the 100% water treatment (**Supplementary Figure 1B**).

The water treatment (drought) affected the mortality of the twigs in the *S. sapinea* treatment (**Supplementary Figure 2**). The number of dead twigs was higher in 25% compared to the 100% water treatment (p = 0.04, **Supplementary Figure 2**). Drought, caused by the reduced water treatment, was not found to have any impact on the number of dead twigs in other fungal/control treatments.

Re-isolations of Inoculated Fungi

Sphaeropsis sapinea did not grow out from the surface sterilized samples of the mock-controls. From all inoculated samples, the respective fungus was isolated 66 days after inoculation and identified as the original inoculated species (**Table 3**).

DISCUSSION

The forest pathosystems' behavior can be unpredictable in the future due to changes in the environment that favor fungal pathogens rather than the hosts' vitality. Similarly, this might have unknown effects on host trees core fungal endophytes. We found that abiotic stress, here defined as drought, increased the aggressiveness of *S. sapinea* (no. of dead twigs, necrosis length) but not the other tested endophytes. In case of *S. sapinea*, the negative impact can be expected to increase. Similarly, we observed different modes of competition between other endophytes against *S. sapinea*. Overall these results indicate that

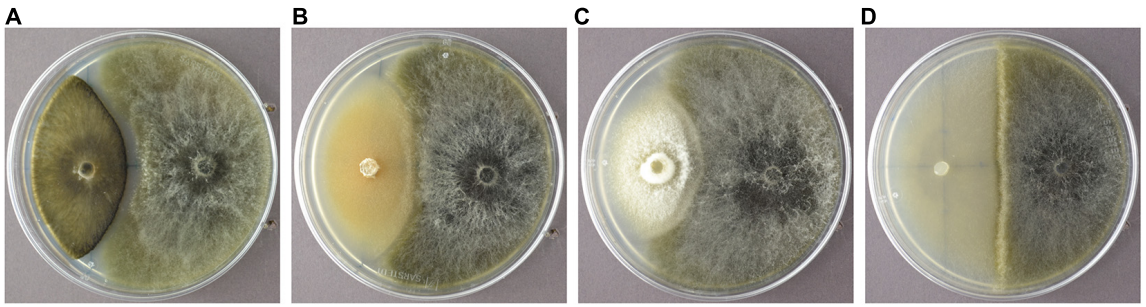

FIGURE 4 | *Sydowia polyspora* **(A)**, *Microsphaeropsis olivacea* **(B)**, *Truncatella conorum-piceae* **(C)**, and *Desmazierella acicola* **(D)** were the endophytes chosen for the infection experiment.

TABLE 4 | Frequency as percent of twig-inhabiting fungal endophytes isolated from two-year-old *Pinus sylvestris*.

Pine plant	**1**	**2**	**3**	**4**	**5**	**6**	**Total**
Stem including shoots of the growth years	2018-2019	2018-2019	2018-2019	2018-2019	2018-2019	2018-2019	
Incubated tissue segments	122	87	88	54	50	56	457
no outgrowth	23	10.3	44.3	7.4	0	3.6	17.9
outgrowth of yeasts	2.5	0	3.4	3.7	6	7.1	3.3
Alternaria alternata	20.5	2.3	5.7	11.1	24	23.2	13.8
Alternaria spp.	11.5	0	0	7.4	0	0	3.9
Didymellaceae sp.	26.2	24.1	15.9	22.2	68	50	30.9
Ascomycete sp. 2	4.9	34.5	12.5	18.5	10	0	13.6
Ascomycete sp. 3	1.6	0	0	35.2	2	16.1	6.8
Ascomycete sp. 4	19.7	28.7	2.3	0	0	0	11.2
Ascomycete sp. 5	0	3.5	6.8	0	0	0	2
Diaporthe sp. 1	10.7	4.6	13.6	14.8	12	12.5	10.9
Diaporthe sp. 2	0	0	8	0	0	0	1.5
Diaporthe sp. 3	0	0	0	7.4	0	1.8	1.1
Epicoccum nigrum	13.9	20.7	18.2	7.4	26	35.7	19.3
Fusarium sp.	0	0	0	11.1	0	1.8	1.5
Microsphaeropsis olivacea	0	0	0	0	0	10.7	1.3
Paraphaeosphaeria sp.	0	1.2	0	0	0	0	0.2
Sordaria fimicola	0	0	0	0	2	0	0.2
Sydowia polyspora	0	3.5	2.3	0	0	0	1.1
Trichoderma spp.	0	0	0	0	2	0	0.2
Truncatella conorum-piceae	0	2.3	0	0	0	0	0.4
Fungus spp.	1.6	2.3	0	0	0	0	0.9
Total No. of identified filamentous species	8	10	9	9	8	8	18

other endophytes in Scots pine tissues (especially in twigs) can play a role in the disease development of "Diplodia Tip Blight." Hypothetically, favoring certain tree microbiome in tree health would produce effective, durable, and environmentally friendly control method against severe disease outbreaks.

Antagonism Studies

Scots pine endophytes and *S. sapinea* interacted with each other in various ways as demonstrated by the *in vitro* antagonism assays. Four interaction categories were found: about half of the tested strains were able to either inhibit *S. sapinea in vitro* or were superior in their growth towards *S. sapinea*. Similar results were presented by Bußkamp (2018). In our study, thirteen species could be considered potential antagonists against *S. sapinea in vitro,* because they had either a faster growth than *S. sapinea* or inhibited the pathogen's development. This partly corresponds with the results of Bußkamp (2018), who found 22% of the tested 89 endophytic strains inhibited the growth of *S. sapinea*. A contactless inhibition of *S. sapinea* was observed for 26% of the endophytes in our study (e.g., *A. alternata* and *Pe. eucrita*). Chemical antagonism can be assumed when a fungus reacts to the presence of an opponent fungus with an inhibition zone between the two fungal colonies. One fungus might excrete secondary metabolites that inhibit the opponent fungus (Schulz et al., 2002).

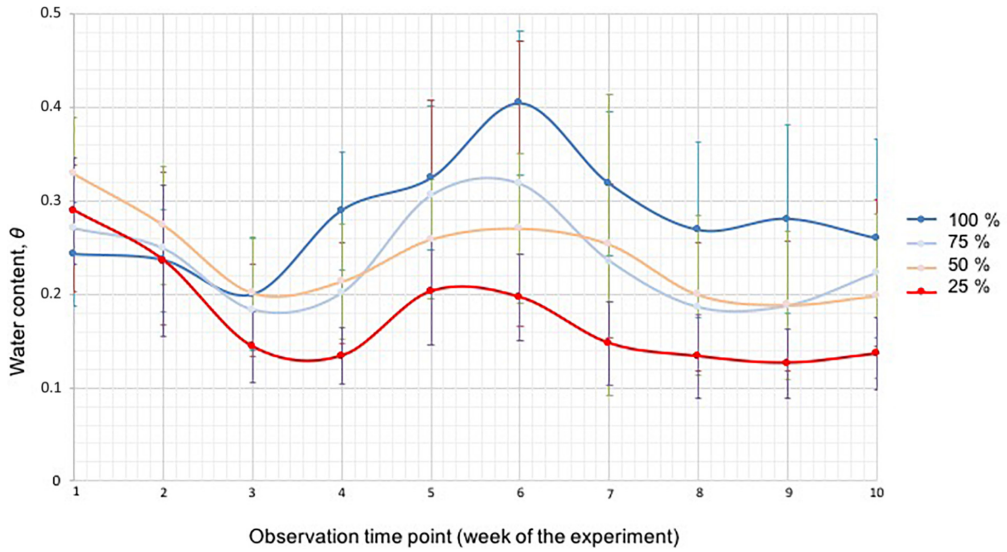

FIGURE 5 | The soil moisture of the four different water treatment groups (100% blue, 75% light blue, 50% green, and 25% red) measured with a soil moisture meter, shown as water content ϴ for each week during the duration of the experiment. The bars represent standard deviation.

Secondary metabolites should be extracted and tested to see whether the same reaction towards the pathogen can be observed, in order to determine whether a certain metabolite can inhibit growth (Tellenbach et al., 2013). *S. sapinea*, could not penetrate the barrier surrounding one of those endophytes.

Several of the tested endophytes in this study over-grew the *S. sapinea* mycelium. This ability might indicate a stronger capacity to metabolize nutrients. The faster growth and better ability to utilize nutrients are two strategies with clear advantages during competition (Mgbeahuruike et al., 2011). The fungi *Sy. polyspora*, *Xylaria* sp. and *Diaporthe* sp. are typical endophytes in Scots pine (Bußkamp et al., 2020). If their growth or infection in the host tissues could be promoted, in theory they could provide strong competition against pathogens in nature (Terhonen et al., 2019a). A co-occurrence analysis of shoot-inhabiting endophytes in mature pines by Oliva et al. (2021) identified a cluster of species that was negatively correlated with *S. sapinea* and could be potential antagonists. The most negatively correlated was an *Alternaria* species, accompanied by *E. nigrum* and *Sy. polyspora*. Similarly, we show that *Sy. polyspora* had antagonistic capability against *S. sapinea*. Oliva et al. (2021) provided some evidence that the competition between *S. sapinea* and other endophytes for stress-related metabolites could prevent the growth of *S. sapinea* and development of Diplodia tip blight symptoms. Our results support this conclusion as the tested endophytes (e.g., *Sy. polyspora*) sharing the same niche (in this case MYP plates) with *S. sapinea* could inhibit the fungus' growth *in vitro*. The co-infection of the studied Scots pines with different endophytes together with *S. sapinea* on different twigs did not cause a visible increase in the host plant's immune system *in planta*. In our study, we did not aim at directly inhibiting *S. sapinea* growth but rather testing for an influence (lower necrosis caused by *S. sapinea*) on the host plant as a consequence of the combined infections (e.g., induced systemic resistance due to the presence of an endophyte).

Several studies indicate that fungal endophytes may increase their host plant's immune system *in vivo* (e.g., Witzell and Martín, 2018). Ganley et al. (2008) demonstrated that *Pinus monticola* Douglas gained resistance against *Cronartium ribicola* J.C. Fisch. as a result of prior infection with certain endophytes. Mejía et al. (2008) were able to enhance *Theobroma cacao* L. plants' defense against herbivore and pathogen attacks, by inoculating the leaves with the endophyte *Colletotrichum tropicale* E.I. Rojas, S.A. Rehner & Samuels. The host plant's defense was enhanced due to a priming effect caused by the endophytes, increasing the expression of suites of host genes involved in in plant defense pathways or e.g., cell wall development (Mejía et al., 2008). Similar results were found by Raghavendra and Newcombe (2013); Martínez-Arias et al. (2019) with endophytic fungi on *Populus* species. Enhancement of resistance to Dutch elm disease by elm endophytes has been recently described by Martínez-Arias et al. (2021). The combination infections did not impact the necrosis length, indicating no activation of systematic resistance. The inoculation method in our study was very aggressive (mycelium) and perhaps, infecting *S. sapinea* later than the endophytes in the host would have produced different results. Similarly, mimicking more natural infection methods through conidia infections would give more legitimate results.

The remaining tested strains in the antagonism assays showed either neutral (33% of strains with equal growth capability) interaction or were inferior to *S. sapinea*. Therefore, they do not appear to be suitable potential antagonists against *S. sapinea*. Pairing with equal growth capability may indicate that the endophytes' and *S. sapinea*s' growth was not disturbed by each other, meaning no antagonism took place. In the host,

TABLE 5 | The General Linear Model values.

Variable	Fixed Effects	Std. Error	*F*	Sig.
Necrosis length	Water treatment	0.141	7.692	0.000
	Inoculation method	0.188	245.600	0.000
	Combination	0.152	0.460	0.710
	Random Effects			
Necrosis length	Tray	0.045		0.108

this might mean the fungi can grow together and neither specifically reacts to the presence of the other. *S. sapinea* has a comparatively high growth rate (Bußkamp, 2018) and therefore, it can be assumed that it has a fast metabolism to use the available nutrients. Is not surprising that *S. sapinea* was found to be superior and occupied a larger area of the plate more rapidly than several more slow growing endophytic test partners, such as *T. conorum-piceae*, *N. serpens*, *Mollisia* sp. and two *Th. fuckelii* strains. When the Scots pine host is weakened due to drought stress for example, the common endophytes inside the tree could be disadvantaged while *S. sapinea* can become more established as secondary pathogen and occupy more tissues faster in the host, thus outcompeting these inferior endophytes. This could be one reason why *S. sapinea* is present in higher numbers in diseased sites (Bußkamp et al., 2020).

Pre-colonization of the Trees With Fungal Community

The pre-examination of the nursery Scots pines indicated a relatively small fungal community. No *S. sapinea* could be detected from the tested seedlings prior to the experiments, whereas the other fungal strains used for the greenhouse-infections were found to be present. We concluded that these species belong to the naturally observed Scots pine endophyte community (Blumenstein et al., 2020; Bußkamp et al., 2020). This corresponds to results of Bihon et al. (2011) who found that *S. sapinea* was not an endophyte of healthy seedlings collected from greenhouses and nurseries. The composition of endophytes isolated from two-year-old Scots pine plants in this study was dominated by *A. alternata* and *E. nigrum*, and was typical of young pines from tree nurseries (own unpublished data). In contrast to intensive studies on the fungal endophytic community of Scots pine shoots of mature trees (Blumenstein et al., 2020; Bußkamp et al., 2020; Oliva et al., 2021), the endophyte α-diversity of the tested two-year old Scots pines was lower. In total, only 18 filamentous, ascomycetous endophytes (8 – 10 species per seedling) were isolated in this study, whereas 103 different species (5 – 22 isolated per tree) were found in mature pine shoots in a study by Bußkamp et al. (2020). Foliar fungal endophyte assemblages have been shown to vary between the developmental stage of the host (mature vs. seedling (Helander et al., 2011; Koukol et al., 2012; Skaltsas et al., 2019). The core foliar endophytes seem to be the same in seedlings and mature Scots pine (Blumenstein et al., 2020; Bußkamp et al., 2020) but community compositions and species differences are probably related to the age of the host (Taudière et al., 2018).

The genesis of the Scots pine endophytic community is poorly known. There are hints that composition of the endophytic community is mainly determined by the host species and organ type (Peršoh, 2013), health condition, composition of the forest trees, and vegetation which is growing in the surroundings of the host tree (Peršoh et al., 2010; Nguyen et al., 2016; Bußkamp, 2018). The latter factor may explain why plants could be species-poorer in a nursery field than in a mixed forest. Horizontal transmission from mature trees in forest stands is probably the main source for young trees to obtain endophyte inocula, as shown for *Pinus patula* Schltdl. & Cham. And *S. sapinea* (Bihon et al., 2011). Additionally, the composition of endophytes depends on the age of the tissue (Fröhlich et al., 2000; Arnold and Herre, 2003; Terhonen et al., 2011,

TABLE 6 | Statistical differences of necrosis length between different groups ($p < 0.01$).

		Water treatment			
Group 1	**Group 2**	**100%**	**75%**	**50%**	**25%**
Mock-inoculated control	*Sphaeropsis sapinea*	0.000	0.00	0.00	0.00
Mock-inoculated control	*Didymellaceae* sp.	0.001	NA	NA	NA
Sphaeropsis sapinea	*Sydowia polyspora*	0.000	0.000	0.000	0.000
Sphaeropsis sapinea	*Truncatella conorum-piceae*	0.000	0.000	0.000	0.000
Sphaeropsis sapinea	*Microsphaeropsis olivacea*	0.000	0.000	0.000	0.000
Sphaeropsis sapinea	*Desmazierella acicola*	0.000	0.000	0.000	0.000
Sphaeropsis sapinea	*Didymellaceae* sp.	0.000	0.000	0.000	0.000
Truncatella conorum-piceae	*Didymellaceae* sp.	0.001	NA	NA	NA
		Inoculation treatment			
Group 1	**Group 2**	**Mock-inoculated control**	***Sphaeropsis sapinea***	***Truncatella conorum-piceae***	
100%	25%	0.001	NA	NA	
100%	75%	NA	0.003	0.002	
75%	25%	NA	0.007	NA	

FIGURE 6 | Pine shoot with combined infections at the end of the experiment. The red labeled side-shoot was infected with *S. sapinea* and shows full necrosis.

2019a; Bußkamp, 2018), which determines whether an endophyte community can accumulate over years or if it represents only annual accumulation, such as in leaves. Peršoh (2013) found that one- and three-year-old pine stem sections had different assemblies of endophytic fungi, supporting the theory that forest trees mainly accumulate their endophytic community as the infection rate tends to increase with age (Guo et al., 2008; Deckert and Peterson, 2011).

Interaction of Endophytes With *S. sapinea* Infection

Necrosis of the Scots pine was marginal when infected with *D. acicola, Didymellaceae* sp., *M. olivacea, Sy. polyspora*, and *T. conorum-piceae*. These fungi (excluding *S. sapinea*) were most likely already endophytically present in the Scots pine plants before inoculation (based on pre-examination). The fact that *D. acicola* (anamorph *Verticicladium trifidum* Preuss) did not cause higher necrosis compared to the control is not surprising, as it is a typical twig endophyte on *Pinus* spp. in Europe (Petrini and Fisher, 1988; Kowalski and Kehr, 1992; Kowalski and Zych, 2002; Bußkamp, 2018) and lives endophytically in pine needles (Kendrick, 1962). This saprotrophic species also colonizes needles after fall (Ponge, 1991) and ascocarps can be found on dead blackened leaves. No pathogenic behavior has ever been described and it is one of the most common fungi growing in pine leaf litter all over the world (Martinoviæ et al., 2016). The tested *Didymellaceae* sp. was not identified to the species level based on the ITS analysis. The *Didymellaceae* is a species rich, cosmopolitan family, assigned to the Pleosporales and includes genera such as *Didymella, Leptosphaerulina, Macroventuria, Monascostroma, Platychora* and moreover some species of *Phoma* and *Ascochyta* (Zhang et al., 2009). Most species of the *Didymellaceae* are associated with dicotyledon plants and mostly hemibiotrophic and saprobic (Zhang et al., 2009) or pathogens, causing leaf and stem lesions (Chen et al., 2017). *M. olivacea* (basionym: *Coniothyrium olivaceum* Bonord.) has been described from *Pinus* plants in very few publications (Petrini and Fisher, 1988; Kowalski and Kehr, 1992; Bußkamp et al., 2020). Petrini and Fisher (1988) described *M. olivacea* as a typical endophytic colonizer of conifers. Bußkamp et al. (2020) were able to confirm this observation as it was the third most common fungus isolated from pine twigs and they found it in nearly all studied stands in Germany. In contrast, Kowalski and Kehr (1992), isolated the fungus endophytically only from very few pine branches. *M. olivacea* is known to be plurivorous and was found on twigs and branches of other tree species (e.g., Hormazabal et al., 2005), causing brown spine rot of Camelthorn (*Alhagi maurorum* Medik.) (Razaghi and Zafari, 2016).

Sydowia polyspora and *T. conorum-piceae*, which can be conifer pathogens (Sutton and Waterston, 1970; Heydeck, 1991; Talgø et al., 2010; Pan et al., 2018), did not cause strong necrosis on the twigs. The reason may be that they are specialized true endophytes of Scots pine (Bußkamp et al., 2020) and the host-fungi continuum is balanced. *Sy. polyspora* is widely distributed all over the world (Muñoz-Adalia et al., 2017; Pan et al., 2018). As an endophyte it has a high consistency and frequency in Scots pine twigs (Sanz-Ros et al., 2015; Blumenstein et al., 2020; Bußkamp et al., 2020). Predominately, *Sy. polyspora* lives saprophytically on dead plant material but also occurs as a secondary pathogen on previously damaged needles and twigs (Heydeck, 1991), as wound pathogen and blue stain-fungus (Sutton and Waterston, 1970), or as causal agent of current season needle necrosis (CSNN) on true fir (*Abies* spp.) (Talgø et al., 2010). Ascomata and pycnidia appear on dead pine branches and needles (Gremmen, 1977). Cleary et al. (2019) suggest that this fungus could benefit from climate change as additional stresses are added to the host so that *Sy. polyspora* can become a more commonly opportunistic pathogen. Here we show that the necrosis caused by *Sy. polyspora* in Scots pine is not affected by drought. In a study by Bußkamp (2018), *Sy. polyspora* did not show antagonistic behavior in dual culture

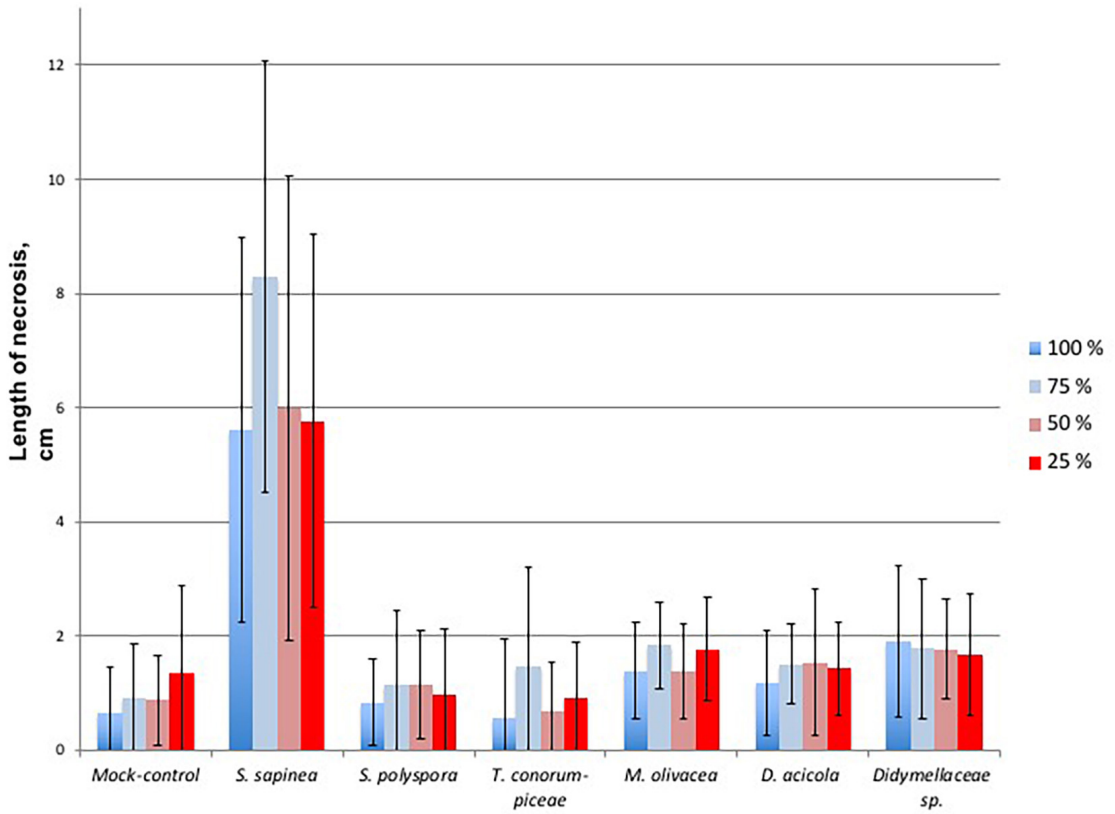

FIGURE 7 | Necrosis length of the single infected shoots per fungal isolate, each in relation to the water treatment groups, where blue is 100% water treatment, light blue 75%, light red 50%, and red 25%. The bars represent standard deviation.

with *S. sapinea* so the observed antagonism in this study might be strain related. *T. conorum-piceae* (≡ *Pestalotia conorum-piceae* Tubeuf) is also a frequently occurring twig endophyte of Scots spine with high consistency in Germany (Bußkamp et al., 2020). Mainly, it is a decomposer of pre-damaged needles of pine and is saprotrophic. However, *T. conorum-piceae* is also known as a secondary pathogen of pine and spruce needles and cones (Landeskompetenzzentrum Forst Eberswalde (LFE) 2015). The fungus is hardly described in the literature, but due to the fact that it is very abundant (Blumenstein et al., 2020; Bußkamp et al., 2020), it is important to gain more knowledge about this species in future studies. Other allied *Amphisphaeriaceae* such as *Pestalotiopsis* species can be primary causal agents of spots, blights and diebacks of various host plants. For example, the very common *Pestalotiopsis funerea* (Desm.) Steyaert, with a worldwide distribution, causes damping off, root and collar rots of seedlings, needle blight, tip-blight, twig dieback, and stem canker of conifers, especially Cupressaceae (Sinclair and Lyon, 2005).

The twig mortality was highest in the 25% water group and different statistically from the 100% treatment. This aspect is important with regard to the disease development in mature trees, as the twig mortality and thus the tree health, increases due to drought. Other studies have shown that water availability can affect the growth of pathogens in conifer trees during water stress. *Heterobasidion* species were able to increase necrosis under water stress (Terhonen et al., 2019b). Similarly, the blue stain fungus *Endoconidiophora polonica* (Siemaszko) Z.W. de Beer, T.A. Duong & M.J. Wingf. caused greater necrosis and mortality in *Pi. abies* seedlings with low water availability compared to those with high water availability (Linnakoski et al., 2017). Even a 25% decrease in water was able to trigger the activity of *S. sapinea*. The necrosis caused by *S. sapinea* was statistically higher in all water treatments compared to other fungi, indicating that host stress can particularly benefit this opportunistic pathogen.

Overall, the findings of our greenhouse-study demonstrate how severe the infection of *S. sapinea* is in drought stressed Scots pines, evidenced by high twig mortality and necrosis. The other fungi with the potential to become pathogens (as described above) did not benefit from host stress. In conclusion, pine endophytes showing antagonism against *S. sapinea* and with no detrimental effect to the host could be applied as inoculants to facilitate host protection. We will plan new research to find innovative and effective ways of utilizing the beneficial tree mycobiome in the context of future challenges. *Sphaeropsis sapinea* is a high-risk Scots pine pathogen because the disease severity (mortality of twigs, necrosis length) is increasing under

drought stress. Climate change, leading to more severe and prolonged drought, will therefore lead to more outbreaks of the disease "Diplodia Tip Blight" in the future.

DATA AVAILABILITY STATEMENT

The raw data supporting the conclusions of this article will be made available by the authors, without undue reservation.

AUTHOR CONTRIBUTIONS

KB planned and performed the greenhouse experiment. JB and GL performed the isolation of the endophytes and the dual-culture study. RS and NPR contributed to the greenhouse experiment, the measurements of the necrosis, and the re-isolation of the fungi. ET contributed to the study design and analyzed the data. KB wrote the first draft. KB, JB, GL, and ET contributed to the final version of the manuscript. All authors contributed to the article and approved the submitted version.

FUNDING

The study was funded by the Faculty of Forest Sciences and Forest Ecology of the University of Göttingen and the Northwest German Forest Research Institute, Göttingen, Germany. We acknowledge support by the Open Access Publication Funds of the Göttingen University.

ACKNOWLEDGMENTS

We thank Annette Ihlemann from the NW-FVA for her contribution to the study during the antagonism assay and Etta Paar for helping with the illustrations. We also thank David Răscuțoi from the Forest Pathology group of University of Göttingen for taking care of the trees and helping with the infections.

SUPPLEMENTARY MATERIAL

The Supplementary Material for this article can be found online at: https://www.frontiersin.org/articles/10.3389/ffgc.2021.655769/full#supplementary-material

Supplementary Figure 1 | Boxplot representing the mortality of the twigs due to fungal **(A)** and water **(B)** treatment.

Supplementary Figure 2 | Boxplot presenting number of dead twigs after *Sphaeropsis sapinea* treatment in different water treatments.

Supplementary Table 1 | Number of dead twigs in the end of the greenhouse-experiment.

REFERENCES

Arnold, A. E., and Herre, E. A. (2003). Canopy cover and leaf age affect colonization by tropical fungal endophytes: ecological pattern and process in *Theobroma cacao* (Malvaceae). *Mycologia* 95, 388–398. doi: 10.1080/15572536.2004.11833083

Arnold, A. E., and Lutzoni, F. (2007). Diversity and host range of foliar fungal endophytes: are tropical leaves biodiversity hotspots? *Ecology* 88, 541–549.

Arnold, A. E., Mejía, L. C., Kyllo, D., Rojas, E. I., Maynard, Z., Robbins, N., et al. (2003). Fungal endophytes limit pathogen damage in a tropical tree. *Proc Natl Acad Sci U.S.A.* 100:15649. doi: 10.1073/pnas.2533483100

Bengtsson-Palme, J., Ryberg, M., Hartmann, M., Branco, S., Wang, Z., Godhe, A., et al. (2013). Improved software detection and extraction of ITS1 and ITS2 from ribosomal ITS sequences of fungi and other eukaryotes for analysis of environmental sequencing data. *Methods Ecol. Evol.* 4, 914–919. doi: 10.1111/2041-210X.12073

Bihon, W., Slippers, B., Burgess, T., Wingfield, M. J., and Wingfield, B. D. (2011). Diverse sources of infection and cryptic recombination revealed in South African *Diplodia pinea* populations. *Fungal Biol.* 116, 112–120. doi: 10.1016/j.funbio.2011.10.006

Blodgett, J. T., Kruger, E. L., and Stanosz, G. R. (1997a). Effects of moderate water stress on disease development by *Sphaeropsis sapinea* on Red Pine. *Phytopathology* 87, 422–428. doi: 10.1094/PHYTO.1997.87.4.422

Blodgett, J. T., Kruger, E. L., and Stanosz, G. R. (1997b). Sphaeropsis sapinea and water stress in a Red Pine plantation in Central Wisconsin. *Phytopathology* 87, 429–434. doi: 10.1094/PHYTO.1997.87.4.429

Blumenstein, K. (2015). *Endophytic Fungi in Elms: Implications for the Integrated Management of Dutch elm Disease*. Alnarp: Swedish University of Agricultural Sciences.

Blumenstein, K., Bußkamp, J., Langer, G. J., Langer, E. J., and Terhonen, E. (2020). The opportunistic pathogen *Sphaeropsis Sapinea* is found to be one of the most abundant fungi in symptomless and diseased Scots Pine in Central-Europe. *BMC Plant Biol.* doi: 10.21203/rs.3.rs-48366/v1

Brodde, L., Adamson, K., Julio Camarero, J., Castaño, C., Drenkhan, R., Lehtijärvi, A., et al. (2019). Diplodia tip blight on its way to the North: drivers of disease emergence in Northern Europe. *Front. Plant Sci.* 9:1818. doi: 10.3389/fpls.2018.01818

Burgess, T. I., Wingfield, M. J., and Wingfield, B. D. (2004). Global distribution of Diplodia pinea genotypes revealed using simple sequence repeat (SSR) markers. *Aust. Plant Pathol.* 33, 513–519. doi: 10.1071/AP04067

Butin, V. H., and Kowalski, T. (1990). Die natürliche astreinigung und ihre biologischen Voraussetzungen. *Eur. J. Forest Pathol.* 20, 44–54. doi: 10.1111/j.1439-0329.1990.tb01272.x

Bußkamp, J. (2018). *Schadenserhebung, Kartierung und Charakterisierung des "Diplodia-Triebsterbens" der Kiefer, insbesondere des endophytischen Vorkommens in den klimasensiblen Räumen und Identifikation von den in Kiefer (Pinus sylvestris) vorkommenden Endophyten*. Kassel: Universität Kassel.

Bußkamp, J., Langer, G. J., and Langer, E. J. (2020). Sphaeropsis sapinea and fungal endophyte diversity in twigs of Scots pine (*Pinus sylvestris*) in Germany. *Mycol. Progress* 19, 985–999. doi: 10.1007/s11557-020-01617-0

CABI (2019). *Sphaeropsis Sapinea (Sphaeropsis Blight) [WWW Document]*. Invasive Species Compendium. Available online at: https://www.cabi.org/isc/datasheet/19160 (accessed November 13, 2019).

Chapela, I. H., and Boddy, L. (1988). Fungal colonization of attached beech branches. *New Phytol.* 110, 47–57. doi: 10.1111/j.1469-8137.1988.tb00236.x

Chen, Q., Hou, L. W., Duan, W. J., Crous, P. W., and Cai, L. (2017). Didymellaceae revisited. *Stud. Mycol.* 87, 105–159. doi: 10.1016/j.simyco.2017.06.002

Cleary, M., Oskay, F., Doğmuş, H. T., Lehtijärvi, A., Woodward, S., and Vettraino, A. M. (2019). Cryptic risks to forest biosecurity associated with the global movement of commercial seed. *Forests* 10:459. doi: 10.3390/f10050459

Compant, S., Saikkonen, K., Mitter, B., Campisano, A., and Mercado-Blanco, J. (2016). Editorial special issue: soil, plants and endophytes. *Plant Soil* 405, 1–11. doi: 10.1007/s11104-016-2927-9

de Wet, J., Burgess, T., Slippers, B., Preisig, O., Wingfield, B. D., and Wingfield, M. J. (2003). Multiple gene genealogies and microsatellite markers reflect relationships between morphotypes of Sphaeropsis sapinea and distinguish

a new species of Diplodia. *Mycol. Res.* 107, 557–566. doi: 10.1017/s0953756203007706

Deckert, R. J., and Peterson, R. L. (2011). Distribution of foliar fungal endophytes of *Pinus strobus* between and within host trees. *Can. J. Forest Res.* 30, 1436–1442. doi: 10.1139/x00-078

Desprez-Loustau, M.-L., Marçais, B., Nageleisen, L.-M., Piou, D., and Vannini, A. (2006). Interactive effects of drought and pathogens in forest trees. *Ann. For. Sci.* 63, 597–612. doi: 10.1051/forest:2006040

Fabre, B., Piou, D., Desprez-Loustau, M.-L., and Marçais, B. (2011). Can the emergence of pine Diplodia shoot blight in France be explained by changes in pathogen pressure linked to climate change? *Glob. Change Biol.* 17, 3218–3227.

Feci, E., Battisti, A., Capretti, P., and Tegli, S. (2002). An association between the fungus *Sphaeropsis sapinea* and the cone bug *Gastrodes grossipes* in cones of *Pinus nigra* in Italy. *Forest Pathol.* 32, 241–247. doi: 10.1046/j.1439-0329.2002.00286.x

Flowers, J., Hartman, J. R., and Vaillancourt, L. J. (2006). Histology of *Diplodia pinea* in diseased and latently infected *Pinus nigra* shoots. *Forest Pathol.* 36, 447–459.

Fröhlich, J., Hyde, K. D., and Petrini, O. (2000). Endophytic fungi associated with palms. *Mycol. Res.* 104, 1202–1212.

Ganley, R. J., Sniezko, R. A., and Newcombe, G. (2008). Endophyte-mediated resistance against white pine blister rust in Pinus monticola. *Forest Ecol. Manag.* 255, 2751–2760. doi: 10.1016/j.foreco.2008.01.052

Gardes, M., and Bruns, T. D. (1993). ITS primers with enhanced specificity for basidiomycetes – application to the identification of mycorrhizae and rusts. *Mol. Ecol.* 2, 113–118. doi: 10.1111/j.1365-294X.1993.tb00005.x

Gremmen, J. (1977). Fungi colonizing living and dead tissue of Pinus sylvestris and P. nigra. *Kew Bull.* 31, 455–460. doi: 10.2307/4119386

Griffith, G. S., and Boddy, L. (1988). Fungal communities in attached ash (*Fraxinus excelsior*) twigs. *Trans. Br. Mycol. Soc.* 91, 599–606. doi: 10.1016/S0007-1536(88)80033-0

Guo, L.-D., Huang, G.-R., and Wang, Y. (2008). Seasonal and tissue age influences on endophytic fungi of *Pinus tabulaeformis* (Pinaceae) in the Dongling Mountains. Beijing. *J. Integr. Plant Biol.* 50, 997–1003. doi: 10.1111/j.1744-7909.2008.00394.x

Helander, M., Wäli, P., Kuuluvainen, T., and Saikkonen, K. (2011). Birch leaf endophytes in managed and natural boreal forests. *Can. J. Forest Res.* 36, 3239–3245. doi: 10.1139/x06-176

Heydeck, P. (1991). Nadelschädigung und triebsterben in verbindung mit *Sclerophoma pithyophila* (Corda) Höhn. *Der. Wald.* 41:142.

Hormazabal, E., Schmeda-Hirschmann, G., Astudillo, L., Rodríguez, J., and Theoduloz, C. (2005). Metabolites from Microsphaeropsis olivacea, an endophytic fungus of Pilgerodendron uviferum. *Z. Naturforsch. C. J. Biosci.* 60, 11–21. doi: 10.1515/znc-2005-1-203

Kehr, R. (1998). Zur bedeutung pilzlicher endophyten bei waldbäumen. *Mitt. Biol. Bundesanst. Land Forstwirtsch. Berlin Dahlem* 349, 8–30.

Kendrick, W. (1962). Biological aspects of the decay of Pinus sylvestris leaf litter. *Nova Hedwigia* 4, 313–342.

Keriö, S., Terhonen, E., and LeBoldus, J. (2020). Safe DNA-extraction protocol suitable for studying tree-fungus interactions. *Bio Protocol* 10:e3634. doi: 10.21769/BioProtoc.3634

Koukol, O., Kolařík, M., Kolářová, Z., and Baldrian, P. (2012). Diversity of foliar endophytes in wind-fallen *Picea abies* trees. *Fungal Divers.* 54, 69–77. doi: 10.1007/s13225-011-0112-2

Kowalski, T., and Kehr, R. (1992). Endophytic fungal colonization of branch bases in several forest tree species. *Sydowia* 44, 137–168.

Kowalski, T., and Zych, P. (2002). Fungi isolated from living symptomless shoots of *Pinus nigra* growing in different site conditions. *Österr. Z. Pilzk.* 11, 107–116.

Kuo, H.-C., Hui, S., Choi, J., Asiegbu, F. O., Valkonen, J. P. T., and Lee, Y.-H. (2014). Secret lifestyles of *Neurospora crassa*. *Sci. Rep.* 4:5135. doi: 10.1038/srep05135

Kusari, S., Hertweck, C., and Spiteller, M. (2012). Chemical ecology of endophytic fungi: origins of secondary metabolites. *Chem. Biol.* 19, 792–798. doi: 10.1016/j.chembiol.2012.06.004

Langer, G. J. (1994). *Die Gattung Botryobasidium DONK (Corticiaceae, Basidiomycetes), Bibliotheca Mycologica*. Stuttgart: J. Cramer, 459.

Linnakoski, R., Kasanen, R., Dounavi, A., and Forbes, K. (2019). Forest health under climate change: effects on tree resilience, and pest and pathogen dynamics. *Front. Plant Sci.* 10:1157. doi: 10.3389/fpls.2019.01157

Linnakoski, R., Sugano, J., Junttila, S., Pulkkinen, P., Asiegbu, F. O., and Forbes, K. M. (2017). Effects of water availability on a forestry pathosystem: fungal strain-specific variation in disease severity. *Sci. Rep.* 7:13501. doi: 10.1038/s41598-017-13512-y

Martín, J. A., Macaya-Sanz, D., Witzell, J., Blumenstein, K., and Gil, L. (2015). Strong in vitro antagonism by elm xylem endophytes is not accompanied by temporally stable in planta protection against a vascular pathogen under field conditions. *Eur. J. Plant Pathol.* 142, 185–196. doi: 10.1007/s10658-015-0602-2

Martínez-Arias, C., Macaya-Sanz, D., Witzell, J., and Martín, J. A. (2019). Enhancement of Populus alba tolerance to *Venturia tremulae* upon inoculation with endophytes showing in vitro biocontrol potential. *Eur. J. Plant Pathol.* 153, 1031–1042. doi: 10.1007/s10658-018-01618-6

Martínez-Arias, C., Sobrino-Plata, J., Ormeño-Moncalvillo, S., Gil, L., Rodríguez-Calcerrada, J., and Martín, J. A. (2021). Endophyte inoculation enhances *Ulmus minor* resistance to Dutch elm disease. *Fungal Ecol.* 50:101024. doi: 10.1016/j.funeco.2020.101024

Martinoviæ, T., Koukol, O., and Hirose, D. (2016). Distinct phylogeographic structure recognized within *Desmazierella acicola*. *Mycologia* 108, 20–30. doi: 10.3852/14-291

McMullin, D. R., Green, B. D., Prince, N. C., Tanney, J. B., and Miller, J. D. (2017). Natural products of Picea endophytes from the Acadian Forest. *J. Nat. Prod.* 80, 1475–1483. doi: 10.1021/acs.jnatprod.6b01157

Mejía, L. C., Rojas, E. I., Maynard, Z., Bael, S. V., Arnold, A. E., Hebbar, P., et al. (2008). Endophytic fungi as biocontrol agents of *Theobroma cacao* pathogens. *Biol. Control* 46, 4–14. doi: 10.1016/j.biocontrol.2008.01.012

Mgbeahuruike, A. C., Sun, H., Fransson, P., Kasanen, R., Daniel, G., Karlsson, M., et al. (2011). Screening of *Phlebiopsis gigantea* isolates for traits associated with biocontrol of the conifer pathogen *Heterobasidion annosum*. *Biol. Control* 57, 118–129. doi: 10.1016/j.biocontrol.2011.01.007

Müller, C. B., and Krauss, J. (2005). Symbiosis between grasses and asexual fungal endophytes. *Curr. Opin. Plant Biol. Biotic Interact.* 8, 450–456. doi: 10.1016/j.pbi.2005.05.007

Muñoz-Adalia, E. J., Sanz-Ros, A. V., Flores-Pacheco, J. A., Hantula, J., Diez, J. J., Vainio, E. J., et al. (2017). *Sydowia polyspora* dominates fungal communities carried by two tomicus species in Pine plantations threatened by *Fusarium circinatum*. *Forests* 8:127. doi: 10.3390/f8040127

Navarro-Meléndez, A. L., and Heil, M. (2014). Symptomless endophytic fungi suppress endogenous levels of salicylic acid and interact with the jasmonate-dependent indirect defense traits of their host, lima bean (*Phaseolus lunatus*). *J. Chem. Ecol.* 40, 816–825. doi: 10.1007/s10886-014-0477-2

Nguyen, D., Boberg, J., Ihrmark, K., Stenström, E., and Stenlid, J. (2016). Do foliar fungal communities of Norway spruce shift along a tree species diversity gradient in mature European forests? *Fungal Ecol.* 23, 97–108. doi: 10.1016/j.funeco.2016.07.003

Oliva, J., Ridley, M., Redondo, M. A., and Caballol, M. (2021). Competitive exclusion amongst endophytes determines shoot blight severity on pine. *Funct. Ecol.* 35, 239–254. doi: 10.1111/1365-2435.13692

Oses, R., Valenzuela, S., Freer, J., Sanfuentes, E., and Rodriguez, J. (2008). Fungal endophytes in xylem of healthy Chilean trees and their possible role in early wood decay. *Fungal Divers.* 33, 77–86.

Osono, T. (2006). Role of phyllosphere fungi of forest trees in the development of decomposer fungal communities and decomposition processes of leaf litter. *Can. J. Microbiol.* 52, 701–716. doi: 10.1139/w06-023

Paez, C. A., and Smith, J. A. (2018). First report of Diplodia sapinea and Diplodia scrobiculata causing an outbreak of tip blight on slash pine in Florida. *Plant Dis.* 102:1657. doi: 10.1094/PDIS-07-17-1093-PDN

Pan, Y., Ye, H., Lu, J., Chen, P., Zhou, X.-D., Qiao, M., et al. (2018). Isolation and identification of *Sydowia polyspora* and its pathogenicity on *Pinus yunnanensis* in Southwestern China. *J. Phytopathol.* 166, 386–395. doi: 10.1111/jph.12696

Peršoh, D. (2013). Factors shaping community structure of endophytic fungi–evidence from the Pinus-Viscum-system. *Fungal Divers.* 60, 55–69.

Peršoh, D., Melcher, M., Flessa, F., and Rambold, G. (2010). First fungal community analyses of endophytic ascomycetes associated with *Viscum album* ssp. austriacum and its host *Pinus sylvestris*. *Fungal Biol.* 114, 585–596.

Peters, S., Draeger, S., Aust, H.-J., and Schulz, B. (1998). Interactions in dual cultures of endophytic fungi with host and nonhost plant calli. *Mycologia* 90, 360–367. doi: 10.1080/00275514.1998.12026919

Petrini, O. (1991). "Fungal endophytes of tree leaves," in *Microbial Ecology of Leaves, Brock/Springer Series in Contemporary Bioscience*, eds J. H. Andrews and S. S. Hirano (New York, NY: Springer), 179–197. doi: 10.1007/978-1-4612-3168-4_9

Petrini, O., and Fisher, P. J. (1988). A comparative study of fungal endophytes in xylem and whole stem of *Pinus sylvestris* and *Fagus sylvatica*. *Trans. Br. Mycol. Soc.* 91, 233–238. doi: 10.1016/S0007-1536(88)80210-9

Phillips, A. J. L., Alves, A., Abdollahzadeh, J., Slippers, B., Wingfield, M. J., Groenewald, J. Z., et al. (2013). The Botryosphaeriaceae: genera and species known from culture. *Stud. Mycol.* 76, 51–167.

Ponge, J. F. (1991). Succession of fungi and fauna during decomposition of needles in a small area of Scots pine litter. *Plant Soil* 138, 99–113. doi: 10.1007/BF00011812

R Core Team (2019). *R: A Language and Environment for Statistical Computing*. Vienna: R Foundation for Statistical Computing.

Raghavendra, A. K. H., and Newcombe, G. (2013). The contribution of foliar endophytes to quantitative resistance to *Melampsora rust*. *New Phytol.* 197, 909–918. doi: 10.1111/nph.12066

Razaghi, P., and Zafari, D. (2016). First report of Microsphaeropsis olivacea causing brown spine rot on *Alhagi Maurorum* in Iran. *J. Plant Pathol.* 98:377. doi: 10.4454/JPP.V98I2.044

Richardson, S. N., Walker, A. K., Nsiama, T. K., McFarlane, J., Sumarah, M. W., Ibrahim, A., et al. (2014). Griseofulvin-producing *Xylaria endophytes* of *Pinus strobus* and *Vaccinium angustifolium*: evidence for a conifer-understory species endophyte ecology. *Fungal Ecol.* 11, 107–113. doi: 10.1016/j.funeco.2014.05.004

Ridout, M., and Newcombe, G. (2015). The frequency of modification of *Dothistroma pine* needle blight severity by fungi within the native range. *Forest Ecol. Manag.* 337, 153–160. doi: 10.1016/j.foreco.2014.11.010

Rigerte, L., Blumenstein, K., and Terhonen, E. (2019). New R-Based methodology to optimize the identification of root endophytes against *Heterobasidion parviporum*. *Microorganisms* 7:102. doi: 10.3390/microorganisms7040102

Rodriguez, R. J., White, J. F. Jr., Arnold, A. E., and Redman, R. S. (2009). Fungal endophytes: diversity and functional roles. *New Phytol.* 182, 314–330. doi: 10.1111/j.1469-8137.2009.02773.x

Romeralo, C., Santamaria, O., Pando, V., and Diez, J. J. (2015). Fungal endophytes reduce necrosis length produced by *Gremmeniella abietina* in *Pinus halepensis* seedlings. *Biol. Control* 80, 30–39.

Rungjindamai, N., Pinruan, U., Hattori, T., and Choeyklin, R. (2008). Molecular characterization of basidiomycetous endophytes isolated from leaves, rachis and petioles of the oil palm, *Elaeis guineensis*, in Thailand. *Fungal Divers.* 33, 139–161.

Saikkonen, K., Faeth, S. H., Helander, M., and Sullivan, T. J. (1998). Fungal endophytes: a continuum of interactions with host plants. *Annu. Rev. Ecol. Syst.* 29, 319–343. doi: 10.1146/annurev.ecolsys.29.1.319

Santamaría, O., Smith, D. R., and Stanosz, G. R. (2012). Interaction between *Diplodia pinea* or *Diplodia scrobiculata* and fungal endophytes isolated from pine shoots. *Can. J. For. Res.* 42, 1819–1826. doi: 10.1139/x2012-132

Sanz-Ros, A. V., Müller, M. M., San Martín, R., and Diez, J. J. (2015). Fungal endophytic communities on twigs of fast and slow growing *Scots pine* (*Pinus sylvestris* L.) in northern Spain. *Fungal Biol.* 119, 870–883. doi: 10.1016/j.funbio.2015.06.008

Sayers, E. W., Barrett, T., Benson, D. A., Bolton, E., Bryant, S. H., Canese, K., et al. (2011). Database resources of the National Center for Biotechnology Information. *Nucleic Acids Res.* 39, D38–D51. doi: 10.1093/nar/gkq1172

Schulz, B., Boyle, C., Draeger, S., Römmert, A.-K., and Krohn, K. (2002). Endophytic fungi: a source of novel biologically active secondary metabolites. *Mycol. Res.* 106, 996–1004. doi: 10.1017/S0953756202006342

Schulz, B., Guske, S., Dammann, U., and Boyle, C. (1998). *Endophyte-Host Interactions. II. Defining Symbiosis of the Endophyte-Host Interaction*. Philadelphia, PA: Symbiosis.

Schulz, B., Haas, S., Junker, C., Andrée, N., and Schobert, M. (2015). Fungal endophytes are involved in multiple balanced antagonisms. *Curr. Sci.* 109, 39–45.

Sherwood, P., Villari, C., Capretti, P., and Bonello, P. (2015). Mechanisms of induced susceptibility to Diplodia tip blight in drought-stressed *Austrian pine*. *Tree Physiol.* 35, 549–562. doi: 10.1093/treephys/tpv026

Sieber, T. N. (2007). Endophytic fungi in forest trees: are they mutualists? *Fungal Biol. Rev. Fungal Endophytes* 21, 75–89. doi: 10.1016/j.fbr.2007.05.004

Sieber, T. N., and Grünig, C. R. (2013). *Plant Roots: The Hidden Half*. Boca Raton, FL: CRC Press.

Sinclair, W. A., and Lyon, H. H. (2005). *Diseases of Trees and Shrubs*, 2nd Edn. Ithaca, NY: Comstock Publishing.

Skaltsas, D. N., Badotti, F., Vaz, A. B. M., Silva, F. F., da Gazis, R., Wurdack, K., et al. (2019). Exploration of stem endophytic communities revealed developmental stage as one of the drivers of fungal endophytic community assemblages in two Amazonian hardwood genera. *Sci. Rep.* 9:12685. doi: 10.1038/s41598-019-48943-2

Smith, H., Wingfield, M., Crous, P., and Coutinho, T. A. (1996). Sphaeropsis sapinea and Botryosphaeria dothidea endophytic in *Pinus* spp. and *Eucalyptus* spp. in South Africa. *S. Afr. J. Bot.* 62, 86–88. doi: 10.1016/S0254-6299(15)30596-2

Stanosz, G. R., Blodgett, J. T., Smith, D. R., and Kruger, E. L. (2001). Water stress and *Sphaeropsis sapinea* as a latent pathogen of red pine seedlings. *New Phytol.* 149, 531–538. doi: 10.1046/j.1469-8137.2001.00052.x

Sturrock, R. N., Frankel, S. J., Brown, A. V., Hennon, P. E., Kliejunas, J. T., Lewis, K. J., et al. (2011). Climate change and forest diseases. *Plant Pathol.* 60, 133–149. doi: 10.1111/j.1365-3059.2010.02406.x

Sumarah, M. W., Kesting, J. R., Sørensen, D., and Miller, J. D. (2011). Antifungal metabolites from fungal endophytes of *Pinus strobus*. *Phytochemistry* 72, 1833–1837. doi: 10.1016/j.phytochem.2011.05.003

Sumarah, M. W., Walker, A. K., Seifert, K. A., Todorov, A., and Miller, J. D. (2015). "Screening of fungal endophytes isolated from Eastern White Pine deedles," in *The Formation, Structure and Activity of Phytochemicals, Recent Advances in Phytochemistry*, ed. R. Jetter (Cham: Springer International Publishing), 195–206. doi: 10.1007/978-3-319-20397-3_8

Suryanarayanan, T. S., Thirunavukkarasu, N., Govindarajulu, M. B., and Gopalan, V. (2012). Fungal endophytes: an untapped source of biocatalysts. *Fungal Divers.* 54, 19–30. doi: 10.1007/s13225-012-0168-7

Sutton, B. C., and Waterston, J. M. (1970). *Sydowia polyspora CMI Descriptions of Pathogenic Fungi and Bacteria*. CAB International, Wallingford, 1–2.

Talgø, V., Chastagner, G., Thomsen, I. M., Cech, T., Riley, K., Lange, K., et al. (2010). Sydowia polyspora associated with current season needle necrosis (CSNN) on true fir (*Abies* spp.). *Fungal Biol.* 114, 545–554. doi: 10.1016/j.funbio.2010.04.005

Tanney, J. B., McMullin, D. R., Green, B. D., Miller, J. D., and Seifert, K. A. (2016). Production of antifungal and antiinsectan metabolites by the *Picea endophyte Diaporthe maritima* sp. nov. *Fungal Biol. Integr. Taxon. Uncovering Fungal Divers.* 120, 1448–1457. doi: 10.1016/j.funbio.2016.05.007

Taudière, A., Bellanger, J.-M., Carcaillet, C., Hugot, L., Kjellberg, F., Lecanda, A., et al. (2018). Diversity of foliar endophytic ascomycetes in the endemic *Corsican pine* forests. *Fungal Ecol.* 36, 128–140. doi: 10.1016/j.funeco.2018.07.008

Tellenbach, C., Sumarah, M. W., Grünig, C. R., and Miller, J. D. (2013). Inhibition of Phytophthora species by secondary metabolites produced by the dark septate endophyte Phialocephala europaea. *Fungal Ecol.* 6, 12–18. doi: 10.1016/j.funeco.2012.10.003

Terhonen, E., Babalola, J., Kasanen, R., Jalkanen, R., and Blumenstein, K. (2021). *Sphaeropsis sapinea* found as symptomless endophyte in Finland. *Silva Fenn.* 55:13. doi: 10.14214/sf.10420

Terhonen, E., Blumenstein, K., Kovalchuk, A., and Asiegbu, F. O. (2019a). Forest tree microbiomes and associated fungal endophytes: functional roles and impact on forest health. *Forests* 10:42. doi: 10.3390/f10010042

Terhonen, E., Kovalchuk, A., Zarsav, A., and Asiegbu, F. O. (2018). "Biocontrol potential of forest tree endophytes," in *Endophytes of Forest Trees: Biology and Applications, Forestry Sciences*, eds A. M. Pirttilä and A. C. Frank (Cham: Springer International Publishing), 283–318. doi: 10.1007/978-3-319-89833-9_13

Terhonen, E., Langer, G. J., Bußkamp, J., Răscuțoi, D. R., and Blumenstein, K. (2019b). Low water availability increases necrosis in *Picea abies* after artificial inoculation with fungal root rot pathogens *Heterobasidion parviporum* and *Heterobasidion annosum*. *Forests* 10:55. doi: 10.3390/f10010055

Terhonen, E., Marco, T., Sun, H., Jalkanen, R., Kasanen, R., Vuorinen, M., et al. (2011). The effect of latitude, season and needle-age on the mycota of Scots pine (*Pinus sylvestris*) in Finland. *Silva Fenn.* 45:104. doi: 10.14214/sf.104

Terhonen, E., Sipari, N., and Asiegbu, F. O. (2016). Inhibition of phytopathogens by fungal root endophytes of Norway spruce. *Biol. Control* 99, 53–63. doi: 10.1016/j.biocontrol.2016.04.006

White, T. J., Bruns, T., Lee, S., and Taylor, J. (1990). "Amplification and direct sequencing of fungal ribosomal RNA genes for phylogenetics," in *PCR Protocols*, eds M. A. Innis, D. H. Gelfand, J. J. Sninsky, White, and J. Thomas (San Diego, CA: Academic Press), 315–322. doi: 10.1016/B978-0-12-372180-8.50042-1

Witzell, J., and Martín, J. A. (2018). "Endophytes and forest health," in *Endophytes of Forest Trees: Biology and Applications, Forestry Sciences*, eds A. M. Pirttilä and A. C. Frank (Cham: Springer International Publishing), 261–282. doi: 10.1007/978-3-319-89833-9_12

Witzell, J., Martín, J. A., and Blumenstein, K. (2014). "Ecological aspects of endophyte-based biocontrol of forest diseases," in *Advances in Endophytic Research*, eds V. C. Verma and A. C. Gange (New Delhi: Springer India), 321–333. doi: 10.1007/978-81-322-1575-2_17

Zhang, Y., Schoch, C. L., Fournier, J., Crous, P. W., de Gruyter, J., Woudenberg, J. H. C., et al. (2009). Multi-locus phylogeny of Pleosporales: a taxonomic, ecological and evolutionary re-evaluation. *Stud. Mycol.* 64, 85–102. doi: 10.3114/sim.2009.64.04

Zhang, Z., Schwartz, S., Wagner, L., and Miller, W. (2000). A greedy algorithm for aligning DNA sequences. *J. Comput. Biol.* 7, 203–214.

Conflict of Interest: The authors declare that the research was conducted in the absence of any commercial or financial relationships that could be construed as a potential conflict of interest.

frontiers in Forests and Global Change

ORIGINAL RESEARCH
published: 24 May 2021
doi: 10.3389/ffgc.2021.673099

Pathogen and Endophyte Assemblages Co-vary With Beech Bark Disease Progression, Tree Decline, and Regional Climate

Eric W. Morrison[1], Matt T. Kasson[2], Jeremy J. Heath[1] and Jeff R. Garnas[1]*

[1] Department of Natural Resources and the Environment, University of New Hampshire, Durham, NH, United States,
[2] Division of Plant and Soil Sciences, West Virginia University, Morgantown, WV, United States

Plant–pathogen interactions are often considered in a pairwise manner with minimal consideration of the impacts of the broader endophytic community on disease progression and/or outcomes for disease agents and hosts. Community interactions may be especially relevant in the context of disease complexes (i.e., interacting or functionally redundant causal agents) and decline diseases (where saprobes and weak pathogens synergize the effects of primary infections and hasten host mortality). Here we describe the bark endophyte communities associated with a widespread decline disease of American beech, beech bark disease (BBD), caused by an invasive scale insect (*Cryptococcus fagisuga*) and two fungal pathogens, *Neonectria faginata* and *N. ditissima*. We show that the two primary fungal disease agents co-occur more broadly than previously understood (35.5% of infected trees), including within the same 1-cm diameter phloem samples. The two species appear to have contrasting associations with climate and stages of tree decline, wherein *N. faginata* was associated with warmer and *N. ditissima* with cooler temperatures. *Neonectria ditissima* showed a positive association with tree crown dieback – no such association was observed for *N. faginata*. Further, we identify fungal endophytes that may modulate disease progression as entomopathogens, mycoparasites, saprotrophs, and/or additional pathogens, including *Clonostachys rosea* and *Fusarium babinda*. These fungi may alter the trajectory of disease via feedbacks with the primary disease agents or by altering symptom expression or rates of tree decline across the range of BBD.

Keywords: fungal community, tree decline, pathogenic fungi, multi-species disease complex, amplicon sequencing

OPEN ACCESS

Edited by:
Nicolas Feau, University of British Columbia, Canada

Reviewed by:
Stephen A. Teale, SUNY College of Environmental Science and Forestry, United States
Eeva Terhonen, University of Göttingen, Germany

****Correspondence:***
Eric W. Morrison
eric.morrison@unh.edu

Specialty section:
This article was submitted to Pests, Pathogens and Invasions, a section of the journal Frontiers in Forests and Global Change

Received: *26 February 2021*
Accepted: *13 April 2021*
Published: *24 May 2021*

Citation:
Morrison EW, Kasson MT, Heath JJ and Garnas JR (2021) Pathogen and Endophyte Assemblages Co-vary With Beech Bark Disease Progression, Tree Decline, and Regional Climate. Front. For. Glob. Change 4:673099. doi: 10.3389/ffgc.2021.673099

INTRODUCTION

Plant–microbe or plant–insect interactions are often considered in a pairwise manner with minimal consideration of the impacts of the broader community on the nature and outcomes of herbivory or pathogen attack. In some systems, tri- or even multipartite interactions have been shown to be important, particularly where fungus-insect or fungus-insect-mite symbioses are involved (Wingfield et al., 2010, 2016). Rarely, however, are broader communities considered, despite the fact that pathogens and insects attacking forest trees are embedded in variable and/or, in the

case of non-native species, novel communities. In the most aggressive and well-studied examples (e.g., Chestnut blight, Dutch elm disease, or the more recent Emerald ash borer) disease agent aggressiveness and ensuing host mortality may be sufficiently rapid such that co-occurrence with other organisms is of minimal relevance to system dynamics. Though, even in these disease systems, colonization with certain endophytic microbes can influence host susceptibility (Feau and Hamelin, 2017) or pathogen aggressiveness (Kolp et al., 2020) in subtle or complex ways. Often, however, interactions with host trees are embedded in a diverse community that varies both spatially and temporally, and disease "complexes" (diseases with multiple causal agents that act in concert to produce symptoms and mediate host decline), are increasingly recognized as important (Desprez-Loustau et al., 2016). Endophytes may influence disease outcome through a variety of mechanisms including competition with pathogens for resources (Oliva et al., 2020) and production of toxins and antifungal compounds (Rodriguez et al., 2009). The role of the community in determining host fate is extremely difficult to ascertain and could proceed via multiple, potentially interacting mechanisms (**Table 1**).

Beech bark disease (BBD) in North America is a canker disease of American beech (*Fagus grandifolia*) caused by an invasive scale insect, *Cryptococcus fagisuga* Lind., and one of two presumptively native fungal pathogens, *Neonectria faginata* and *N. ditissima*. BBD is referred to as a disease complex because it involves both insects and fungi with at least some degree of ecological redundancy with respect to disease etiology and symptom development. The invasive felted beech scale (*C. fagisuga*) is recognized as the primary initiating agent of BBD symptoms, but only inasmuch as it facilitates the initial infection of beech trees by the fungal BBD pathogens *Neonectria faginata* and *N. ditissima* (Ehrlich, 1934) particularly in stands without previous disease exposure (Cale et al., 2012). Both *N. faginata* and *N. ditissima* cause similar cankering infections and bole defects resulting in host callus tissue formation (Cotter and Blanchard, 1981). In addition to the primary disease agents, at least two fungal mycoparasites are known from the BBD system – *Clonostachys rosea* (the anamorph and preferred name of *Bionectria ochroleuca*; Houston et al., 1987; Schroers et al., 1999; Rossman et al., 2013; Stauder et al., 2020b) and *Nematogonum ferrugineum* (Houston, 1983). Other fungi are regularly isolated from infected trees (i.e., *Fusarium babinda*; Stauder et al., 2020b) though their roles are less clear. Further, saprotrophic fungi [e.g., *Inonotus glomeratus*, *Phellinus igniarius* (Cale et al., 2015a)] are likely involved in late stages of disease wherein host stem tissue is weakened to the point of mechanical failure ("beech snap," Houston, 1994), though the presence or importance of wood-rot fungi on disease progression remains unclear.

TABLE 1 | Summary of ecological guilds in addition to primary pests and pathogens that are potentially involved in tree decline associated with multi-species disease complexes.

Functional role (guild)	Effect on host	Description
Other pathogens	–	Direct effects on host, could synergize or antagonize primary insect/pathogen impacts
Decay fungi	–/0	Increase susceptibility to snap, interrupt vascular transport, reduce resource quality or availability for primary insect/pathogen (potential benefit for host)
Other insects	–/0	Competition for resources, tree defense induction, predation (including intra-guild), vectors (for other microbes, mites, nematodes)
Mycoparasites	+	Reduce growth, survival/longevity, or spore production of primary and secondary pathogens
Entomopathogens	+/0	Reduce survival, longevity of primary and secondary insects
Non-pathogenic microbes	+/–/0	Competition for resources, tree defense induction, potential viral reservoirs
Endophytes	+/–/0	Roles variable and largely unknown, potential defensive symbionts, latent pathogens, early colonizing saprotrophs, etc.

These include both insects and fungi and may have negative (–), positive (+) or no effect (0) on hosts.

In addition to questions of the role of the broader community in disease dynamics, the relative frequency and ecological importance of the two primary (*Neonectria*) pathogens has long been the subject of study and debate. While apparently ecologically similar within the BBD system, the life histories of these fungi differ in important ways. For example, *Neonectria ditissima* is a generalist that infects many diverse tree hosts including species of birch, maple, walnut, mountain ash, and holly, among others (Castlebury et al., 2006; Stauder et al., 2020b). The species is also an important pathogen of apple (Gómez-Cortecero et al., 2016). The diversity and abundance of alternative hosts could plausibly influence ecological and evolutionary dynamics (Houston, 1994; Kasson and Livingston, 2009), though this question has not been adequately studied to date. In contrast, *N. faginata* has never been observed outside of the BBD complex in North America (Castlebury et al., 2006) despite recent surveys focused on uncovering possible cryptic native reservoirs for this pathogen (Stauder et al., 2020b).

These fungi exhibit spatiotemporal trends with respect to the timing of site-level infestation with the felted scale. The current range of BBD is defined by the range of the felted beech scale, which, unlike many forest pests, has spread slowly (∼13 km per year; Morin et al., 2007) from the site of initial introduction in Halifax, Nova Scotia in 1890 (Hewitt, 1914). This progression, together with a handful of long-distance dispersal events (i.e., to North Carolina, West Virginia, and Michigan) has resulted in a gradient of duration of infestation ranging from very recent (∼9 years in Wisconsin) to more than eight decades (86 years in Maine) (Houston, 1994; Cale et al., 2017). Surveys of *Neonectria* species distribution have generally found *N. ditissima* to be more prevalent in the killing front of the disease (i.e., 10–20 years post scale insect arrival; Cale et al., 2017 and references therein). *Neonectria faginata* appears to dominate aftermath forests to the degree that researchers have suggested near replacement of *N. ditissima* with *N. faginata* as early as 7 years after pathogen attack becomes apparent

(Houston, 1994; Cale et al., 2017). However, *N. ditissima* can maintain a presence in stands dominated by *N. faginata*, including within the same tree (Kasson and Livingston, 2009). Persistence of *N. ditissima* in areas that are previously BBD-affected may be attributed to reinfection from reservoirs of this fungus in non-beech hardwood tree hosts (Kasson and Livingston, 2009), and/or the development of secondary killing fronts when climatic conditions allow beech scale to colonize areas where it was previously inhibited (e.g., release from killing winter temperatures by warm periods; Kasson and Livingston, 2012). These species – while morphologically indistinguishable in the field – can be separated using culture morphology and spore size measurements, though the latter process is tedious and is dependent on the presence of sexually produced ascospores. Further, spore size comparisons can only detect co-infection if either both species are simultaneously producing perithecia (sexual spore structures) or multiple isolates are collected, cultured, and induced to mate and produce sexual structures (Cotter and Blanchard, 1981; Stauder et al., 2020a). Partly because of these challenges, it is yet unclear whether trends in species dominance with infection duration are consistent, whether *N. ditissima* plays an important and/or predictable role in aftermath forests, and how the prevalence and distribution of each species reflects climate, disease stage, and other tree host and environmental conditions.

The objectives of this study are twofold. First, we examine patterns of occurrence (and co-occurrence) of *N. faginata* and *N. ditissima* across the current range of BBD and use joint species distribution modeling to evaluate hypothesized biotic and abiotic drivers of the prevalence and relative dominance of these species. Second, we characterize the bark mycobiome of American beech using Illumina-based metabarcoding on bark samples collected from across the range of BBD to ask how disease-associated communities vary geographically and to assess the fidelity and potential role of key species within the BBD system, whether as direct or indirect drivers or as indicators of disease state. Based on previously observed patterns with respect to disease dynamics across the range of BBD, we evaluated the relative contribution of hypothesized drivers of pathogen and associated community distribution. These included the number of years since regional infestation with scale insect (hereafter referred to as duration of BBD infection), disease severity (i.e., tree condition as well as beech scale and *Neonectria* perithecia density), and climate.

MATERIALS AND METHODS

Site Description and Sample Collection

Bark disks including phloem tissue were collected from American beech (*Fagus grandifolia*) from 10 sites across the range of BBD. Sites ranged from northern Maine, western North Carolina, and eastern Wisconsin, representing latitudinal and longitudinal transects across the current range of BBD with a range of infection duration (**Table 2**). Sampling was performed from December 2017 through January 2019. At each site American beech trees were surveyed for levels of *Neonectria* perithecium density, beech scale density, crown dieback, and amount of cankering. Scale insect and *Neonectria* perithecium density were scored on a 0–5 ordinal scale (Houston et al., 2005; Garnas et al., 2011b) and tree condition on a 0–4 scale. Distinct cankering types were pooled and measured as roughly corresponding to 20% bins by bole coverage. Trees were sampled along 100 × 5 m transects in a random direction from starting point up to a maximum of 50 trees or 400 m. All trees were measured along the transects to facilitate estimation of site-level tree size distribution and mean disease severity. Where possible, stratified random sampling was performed for bark plug collection so as to obtain an unbiased sample across a range of tree conditions. Stratified sampling levels were tree size (three levels 1st, 2nd/3rd, and 4th quartile of diameter at breast height [DBH]), four levels of *Neonectria* perithecium density (0, 1, 2–3, 4–5), and two levels of beech scale density (0–1 vs. 2–5), yielding 24 possible stratification levels. It was not possible to collect all combinations at all sites, but most sites had representative trees in most categories. In particular, in one site (Wisconsin) there were no visible *Neonectria* perithecia and we instead stratified within DBH and the available levels of beech scale density (2–3, 4–5) with four replicates per stratum (n = 24). Bark plugs were collected using a flame-sterilized 1-cm diameter hollow leather punch and stored on ice in sterile 24-well plates. The punch was flame-sterilized by first wiping it

TABLE 2 | Site locations, sampling effort, and duration of BBD infection in terms of years since beech scale first observed.

State	Latitude	Longitude	No. trees with ≥ 1000 sequences	No. plugs with ≥ 1000 sequences	No. plugs with perithecia	Duration of infection (years)
Maine	46.6585	−68.6913	10	12	7	68
Maine	44.8307	−68.5996	7	17	12	68
New Hampshire	43.134	−70.951	13	20	12	59
New York	44.4924	−74.0295	6	17	15	43
New York	43.0841	−74.4406	11	30	28	58
Pennsylvania	41.2144	−75.3834	8	8	1	42
Michigan	45.3179	−84.6723	11	21	13	12
Wisconsin	44.9284	−87.1891	21	21	0	9
West Virginia	38.6074	−79.8443	10	19	16	19
North Carolina	35.3203	−82.8439	5	5	5	20

Beech scale observations based on Cale et al. (2017).

free of surface debris using a clean Kim wipe and then applying a butane torch flame for 20 s. Multiple plugs were taken from a random subset of trees with number of plugs ranging from 1–6. Where perithecia were present we targeted plugs to include perithecia that were accessible from the ground (0–2 m). Samples were stored on ice and then frozen within 48 h of sampling and stored at −20°C until processed for DNA extraction.

We used the PRISM dataset (4 km^2-daily resolution, PRISM Climate Group, 2020) to calculate climate variables for each site. We first determined the start and end dates of the growing season in each year based on empirical values describing heat accumulation for American beech leaf out and leaf drop (Richardson et al., 2006), wherein bud break for a given site and year was estimated as the date when a site had accumulated 100 cumulative GDD_4 (base 4°C) from January 1. Leaf drop was defined by 500 cumulative chilling degree days (below 20°C) from August 15. These calculations resulted in leaf out estimates ranging from March 15 to May 12 and leaf fall estimates from October 20 to November 8 along the natural climate gradient among sites. We considered non-growing season climate because fungi are likely to grow in periods where minimum temperatures are non-limiting, and growth during periods of tree host dormancy may be important for fungal establishment, growth, and/or aggressiveness. We then summed GDD_4, daily precipitation, and freeze-thaw frequency (the number of days that temperatures crossed 0°C) for both the growing season and non-growing season.

DNA Extraction, PCR, and Sequencing

Phloem plugs were prepared for DNA extraction by removing surface debris, *Neonectria* perithecia, and the periderm layer using a sterile scalpel that was cleaned with 70% ethanol and flamed-sterilized between samples. Plugs were then washed under a steady stream of 1 ml sterile 1x PBS pH 7.2 buffer. Phloem plugs were freeze-dried for 24 h then crushed and homogenized, and a subsample of phloem (mean 56 mg ± 18 mg s.d.) was subjected to bead bashing. DNA was extracted from ground phloem samples using a QIAGEN DNeasy Plant Mini Kit following the factory protocol. Extracted DNA was then purified using a Zymo OneStep PCR Inhibitor Removal Kit following the factory protocol and diluted 1:10 in PCR grade water. Positive and negative controls for *Neonectria* detection were created by collecting phloem from an asymptomatic beech tree in Durham, NH. The phloem was prepared following the protocol above, but with the addition of three cycles of autoclaving at 121°C for 30 min prior to the freeze-drying step. Negative controls were processed through DNA extraction as described above, whereas for positive controls 1–3 mg of mycelium from axenic cultures of *N. ditissima* and *N. faginata* was added to phloem subsamples prior to the bead-bashing step. Two replicates of each positive and three replicates of negative controls were included as separate samples in downstream PCR and sequencing.

The ITS2 region was amplified in duplicate PCR reactions with the primers 5.8S-Fun and ITS4-Fun using Phusion High Fidelity polymerase, a 58°C annealing temperature, and 30 PCR cycles (Taylor et al., 2016). Primers included the Illumina TruSeq adapters and sample identification tags were added to amplicons via a second round PCR at the University of New Hampshire Hubbard Center for Genome Studies. A dual-unique indexing strategy was used such that each sample had a matching pair of indices on forward and reverse reads in order to reduce potential for sample misassignment due to index switching or index bleed. We included PCR negatives (one per PCR plate) and DNA extraction negatives (one per kit) in the sequencing run.

Bioinformatic Analyses

Amplicon sequence variant (ASV) calling was performed using the DADA2 (Callahan et al., 2016) protocol v1.8 for ITS sequences in R 3.6.2 (DADA2 version 1.14.0), with an additional step to extract the ITS2 region from 5.8S-Fun–ITS4-Fun amplicon sequences using *itsxpress* (Rivers et al., 2018). The core DADA2 algorithm was run with option 'pool = TRUE' to allow greater sensitivity for ASVs that were rare in a single sample but more abundant across the entire dataset, and putative chimeras were removed using DADA2::*removeBimeraDenovo*. Sequences from trees with multiple plugs were pooled at the tree level before ASV calling. Taxonomy was assigned to ASV representative sequences by comparison to the UNITE dynamically clustered database (release date 04/02/2020; Nilsson et al., 2019) using the DADA2::*assignTaxonomy* algorithm.

We used the LULU post-processing algorithm to group putatively erroneous ASVs with their parent ASVs based on sequence similarity and co-occurrence patterns (Frøslev et al., 2017), which has been shown to improve reconstruction of biological taxa for fungi relative to ASV denoising alone (Pauvert et al., 2019). We note that this is not a clustering algorithm but rather uses minimum sequence similarity as the first of three criteria for culling of likely error variants. After comparing a range of minimum sequence similarity thresholds (84, 90, 93, 95%) we selected a 93% threshold, which maximized the identification and removal of likely erroneous ASVs while minimizing taxonomic reassignment.

One of the goals of this study was to determine the distribution of *N. faginata* and *N. ditissima* across the range of BBD. In order to increase sensitivity for the detection, after calling ASVs we subsequently mapped the original quality filtered reads to representative sequences for ASVs identified as *N. faginata* and *N. ditissima* using the 'vsearch usearch_global' algorithm (Rognes et al., 2016). This approach increases detection sensitivity by including reads that may have otherwise been discarded or misassigned during ASV calling steps (Edgar, 2013; Pauvert et al., 2019). Samples were scored as containing *N. faginata* or *N. ditissima* if the species were discovered in a sample using either the ASV calling or mapping-based approaches. Singleton ASVs were removed from the dataset and samples with less than 1000 sequences after singleton filtering were also excluded.

Statistical Analyses

We first performed pairwise correlations of site characteristics data to examine relationships between disease severity and climate variables using the R package Hmisc (Harrell et al., 2019). These were either means of disease severity variables collected from random transects, or 10-year mean climate variables for each site extracted from the PRISM database. We first tested for

normality using a Shapiro–Wilk test (Shapiro and Wilk, 1965). We report Spearman rank correlation (ρ) where one or both variables were non-normal (including all ordinal variables) – for other variables we report Pearson correlation (r).

To test for deviations from random patterns of co-occurrence of the two *Neonectria* species we used a probabilistic model (Veech, 2013; Griffith et al., 2016). In brief, all possible permutations of species occurrence were determined based on the number of samples and observed species frequencies. A probability distribution was then calculated wherein the probability of a given co-occurrence frequency was equal to the number of permutations with that co-occurrence frequency as a proportion of the total possible permutations. Significant deviations from random were then assessed by comparing the observed co-occurrence to the probability distribution with P equal to the sum of probabilities for co-occurrence in less than (P_{lt}) or greater than (P_{gt}) the observed number of samples. We excluded samples from the Wisconsin site, which at 9 years post-beech scale colonization had a considerable number of uninfected trees that would have skewed the analysis toward detecting aggregation.

To examine the effects of environmental covariates on *N. faginata* and *N. ditissima* occurrence, we applied spatially explicit joint species distribution modeling implemented in the R HMSC package (Ovaskainen et al., 2016, 2017; Tikhonov et al., 2017). We used the *N. faginata* and *N. ditissima* presence-absence matrix as the dependent variables and employed a probit link function. Pairwise site geographic distance was included as a random effect to control for spatial correlations between predictors and *Neonectria* occurrence. Tree was included as nested random effect (within site); natural log of sequence count was included as a fixed effect to account for sampling depth effects on species detection probability (Ovaskainen et al., 2017). Non-growing season climate variables were stronger predictors of *Neonectria* occurrence in exploratory analyses, and we therefore only considered non-growing season variables in subsequent models. The primary model included climate variables and disease severity variables in order to determine the best predictors of *N. faginata* and *N. ditissima* occurrence. Independent variables were standardized to their respective means and standard deviations to obtain comparable slope estimates. We report Tjur's R^2, a coefficient of determination for logistic regression (Tjur, 2009; Ovaskainen et al., 2017) along with slope coefficients. To minimize issues with multicollinearity, precipitation was excluded from the model due to strong correlations with beech scale density ($\rho = -0.88$, $P < 0.001$) and DBH ($\rho = -0.73$, $P = 0.02$, **Supplementary Table 1**).

We used PERMANOVA (*vegan::adonis* function, Oksanen et al., 2019) to determine whether *Neonectria* species occurrences were associated with differences in composition of the remaining community. We used the presence-absence of each ASV with greater than 10% frequency as predictors of community composition, by first randomly subsampling the dataset to 1000 sequences per sample, iteratively removing each predictor ASV from the dependent variable matrix, and then performing PERMANOVA on transformed sequence counts ($\log_{10} + 1$) with the removed ASV as a categorical predictor. We tested for a relationship between ASV frequency and its strength as a predictor of community composition by regressing PERMANOVA R^2 against ASV sample incidence.

We next used indicator species analysis to explore whether certain species were associated with *Neonectria* species occurrence, or ordinal measures of *Neonectria* perithecia density, beech scale density, crown dieback, or cankering using the *indicspecies::multipatt* function (De Caceres and Legendre, 2009). We chose these variables because in combination they describe various stages of tree decline and aspects of disease and are amenable to transformation to categorical predictors (and therefore appropriate for ISA analysis). We used the sample-ASV matrix, randomly selecting 1000 sequences per sample for this analysis. We then identified ASVs that were indicators of at least two measures of disease severity. The goal of filtering out ASVs that were indicators of only one disease severity measure was to increase interpretability and reduce misclassification of ecological roles due to spurious correlations. We then performed functional classifications of ASVs using the FungalTraits database (Põlme et al., 2021). We noted primary and secondary lifestyles, and where additional functional potential was noted, such as endophytic capacity, we recorded this as tertiary lifestyle. We also noted "wood saprotroph" as a separate category, but collapsed other saprotrophic categories (i.e., "unspecified saprotroph," "litter saprotroph," "soil saprotroph") into a single "saprotroph" designation.

Data Accessibility

Raw sequence data and associated sample metadata are archived at the National Center for Biotechnology Information Sequence Read Archive under BioProject accession PRJNA701888.

RESULTS

Disease Severity and Site Characteristics

We performed a pairwise cross-correlation analysis using site-level means of disease severity variables and climactic variables (**Supplementary Table 1**). As expected, there were strong correlations between climate variables and latitude. Specifically, latitude was negatively correlated with heat accumulation (GDD_4) in both the growing ($r = -0.64$, $P = 0.047$) and non-growing season ($r = -0.95$, $P < 0.001$) and with precipitation in the growing season (Spearman's $\rho = -0.96$, $P < 0.001$). Latitude was also negatively correlated with elevation ($r = -0.73$, $P = 0.016$) with more southerly sites tending to be at higher elevation. Longitude was not significantly correlated with the climate variables tested but was strongly positively correlated with duration of BBD infection ($r = 0.97$, $P < 0.001$) and cankering ($\rho = 0.83$, $P = 0.003$) and negatively with elevation ($r = -0.69$, $P = 0.03$). Various climate parameters correlated with disease severity. Non-growing season precipitation was negatively correlated with both scale insect density ($\rho = -0.88$, $P = 0.001$) and DBH ($\rho = -0.73$, $P = 0.02$), while growing season precipitation was negatively correlated with scale insect density ($\rho = -0.81$, $P = 0.005$). We also found correlations among

some of the disease severity indicators we measured. Duration of infection correlated positively with cankering (ρ = 0.81, P = 0.004), while scale insect density and DBH were also positively correlated (ρ = 0.65, P = 0.043). No other correlations with disease severity indicators were found. We note, however, that the youngest site (Wisconsin, infested in 2010) had high mean wax density but no visible *Neonectria* perithecia at the time of sampling. We performed pairwise partial-correlation analysis using non-growing season precipitation, DBH, and beech scale while controlling for the effect of the third of these variables in each pairwise combination. Partial correlation analysis showed that only non-growing season precipitation and beech scale retained a significant correlation after controlling for the effect of DBH ($\rho_{\text{precip,scale.DBH}} = -0.78$, $P = 0.013$), whereas the other relationships were no longer significant ($\rho_{scale,DBH.precip} = 0.12$, $P = 0.97$; $\rho_{\text{precip,DBH.scale}} = -0.45$, $P = 0.22$).

Sequencing Results

After sequence processing and ASV denoising the number of sequences per sample (tree) ranged from <100 to 331,624 (median 21,315) across 117 samples. The LULU post-processing algorithm resulted in the identification of 149 ASVs (13% of 1132 original ASVs) that were better interpreted as variants of existing "parent" ASV's (either due to minor sequence variation or sequencing error; **Supplementary Table 2**). Over 90% of the ASVs culled in this way shared full taxonomic identity with their respective parent ASVs. For example, the dominant *N. faginata* and *N. ditissima* ASVs each subsumed 8 and 3 "children" variants respectively with no taxonomic reassignment. Fourteen ASVs were taxonomically reassigned, but in all cases this involved reassignment to a higher taxonomic rank (i.e., species designations were removed but the genus [13 ASVs] or family [1 ASV] was retained). After LULU post-processing and removing samples with fewer than 1000 sequences 796 ASVs remained across 102 samples retained of the 117 original samples, with the number of ASVs per sample ranging from 12 to 172 (median 60). Rarefying (to 1000 sequences per sample) led to a further drop in ASV retention; ASVs richness ranged from 7 to 67 per sample (median 25). The mean ASV richness per site ranged from 13.2 ± 4.4 s.d. to 46.8 ± 16.4 s.d. and total site richness ranged from 66 to 412 ASVs. Further exploration of the relationships between disease severity, climate, and broad trends in community composition and diversity are possible using this dataset and are currently underway. We focus here on the primary fungal disease agents and description of species that may play a role in disease progression (**Table 1**).

We did not observe sequences in our DNA extraction negative or PCR negative controls (**Supplementary Figure 1**). Only one of the three negative controls composed of autoclaved phloem produced sequences – the three total sequences from that sample included two sequences from a *Neocucurbitaria* ASV and one sequence from a *Corynespora* ASV. Sequence counts from the nine samples of PBS buffer that had been used to wash plugs were likewise extremely low (1–8 sequences). Three of the PBS buffer wash samples contained *N. faginata* whereas *N. ditissima* was not detected in any of the samples. We included two positive controls for each of *N. ditissima* and *N. faginata* and observed the expected species and no other taxa in each of those samples, though one *N. faginata* positive control produced only a single sequence.

Neonectria Species Distribution and Its Drivers

Neonectria faginata was present in all 10 sites and *N. ditissima* was found in all but the southernmost site in North Carolina (**Figure 1**). Importantly, the two species often co-occurred both in sites and within the same tree, including within the same 1-cm phloem disc. Overall, *N. faginata* was present in 135 of 170 phloem plugs (79.4%) and 71 of 102 trees (69.6%), while *N. ditissima* was present in 46 of 170 plugs (27.1%) and 32 of 102 trees (31.4%). The two species co-occurred in 38 of 170 plugs (22.4%) and 27 of 102 trees (26.5%) including 35.5% of the 76 trees infected with at least one species. Both species were absent in 27 of 170 plugs (15.9%) and 26 of 102 trees (25.5%). At least one of the two species was detected in all 109 plugs where perithecia were present on the plug periderm surface prior to processing for DNA extraction (64.1% of plugs). *Neonectria faginata* was detected in 107 (98.2%) of the plugs with fruiting structures present while *N. ditissima* was detected in 31 plugs (29.4%). The species co-occurred in 29 of 109 plugs (26.6%). Sixty plugs had no perithecia present and one plug of the 170 total had degraded periderm such that it was not possible to record perithecia presence-absence. Of the 60 plugs with no perithecia at least one species was detected in 33 plugs (55%), wherein *N. faginata* was detected in 27 (45%) and *N. ditissima* in 15 (25%). The two species co-occurred in nine plugs without perithecia (15%), and were both absent in 27 plugs (45%).

Neonectria ditissima was only found in isolation at the tree level (i.e., without *N. faginata*) at the three northernmost sites we sampled (MI, WI, and northern ME). In the remaining seven of the 10 sites, *N. ditissima* was only detected in trees where *N. faginata* was also present. In terms of species prevalence, *N. faginata* occurred in a greater number of trees than *N. ditissima* in all but the three northernmost sites (90% mean occurrence versus 25% mean occurrence for *N. faginata* and *N. ditissima*, respectively, in the seven more southerly sites). The two species each occurred in isolation in two trees in Wisconsin and co-occurred in one tree, and in Michigan each species occurred in isolation in one tree and co-occurred in six trees. *Neonectria ditissima* was more prevalent in our northern Maine site (70% versus 60% of trees for *N. ditissima* and *N. faginata*, respectively, including 50% of trees where the species co-occurred). In sites within the killing front and aftermath zone (i.e., excluding the Wisconsin site within "advancing front" of the disease), *N. faginata* was detected in 84% of all trees across our sites, whereas *N. ditissima* was detected in 36% of trees. Given these observed occurrence frequencies, co-occurrence did not differ from a random distribution [32% observed vs. 30% expected; $P_{gt} = 0.24$ *sensu* Veech (2013)].

We next examined correlations between *Neonectria* species incidence across sites (i.e., presence-absence at the tree level) and indices of disease severity and climate using spatially explicit joint species distribution modeling (HMSC, Ovaskainen et al., 2017). We first tested for effects of growing season versus non-growing

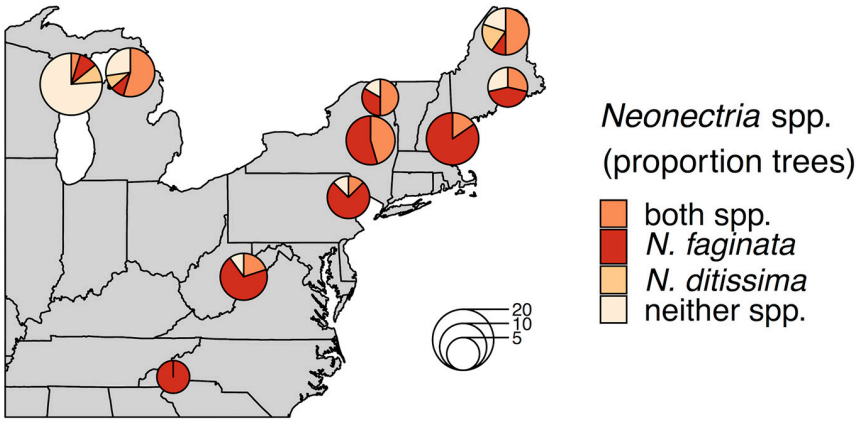

FIGURE 1 | *Neonectria* species occurrence across 10 sites. Proportions in pie charts indicate the number of trees in a site where a species was detected using metabarcoding. The number of trees per site is indicated by pie chart diameter as indicated by the inset scale legend.

season climate parameters and found that climate during the non-growing season was overall a stronger predictor of patterns of *Neonectria* occurrence (**Supplementary Figure 2**). Specifically, heat accumulation (GDD_4) during the non-growing season was significantly associated with incidence of both species, while growing season GDD_4 was generally a poor predictor of incidence. Non-growing season freeze-thaw was significantly associated with *N. faginata* (posterior support $P = 0.99$) but not *N. ditissima* incidence ($P = 0.86$). In the growing season neither of these variables was correlated with *Neonectria* species occurrence.

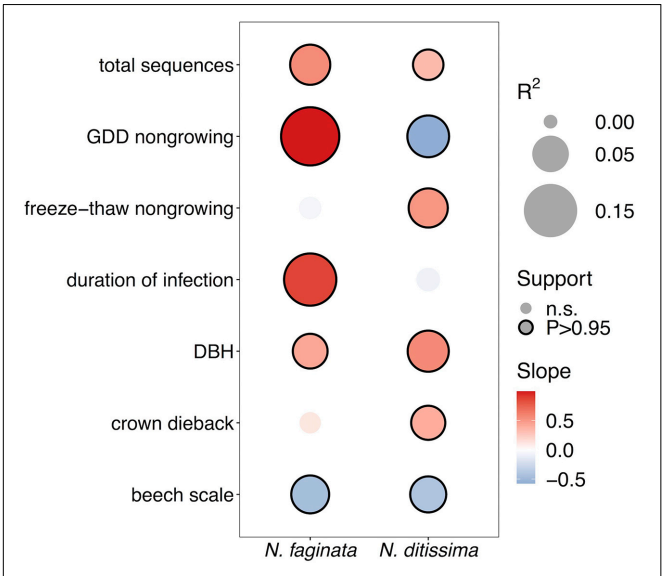

FIGURE 2 | Effects of disease severity and climate on *Neonectria* species occurrence within trees. Points with solid outlines represent significant effects at posterior probability $P > 0.95$ (analogous to a p-value of $P < 0.05$). Box fill indicates the strength and direction of the relationship with blue indicating a negative slope, and red indicating a positive slope. Point size indicates magnitude of R^2 with overall fits for *N. faginata* and *N. ditissima* of Tjur $R^2 = 0.54$ and 0.37, respectively.

After controlling for sampling effort and spatial structure, our models explained 54% and 37% of variance in *N. faginata* and *N. ditissima* incidence, respectively, based on Tjur R^2 (Tjur, 2009). The full model indicated that *N. faginata* had a significant, positive relationship with non-growing season heat accumulation ($R^2 = 0.19$), duration of infection ($R^2 = 0.14$) and DBH ($R^2 = 0.04$), and a negative association with beech scale density ($R^2 = 0.06$) (**Figure 2**). Heat accumulation was the strongest predictor of *N. faginata* incidence ($R^2 = 0.19$). *Neonectria ditissima* incidence was positively associated with DBH ($R^2 = 0.07$), freeze-thaw cycle frequency ($R^2 = 0.07$), and crown dieback ($R^2 = 0.04$), but negatively associated with non-growing season heat accumulation ($R^2 = 0.07$) and beech scale density ($R^2 = 0.05$). Results were unchanged when non-growing season precipitation was included in the model, except there was no significant correlation between *N. faginata* and beech scale or infection duration (**Supplementary Figure 3**). Neither species showed a significant correlation with non-growing season precipitation. The HMSC approach also allows examination of residual correlation between dependent variables (i.e., *N. faginata* and *N. ditissima* occurrence) after accounting for the effect of independent predictors. We found no residual correlation between the two species after accounting for the effects of disease severity and climate, and also found no correlation between the species using a reduced model that only controlled for sampling effort (i.e., sequence count) and spatial structure. This result suggests that distribution of the two species is not strongly structured by inter-species interactions (e.g., competition or facilitation).

In light of the significant positive association of *N. ditissima* with crown dieback indicated in HMSC modeling, we visually explored patterns of species incidence across levels of crown dieback and cankering (**Figure 3**). *Neonectria ditissima* occurrence increased across crown dieback classes (crown dieback level 0 = 21%, 1 = 24%, 2 = 38%, 3 = 58%), whereas *N. faginata* occurrence was relatively stable or modestly declined (crown dieback level 0 = 79%, 1 = 71%, 2 = 62%, 3 = 67%). The increase in *N. ditissima* with increasing crown dieback

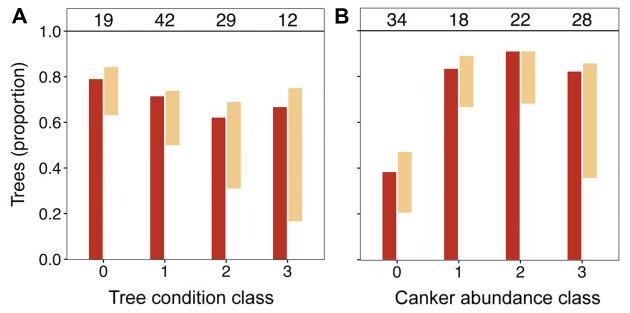

FIGURE 3 | Occurrence of *N. faginata* and *N. ditissima* across levels of crown dieback **(A)** and cankering **(B)**. The proportion of trees in which each species was detected is indicated for *N. faginata* (dark red) and *N. ditissima* (light red). The proportion of co-occurrence is indicated by overlap of the bars and the remaining white space indicates the proportion of trees where neither species was detected. The number of trees per grouping (n) is indicated above respective bars.

resulted in an increase in co-infection by the two species at the tree level. *Neonectria ditissima* occurred in isolation in 2–8% of trees in each dieback class, whereas trees co-infected with both *Neonectria* species increased across dieback classes (crown dieback level 0 = 16%, 1 = 21%, 2 = 31%, 3 = 50%). When discrete cankers were absent both species were at relatively low occurrence (38 and 26% for *N. faginata* and *N. ditissima*, respectively). However, *N. faginata* more than doubled in trees with cankers compared to no cankers (85% *versus* 38%, respectively; $\chi^2 = 21.6$, $P < 0.001$), and *N. ditissima* doubled in the highest cankering level compared to levels 0–2 (50% *versus* 25%, respectively; $\chi^2 = 5.1$, $P = 0.02$) resulting in elevated co-infection at the highest cankering category (46% of trees compared to 17–23% in remaining categories).

In this work we were also interested in whether *N. faginata* or *N. ditissima* was structuring or responding to different fungal endophyte communities. Of the 62 most commonly detected ASVs (minimum 10% incidence across all samples) *N. faginata* was the fifth best predictor of mycobiome composition (PERMANOVA $R^2 = 0.076$, $P = 0.001$) while *N. ditissima* was the 42nd best predictor ($R^2 = 0.023$, $P = 0.007$; **Supplementary Figure 4A**). We tested for a relationship between PERMANOVA R^2 and sample incidence to examine the possibility that species presence-absence effects on community composition were primarily driven by the frequency of ASV occurrence. There was a weak but significant relationship between incidence and PERMANOVA R^2 ($R^2 = 0.165$, $P = 0.001$; **Supplementary Figure 4B**) with the top five most predictive ASVs occurring in between 13 and 61% of samples.

Ecological Roles of Fungi in the BBD System

We used a combination of Indicator Species Analysis (ISA; De Caceres and Legendre, 2009) and literature-based functional classification (Põlme et al., 2021) to discern degrees of statistical association and potential ecological roles for fungal species that appear as beech bark endophytes across the range of disease and tree decline levels sampled. Overall, 38 ASVs were identified as indicator species of at least two disease categories. All but two of these ASVs were indicators of different levels of crown dieback or cankering (**Table 3**). Nine of the 38 ASVs were indicators of the absence of crown dieback and either low levels of cankering or the absence of scale insect (see **Table 3**, "Healthy beech" indicators). Of these nine, only three were taxonomically identified to the genus level, with six other ASVs identified to order, phylum or kingdom. Another five ASVs were indicators of both low levels of cankering and absence of scale insect (**Table 3**, "Minor cankering, scale absent"), with two being taxonomically identified to the genus level.

In total, 16 ASVs were associated with intermediate to high levels of either cankering or crown dieback. Six ASVs were indicators of intermediate to high levels of cankering, low scale density, and/or presence of *Neonectria* species (**Table 3**, "Intermediate BBD severity"). These included *N. faginata*, as well as ASVs annotated as animal pathogens/entomopathogens, mycoparasites, plant pathogens, and saprotrophs or wood saprotrophs, the latter two functional groupings accounting for five of the six ASVs. Ten ASVs were indicators of intermediate to high levels of crown dieback (**Table 3**, "High BBD severity"). Four of these 10 were also indicators of high scale density, and another four were indicators of high levels of cankering. Eight of the 10 ASVs associated with high levels of crown dieback were annotated as either saprotrophs or wood saprotrophs, and five were annotated as plant pathogens. All five of the ASVs assigned a plant pathogen function mapped to multiple functional groups, with saprotrophic lifestyle assigned as primary or secondary functions. Three ASVs associated with high levels of crown dieback were also among the top five predictors of community composition (**Supplementary Figure 3**), and were annotated to entomopathogen (animal pathogen), plant pathogen-saprotroph-mycoparasite, or saprotroph-plant pathogen-endophyte functions, respectively. We note that *N. ditissima* was also an indicator of high levels of crown dieback (crown dieback 2–3) but was not formally included in this analysis due to lack of association with additional disease indicators.

Eight ASVs were associated with presence or absence of the primary disease agents (**Table 3**, "Scale and *Neonectria* associates"), including ASVs associated with high beech scale density and *Neonectria* absence (two ASVs), high density of both beech scale and *Neonectria* perithecia (one ASV), or absence of both beech scale and *Neonectria* (one ASV). Six of the eight ASVs were also associated with absence of cankering. Five of these eight ASVs were annotated to saprotroph or wood saprotroph functions, three as entomopathogens/animal pathogen, and two as endophytes, including three ASVs with multiple functional mappings.

We also specifically explored the distributions of *Clonostachys rosea, Nematogonum ferrugineum*, and *Fusarium babinda* given their previously described roles as BBD associates as either mycoparasites of *Neonectria* (*C. rosea* and *N. ferrugineum*; Barnett and Lilly, 1962; Houston, 1983; Stauder et al., 2020b) or potential entomopathogens or secondary beech pathogens (Stauder et al., 2020b). Two ASVs were annotated as *C. rosea*

TABLE 3 | Amplicon sequence variant (ASVs) associated with at least two indicators of disease according to ISA [columns "Disease indicators (ISA)"].

	Disease indicators (ISA)							
Disease state	**Crown dieback**	**Cankers**	**Beech scale**	**Perithecia**	**Nf/Nd**	**Taxonomy (order, genus/species)**	**Function†,‡**	**ASV**
Healthy beech	0	0				Unidentified ascomycota		ASV_229
	0	1				Lecanorales, Lecania croatica	L	ASV_169
	0		0			Hypocreales, Microcera sp.	A	ASV_575
	0		0			Chaetothyriales, Capronia sp.	S[1], E[2], A[3], M[3]	ASV_427
	0		0			Unidentified Capnodiales		ASV_272
	0		0			Unidentified Fungi		ASV_441
	0		0			Unidentified Ascomycota		ASV_524
	0		0			Unidentified Capnodiales		ASV_596
	0		0			Unidentified Ascomycota		ASV_688
Minor cankering		1	0			Chaetothyriales, Capronia sp.	S[1], E[2], A[3], M[3]	ASV_190
scale absent		1	0			Togniniales, Phaeoacremonium sp.	P	ASV_135
		1	0			Unidentified Capnodiales		ASV_166
		1	0			Unidentified ASV		ASV_181
		1	0			Unidentified Capnodiales		ASV_200
Intermediate BBD		**1–3**	**0–2**	**2–5**		**Hypocreales, Neonectria faginata**	P	**ASV_1**
severity		1–3	0–2			Pleosporales, Neocucurbitaria sp.	S	ASV_2
		1–3	0–2			Pleosporales, Unidentified Thyridariaceae	S, WS	ASV_18
		1–3		3–5		Orbiliales, Hyalorbilia erythrostigma	WS[1], A[2]	ASV_26
		1–3			Nd+	Agaricostilbales, Unidentified Chionosphaeraceae	E, M, S	ASV_78
		3			Nd+	Chaetothyriales, Exophiala castellanii	A[1], S[2], E[3]	ASV_343
High BBD severity	1–3		2–5			Hypocrelaes, Fusarium babinda	P[1], S[2], E[3]	ASV_19
	1–3		**3–5**			**Tremellales, Hannaella surugaensis**	A	**ASV_5**
	1–3		**3–5**		**Nd+**	**Pleosporales, Coniothyrium sp.**	P[1], S[2], M[3]	**ASV_10**
	1–3		**3–5**		**Nf/Nd –**	**Capnodiales, Cladosporium sp.**	S[1], P[2], E[3]	**ASV_12**
	3	3				Hypocreales, Microcera rubra	A	ASV_94
	3	3				Myriangiales, Unidentified Elsinoaceae	P[1], S[2]	ASV_79
	3	2–3			Nf/Nd+	Pleosporales, Brunneofusispora sinensis	WS	ASV_14
	3	2–3				Pleosporales, Acericola italica	WS	ASV_11
	3		0			Chaetothyriales, Exophiala sp.	A[1], S[2], E[3]	ASV_320
	3			5		Diaporthales, Cytospora prunicola	P[1], S[2], E[3]	ASV_474
Scale and Neonectria		**0**	**3–5**		**Nf/Nd–**	**Tremellales, Vishniacozyma taibaiensis**	S	**ASV_27**
associates		0	3–5		Nf/Nd –	Tremellales, Hannaella surugaensis	A	ASV_234
		0	3–5			Chaetothyriales, Cyphellophora sp.	S[1], A[2]	ASV_119
		0	3–5			Pleosporales, Acericola italica	WS	ASV_212
		0	3–5			Unidentified Cystobasidiomycetes		ASV_136
		0			Nf/Nd–	Hypocreales, Acremonium alternatum	A	ASV_126
			0	5		Xylariales, Phialemoniopsis ocularis	S[1], E[2]	ASV_69
			0		Nf/Nd –	Helotiales, Cadophora melinii	S[1], P[2], E[3]	ASV_217

Taxonomy is listed as order, species epithet where available, or most informative taxonomic level. Those five ASVs that were strongest predictors of community composition according to PERMANOVA are bolded. Functional classifications are provided (sensu Põlme et al., 2021).

†Functional classifications: A, animal pathogen including entomopathogens; E, endophyte; M, mycoparasite; P, plant pathogen; S, Saprotroph; WS, wood saprotroph; L, lichenized.

‡Primary and secondary lifestyles according to Põlme et al. (2021) are indicated by [1] and [2]. Where tertiary lifestyles such as endophytic capacity is provided by Põlme et al. (2021), those are indicated by [3]. Where classifications at the family level were performed all potential guild information is listed without indicating primary or secondary lifestyle status.

and together they occurred in four of our 10 sites ranging from 10 to 27% of trees in respective sites (**Figure 4A**). One of these ASVs was also an indicator of the highest level of *Neonectria* perithecia. One ASV of putative importance as a mycoparasite of the BBD fungi, *N. ferrugineum*, only occurred at two sites at low frequency (9 and 20% of trees **Figure 4B**) and was not a statistical indicator of any disease categories. Another ASV (ASV 19) was identified as *Fusarium babinda*, which has been previously

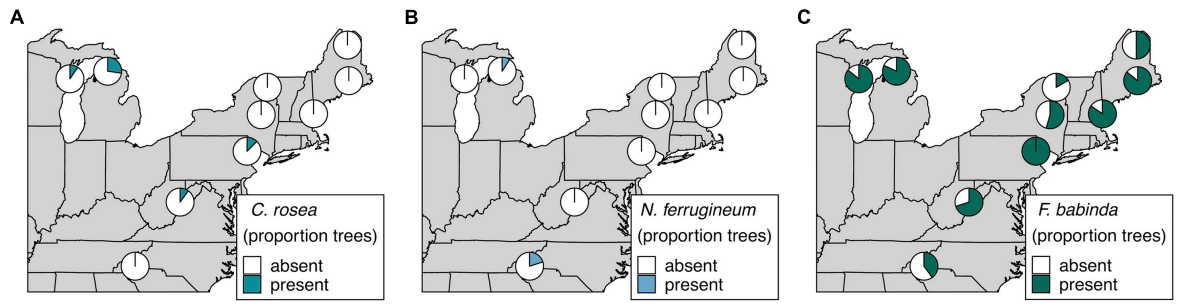

FIGURE 4 | Occurrence of ASVs 16 and 21, *Clonostachys rosea* **(A)**, ASV 807, *Nematogonum ferrugineum* **(B)**, and ASV 19, *Fusarium babinda* **(C)**, across 10 sites. Proportions in pie charts indicate the number of trees in a site where the species was detected using metabarcoding.

identified in association with BBD and is a suspected beech scale associate (Stauder et al., 2020b). This ASV was associated with high wax density and high crown dieback (**Table 3**) and occurred in all 10 of our sites (**Figure 4C**). Of these three species only *C. rosea* showed a statistical association with either *Neonectria* species. *Clonostachys rosea* was positively associated with *N. ditissima* (Fisher's exact test odds ratio = 6.3, $P = 0.03$) and only occurred in one sample where both species were absent (**Supplementary Figure 5**).

DISCUSSION

In the present study we explored the distribution of *N. faginata* and *N. ditissima*, the primary pathogens involved in BBD, in relation to disease severity and climate characteristics in 10 sites across the range of BBD. We further explored patterns of association with other fungal taxa in the beech bark endophytic community in relation to tree disease state, and used these relationships to highlight and hypothesize ecological roles of potential relevance to BBD severity and progression. We show that *N. faginata* and *N. ditissima* have divergent correlations with climate and may be associated with different stages of tree decline. Further, we show that fungal taxa occurring in association with the primary BBD agents (i.e., the host, *F. grandifolia*; the scale insect initiating agent, *C. fagisuga*, and the fungal pathogens, *N. faginata* and *N. ditissima*) may contribute to disease outcomes in complex and interacting ways in this system. We suspect that these types of feedbacks are not unique to the BBD system, but rather are likely to generalize to other complex diseases where variation in the occurrence, relative densities, or interactions among ecologically redundant disease agents influence the trajectory of disease (Cobb and Metz, 2017). Outcomes are likely to be especially hard to predict where component species respond uniquely to key biotic and biophysical drivers.

Correlations Among Disease Agents and Climate

We found that precipitation in both growing and non-growing seasons was negatively correlated with scale insect density. Non-growing season precipitation also correlated negatively with DBH. Negative correlations between beech scale and precipitation are consistent with a hypothesized causal relationship whereby precipitation reduces scale insect population density by washing colonies off of tree boles (Houston and Valentine, 1988; Dukes et al., 2009; Garnas et al., 2011b; Kasson and Livingston, 2012). The latter relationship between precipitation and DBH is likely driven by multicollinearity between infection duration (and thus disease severity indicators), geographic distribution, and climate. Sites with older infections tend to be dominated by small diameter trees and also occur in lower precipitation sites in our dataset. That said cankering (which constitutes evidence of past, non-lethal infection) was the only index of disease status that was related statistically (positively in this case) with duration of infection. Our dataset included sites ranging from nine to 68 years from the arrival of beech scale based on county-level data (Cale et al., 2017), but only one site was in the "advancing front" stage of infection as typically defined (i.e., ≤10 years post scale insect arrival; Houston et al., 2005). At least one further site, and possibly up to three sites, occurred in the "killing front" stage of infection (i.e., 5–10 years after advancing front conditions, or 15–20 years after scale insect arrival; Houston et al., 2005), whereas the remaining sites were sampled in an aftermath forest infection stage. Interactions between disease agents are variable in aftermath forests despite density dependent growth within populations of insects or fungi (Garnas et al., 2011b). Our sampling design, which was weighted toward aftermath forest stands, may have obscured the typically observed patterns across disease stages in beech scale and fungal pathogen abundance. However, there were signals of duration of infection-driven patterns in our dataset. For example, our advancing front site had high mean wax density but no visible *Neonectria* perithecia production, as is typical of advancing front stage forests (Shigo, 1972). Further, scale insect density and DBH were positively correlated, likely reflecting both a positive relationship at the tree scale (Latty et al., 2003; Garnas et al., 2011a) or an effect of our sampling design. Specifically, since we included stands within the advancing front, sites with higher beech scale density, as is common in recently infested stands, also tended to have larger trees prior to experiencing BBD-induced mortality. Thus, inclusion of both aftermath and advancing front sites is likely to over-represent the scale insect-tree size relationship,

which is considerably weaker within the aftermath forest alone (Garnas et al., 2013).

Neonectria Species Distribution and Its Drivers

Both *Neonectria* species were widely distributed geographically and in terms of disease stage (i.e., infection duration). *Neonectria faginata* was detected in all 10 sites, and *N. ditissima* in nine of 10 sites, with both occurring in advancing front, killing front, and aftermath forests. Importantly, the two species regularly co-occurred, not only within the same tree (26% co-occurrence), but within the same 1-cm phloem disk (22% co-occurrence). The prevailing understanding of the dynamics of BBD is that infected stands undergo a progression from initial infection by *N. ditissima* to near-total replacement by *N. faginata* in later disease stages in most cases (Houston, 1994; Cale et al., 2017). This idea persists despite evidence of *N. ditissima* persistence and co-occurrence of the two pathogens (Kasson and Livingston, 2009). Here we show that while *N. faginata* is the dominant species throughout killing front and aftermath forests (84% of all trees), *N. ditissima* maintained a substantial foothold throughout these stands (36% of all trees). Such relatively high incidence indicates that spillover of *N. ditissima* to non-beech trees could be an important mechanism by which this disease impacts forest structure, function, and diversity. Further, given random co-occurrence patterns between *N. faginata* and *N. ditissima*, we found no evidence of strong facilitation such that co-infection frequency would be elevated nor obvious competitive exclusion within sites or trees.

Despite approximately random co-occurrence between the two species we did observe patterns with regard to species distributions, stand characteristics, and climate. For example, in accordance with previous research (Houston, 1994) we found evidence that *N. faginata* becomes more prevalent as disease progresses over decades. Generally, the two species appear to have divergent climate associations, where *N. faginata* was associated with warmer climates, and *N. ditissima* with colder climates. It is possible that these patterns arise from infection duration dynamics that are obscured by our use of coarse-grained county level data. For example, northern Maine has experienced secondary killing fronts after release of beech scale populations from suppression by winter killing temperatures as temperature warms (Kasson and Livingston, 2012). However, the two warmest sites in our dataset were also of intermediate infection duration (19 and 20 years) and so infection duration is unlikely to fully explain the climate-driven distribution patterns we observed. Indeed, non-growing season heat accumulation was the strongest predictor of *N. faginata* occurrence while infection duration was the second strongest predictor, suggesting climate as an important influence on prevalence of these species within the BBD system.

Both *Neonectria* species exhibited significant associations with various disease severity metrics. For example, both species were negatively correlated with *C. fagisuga* density. Despite the fact that scale insects appear to be obligate initiating agents of BBD in the advancing front, correlations between insect and fungal components of BBD are weak or negative in aftermath forests (Cale et al., 2012; Garnas et al., 2013). Our data support this pattern. Alternative hypotheses have been offered for the priming of trees for fungal infection, including a role for the native birch margodid scale insect, *Xylococculus betulae,* as a predisposing agent specifically for *N. ditissima* (Cale et al., 2015b). While this insect can be locally abundant in certain sites and years, we did not encounter it in sufficient densities to warrant inclusion in our models. Nor does it seem likely that *X. betulae* is an important driver of fungal dynamics across the range of BBD.

Occurrence of *Neonectria* was most strongly associated with tree condition and with aspects of climate. *Neonectria ditissima* but not *N. faginata* was positively correlated with crown dieback class, a result supported by both HMSC modeling and indicator species analysis (ISA). This pattern resulted in increased co-infection by the two species in higher crown-dieback classes. Higher rates of co-infection associated with increasing crown dieback may indicate that a synergistic attack by the two species contributes to tree decline. For example, *N. ditissima* showed higher prevalence in sites with lower temperatures during the non-growing season. Maintaining growth during the non-growing season, however slow, could result in higher apparent aggressiveness if attacking dormant hosts limits host defensive response or wound compartmentalization (Manion, 2003; Dukes et al., 2009; Copini et al., 2014). Alternatively, *N. ditissima* may be more prevalent in later stages of tree decline as a secondary pathogen that is favored by weakened host tissue (Houston, 1981; Manion, 1981).

There is some evidence that trees infected with heart-rot decay fungi have higher density of *Neonectria*-induced lesions, potentially indicating that modification of tree tissues by either *Neonectria* pathogens or decay fungi facilitates host colonization (Cale et al., 2015a). However, the directionality or strength of this relationship is unclear. Indeed, *N. faginata* was among the top five predictors of community composition of the bark endophyte community overall, whereas *N. ditissima* was a relatively poor predictor, suggesting that colonization by *N. faginata* may be a predisposing factor for colonization of bark by a suite of other disease-associated fungi. However, the two species produced similar sized cankers on American beech in inoculation trials (Stauder et al., 2020b) suggesting that *N. ditissima* is not restricted to tissues already weakened by primary *N. faginata* infection.

Since our results suggest a much more central role for *N. ditissima* in the aftermath forest than has been previous indicated, it is important to attempt to reconcile differences between our study and previous work on BBD-associated *Neonectria* species. For example, in a recent study, *N. ditissima* represented just 4.2% of perithecial isolates from American beech across the central Appalachian Mountains and was recovered from only two of 13 sampled locations (Stauder et al., 2020b). This is considerably lower than the 27% of bark samples we estimate here. Most studies to date rely on culturing from ascospores or spore measurement as direct isolation from bark tissue is challenging. Higher rates of perithecium production, seasonal or within-tree differences in sporocarp

production and/or spore viability could favor the collection or successful rearing of *N. faginata* over *N. ditissima*, particular in cases of co-infection. While all sampling methodologies likely suffer from some form of bias, our metabarcoding approach using DNA extracted directly from bark tissue likely represents an improvement on historical detection of BBD fungal agents and associates.

Ecological Roles of Fungi in the BBD System

We used a combination of ISA and literature searches to describe the ecological roles of fungi occurring in the context of the BBD complex. ISA delineated clear groups of fungi associated with different stages of disease or disease agents, including healthy beech associates, fungi associated with intermediate or high BBD severities and associated tree decline, and fungi associated with presence and/or absence of the primary disease agents (i.e., *Neonectria* and beech scale).

The majority of healthy beech associates were not taxonomically identified past the order level (67%). In addition, only 40% of ASVs associated with low levels of cankering and absence of beech scale were identified past the order level. Of the 24 remaining indicator ASVs 96% (23 ASVs) were taxonomically identified to at least the genus level, suggesting that bark endophytic communities of healthy American beech are a relatively unexplored reservoir of fungal diversity given comparatively low taxonomic identification. Bark endophytes have historically received less attention than foliar endophytes in temperate forests (Unterseher, 2011), and further exploration of bark endophyte diversity and functioning is warranted.

We observed a shift in both taxonomic composition and functional potential in the indicators of intermediate to high BBD severity compared to healthy beech. Overall, 13 of the 16 ASVs (81%) associated with intermediate to high BBD severity were annotated to saprotrophic functional groups, and five of the putatively saprotrophic ASVs associated with high BBD severity were further identified as facultative plant pathogens. Four ASVs in intermediate- and high BBD severity categories, including *N. faginata*, were also among the top five predictors of community composition. Many endophytes and plant pathogens function as facultative saprotrophs (Frankland, 1998; Stone et al., 2004); a shift in community function toward saprotrophy may be an important indicator of later stages of tree decline. Decay fungi may have negative and weak positive associations with beech scale and *Neonectria*, respectively (Cale et al., 2015a), suggesting complex interactions between disease organisms and co-occurring fungi potentially mediated by host tissue modification. The fungal communities associated with late stages of tree decline in particular, as indicated by high levels of crown dieback, may contribute to tree death by weakening tissues to the point of mechanical failure (i.e., "beech snap"; Houston, 1981; Manion, 1981). Together, enrichment of saprotrophs and plant pathogens along with an apparent consistent shift in community composition indicate that the endophytic fungal community may play an important role in disease progression beyond the direct action of the primary disease agents.

We observed eight ASVs that were associated with presence or absence of the primary disease agents (*Neonectria* and beech scale). It is difficult to assign ecological roles or the nature of interactions based on pairwise species associations. For example, a positive correlation between species may indicate facilitation, overlapping habitat or microclimatic preferences, or may indicate deadlocked competition or mycoparasitic relationships (Maynard et al., 2018). Indeed, some of the ASVs in this group were associated with high beech scale density and absence of *Neonectria*, or vice versa. Two of these (ASVs 27 and 234) were restricted geographically – occurring primarily in our Wisconsin site, which, at 9 years infection duration, was unique in our dataset with high average beech scale density and low *Neonectria* incidence. As such, these two ASVs may be indicators of early stage BBD infection or geographic location rather than of interactions with beech scale or *Neonectria*, *per se*. However, two other ASVs (ASVs 69 and 217) that were geographically widespread, occurring in 4-5 sites, were both indicators of beech scale absence, with one also being an indicator of high *Neonectria* perithecium density and the other an indicator of *Neonectria* absence. It is possible that these taxa function as facultative entomopathogens and/or mycoparasites depending on BBD disease stage and available hosts.

We also examined distribution of two species previously reported as mycoparasites (*N. ferrugineum* and *C. rosea*) and one reported as a potential additional plant pathogen and/or an entomopathogen (*F. babinda*) in the BBD system. One of these, *N. ferrugineum* (ASV 807) occurred at only two sites and was not a statistical indicator of any disease categories. Despite its prevalence in visual surveys (Houston, 1983) our data suggest that given its relative rarity, this fungus may not play a primary role in limiting growth of *Neonectria* pathogens involved in BBD. In contrast, two ASVs were identified as *C. rosea*, which together were detected at four of our 10 sites including recently infested sites in Wisconsin and Michigan, suggesting this fungus is present in BBD-affected forest stands even at the earliest stages of *Neonectria* establishment. In addition, one of the *C. rosea* ASVs was an indicator of high *Neonectria* perithecia density, consistent with its hypothesized mycoparasitic status in this system (Stauder et al., 2020b). This species has long been used as a biocontrol agent against plant pathogenic fungi (Schroers et al., 1999). Genomic mechanisms of mycoparasitism have also been described in this species (Karlsson et al., 2015) making this an intriguing candidate for further study in terms of interactions with the primary *Neonectria* disease agents. *Fusarium babinda* (ASV 19) was an indicator of high BBD severity and was found at all 10 of our sites, suggesting this fungus is a geographically widespread and consistent member of late-stage decline communities associated with BBD. In particular, *F. babinda* was associated with high wax density supporting its hypothesized association with beech scale (Stauder et al., 2020b). Whether this fungus is parasitizing the scale insects remains unclear. Previous literature supports a possible entomopathogenic lifestyle, having been previously recovered from other non-native forest insect pests (*Lymantria dispar* and *Adelges tsugae*) in the eastern U.S. (Jacobs-Venter et al., 2018).

CONCLUSION

This study explores new aspects of the fungal community ecology of the BBD system. We combined structured sampling at a landscape scale and across a known gradient of duration of infestation with beech scale with robust characterization of the beech bark mycobiome using high-throughput, metabarcoding sequencing. We found that one of the primary BBD agents, *N. ditissima,* occurs far more widely than previously known, co-occurring with *N. faginata* in nearly all of the sites and regularly within the same tree and even the same 1-cm phloem disk. The two species have apparently contrasting climate associations with *N. faginata* being associated with warmer temperatures and *N. ditissima* with cooler temperatures. Further, the two species are non-randomly associated with different stages of disease. While *N. faginata* is indeed the dominant pathogen, *N. ditissima* becomes most prevalent both very early during stand BBD-level infection and also at later stages of tree decline within the aftermath forest. The role of this pathogen, both in conjunction *N. faginata* and as trees progress through stages of the decline cycle, should be further explored. We also identified fungi that regularly occur in association with BBD with the potential to influence disease trajectory by functioning as entomopathogens, mycoparasites, saprotrophs and/or alternate or additional pathogens, and resulting in downstream shifts in community composition in the fungal communities of beech bark.

DATA AVAILABILITY STATEMENT

The datasets presented in this study can be found in online repositories. The names of the repository/repositories and accession number(s) can be found below: https://www.ncbi.nlm.nih.gov/, PRJNA701888.

AUTHOR CONTRIBUTIONS

JG and EM designed the study. JH and EM collected and processed the samples. EM and JG designed the data analysis approach. EM performed the data analysis and wrote the first draft of the manuscript. EM, JG, and MK wrote sections of the manuscript. All the authors contributed to manuscript revision, read, and approved the submitted version.

FUNDING

This work was funded in part by the New Hampshire Agricultural Experiment Station including support for open-access publishing fees. This is Scientific Contribution Number 2895. This work was supported by the USDA National Institute of Food and Agriculture McIntire-Stennis Project 1023443.

ACKNOWLEDGMENTS

We thank Paul Super and Bambi Teague at the National Parks Service in North Carolina as well as Keith Kanoti at the University of Maine for their help in obtaining collection permits. We appreciate the cooperation of the New York Department of Environmental Conservation, and the Michigan, Pennsylvania, and Wisconsin Departments of Natural Resources for granting collection permits.

SUPPLEMENTARY MATERIAL

The Supplementary Material for this article can be found online at: https://www.frontiersin.org/articles/10.3389/ffgc.2021.673099/full#supplementary-material

REFERENCES

Barnett, H. L., and Lilly, V. G. (1962). A Destructive Mycoparasite, *Gliocladium roseum*. *Mycologia* 54, 72–77. doi: 10.1080/00275514.1962.12024980

Cale, J. A., Ashby, A. W., West, J. L., Teale, S. A., Johnston, M. T., and Castello, J. D. (2015a). Scale insects, decay and canker fungi in American beech. *For. Pathol.* 45, 71–75. doi: 10.1111/efp.12127

Cale, J. A., Teale, S. A., Johnston, M. T., Boyer, G. L., Perri, K. A., and Castello, J. D. (2015b). New ecological and physiological dimensions of beech bark disease development in aftermath forests. *For. Ecol. Manag.* 336, 99–108. doi: 10.1016/j.foreco.2014.10.019

Cale, J. A., Garrison-Johnston, M. T., Teale, S. A., and Castello, J. D. (2017). Beech bark disease in North America: over a century of research revisited. *For. Ecol. Manag.* 394, 86–103. doi: 10.1016/j.foreco.2017.03.031

Cale, J. A., Letkowski, S. K., Teale, S. A., and Castello, J. D. (2012). Beech bark disease: an evaluation of the predisposition hypothesis in an aftermath forest. *For. Pathol.* 42, 52–56. doi: 10.1111/j.1439-0329.2011.00722.x

Callahan, B. J., McMurdie, P. J., Rosen, M. J., Han, A. W., Johnson, A. J. A., and Holmes, S. P. (2016). DADA2: high-resolution sample inference from Illumina amplicon data. *Nat. Methods* 13, 581–583. doi: 10.1038/nmeth.3869

Castlebury, L. A. C. A., Rossman, A. Y. R. Y., and Hyten, A. S. H. S. (2006). Phylogenetic relationships of *Neonectria/Cylindrocarpon* on Fagus in North America. *Botany* 84, 1417–1433. doi: 10.1139/b06-105

Cobb, R. C., and Metz, M. R. (2017). Tree Diseases as a Cause and Consequence of Interacting Forest Disturbances. *Forests* 8:147. doi: 10.3390/f8050147

Copini, P., den Ouden, J., Decuyper, M., Mohren, G. M. J., Loomans, A. J. M., and Sass-Klaassen, U. (2014). Early wound reactions of Japanese maple during winter dormancy: the effect of two contrasting temperature regimes. *AoB Plants* 6:plu059. doi: 10.1093/aobpla/plu059

Cotter, H. V., and Blanchard, R. O. (1981). Identification of the two *Nectria* taxa causing bole cankers on American beech. *Plant Dis.* 65, 332–334. doi: 10.1094/PD-65-332

De Caceres, M., and Legendre, P. (2009). Associations between species and groups of sites: indices and statistical inference. *Ecology* 90, 3566–3574. doi: 10.1890/08-1823.1

Desprez-Loustau, M. L., Aguayo, J., Dutech, C., Hayden, K. J., Husson, C., Jakushkin, B., et al. (2016). An evolutionary ecology perspective to address forest pathology challenges of today and tomorrow. *Ann.For. Sci.* 73, 45–67.

Dukes, J. S. D. S., Pontius, J. P., Orwig, D. O., Garnas, J. R. G. R., Rodgers, V. L. R. L., Brazee, N. B., et al. (2009). Responses of insect pests, pathogens, and invasive plant species to climate change in the forests of northeastern North America: what can we predict?. *Can. J. For. Res.* 39:2. doi: 10.1139/X08-171

Edgar, R. C. (2013). UPARSE: highly accurate OTU sequences from microbial amplicon reads. *Nat. Methods* 10, 996–998. doi: 10.1038/nmeth.2604

Ehrlich, J. (1934). The beech bark disease: a *Nectria* disease of *Fagus*, following *Cryptococcus fagi* (BAER.). *Can. J. Res.* 10:6. doi: 10.1139/cjr34-070

Feau, N., and Hamelin, R. C. (2017). Say hello to my little friends: how microbiota can modulate tree health. *New Phytol.* 215, 508–510. doi: 10.1111/nph.14649

Frankland, J. C. (1998). Fungal succession — unravelling the unpredictable. *Mycol. Res.* 102, 1–15. doi: 10.1017/S0953756297005364

Frøslev, T. G., Kjøller, R., Bruun, H. H., Ejrnæs, R., Brunbjerg, A. K., Pietroni, C., et al. (2017). Algorithm for post-clustering curation of DNA amplicon data yields reliable biodiversity estimates. *Nat. Commun.* 8:1188. doi: 10.1038/s41467-017-01312-x

Garnas, J. R., Houston, D. R., Ayres, M. P., and Evans, C. (2011b). Disease ontogeny overshadows effects of climate and species interactions on population dynamics in a nonnative forest disease complex. *Ecography* 35, 412–421. doi: 10.1111/j.1600-0587.2011.06938.x

Garnas, J. R., Ayres, M. P., Liebhold, A. M., and Evans, C. (2011a). Subcontinental impacts of an invasive tree disease on forest structure and dynamics. *J. Ecol.* 99, 532–541. doi: 10.1111/j.1365-2745.2010.01791.x

Garnas, J. R., Houston, D. R., Twery, M. J., Ayres, M. P., and Evans, C. (2013). Inferring controls on the epidemiology of beech bark disease from spatial patterning of disease organisms. *Agric. For. Entomol.* 15, 146–156. doi: 10.1111/j.1461-9563.2012.00595.x

Gómez-Cortecero, A., Saville, R. J., Scheper, R. W. A., Bowen, J. K., Agripino De Medeiros, H., Kingsnorth, J., et al. (2016). Variation in Host and Pathogen in the *Neonectria/Malus* Interaction; toward an Understanding of the Genetic Basis of Resistance to European Canker. *Front Plant Sci.* 7:1365. doi: 10.3389/fpls.2016.01365

Griffith, D. M., Veech, J. A., and Marsh, C. J. (2016). cooccur: probabilistic Species Co-Occurrence Analysis in R. *J. Stat. Softw.* 69, 1–17. doi: 10.18637/jss.v069.c02

Harrell, F. E. Jr., Dupont, C., et al. (2019). *Hmisc: Harrell Miscellaneous. R package version 4.3-0*. URL: https://CRAN.R-project.org/package=Hmisc.

Hewitt, C. G. (1914). Note on the occurrence of the felted beech coccus *Cryptococcus fagi* (Baerens) Dougl. in Nova Scotia. *Can. Entomol.* 46, 15–16. doi: 10.4039/Ent4615-1

Houston, D. R. (1981). *Stress Triggered Tree Diseases: The Diebacks and Declines*. Broomall, PA: U.S. Department of Agriculture, Forest Service.

Houston, D. R. (1983). "Effects of parasitism by Nematogonum ferrugineum (Gonstorrhodiella highlei) on pathogenicity of Nectria coccinea var. faginata and Nectria galligena," in *Proceedings, I.U.F.R.O. Beech Bark Disease Working Party Conference; 1982 September 26-October 8; Hamden, CT. Sponsored by the USDA Forest Service, Northeastern Forest Experiment Station* (Washington, DC: U.S. Department of Agriculture, Forest Service), 109–114.

Houston, D. R. (1994). Major new tree disease epidemics: beech bark disease. *Annu. Rev. Phytopathol.* 32, 75–87. doi: 10.1146/annurev.py.32.090194.000451

Houston, D. R., Mahoney, E. M., and McGauley, B. H. (1987). Beech bark disease – association of Nectria ochroleuca in W. VA, PA, and Ontario. *Phytopathology* 77, 1615-1615.

Houston, D. R., Rubin, B. D., Twery, M. J., Steinman, J. R., and Steinman, J. R. (2005). "Spatial and Temporal Development of Beech Bark Disease in the Northeastern United States," in *Beech Bark Disease: Proceedings of the Beech Bark Disease Symposium; 2004 June 16-18; Saranak Lake, NY. Gen. Tech. Rep. NE-331*, eds A. E. vans Celia, A. Lucas Jennifer, and J. Twery Mark (Newtown Square: US. Department of Agriculture, Forest Service, Northeastern Research Station), 43–47.

Houston, D. R., and Valentine, H. T. (1988). Beech bark disease: the temporal pattern of cankering in aftermath forests of Maine. *Can. J. For. Res.* 18, 38–42. doi: 10.1139/x88-007

Jacobs-Venter, A., Laraba, I., Geiser, D. M., Busman, M., Vaughan, M. M., Proctor, R. H., et al. (2018). Molecular systematics of two sister clades, the *Fusarium concolor* and *F. babinda* species complexes, and the discovery of a novel microcycle macroconidium–producing species from South Africa. *Mycologia* 110, 1189–1204. doi: 10.1080/00275514.2018.1526619

Karlsson, M., Durling, M. B., Choi, J., Kosawang, C., Lackner, G., Tzelepis, G. D., et al. (2015). Insights on the evolution of mycoparasitism from the genome of *Clonostachys rosea*. *Genome Biol. Evol.* 7, 465–480. doi: 10.1093/gbe/evu292

Kasson, M. T., and Livingston, W. H. (2009). Spatial distribution of *Neonectria* species associated with beech bark disease in northern Maine. *Mycologia* 101, 190–195. doi: 10.3852/08-165

Kasson, M. T., and Livingston, W. H. (2012). Relationships among beech bark disease, climate, radial growth response and mortality of American beech in northern Maine, USA. *For. Pathol.* 42, 199–212. doi: 10.1111/j.1439-0329.2011.00742.x

Kolp, M., Double, M. L., Fulbright, D. W., MacDonald, W. L., and Jarosz, A. M. (2020). Spatial and temporal dynamics of the fungal community of chestnut blight cankers on American chestnut (*Castanea dentata*) in Michigan and Wisconsin. *Fungal Ecol.* 45:100925. doi: 10.1016/j.funeco.2020.100925

Latty, E. F., Canham, C. D., and Marks, P. L. (2003). Beech bark disease in northern hardwood forests: the importance of nitrogen dynamics and forest history for disease severity. *Can. J. For. Res.* 33:2. doi: 10.1139/x02-183

Manion, P. D. (1981). *Tree disease concepts*. Available online at: https://www.cabdirect.org/cabdirect/abstract/19810672031 [accessed on Feb 10, 2021]

Manion, P. D. (2003). Evolution of Concepts in Forest Pathology. *Phytopathology* 93, 1052–1055. doi: 10.1094/PHYTO.2003.93.8.1052

Maynard, D. S., Covey, K. R., Crowther, T. W., Sokol, N. W., Morrison, E. W., Frey, S. D., et al. (2018). Species associations overwhelm abiotic conditions to dictate the structure and function of wood-decay fungal communities. *Ecology* 99, 801–811. doi: 10.1002/ecy.2165

Morin, R. S. M. S., Liebhold, A. M. L. M., Tobin, P. C. T. C., Gottschalk, K. W. G. W., and Luzader, E. L. (2007). Spread of beech bark disease in the eastern United States and its relationship to regional forest composition. *Can. J. For. Res.* 37, 726–736. doi: 10.1139/X06-281

Nilsson, R. H., Larsson, K.-H., Taylor, A. F. S., Bengtsson-Palme, J., Jeppesen, T. S., Schigel, D., et al. (2019). The UNITE database for molecular identification of fungi: handling dark taxa and parallel taxonomic classifications. *Nucleic Acids Res.* 47, D259–D264. doi: 10.1093/nar/gky1022

Oksanen, J. F., Blanchet, G., Friendly, M., Kindt, R., Legendre, P., McGlinn, D., et al. (2019). *vegan: Community Ecology Package. R package version 2.5-6*. URL: https://CRAN.R-project.org/package=vegan.

Oliva, J., Ridley, M., Redondo, M. A., and Caballol, M. (2020). Competitive exclusion amongst endophytes determines shoot blight severity on pine. *Funct. Ecol.* 35, 239–254. doi: 10.1111/1365-2435.13692

Ovaskainen, O., Roy, D. B., Fox, R., and Anderson, B. J. (2016). Uncovering hidden spatial structure in species communities with spatially explicit joint species distribution models. *Methods Ecol. Evol.* 7, 428–436. doi: 10.1111/2041-210X.12502

Ovaskainen, O., Tikhonov, G., Norberg, A., Blanchet, F. G., Duan, L., Dunson, D., et al. (2017). How to make more out of community data? A conceptual framework and its implementation as models and software. *Ecol. Lett.* 20, 561–576. doi: 10.1111/ele.12757

Pauvert, C., Buée, M., Laval, V., Edel-Hermann, V., Fauchery, L., Gautier, A., et al. (2019). Bioinformatics matters: the accuracy of plant and soil fungal community data is highly dependent on the metabarcoding pipeline. *Fungal Ecol.* 41, 23–33. doi: 10.1016/j.funeco.2019.03.005

Põlme, S., Abarenkov, K., Nilsson, H. R., Lindahl, B. D., Clemmensen, K. E., Kauserud, H., et al. (2021). FungalTraits: a user-friendly traits database of fungi and fungus-like stramenopiles. *Fungal Divers*. 105, 1–16. doi: 10.1007/s13225-020-00466-2

PRISM Climate Group. (2020). *Oregon State University*. Available online at: http://prism.oregonstate.edu [accessed on May 28, 2020]

Richardson, A. D., Bailey, A. S., Denny, E. G., Martin, C. W., and O'keefe, J. (2006). Phenology of a northern hardwood forest canopy. *Glob. Change Biol.* 12, 1174–1188. doi: 10.1111/j.1365-2486.2006.01164.x

Rivers, A. R., Weber, K. C., Gardner, T. G., Liu, S., and Armstrong, S. D. (2018). ITSxpress: software to rapidly trim internally transcribed spacer sequences with quality scores for marker gene analysis. *F1000Res.* 7:1418. doi: 10.12688/f1000research.15704.1

Rodriguez, R. J., White, J. F., Arnold, A. E., and Redman, R. S. (2009). Fungal endophytes: diversity and functional roles. *New Phytol.* 182, 314–330. doi: 10.1111/j.1469-8137.2009.02773.x

Rognes, T., Flouri, T., Nichols, B., Quince, C., and Mahé, F. (2016). VSEARCH: a versatile open source tool for metagenomics. *PeerJ* 4:e2584. doi: 10.7717/peerj.2584

Rossman, A. Y., Seifert, K. A., Samuels, G. J., Minnis, A. M., Schroers, H.-J., Lombard, L., et al. (2013). Genera in *Bionectriaceae, Hypocreaceae, and Nectriaceae* (Hypocreales) proposed for acceptance or rejection. *IMA Fungus* 4, 41–51. doi: 10.5598/imafungus.2013.04.01.05

Schroers, H.-J., Samuels, G. J., Seifert, K. A., and Gams, W. (1999). Classification of the mycoparasite *Gliocladium roseum* in *Clonostachys* as *C. rosea*, its

relationship to *Bionectria ochroleuca*, and notes on other *Gliocladium*-like fungi. *Mycologia* 91, 365–385. doi: 10.1080/00275514.1999.12061028

Shapiro, S. S., and Wilk, M. B. (1965). An Analysis of Variance Test for Normality (Complete Samples). *Biometrika* 52, 591–611. doi: 10.2307/2333709

Shigo, A. L. (1972). The Beech Bark Disease Today in the Northeastern U.S. *J. For.* 70, 286–289. doi: 10.1093/jof/70.5.286

Stauder, C. M., Utano, N. M., and Kasson, M. T. (2020b). Resolving host and species boundaries for perithecia-producing nectriaceous fungi across the central Appalachian Mountains. *Fungal Ecol.* 47:100980. doi: 10.1016/j.funeco.2020.100980

Stauder, C. M., Garnas, J. R., Morrison, E. W., Salgado-Salazar, C., and Kasson, M. T. (2020a). Characterization of mating type genes in heterothallic *Neonectria* species, with emphasis on *N. coccinea. N. ditissima, and N. faginata*. *Mycologia* 112, 880–894. doi: 10.1080/00275514.2020.1797371

Stone, J. K., Polishook, J. D., and White, J. F. (2004). "Endophytic fungi," in *Biodiversity of Fungi*, eds M. Foster and G. Bills (Burlington: Elsevier Academic Press), 241–270. doi: 10.13140/RG.2.1.2497.0726

Taylor, D. L., Walters, W. A., Lennon, N. J., Bochicchio, J., Krohn, A., Caporaso, J. G., et al. (2016). Accurate Estimation of Fungal Diversity and Abundance through Improved Lineage-Specific Primers Optimized for Illumina Amplicon Sequencing. *Appl. Environ. Microbiol.* 82, 7217–7226. doi: 10.1128/AEM.02576-16

Tikhonov, G., Abrego, N., Dunson, D., and Ovaskainen, O. (2017). Using joint species distribution models for evaluating how species-to-species associations depend on the environmental context. *Methods Ecol. Evol.* 8, 443–452. doi: 10.1111/2041-210X.12723

Tjur, T. (2009). Coefficients of Determination in Logistic Regression Models—A New Proposal: the Coefficient of Discrimination. *Am. Stat.* 63, 366–372. doi: 10.1198/tast.2009.08210

Unterseher, M. (2011). "Diversity of Fungal Endophytes in Temperate Forest Trees," in *Endophytes of Forest Trees: Biology and Applications* Forestry Sciences, eds A. M. Pirttilä and A. C. Frank (Dordrecht: Springer Netherlands), 31–46. doi: 10.1007/978-94-007-1599-8_2

Veech, J. A. (2013). A probabilistic model for analysing species co-occurrence. *Glob. Ecol. Biogeogr.* 22, 252–260. doi: 10.1111/j.1466-8238.2012.00789.x

Wingfield, M. J., Garnas, J. R., Hajek, A., Hurley, B. P., de Beer, Z. W., and Taerum, S. J. (2016). Novel and co-evolved associations between insects and microorganisms as drivers of forest pestilence. *Biol. Invasions* 18, 1045–1056. doi: 10.1007/s10530-016-1084-7

Wingfield, M. J., Slippers, B., and Wingfield, B. D. (2010). Novel associations between pathogens, insects and tree species threaten world forests. *N. Z. J. For. Sci.* 40, S95-S103.

Conflict of Interest: The authors declare that the research was conducted in the absence of any commercial or financial relationships that could be construed as a potential conflict of interest.

frontiers in Forests and Global Change

ORIGINAL RESEARCH
published: 08 September 2021
doi: 10.3389/ffgc.2021.725066

Competitive Advantage of *Geosmithia morbida* in Low-Moisture Wood May Explain Historical Outbreaks of Thousand Cankers Disease and Predict the Future Fate of *Juglans nigra* Within Its Native Range

Geoffrey M. Williams[1] *and Matthew D. Ginzel*[1,2]*

[1] *Department of Forestry and Natural Resources, Hardwood Tree Improvement and Regeneration Center, Purdue University, West Lafayette, IN, United States,* [2] *Department of Entomology, Purdue University, West Lafayette, IN, United States*

OPEN ACCESS

Edited by:
Richard Hamelin, University of British Columbia, Canada

Reviewed by:
Pedro Miguel Naves, Instituto Nacional Investigaciao Agraria e Veterinaria (INIAV), Portugal
Jennifer Gene Klutsch, University of Alberta, Canada

***Correspondence:**
Matthew D. Ginzel
mginzel@purdue.edu

Specialty section:
This article was submitted to Pests, Pathogens and Invasions, a section of the journal Frontiers in Forests and Global Change

Received: *14 June 2021*
Accepted: *04 August 2021*
Published: *08 September 2021*

Citation:
Williams GM and Ginzel MD (2021) Competitive Advantage of Geosmithia morbida in Low-Moisture Wood May Explain Historical Outbreaks of Thousand Cankers Disease and Predict the Future Fate of Juglans nigra Within Its Native Range. Front. For. Glob. Change 4:725066. doi: 10.3389/ffgc.2021.725066

Bark beetles vector symbiotic fungi and the success of these mutualisms may be limited by competition from other microbes. The outcome of fungal competition is strongly influenced by the physical and chemical conditions of the wood they inhabit. These conditions are in turn subject to climatic variation. In particular, wood moisture content (MC) influences fungal competition and, therefore, could help determine environmental suitability for thousand cankers disease (TCD) caused by *Geosmithia morbida* and its vector *Pityophthorus juglandis*. We conducted competition experiments in *Juglans nigra* wood that was naturally or artificially colonized by *G. morbida* and other fungi over a range of wood MC expected across prevailing United States climatic conditions. *G. morbida* outcompeted antagonistic fungi *Clonostachys* and *Trichoderma* spp. at <5% equilibrium moisture content. *Aspergillus* spp. outcompeted *G. morbida* at low moisture in wood from Indiana. We fit a logistic regression model to results of the competition experiments to predict survival of *G. morbida* across the United States. Expected survival of *G. morbida* was highest in historical TCD epicenters and accounted for the low incidence and severity of TCD in the eastern United States. Our results also predict that under future climate scenarios, the area impacted by TCD will expand into the native range of *J. nigra*. Given its role in emergent forest health threats, climate change should be a key consideration in the assessment of risks to hardwood resources.

Keywords: climate change, forest health, walnut, wood sorption, fungi, competition, bark beetle, central hardwood region

INTRODUCTION

Range expansions of native pests caused by climate change are a major threat to the health and productivity of forest ecosystems (Ramsfield et al., 2016; Pureswaran et al., 2018). In particular, abiotic factors are known to influence dispersal and reproduction of scolytine beetles (Coleoptera: Curculionidae) and primary symbiotic fungi (Wood, 1982; Six and Bentz, 2007). Beetles and fungi mutualistically rely upon one another for successful host colonization and to satisfy metabolic requirements (Hofstetter et al., 2007, 2015; Six and Bentz, 2007; Mitton and Ferrenberg, 2012). Physicochemical conditions in bark and wood, including nutrient availability, temperature, and moisture, determine the outcome of competition between the primary mutualist of a beetle species and other fungi, and consequently, affect reproductive success and dispersal (Rayner and Boddy, 1988; Ranger et al., 2018).

Co-dispersal of the walnut twig beetle (*Pityophthorus juglandis* Blackman) and its primary mutualist, the pathogenic fungus *Geosmithia morbida* Kolařík, Freeland, Utley, and Tisserat, to walnut trees (*Juglans* spp.) is contingent on physicochemical conditions that favor competitive success and sporulation of *G. morbida* in walnut wood. Many species of scolytine beetles have evolved specialized structures, glands, and behaviors that maximize favorability of growth conditions for the successful colonization of wood by their mutualistic fungi (Francke-Grosmann, 1967; Weed et al., 2015; Nuotclà et al., 2019). Other species, including *P. juglandis,* lack specialized structures but rather rely on passive co-dispersal of fungi (Bright, 1981). The hydrophobic spores of *G. morbida* are borne on conidiophores inside beetle galleries (Tisserat et al., 2009; Kolařík et al., 2011) and picked up by static adhesion to the cuticle of adult *P. juglandis* as they emerge (Seybold et al., 2016).

Geographic variation in severity and impact of thousand cankers disease (TCD) and establishment of *P. juglandis* and *G. morbida* across North America (Tisserat et al., 2011; Griffin, 2015; Juzwik et al., 2020) suggest that climatic factors such as temperature and humidity may be important in determining environmental favorability for development and spread of the disease. TCD results from mass attack of *P. juglandis* that introduce *G. morbida* to the inner bark of *Juglans* and *Pterocarya* spp., which causes necrotic cankers in the phloem and outer sapwood that interfere with the translocation of nutrients and photosynthate from distal branches and leaves to other parts of the plant (Tisserat et al., 2009).

Geosmithia morbida is evolutionarily adapted to the seasonally dry climate of the western United States (Williams and Newcombe, 2017). Population genetics and historical records indicate that both *P. juglandis* (Seybold et al., 2012; Rugman-Jones et al., 2015) and *G. morbida* (Hadziabdic et al., 2014; Zerillo et al., 2014) are native to semiarid southwest North America where the range of their ancestral host, *Juglans major* (Torr.) A. Heller, crosses into the United States from Mexico (Little, 1976). Large-scale tree mortality attributed to TCD has been restricted to other native and introduced *Juglans* spp. west of the Great Plains (Seybold et al., 2019). *G. morbida* is thermophilic (Kolařík et al., 2011) and xerotolerant (Williams and Newcombe, 2017), and commonly found sporulating inside *P. juglandis* galleries in black walnut (*Juglans nigra* L.) in the western, but not the eastern, United States (D. Hadziabdic, pers. comm.). In eastern states, including Tennessee (TN) in the Appalachian Mountains and piedmont, fungal antagonists such as *Trichoderma* spp. are frequently found instead of *G. morbida* in *P. juglandis* galleries (Gazis et al., 2018). Native populations of *J. nigra* in the eastern United States have been largely unaffected by TCD despite detections of the beetle or fungus in nine states (Moore et al., 2019; Seybold et al., 2019; Juzwik et al., 2020; Stepanek, 2020), and moribund trees recovered in disease epicenters in Virginia (VA) and Tennessee (TN) (Griffin, 2015).

Climatic differences between the eastern and western United States provide one possible explanation for geographical difference in the prevalence and spread of TCD within the native and non-native range of *J. nigra*. In particular, intracontinental differences in prevailing climatic conditions may lead to differences in moisture content (MC) of senescent woody tissues around *P. juglandis* galleries and affect the relative competitive success and sporulation of *G. morbida*. When wood dries, its equilibrium moisture content (EMC) is determined by air temperature and relative humidity. Moisture content—the amount of moisture in wood—typically falls below 10% in spring, summer, and autumn in locations in the western United States where TCD has been severe (Seybold et al., 2019) but remains above 10% throughout much of the native range of *J. nigra* (Eckelman, 1998; Simpson, 1998). For example, in Tippecanoe Co., Indiana (IN), in the humid midwestern United States, summer MC of *J. nigra* wood was much higher, at 14.9 $\pm$ 0.20% (n = 156) for air-dried lumber and 20.1 $\pm$ 0.29% (n = 180) for retail firewood (Williams and Ginzel, unpublished data), the predominant pathway for the movement of invasive wood-boring pests (Newton and Fowler, 2009; Jacobi et al., 2012). Furthermore, the peak flight of *P. juglandis* typically occurs in the spring (Sitz et al., 2017; Chen et al., 2020), coinciding with high levels of precipitation in the Midwest.

Geographical variation in TCD incidence and severity could be partly explained by a competitive advantage for *G. morbida* over other xylotropic fungi in the western United States. However, under higher prevailing MC in the eastern United States (Eckelman, 1998), the colonization and spread of *G. morbida* may be inhibited by competition with other fungi that may be better adapted to those conditions. *G. morbida* was recovered after 133 days from wood dried to a MC of 7% and grown on 25% glycerol agar (Williams and Newcombe, 2017) with a water potential of −20 MPa (Ridout et al., 2017). These moisture levels fall below known limits for fungal wood decomposition (−4 MPa; Griffin, 1977), between limits for biological activity in soils (−14 MPa) and surface litter (−36 MPa; Manzoni et al., 2012), and between limits for soil-dwelling *Fusarium* (−10 MPa) and extremely xerophilic *Penicillium* spp. (−40 MPa; Harris, 1981). Water potential supporting the growth of *G. morbida* is similar to those that support *Penicillium* and *Phialocephala* from roots of conifers that withstand seasonal droughts in the seasonally dry western United States (Ridout et al., 2017). To our knowledge, the role of temperature and wood MC in determining the outcome of

competition between *G. morbida* and other fungi in walnut wood has not yet been investigated.

Understanding the environmental parameters that favor TCD is essential for risk assessments to help predict the future threat to *J. nigra* in a changing climate. Wood MC may have historically limited the spread of TCD in the native range of *J. nigra*. Nevertheless, conditions could still become favorable for TCD in the eastern United States if prevailing temperature, precipitation, and humidity change as predicted by climate models (USGCRP, 2018). We hypothesized that the success of *G. morbida* and *P. juglandis* is limited by competition between *G. morbida* and other native fungi better adapted to the prevailing temperature and humidity regimes in the native range of *J. nigra*. To test this hypothesis, we first carried out a series of competition experiments in wood that had been naturally or artificial colonized by *G. morbida* and other fungi. We used lethal and non-lethal heat treatments to create fungal wood microcosms to reduce the abundance of native fungi in the wood and then inoculated it with *G. morbida*. In another experiment, we characterized competition between *G. morbida* and other fungi in nontreated wood that was naturally infested. We calibrated the incubation conditions of the experiments to a range of EMC corresponding to climatic conditions across the United States (Eckelman, 1998; Simpson, 1998). We predicted that *G. morbida* would have a competitive advantage over other fungi that occur in wood that equilibrated to extremely low MC but would be increasingly outcompeted by other fungi in wood that equilibrated to intermediate and high MC. We validated our interpretation of the results from our competition experiments by first extrapolating expected survival of *G. morbida* across the United States based on historical climate data, and then comparing inferred TCD severity with historical observations. Finally, we extrapolated the model to climate change scenarios based on high- and low-carbon emission to predict the portions of the native range of *J. nigra* that will be threatened by TCD 10 and 50 years into the future.

MATERIALS AND METHODS

Collection of Branches and *G. morbida* Isolates

Branches (6–8-cm diameter) of black walnut (*Juglans nigra*) were collected in 2018 and 2019, cut into 20–25-cm lengths and brought or shipped to an authorized containment facility at Purdue University (West Lafayette, IN, United States). All branches were cut laterally into disks to a thickness of 4 mm. *G. morbida* (Gm-10) used in experiments 1–3 was originally isolated from TCD-symptomatic trees in Tennessee (Hadziabdic et al., 2014) and obtained courtesy of the laboratory collection of Dr. Denita Hadziabdic-Guerry (UT-Knoxville). To inoculate wood disks with *G. morbida,* they were placed on cultures of Gm-10 growing on 1/8-strength potato dextrose agar (4.9 g PDA powder + 13.1 g agar per 1 L H_2O) in vented, high-profile dimension polystyrene petri dishes (100-mm diameter 26-mm deep, Thermo Fisher Scientific, Waltham, MA, United States). Cultures of *G. morbida* were allowed to grow until colony diameter matched the diameter of the wood disks (8–21 days).

Humidity Chambers

Four fungal competition experiments were conducted in the dark. Humidity chambers with different expected equilibrium relative humidity and wood MC were constructed by preparing supersaturated salt solutions in 250-ml beakers and placing one beaker of each solution inside of a tightly sealed six-quart plastic storage container (Simpson, 1973; Greenspan, 1977). Wood disks were placed inside of sterile standard-size (100-mm diameter by 17-mm deep) polystyrene petri dishes, which were placed inside the humidity chambers with the beakers containing the salt solutions. In all experiments, wood disks that were from the same parts of the same branch were distributed equally and randomly among humidity treatments to obtain independent data on survival of fungi from each portion of the branch or branches for each treatment. Temperature was maintained at 30°C by keeping the plastic storage containers containing the petri dishes and beakers with salt solutions inside a Precision 818 low-temperature incubator (Thermo Fisher), or at 23°C by keeping the containers in a laboratory cabinet. Most treatments were conducted at the optimal growth temperature for *G. morbida* (30°C) to provide conservative inferences on the effect of wood moisture on its competitive success. In Experiments 3 and 4 described below, an additional temperature treatment at 23°C was included to increase the relative humidity and, thereby, increase wood MC and decrease the competitive advantage of *G. morbida*.

Experiment 1: High-Heat Pretreatment of Wood Disks and Inoculation With *G. morbida*

Branches were collected from Purdue University Martell Forest in West Lafayette, IN (40°25′60.0″N, 87°02′07.3″W), where neither *G. morbida* or *P. juglandis* have been detected, and allowed to dry on a lab bench for approximately 30 days prior to cutting them into disks. Walnut branch disks from Indiana were wrapped in aluminum foil and placed in an oven at 90°C for 48 h to dry and kill most fungi. The heat-treated disks were then transferred to cultures of *G. morbida*. After 24 h, disks with visible growth of fungi other than *G. morbida* were discarded, and the remaining inoculated disks were transferred to sterile plastic petri dishes. Discarding disks with substantial growth of other fungi left a slightly unbalanced sample size across treatments: LiCl (n = 11 inoculated wood disks), KOAc (n = 9), $MgNO_3$ (n = 9), and NH_4Cl (n = 11). Disks were then allowed to equilibrate and incubate in the chambers at 30°C for 48 days.

At the conclusion of the incubation period, disks were weighed to record wet mass (m_i), and fungal growth was examined under a stereomicroscope (e.g., **Figures 1B,F**). Fungi growing on the surface of each wood disk were categorized into morphospecies while examining them under 400× magnification. Presence and absence of each morphospecies were recorded for each disk (**Figure 1**). Mycelia or spores from the most frequently encountered and dominant morphospecies

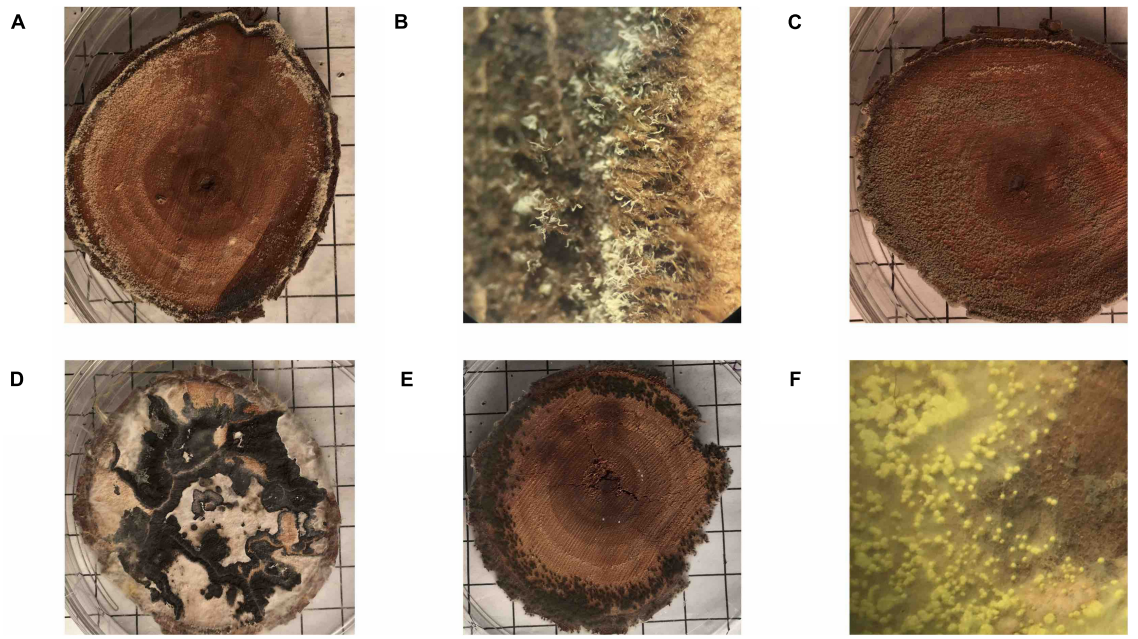

FIGURE 1 | Representative images of wood disks colonized by fungi from Experiments 1 **(A,C–E)** and 4 **(B,F)**. Wood disk colonized by *Geosmithia morbida* **(A,B)**, *Aspergillus* sp. and *G. morbida* **(C)**, Xylariaceae sp. **(D)**, *Trichoderma* sp. **(E)**, and *Aspergillus* (both anamorph and *Eurotium* sexual stage) sp. and *Clonostachys* sp. **(F)** Each grid line is 1 cm^2 **(A,C–E)**.

were collected directly into tubes with buffer to extract DNA or cultured to obtain voucher samples. If present, white-to-pink penicilliate conidiophores that resembled those of *G. morbida* (**Figures 1A–C**) were mounted on slides and examined at 1000× to confirm their identity. *G. morbida* was also cultured from conidiophores to verify viability of the spores across the range of final abiotic conditions. All wood disks were then dried at 70°C for at least 96 h and weighed again to record dry mass (m_f). Final wood *MC* of each individual wood disk was calculated gravimetrically according to Eckelman (1998): $MC = \frac{m_i - m_f}{m_f}$.

Experiment 2: Low-Heat Pretreatment of Wood Disks and Inoculation With *G. morbida*

Wood disks were collected, dried, inoculated, and incubated as described for Experiment 1 with the following exceptions: a less intense heat treatment (70°C for 24 h) and longer incubation period in humidity chambers (88 days) was employed to allow more fungal endophytes to persist in the wood prior to being challenged with *G. morbida* and a longer period to compete in humidity chambers. The final number of disks in each treatment was balanced (n = 8 per saturated salt solution). Fungi were counted and sampled and wood MC was determined gravimetrically as described above.

Experiment 3: Lethal Heat Pretreatment of Wood Disks and Inoculation With *G. morbida*

A control experiment was designed to demonstrate that fungi capable of growing and competing with *G. morbida* could be completely removed from the wood at sufficiently high temperature. Growth and survival of *G. morbida* at all MCs in the absence of other fungi would suggest that the low survival of *G. morbida* at higher moisture levels in Experiments 1, 2, and 4 was due to competition with other fungi. To ensure full removal of other fungi that had already colonized the wood disks, they were heat-treated at 105°C for 2 days. To ensure colonization by *G. morbida*, disks were left on cultures for 10 days before being transferred to humidity chambers. Two *G. morbida*-inoculated disks and four control disks were included in each of the four humidity chamber treatments to verify *G. morbida* survival and the absence of other fungi. The saturated salt solutions, temperature, and incubation times employed were LiCl, NaCl, or no salt, incubated for 57 days at 30°C. An additional no-salt treatment was incubated at room temperature (23°C), and expected to result in higher relative humidity and final MC. Fungi were sampled and wood MC was determined as described above.

Experiment 4: Fungal Competition in Wood Naturally Colonized by *G. morbida*

Branches that were already naturally colonized with *G. morbida* were collected from a TCD disease epicenter. The trees grew on a privately owned plantation of black walnut in Walla Walla, WA, United States. Six branches were collected from six TCD-symptomatic trees and shipped to Purdue University under permit (17-IN-20-007). Two freshly cut disks from each branch were placed directly in sterile petri dishes inside of each of the humidity chambers (n = 18 per treatment). Salt solutions and temperatures employed were the same as described

above for Experiment 3. Fully saturated wood disks were allowed to incubate for 111 days to reach their EMC. Fungi were sampled and wood MC determined by drying disks at 100°C for 72 h.

Molecular Identification of Fungi

DNA extraction, polymerase chain reaction (PCR) of the ITS region, and sequence assembly were performed as described previously (Williams and Ginzel, in press). ITS sequences were extracted with ITSX and assigned to genera through Tree-Based Assignment Selector (TBAS; Miller et al., 2015; Carbone et al., 2019) on DeCIFR public high-performance computing clusters (Center for Integrated Fungal Research, North Carolina State University)[1]. For high-level classification, all sequences were first aligned to a reference tree for all fungi. Isolates assigned to Ascomycetes were then aligned to the tree Pezizomyctonia 2.1, whereas Basidiomycetes were assigned taxonomy with the RDP Bayesian classifier with the Warcup database (Deshpande et al., 2016). Sequences were submitted to GenBank under accession numbers MW584687-MW584698.

Logistic Regressions

To test the hypothesis that the presence or absence of *G. morbida* and other fungi in each wood disk was significantly correlated to final MC, logistic regression and accompanying analytics were performed in R v 3.6.0 (R Core Team, 2019) using the function *glm* and tools from the package *ROCR* (Sing et al., 2005). Because we expected survival rate of each fungus to peak at an optimum MC, we also fit models that included second-order terms for MC. Second-order terms were only retained in the model if they were significant ($p < 0.05$). Drop-in-deviance χ^2 tests and area under the receiver-operating curve (AUC) were used to assess overall regression significance and fit, respectively.

Geographical Prediction of *G. morbida* Survival

To create maps of expected *G. morbida* survival across the United States for historical and future prevailing climates, we used climate layers from Multivariate Constructed Analogs (MACA) statistical downscaling method, Version 2 (Abatzoglou, 2013). We derived a map of expected EMC from MACA by first calculating monthly average humidity and temperatures from monthly minimums and maximums for 5 months (i.e., May, June, July, August, and September) between 1995 and 2004. This time period from late spring to early fall corresponds to the time when *P. juglandis*, the vector of *G. morbida*, is most active. Next, we inputted monthly averages into Simpson's (1973) model for wood moisture sorption with parameters estimated by Glass and Zelinka (2010). The Glass and Zelinka (2010) sorption isotherm model used to calculate *EMC* as a function of ambient air temperature (t, °C) and relative humidity (h, decimal) is given by the following system of equations with constants from Simpson (1973):

$$EMC = \frac{18}{W}\left(\frac{Kh}{1-Kh} + \frac{KK_1h + 2K_1K_2K^2h^2}{1 + KK_1h + K_1K_2K^2h^2}\right)$$

$$W = 349 + 1.29t + 0.0135t^2$$

$$K = 0.805 + 0.000736t - 0.00000273t^2$$

$$K_1 = 6.27 - 0.00938t - 0.000303t^2$$

$$K_2 = 1.91 + 0.0407t - 0.000293t^2$$

For each year between 1995 and 2004, expected *G. morbida* survival from May to September was calculated from the best logistic model fit to Experiment 4 as a function of EMC from the Glass and Zelinka (2010) model. Expected survival rates for each month (between 0 and 1) were then multiplied across all 5 months to obtain a conservative, cumulative expected probability of survival for each year. Finally, cumulative probabilities of survival for each year were averaged across ten years (1995–2004) for historical analysis. For future climate, we used MACA data generated by the Geophysical Fluids Dynamic Laboratory Earth System Models II (GFDL-ESM2M) under the Representative Concentration Pathway low- (RCP4.5) and high-emission (RCP8.5) scenarios for 10 (2031) and 50 years (2071) into the future. RCP scenarios are coded by the amount of thermal radiation (i.e., 4.5 W/m^2 vs. 8.5 W/m^2) that is expected to be absorbed and retained by the atmosphere in year 2100. According to the United States National Oceanic and Atmospheric Administration (NOAA), the atmosphere held ~400 ppm CO_2 as of 2019[2], RCP4.5 projects ~500 ppm CO_2, and RCP8.5 projects ~800 ppm CO_2 in 2071 (IPCC, 2014).

RESULTS

Competition Experiments

Competition with other fungi limited the survival of *G. morbida* at higher wood moisture levels (**Figure 2**). *G. morbida* was released from competition at low wood moisture levels (Experiments 1 and 4; **Figures 2A,D**) or in the absence of other fungi (Experiment 3; **Figure 2C**). In general, when other fungi were present in wood disks, *G. morbida* was most successful at <5% final MC and did not grow or sporulate >30% final MC. Saturated salt solutions were effective at bringing wood disks incubated in the humidity chambers to the target range of MC.

In Experiment 1, when wood from Indiana was pretreated at a high (90°C) non-lethal temperature prior to inoculation with *G. morbida*, final MC significantly accounted for the survival and sporulation of *G. morbida* (**Figure 2A** and **Table 1**). Control disks that were not inoculated with *G. morbida* supported growth of other fungi at all final MC levels.

When wood from Indiana was pretreated at a lower (70°C) non-lethal temperature (Experiment 2), final MC

[1] decifr.hpc.ncsu.edu

[2] www.climate.gov

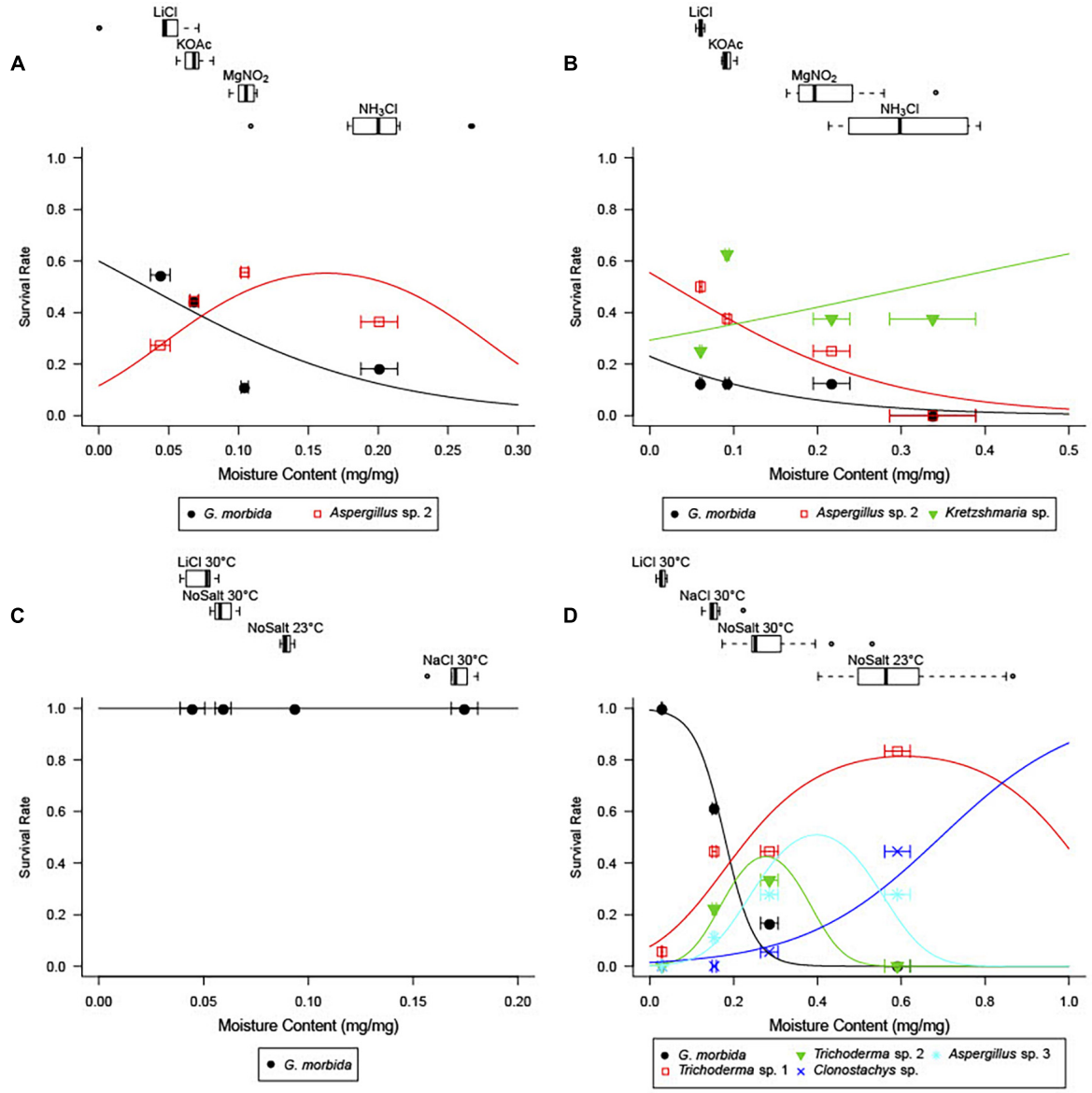

FIGURE 2 | Wood moisture content (MC) by treatment (top panels) and observed and predicted survival of fungal species as a function of wood MC from best-fit logistic regressions (bottom panels) in Experiments 1 **(A)**, 2 **(B)**, 3 **(C)**, and 4 **(D)**. For each saturated salt solution treatment, boxes-and-whiskers show percentiles of final wood MC, and points and error bars in the plotting area give observed mean survival ± SE final MC.

did not significantly account for survival of *G. morbida* ($p > 0.05$) due to the growth of other fungi at low final MC (**Figure 2B**). Fungi from Indiana wood samples in Experiments 1 and 2 included *Aspergillus* sp. (Eurotiomycetes: Eurotiales), *Nothophoma* sp. (Dothidiomycetes: Pleosporales), and *Kretzschmaria* sp. (Sordariomycetes: Xylariales) at low final MC, and *Diplodia* sp. (Dothidiomycetes: Botryosphaeriales) at intermediate final MC (**Table 2**).

However, the higher temperature and duration (105°C for 2 days) treatment was sufficient to remove fungi from the wood from Indiana prior to inoculation (Experiment 3). In the absence of other fungi, *G. morbida* grew and sporulated on all inoculated wood disks regardless of final MC (**Figure 2C**). Other fungi were not found growing on control or *G. morbida*-inoculated wood disks (data not shown).

In Experiment 4, final MC accounted for the survival and sporulation of *G. morbida* in naturally infested wood from TCD-symptomatic trees from Washington (**Figure 2D** and **Table 1**). Fungi from Washington wood samples were represented by *Aspergillus*, *Trichoderma*, and *Clonostachys* spp. (Sordariomycetes: Hypocreales) at low and intermediate MC and *Rosellinia* spp. (Sordariomycetes: Xylariales) and Basidiomycota including *Cryptococcus* (Tremellomycetes: Tremellales), *Schizophyllum*, and *Steccherinum* spp. (Agaricomycetes:

TABLE 1 | Model statistics for logistic regression of survival of fungi on final wood moisture content (MC).

Experiment	Species	p_{MC} (1st)[1]	p_{MC} (2nd)[2]	p (χ^2)†	AUC‡
1	*G. morbida*	0.037	0.005	<0.001	0.863
4	*G. morbida*	<0.001	–	<0.001	0.957
4	*Aspergillus* sp. 3	0.199	0.020	<0.001	0.721
4	*Trichoderma* sp. 1	0.111	0.025	<0.001	0.826
4	*Trichoderma* sp. 2	<0.001	0.054	<0.001	0.800
4	*Clonostachys* sp.	0.001	–	<0.001	0.859

[1,2]*p-Values for first- (1) and second-order (2) terms for MC.*
†*p-Value for overall regression from a drop-in-deviance chi-square test.*
‡*Area under receiver-operating curve goodness-of-fit statistic for overall regression.*

Polyporales) at higher final MC (**Table 2**). The best-fit model for probability of *G. morbida* survival (P) as a function of final MC was:

$$P = \frac{1}{1 + e^{2.2457 - 2.1217MC}}$$

Geographical Trends in Expected *G. morbida* Survival

When predicting survival using the model above from EMC calculated from climate models, survival for the 10-year period from 1995 to 2004 closely followed geographical patterns of TCD severity observed from that time to the present (**Figure 3A**). West of the Great Plains and east of the Cascades, predicted survival generally ranged from 50 to 80%. Epicenters of TCD in seasonally dry intermountain western and northwestern states such as Washington (WA), Utah (UT), Idaho (ID), and the native range of *P. juglandis* in arid southwestern states of Arizona (AZ) and New Mexico (NM) exceeded 70% expected *G. morbida* survival. Elsewhere in the West, TCD epicenters in Oregon (OR), California (CA), and Colorado (CO) were predicted to support ∼60% expected survival of *G. morbida*.

In the native range of *J. nigra*, expected survival for *G. morbida* was generally below 20% (**Figure 3A**). However, known TCD epicenters along the north Atlantic seaboard in eastern Pennsylvania (PA), Maryland (MD), and VA are located in some of the only pockets in the East where expected *G. morbida* survival reached ∼50% according to our model. By contrast, in Knox and Polk Cos., TN, where TCD caused a local and transient outbreak, suitability for *G. morbida* fell to 20% or below.

Under RCP 4.5, the geographical envelope in which *G. morbida* survival rates exceed 50% in the United States is expected to remain relatively stable from 2021 to 2071 (**Figures 3B,C**). However, this envelope would expand across the Great Plains and Mississippi Valley into the humid midwestern and southeastern states under RCP 8.5 (**Figures 3D,E**).

DISCUSSION

Wood Moisture, Fungal Competition, and TCD

Our research demonstrates that fungal competition mediated by abiotic conditions potentially limits the success and dispersal of *G. morbid*a and adds to a growing body of evidence that environmental conditions, including abiotic factors and the host microbiome, account for the lower severity of TCD in the native range of *J. nigra* (Griffin, 2015; Seybold et al., 2019; Onufrak et al., 2020). There were also notable differences in *G. morbida* competition and survival between branches from WA and those from IN, where xerophilic-thermotolerant fungi, including

TABLE 2 | Final MC range, molecularly and/or morphologically inferred taxonomy, and GenBank accession numbers for DNA extracted directly (D) and/or from cultures (C) from fungi growing on wood disks in competition experiments.

MC (%)		Experiment	Locale	TBAS / Warcup determination			DNA sample (*C* = Culture, *D* = Direct)	GenBank Acc. #
Low	High			Phylum*	Family	Genus (sp)		
0	26.8	1, 2 and 4	E. WA	A	Bionectriaceae	*Geosmithia morbida***	C, D	MG008828
2.7	26.7	4	E. WA	A	Aspergillaceae	*Aspergillus* sp. 1†	–	–
3.1	85.0	4	E. WA	A	Hypocreaceae	*Trichoderma* sp. 1	C, D	MW584687
4.7	34.1	1 and 2	IN	A	Aspergillaceae	*Aspergillus* sp. 2	C	MW584688
5.5	65.8	2	IN	A	Xylariaceae	*Kretzshmaria* sp.	C	MW584689
6.0	6.0	1 and 2	IN	A	Didymellaceae	*Nothophoma* sp.	C	MW584690
14.3	39.4	4	E. WA	A	Hypocreaceae	*Trichoderma* sp. 2	C	MW584691
16.4	58.4	4	E. WA	A	Aspergillaceae	*Aspergillus* sp. 3†	–	–
16.7	16.7	4	E. WA	A	Hyaloscyphaceae	*Hyaloscypha* sp.	D	MW584692
17.2	86.6	4	E. WA	A	Bionectriaceae	*Clonostachys* sp.	C, D	MW584693
17.9	52.9	4	E. WA	B	Tremellaceae	*Cryptococcus* sp.	D	MW584694
23.3	23.3	4	E. WA	B	Schizophyllaceae	*Schizophyllum* sp.	C, D	MW584695
25.6	25.6	4	IN	A	Botryosphaeriaceae	*Diplodia* sp.	C	MW584696
56.1	56.1	4	E. WA	A	Xylariaceae	*Rosellinia* sp.	D	MW584697
56.2	62.8	4	E. WA	B	Steccherinaceae	*Steccherinum* sp.	D	MW584698

**Ascomycota (A) and Basidiomycota (B).*
***Geosmithia morbida reisolated from wood disks were BLAST-aligned to sequences from original cultures used for inoculations.*
†*Isolate taxonomy determined by morphology without the aid of molecular data.*

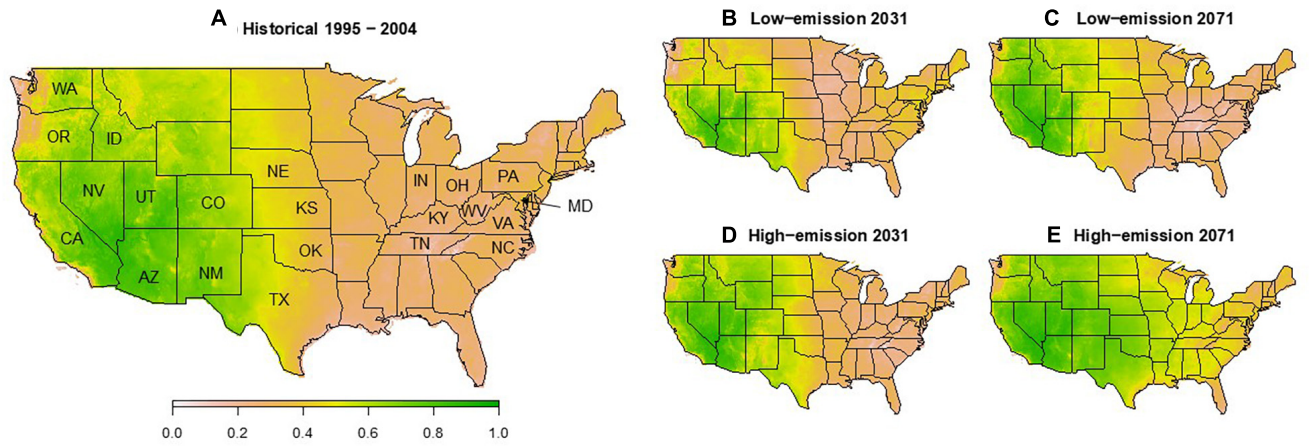

FIGURE 3 | Annotated map of regions and States of the United States referred to in the text and modeled survival of *G. morbida* as a function of equilibrium moisture content (EMC) for average historical **(A)** and future low- (**B,C**, RCP4.5) and high-emission (**D,E**, RCP8.5) climate scenarios 20 **(B,D)** and 50 years **(C,E)** into the future. Survival for each year was obtained by multiplying monthly survival estimates from a logistic regression fit to results from Experiment 4 for May through September. For historical survival **(A)**, yearly survival estimates were averaged across the 10-year timespan. Monthly average EMC was calculated using the model of Glass and Zelinka (2010) as a function of monthly average temperature and humidity averaged from Multivariate Constructed Analogs (MACA) statistical downscaling method, Version 2 (Abatzoglou, 2013) and Geophysical Fluids Dynamic Laboratory Earth System Models II (GFDL-ESM2M) under the Representative Concentration Pathway scenarios (IPCC, 2014).

Xylariaceae and *Aspergillus* spp., outcompeted *G. morbida* at low moisture. These fungi survived temperatures up to 70° and even 90°C (*Aspergillus* sp.) for 48 h. Prior colonization of the substrate by these fungi could have prevented *G. morbida* from colonizing wood disks at lower moisture levels. These findings raise the possibility that other fungi in walnut wood inhibit colonization and growth of *G. morbida* under climatic conditions that would otherwise favor the development of disease and could have important management implications under future climate.

In ambrosia beetle galleries, *Aspergillus* spp. are known to be parasites of beetle–fungal mutualisms, where they outcompete symbiotic fungi, decrease fecundity, or cause disease of beetles (Moore, 1971, 1973; Nuotclà et al., 2019). This exploitation is more successful when physicochemical conditions favor *Aspergillus* spp. over ambrosia fungi (Ranger et al., 2018). *Aspergillus* sp. outcompeted *G. morbida* in our experiments, suggesting it could also interfere with the mutualism between *G. morbida* and *P. juglandis*.

The ability of *G. morbida* to outcompete *Trichoderma* spp. and other fast-growing fungi at low wood moisture has potentially important implications for efforts to employ them as biological control agents (Gazis et al., 2018). Both *Trichoderma* spp. from WA grew well and partly outcompeted *G. morbida* at 15% MC, which is equivalent to levels in air-dried walnut wood in the Midwest (Williams and Ginzel, unpublished data). However, *G. morbida* was still observed successfully growing and sporulating more frequently than either *Trichoderma* spp. on wood disks at 15% MC (*cf.* Gazis et al., 2018). Our findings support exercising caution when drawing biological inferences from competition assays conducted in standard laboratory media to inform management decisions. When the target organism is a specialist, stress-tolerant, or ruderal species, such laboratory assays are likely to favor competitive, resource-demanding putative antagonists when the target organism would otherwise outcompete them under realistic field conditions (Newcombe, 2011; Fierer, 2017; Whitaker and Bakker, 2019).

Mapping the expected survival of *G. morbida* across the United States based on EMC reproduced with high fidelity the historical geography of well-known TCD epicenters which have been reviewed elsewhere (Seybold et al., 2019). Our experiments suggest that the higher EMC in walnut wood in the Midwest, Appalachia, and Atlantic United States limits the rates of successful establishment and spread of *G. morbida* due to competition with other fungi. In parts of MD, VA, PA, Ohio (OH), and IN, expected survival of *G. morbida* was higher than the rest of the native range of *J. nigra*, but below 50%. In these locations, *P. juglandis* and/or *G. morbida* have been detected transiently or incidentally since the early to mid-2010s without the accompanying widespread decline and mortality of *J. nigra*, indicating less success in these areas than in the western United States. We infer that areas of transient TCD outbreaks in eastern TN and western North Carolina (NC) that occurred following years of below-average precipitation (Griffin, 2015) have nevertheless been historically unfavorable for *G. morbida*. However, this prediction that wood moisture and fungal competition limit *G. morbida* and TCD severity will require future validation through field studies of galleries in branches of mature trees.

Drought and above-average temperatures may have increased host stress and susceptibility, leading to successful attack and colonization by *P. juglandis* as suggested by Griffin (2015). Even though the expected survival of *G. morbida* is extremely low in Appalachia, TN and neighboring parts of NC experienced severe and extreme drought starting in March of 2007 that

persisted in Knoxville, TN, until November 2008 [Palmer drought severity index, Palmer, 1965; National Oceanic and Atmospheric Administration (NOAA), 2020]. During this time, there was also a drought in CA that persisted into the end of 2009 [National Oceanic and Atmospheric Administration (NOAA), 2020]. These conditions likely led to physiological stress and could have facilitated low bark moisture and heightened susceptibility of *Juglans* spp. to attack in the years leading up to outbreaks of TCD that were detected in these areas in 2010.

The dependence of *G. morbida* on low-moisture wood for competitive success over other wood-inhabiting fungi may also partly explain the severity of TCD in urban and periurban forests and plantations (Seybold et al., 2019). Closed canopies provide a cool, humid microclimate, which may favor natural competitors of *G. morbida* in walnut wood. By comparison, the canopies of trees in plantations are likely to provide a more diminished effect on moisture retention compared to natural forests. In urban areas, relative humidity would be expected to be even lower because trees are even more widely spaced and heat islands generate higher temperatures (Imhoff et al., 2010). Forest diversity, management activities, buildup of other host-specific biotic disturbance agents, or abundance of opportunistic pathogens (Williams and Ginzel, in press) could also partly account for the higher incidence of TCD in plantations and urban forests. Nevertheless, wood MC is not the only abiotic factor likely to limit the potential geographic range of *G. morbida* and *P. juglandis* in *J. nigra* (Kolařík et al., 2011; Sitz et al., 2017). Most importantly, climatic differences may impact the flight activity and survival of *P. juglandis* (Luna et al., 2013; Hefty et al., 2017, 2018; Chen et al., 2020). Within the native range of black walnut, it is also possible that xerophilic and thermotolerant fungi such as Xylariaceae and *Aspergillus* spp. from this study might outcompete *G. morbida* and thereby limit the spread of TCD.

Linking the geographical limitations of the potential range of *G. morbida* in the native range of *J. nigra* to the limited reproduction and dispersal of *P. juglandis* rests on the assumptions that the symbiosis is truly mutualistic. Evidence for a causal link between MC and TCD severity would be further strengthened if this mutualism was found to be obligate. Primary symbiotic fungi not only weaken hosts to facilitate mass attack by bark beetles but also provide nutritional and/or detoxifying functions and/or supplement primary and secondary metabolic processes by producing or providing precursors to bark beetle pheromones and hormones (Six, 2003, 2013). For these reasons, bark beetles typically have greatly decreased fecundity or fail to reproduce without their primary fungal symbiont (Six, 2003). If *G. morbida* provided such benefits to *P. juglandis*, the beetle would be expected to have lower establishment success in areas where *G. morbida* is unable to compete with other locally adapted fungi unless alternative symbionts were available (Six and Bentz, 2007).

Our mapping of expected survival of *G. morbida* across historic and future climatic conditions also rests on the additional key assumption that MC of inner bark and outer sapwood fully equilibrate to ambient conditions within the timeframe of the *P. juglandis* lifecycle. Woody tissues lose moisture quickly following successful attacks by bark beetles and other wood-boring insects (Nikolov and Encev, 1967; Pinard and Huffman, 1997; Magnussen and Harrison, 2008; Negi and Joshi, 2009; Lawes et al., 2011). Under constant environmental conditions, EMC of bark also reflects that of the wood (Martin, 1967) across angiosperms and gymnosperms (Reeb and Brown, 2007; Glass and Zelinka, 2010). Compared to other woody tissues, bark is by far the fastest to equilibrate its moisture level to ambient conditions (Negi and Joshi, 2009). Furthermore, humidity is low and vapor pressure deficit is high during spring and summer in the western United States, and senescent bark tissues are therefore likely to dry faster west of the Great Plains.

Natural History and Implications for Forest Health in a Changing Climate

Pityophthorus juglandis and *G. morbida* have a co-evolved history in native forest ecosystems of the western and southwestern United States, where they would be presumed to be coadapted with their ancestral host, *J. major* (Seybold et al., 2012; Hadziabdic et al., 2014; Zerillo et al., 2014; Rugman-Jones et al., 2015). An ancestral *Juglans* sect. *Rhysocaryon* sp. diverged into *J. major*, *J. nigra*, and other species during a climatologically cooler period, 2.6–5.3 Ma (Stone et al., 2009; Mu et al., 2020; Song et al., 2020). *J. nigra* would then have radiated across humid eastern North America during interglacial periods. Over the last 10,000 years, *J. major*, *P. juglandis*, and *G. morbida* were restricted to moist canyons and cooler montane regions of the arid southwestern United States and Mexico (Little, 1976), and TCD was likely precluded from the current range of *J. nigra* by a lack of connectivity in host populations as well as an unfavorable moisture regime for the fungus. Across the state of Kansas alone, relative humidity varies twofold from ∼40% near the Colorado border in the West to ∼80% along the Missouri River [National Oceanic and Atmospheric Administration (NOAA), 2021], which corresponds to ∼7.5 and 15.6% EMC (Glass and Zelinka, 2010) at the thermal optimum for *G. morbida* growth of 30°C (Kolařík et al., 2011).

However, in the far western portion of its range, *J. nigra* is a strictly riparian species, much like its western relatives including *J. microcarpa* in Texas (TX) and Oklahoma (OK). This adaptation for riparian areas, along with the activities of humans who used black walnut for food, fiber, and fuel, likely permitted eastern–western connectivity between *J. nigra*, *J. major* and *J. microcarpa* over the last 10,000 years. Evidence that western populations of *J. nigra* have the greatest resistance to *G. morbida* provides support for interceding periods of genetic connectivity with *J. major* and periodic pressure from TCD in western *J. nigra* (Sitz et al., 2021). Transient periods of connectivity favored by shifting climatic conditions may have facilitated gene flow through hybridization zones and provided a corridor for pest-pathogen complexes such as TCD to reach far-western *J. nigra* populations in the Great Plains.

During the last 200 years, the introduction of evolutionarily naïve (Ploetz et al., 2013) eastern *J. nigra* families to regions where environmental conditions remain favorable to the development of TCD may have led to runaway mortality in urban forests and plantations in the western United States (Tisserat et al., 2011;

Seybold et al., 2019; Moricca et al., 2020). Moreover, the failure of *P. juglandis* to successfully establish in the native range of *J. nigra* despite incidental introductions and high host susceptibility may be due to unfavorable conditions for its symbiont (Utley et al., 2013; Moore et al., 2019), in addition to differences in temperature and seasonal precipitation that may affect beetle flight, dispersal, and survival (Luna et al., 2013; Hefty et al., 2017, 2018; Chen et al., 2020).

Conclusion and Relevance to Other Pathosystems

The geographical and realized host ranges of destructive, native, and non-native forest insects will continue to expand as global temperatures rise and climates shift in future decades (Cullingham et al., 2011; Ramsfield et al., 2016; Pureswaran et al., 2018). Such expansions are strongly determined by the environmental conditions that support the growth and reproduction of beetles and their symbiotic fungi (Six and Bentz, 2007). Based on our findings, these conditions include MC and its influence on competition between *G. morbida* and secondary fungi in walnut wood.

The effect of climatic conditions on fungal competition and dispersal may be applied to other emergent beetle-fungal disease complexes, but its relevance will depend on the nature of the symbiosis. Other factors determining the relevance of fungal competition in other pathosystems include whether the fungus is obligate for the beetle, availability of alternative fungal symbionts (Six and Bentz, 2007), strength of the pathogen, and the ecophysiology of the fungal symbiont and competing fungi. *Geosmithia morbida* is highly xerotolerant (Williams and Newcombe, 2017), while other primary fungal symbionts of bark beetles in the Ophiostomatales and Microascales may be less xerotolerant (Kirisits, 2013). These fungi may also vary in their ability to withstand desiccation (Temple et al., 1997) and/or more highly virulent (Caballero et al., 2019) and, thus, less likely to be limited by other fungi or the presence of moderate wood moisture.

Juglans nigra is among the most valuable hardwood species native to the eastern United States (Duval et al., 2013), with an estimated value of over USD 500 billion in merchantable timber alone (Newton and Fowler, 2009). Our study of fungal competition in walnut wood indicates that TCD presents a risk to the long-term sustainability of *J. nigra* within its native range. In light of these findings, investigations of bark beetle–fungal mutualisms will be critical to build a better understanding of the joint influence that climate and biotic interactions have on the reproductive success of pathogens and their vectors and forest disease epidemiology.

DATA AVAILABILITY STATEMENT

The datasets presented in this study can be found in online repositories. The names of the repository/repositories and accession number(s) can be found below: https://www.ncbi.nlm.nih.gov/genbank/, accession numbers MW584687-MW584698. All data and R scripts are available at: https://github.com/readingradio/WilliamsGinzel.TCD.Xerotolerance.2021.

AUTHOR CONTRIBUTIONS

GW and MG conceived of the project and wrote the manuscript. GW performed the experiments and analyses. Both the authors contributed to the article and approved the submitted version.

FUNDING

This project was supported by a Fred M. Van Eck Foundation Memorial Scholarship from Purdue University.

ACKNOWLEDGMENTS

We thank Caleb Kell, Holly Wantuch, Felix Coronado, Ashley Howes, and Dan Bollock for technical support. We also thank Bart Nelson, Brian Beheler, Jim McKenna, and Dan Cassens for access to field sites, host material, and assistance. Publication of this article was funded in part by Purdue University Libraries Open Access Publishing Fund. This research was in partial fulfillment of a doctoral degree for GW from Purdue University.

REFERENCES

Abatzoglou, J. T. (2013). Development of gridded surface meteorological data for ecological applications and modelling. *Int. J. Climatol.* 33, 121–131. doi: 10.1002/joc.3413

Bright, D. E. (1981). Taxonomic monograph of the genus *Pityophthorus* eichoff in North and Central Americs (Coleoptera: Scolytidae). *Mem. Entomol. Soc. Canada* 113, 1–378. doi: 10.4039/entm113118fv

Caballero, J. R. I., Jeon, J., Lee, Y. H., Fraedrich, S., Klopfenstein, N. B., Kim, M. S., et al. (2019). Genomic comparisons of the laurel wilt pathogen, *Raffaelea lauricola*, and related tree pathogens highlight an arsenal of pathogenicity related genes. *Fun. Gen. Biol.* 125, 84–92. doi: 10.1016/j.fgb.2019.01.012

Carbone, I., White, J. B., Miadlikowska, J., Arnold, A. E., Miller, M. A., Magain, N., et al. (2019). T-BAS version 2.1: tree-based alignment selector toolkit for evolutionary placement of DNA sequences and viewing alignments and specimen metadata on curated and custom trees. *Microbiol. Resour. Announc.* 8:e00328-19.

Chen, Y., Aukema, B. H., and Seybold, S. J. (2020). The effects of weather on the flight of an invasive bark beetle, *Pityophthorus juglandis*. *Insects* 11, 156. doi: 10.3390/insects11030156

Cullingham, C. I., Cooke, J. E. K., Dang, S., Davis, C. S., Cooke, B. J., and Coltman, D. W. (2011). Mountain pine beetle host-range expansion threatens the boreal forest. *Mol. Ecol.* 20, 2157–2171. doi: 10.1111/j.1365-294x.2011.05086.x

Deshpande, V., Wang, Q., Greenfield, P., Charleston, M., Porras-Alfaro, A., Kuske, C. R., et al. (2016). Fungal identification using a Bayesian classifier and the Warcup training set of internal transcribed spacer sequences. *Mycologia* 108, 1–5. doi: 10.3852/14-293

Duval, R. P., McConnell, T. E., and Hix, D. M. (2013). Annual change in Ohio hardwood stumpage prices, 1960 to 2011. *For. Prod. J.* 64, 19–25. doi: 10.13073/FPJ-D-13-00075

Eckelman, C. A. (1998). *The Shrinking and Swelling of Wood and Its Effect on Furniture.* Purdue University Cooperative Extension Service. FNR 163. Available online at: https://www.extension.purdue.edu/extmedia/fnr/fnr-163.pdf (accessed August 17, 2021).

Fierer, N. (2017). Embracing the unknown: disentangling the complexities of the soil microbiome. *Nat. Rev. Microbiol.* 15, 579–590. doi: 10.1038/nrmicro.2017.87

Francke-Grosmann, H. (1967). "Ectosymbiosis in wood-inhabiting insects," in *Symbiosis*, ed. S. M. Henry (New York, NY: Academic Press), 141–205. doi: 10.1016/b978-1-4832-2758-0.50010-2

Gazis, R., Poplawski, L., Klingeman, W., Boggess, S. L., Trigiano, R. N., Graves, A. D., et al. (2018). Mycobiota associated with insect galleries in walnut with thousand cankers disease reveals a potential natural enemy against *Geosmithia morbida*. *Fungal Biol.* 122, 241–253. doi: 10.1016/j.funbio.2018.01.005

Glass, S. V., and Zelinka, S. L. (2010). "Chapter 4: moisture relations and physical properties of wood," in *Forest Products Laboratory. Wood Handbook: Wood as an Engineering Material, Centennial*, Vol. 2010, ed. General Technical Report FPL-GTR-190 (Madison, WI: U.S. Dept. of Agriculture, Forest Service, Forest Products Laboratory), 4.1–4.19.

Greenspan, L. (1977). Humidity fixed points of binary saturated aqueous solutions. *J. Res. Natl. Bur. Stand.* 81, 89–96. doi: 10.6028/jres.081a.011

Griffin, D. M. (1977). Water potential and wood-decay fungi. *Annu. Rev. Phytopathol.* 15, 315–326. doi: 10.1146/annurev.py.15.090177.001535

Griffin, G. J. (2015). Status of thousand cankers disease on eastern black walnut in the eastern United States at two locations over 3 years. *For. Pathol.* 45, 203–214. doi: 10.1111/efp.12154

Hadziabdic, D., Vito, L. M., Windham, M. T., Pscheidt, J. W., Trigiano, R. N., and Kolarik, M. (2014). Genetic differentiation and spatial structure of *Geosmithia morbida*, the causal agent of thousand cankers disease in black walnut (*Juglans nigra*). *Curr. Genet.* 60, 75–87. doi: 10.1007/s00294-013-0414-x

Harris, R. F. (1981). "Effect of water potential on microbial growth and activity," in *Water Potential Relations Soil Microbiology*, Vol. 9, eds J. F. Parr, W. R. Gardner, and L. F. Elliot (Madison, WI: Soil Science Society of America), 23–95. doi: 10.2136/sssaspecpub9

Hefty, A. R., Aukema, B. H., Venette, R. C., Coggeshall, M. V., McKenna, J. R., and Seybold, S. J. (2018). Reproduction and potential range expansion of walnut twig beetle across the Juglandaceae. *Biol. Invasions* 20, 2141–2155. doi: 10.1007/s10530-018-1692-5

Hefty, A. R., Seybold, S. J., Aukema, B. H., and Venette, R. C. (2017). Cold tolerance of *Pityophthorus juglandis* (Coleoptera: Scolytidae) from northern California. *Environ. Entomol.* 46, 967–977. doi: 10.1093/ee/nvx090

Hofstetter, R. W., Dempsey, T., Klepzig, K., and Ayres, M. (2007). Temperature-dependent effects on mutualistic, antagonistic, and commensalistic interactions among insects, fungi and mites. *Commun. Ecol.* 8, 47–56. doi: 10.1556/comec.8.2007.1.7

Hofstetter, R. W., Dinkins-Bookwalter, J., Davis, T. S., and Klepzig, K. D. (2015). "Symbiotic associations of bark beetles," in *Bark Beetles: Biology and Ecology of Native and Invasive Species*, eds F. Vega and R. Hofstetter (San Diego, CA: Academic Press), 209–245. doi: 10.1016/b978-0-12-417156-5.00006-x

Imhoff, M. L., Zhang, P., Wolfe, R. E., and Bounoua, L. (2010). Remote sensing of the urban heat island effect across biomes in the continental USA. *Remote Sens. Environ.* 114, 504–513. doi: 10.1016/j.rse.2009.10.008

IPCC (2014). *Climate Change 2014: Synthesis Report. Contribution of Working Groups I, II and III to the Fifth Assessment Report of the Intergovernmental Panel on Climate Change*, eds R. K. Pachauri and L. A. Meyer (Geneva: IPCC), 151.

Jacobi, W. R., Hardin, J. G., Goodrich, B. A., and Cleaver, C. M. (2012). Retail firewood can transport live tree pests. *J. Econ. Entomol.* 105, 1645–1658. doi: 10.1603/ec12069

Juzwik, J., Moore, M., Williams, G., and Ginzel, M. (2020). "Assessment and etiology of thousand cankers disease within the native range of black walnut (*Juglans nigra*)," in *Forest Health Monitoring: National Status, Trends, and Analysis 2019. Gen. Tech. Rep. SRS-250*, eds K. M. Potter and B. L. Conkling (Asheville, NC: US Department of Agriculture, Forest Service, Southern Research Station), 169–178.

Kirisits, T. (2013). "12 Dutch Elm disease and other ophiostoma diseases," in *Infectious Forest Diseases*, eds P. Gonthier and G. Nicolotti (Wallingford: CAB International), 256. doi: 10.1079/9781780640402.0256

Kolařík, M., Freeland, E., Utley, C., and Tisserat, N. (2011). *Geosmithia morbida* sp. nov., a new phytopathogenic species living in symbiosis with the walnut twig beetle (*Pityophthorus juglandis*) on Juglans in USA. *Mycologia* 103, 325–332. doi: 10.3852/10-124

Lawes, M. J., Richards, A., Dathe, J., and Midgley, J. J. (2011). Bark thickness determines fire resistance of selected tree species from fire-prone tropical savanna in north Australia. *Plant Ecol.* 212, 2057–2069. doi: 10.1007/s11258-011-9954-7

Little, E. L. (1976). *Atlas of United States Trees: Minor Western Hardwoods*, Vol. 3. Washington, DC: U.S. Department of Agriculture, Forest Service.

Luna, E. K., Sitz, R. A., Cranshaw, W. S., and Tisserat, N. A. (2013). The effect of temperature on survival of *Pityophthorus juglandis* (Coleoptera: Curculionidae). *Environ. Entomol.* 42, 1085–1091. doi: 10.1603/en13151

Magnussen, S., and Harrison, D. (2008). Temporal change in wood quality attributes in standing dead beetle-killed lodgepole pine. *For. Chron.* 84, 392–400. doi: 10.5558/tfc84392-3

Manzoni, S., Schimel, J. P., and Porporato, A. (2012). Responses of soil microbial communities to water stress: results from a meta-analysis. *Ecology* 93, 930–938. doi: 10.1890/11-0026.1

Martin, R. E. (1967). Interim equilibrium moisture content values of bark. *For. Prod. J.* 17, 30–31.

Miller, M. A., Schwartz, T., Pickett, B. E., He, S., Klem, E. B., Scheuermann, R. H., et al. (2015). A RESTful API for access to phylogenetic tools via the CIPRES science gateway. *Evol. Bioinform. Online* 11, 43–48. doi: 10.4137/EBO.S21501

Mitton, J. B., and Ferrenberg, S. M. (2012). Mountain pine beetle develops an unprecedented summer generation in response to climate warming. *Am. Nat.* 179, E163–E171.

Moore, G. E. (1971). Mortality factors caused by pathogenic bacteria and fungi of the southern pine beetle in North Carolina. *J. Invertebr. Pathol.* 17, 28–37. doi: 10.1016/0022-2011(71)90121-2

Moore, G. E. (1973). Pathogenicity of three entomogenous fungi to the southern pine beetle at various temperatures and humidities. *Environ. Entomol.* 2, 54–57. doi: 10.1093/ee/2.1.54

Moore, M., Juzwik, J., Miller, F., Roberts, L., and Ginzel, M. D. (2019). Detection of *Geosmithia morbida* on numerous insect species in four eastern states. *Plant Heal. Prog.* 20, 133–139. doi: 10.1094/php-02-19-0016-rs

Moricca, S., Bracalini, M., Benigno, A., Ghelardini, L., Furtado, E. L., Marino, C. L., et al. (2020). Observations on the non-native thousand cankers disease of walnut in Europe's southernmost outbreak. *Glob. Ecol. Conserv.* 23:e01159. doi: 10.1016/j.gecco.2020.e01159

Mu, X.-Y., Tong, L., Sun, M., Zhu, Y.-X., Wen, J., Lin, Q.-W., et al. (2020). Phylogeny and divergence time estimation of the walnut family (Juglandaceae) based on nuclear RAD-Seq and chloroplast genome data. *Mol. Phylogenet. Evol.* 147:106802. doi: 10.1016/j.ympev.2020.106802

National Oceanic and Atmospheric Administration (NOAA) (2020). *Historical Palmer Drought Indices*. Available online at: https://www.ncdc.noaa.gov/temp-and-precip/drought/historical-palmers/ (accessed February 11, 2020).

National Oceanic and Atmospheric Administration (NOAA) (2021). *Climate Data Online*. Available online at: https://www.ncdc.noaa.gov/cdo-web/ (accessed July 27, 2021).

Negi, S., and Joshi, V. D. (2009). Role of moisture content in rendering the sal tree component susceptible to the borer (*Hoplocerambyx spinicornis*) attack. *Asian J. Anim. Sci.* 3, 190–192.

Newcombe, G. (2011). "Endophytes in forest management: four challenges," in *Endophytes of Forest Trees*, eds A. M. Pirttilä and A. C. Frank (Berlin: Springer), 251–262. doi: 10.1007/978-94-007-1599-8_16

Newton, L., and Fowler, G. (2009). *Pathway Assessment: Geosmithia sp. and Pityophthorus juglandis Blackman movement from the western into the eastern United States*. Available online at: https://www.uaex.edu/environment-nature/ar-invasives/invasive-diseases/docs/Thousand-Cankers%20Disease.pdf (accessed August 17, 2021).

Nikolov, S., and Encev, E. (1967). *Moisture Content of Green Wood*. Sofia: Zemizdat.

Nuotclà, J. A., Biedermann, P. H. W., and Taborsky, M. (2019). Pathogen defence is a potential driver of social evolution in ambrosia beetles. *Proc. R. Soc. B* 286:20192332. doi: 10.1098/rspb.2019.2332

Onufrak, A. J., Williams, G. M., Klingeman, W. E., Cregger, M. A., Klingeman, D. M., DeBruyn, J. M., et al. (2020). Regional differences in the structure of *Juglans nigra* phytobiome reflect geographical differences in thousand cankers disease severity. *Phytobiomes J.* 4, 388–404. doi: 10.1094/PBIOMES-05-20-0044-R

Palmer, W. C. (1965). *Meteorologic Drought*. U.S. Weather Bureau, Research Paper No. 45. Washington, DC: U.S. Weather Bureau.

Pinard, M. A., and Huffman, J. (1997). Fire resistance and bark properties of trees in a seasonally dry forest in eastern Bolivia. *J. Trop. Ecol.* 13, 727–740. doi: 10.1017/S0266467400010890

Ploetz, R. C., Hulcr, J., Wingfield, M. J., and de Beer, Z. W. (2013). Destructive tree diseases associated with ambrosia and bark beetles: black swan events in tree pathology? *Plant Dis.* 97, 856–872. doi: 10.1094/PDIS-01-13-0056-FE

Pureswaran, D. S., Roques, A., and Battisti, A. (2018). Forest insects and climate change. *Curr. For. Rep.* 4, 35–50. doi: 10.1007/s40725-018-0075-6

R Core Team (2019). *R: A Language and Environment for Statistical Computing*. Vienna: R Foundation for Statistical Computing.

Ramsfield, T. D., Bentz, B. J., Faccoli, M., Jactel, H., and Brockerhoff, E. G. (2016). Forest health in a changing world: effects of globalization and climate change on forest insect and pathogen impacts. *For. An Int. J. For. Res.* 89, 245–252. doi: 10.1093/forestry/cpw018

Ranger, C. M., Biedermann, P. H. W., Phuntumart, V., Beligala, G. U., Ghosh, S., Palmquist, D. E., et al. (2018). Symbiont selection via alcohol benefits fungus farming by ambrosia beetles. *Proc. Natl. Acad. Sci. U.S.A.* 115:201716852. doi: 10.1073/pnas.1716852115

Rayner, A. D. M., and Boddy, L. (1988). *Fungal Decomposition of Wood: Its Biology and Ecology*. Hoboken, NJ: Wiley and Sons, doi: 10.1086/416403

Reeb, J., and Brown, T. (2007). *Air- and Shed-Drying Lumber. Oregon State University Extension EM 8612-E*. Available online at: https://catalog.extension.oregonstate.edu/sites/catalog/files/project/pdf/em8612.pdf (accessed August 17, 2021).

Ridout, M., Houbraken, J., and Newcombe, G. (2017). Xerotolerance of *Penicillium* and *Phialocephala* fungi, dominant taxa of fine lateral roots of woody plants in the intermountain Pacific Northwest. *USA. Rhizosphere* 4, 94–103. doi: 10.1016/j.rhisph.2017.09.004

Rugman-Jones, P. F., Seybold, S. J., Graves, A. D., and Stouthamer, R. (2015). Phylogeography of the walnut twig beetle, *Pityophthorus juglandis*, the vector of thousand cankers disease in North American walnut trees. *PLoS One* 10:e0118264. doi: 10.1371/journal.pone.0118264

Seybold, S. J., Coleman, T. W., Dallara, P. L., Dart, N. L., Graves, A. D., Pederson, L. A., et al. (2012). Recent collecting reveals new state records and geographic extremes in the distribution of the walnut twig beetle, *Pityophthorus juglandis* Blackman (Coleoptera: Scolytidae), in the United States. *Pan Pac. Entomol.* 88, 277–280. doi: 10.3956/2012-32.1

Seybold, S. J., Klingeman, W. E. III, Hishinuma, S. M., Coleman, T. W., and Graves, A. D. (2019). Status and Impact of Walnut twig beetle in Urban Forest, Orchard, and native forest ecosystems. *J. For.* 117, 152–163. doi: 10.1093/jofore/fvy081

Seybold, S. J., Penrose, R. L., and Graves, A. D. (2016). "Invasive bark and ambrosia beetles in California Mediterranean forest ecosystems," in *Insects and Diseases of Mediterranean Forest Systems*, eds T. D. Paine and F. Lieutier (Berlin: Springer), 583–662. doi: 10.1007/978-3-319-24744-1_21

Simpson, W. T. (1973). Predicting equilibrium moisture content of wood by mathematical models. *Wood Fiber Sci.* 5, 41–49.

Simpson, W. T. (1998). *Equilibrium Moisture Content of Wood in Outdoor Locations in the United States and Worldwide.* FPL-RN-0268. Madison, WI: US Dept. of Agriculture, Forest Service.

Sing, T., Sander, O., Beerenwinkel, N., and Lengauer, T. (2005). ROCR: visualizing classifier performance in R. *Bioinformatics* 21:7881.

Sitz, R., Utley, C., Hall, A., Tisserat, N., and Cranshaw, W. (2017). Trapping the Walnut twig beetle to determine flight patterns in colorado. *Southwest. Entomol.* 42, 347–356. doi: 10.3958/059.042.0204

Sitz, R. A., Luna, E., Ibarra Caballero, J., Tisserat, N., Cranshaw, W. S., McKenna, J. R., et al. (2021). Eastern black walnut (*Juglans nigra* L.) originating from native range varies in their response to inoculation with *Geosmithia morbida*. *Front. For. Global Change* 4:12. doi: 10.3389/ffgc.2021.627911

Six, D. L. (2003). Bark beetle-fungus symbioses. *Insect Symbiosis* 1, 97–114. doi: 10.1201/9780203009918.ch7

Six, D. L. (2013). The bark beetle holobiont: why microbes matter. *J. Chem. Ecol.* 39, 989–1002. doi: 10.1007/s10886-013-0318-8

Six, D. L., and Bentz, B. J. (2007). Temperature determines symbiont abundance in a multipartite bark beetle-fungus ectosymbiosis. *Microb. Ecol.* 54, 112–118. doi: 10.1007/s00248-006-9178-x

Song, Y.-G., Fragnière, Y., Meng, H.-H., Li, Y., Bétrisey, S., Corrales, A., et al. (2020). Global biogeographic synthesis and priority conservation regions of the relict tree family Juglandaceae. *J. Biogeogr.* 47, 643–657. doi: 10.1111/jbi.13766

Stepanek, L. (2020). *Walnut Twig Beetle & Thousand Cankers Disease*. Lincoln, NE. Available online at: https://nfs.unl.edu/publications/walnut-twig-beetle-nebraska (accessed June 13, 2021).

Stone, D. E., Oh, S.-H., Tripp, E. A., and Manos, P. S. (2009). Natural history, distribution, phylogenetic relationships, and conservation of Central American black walnuts (*Juglans* sect. *Rhysocaryon*). *J. Torrey Bot. Soc.* 136, 1–25. doi: 10.3159/08-ra-036r.1

Temple, B., Horgen, P. A., Bernier, L., and Hintz, W. E. (1997). Cerato-ulmin, a hydrophobin secreted by the causal agents of Dutch elm disease, is a parasitic fitness factor. *Fun. Gen. Biol.* 22, 39–53. doi: 10.1006/fgbi.1997.0991

Tisserat, N., Cranshaw, W., Leatherman, D., Utley, C., and Alexander, K. (2009). Black Walnut Mortality in Colorado caused by the walnut twig beetle and thousand cankers disease. *Plant Heal. Prog.* 11:10. doi: 10.1094/php-2009-0811-01-rs

Tisserat, N., Cranshaw, W., Putnam, M. L., Pscheidt, J., Leslie, C. A., Murray, M., et al. (2011). Thousand cankers disease is widespread in black Walnut in the Western United States. *Plant Heal. Prog.* 12:35. doi: 10.1094/PHP-2011-0630-01-BR

USGCRP (2018). "Chapter 24: Northwest," in *Impacts, Risks, and Adaptation in the United States: Fourth National Climate Assessment*, Vol. II, eds D. R. Reidmiller, C. W. Avery, D. R. Easterling, K. E. Kunkel, K. L. M. Lewis, T. K. Maycock, et al. (Washington, DC: U.S. Global Change Research Program). doi: 10.7930/NCA4.2018

Utley, C., Nguyen, T., Roubtsova, T., Coggeshall, M., Ford, T. M., Grauke, L. J., et al. (2013). Susceptibility of Walnut and Hickory species to *Geosmithia morbida*. *Plant Dis.* 97, 601–607. doi: 10.1094/PDIS-07-12-0636-RE

Weed, A. S., Ayres, M. P., and Bentz, B. J. (2015). "Population dynamics of bark beetles," in *Bark Beetles: Biology and Ecology of Native and Invasive Species*, eds F. Vega and R. W. Hofstetter (San Diego, CA: Academic Press), 209–245. doi: 10.1016/B978-0-12-417156-5.00004-6

Whitaker, B. K., and Bakker, M. G. (2019). Bacterial endophyte antagonism toward a fungal pathogen in vitro does not predict protection in live plant tissue. *FEMS Microbiol. Ecol.* 95:fiy237.

Williams, G. M., and Ginzel, M. D. (2021). Forest and plantation soil microbiomes differ in their capacity to suppress feedback between geosmithia morbida and rhizosphere pathogens of *J. nigra* seedlings. *Phytobiomes J.* (in press).

Williams, G. M., and Newcombe, G. (2017). "Xerotolerance of *Geosmithia morbida*," in *Proceedings of the 2016 Society of American Foresters National Convention*, Madison, WI. doi: 10.5849/jof.2016-108

Wood, S. L. (1982). The bark and ambrosia beetles of North and Central America (Coleoptera: Scolytidae), a taxonomic monograph. *Great Basin Nat. Mem.* 6:11356.

Zerillo, M. M., Caballero, J. I., Woeste, K., Graves, A. D., Hartel, C., Pscheidt, J. W., et al. (2014). Population structure of *Geosmithia morbida*, the causal agent of thousand cankers disease of walnut trees in the United States. *PLoS One* 9:e112847. doi: 10.1371/journal.pone.0112847

Conflict of Interest: The authors declare that the research was conducted in the absence of any commercial or financial relationships that could be construed as a potential conflict of interest.

Publisher's Note: All claims expressed in this article are solely those of the authors and do not necessarily represent those of their affiliated organizations, or those of the publisher, the editors and the reviewers. Any product that may be evaluated in this article, or claim that may be made by its manufacturer, is not guaranteed or endorsed by the publisher.

frontiers in Forests and Global Change

OPINION
published: 18 November 2021
doi: 10.3389/ffgc.2021.737445

The Future of Forest Pathology in North America

Denita Hadziabdic[1], Pierluigi Bonello[2], Richard Hamelin[3], Jennifer Juzwik[4], Bruce Moltzan[5], David Rizzo[6], Jane Stewart[7] and Caterina Villari[8]*

[1] Department of Entomology and Plant Pathology, University of Tennessee, Knoxville, Knoxville, TN, United States, [2] Department of Plant Pathology, The Ohio State University, Columbus, OH, United States, [3] Department of Forest and Conservation Sciences, The University of British Columbia, Vancouver, BC, Canada, [4] Northern Research Station, U.S. Department of Agriculture, Forest Service, St. Paul, MN, United States, [5] Forest Health Protection, U.S. Department of Agriculture, Forest Service, Washington, DC, United States, [6] Department of Plant Pathology, University of California, Davis, Davis, CA, United States, [7] Department of Agricultural Biology, Colorado State University, Fort Collins, CO, United States, [8] Warnell School of Forestry and Natural Resources, University of Georgia, Athens, GA, United States

Keywords: forest pathology, changing climate, healthy forests, invasive pathogens, insect pests, chestnut blight, Dutch elm disease, sudden oak death

HEALTHY FORESTS FOR A HEALTHY PLANET

Forests provide key ecosystem services globally, with economic values ranging from $125 to $145 trillion per year (Costanza et al., 2014). Forests are important not only for carbon sequestration goals and global biodiversity (Bonello et al., 2020a; Di Sacco et al., 2021; Palmer, 2021), but also for the economic (e.g., timber), environmental (e.g., water purification), and social (e.g., recreational activities) benefits (Trumbore et al., 2015) they provide (Bastin et al., 2019, 2020). Increasingly, forests are viewed as directly important to human health (Donovan et al., 2013); indeed, urban green environments are now considered essential in city planning (Nowak et al., 2006; Donovan and Butry, 2009; Donovan et al., 2013; Ideno et al., 2017).

The health of forests impacts their value and ability to deliver these ecosystem services. However, the definition of a healthy forest is actually quite complex and has long been debated (Raffa et al., 2009). In the absence of significant exogenous disturbances, forest ecosystems are ecologically dynamic, yet holistically stable and resilient. A healthy forest is not disease-free, but rather one that can self-perpetuate in a state of dynamic equilibrium, equivalent to a forest on its way to, or at, the climax state. A healthy forest, therefore, "encompasses a mosaic of successional patches representing all stages of the natural range of disturbance and recovery" (Trumbore et al., 2015). Indeed, a healthy forest supports pathogens and other disturbance agents that are essential for natural forest regeneration and nutrient cycling and, ultimately, increased resilience. Unfortunately, in the Anthropocene, forests have become increasingly threatened by human-mediated intensification of natural stressors, e.g., higher temperatures and lower water availability due to global warming, which make trees maladapted to their current habitats and thus more susceptible to insect pest and/or pathogen attacks (Sherwood et al., 2015).

THE ANTHROPOCENE IS DISRUPTING THE NATURAL BALANCE

Land-use changes and tree domestication aimed at large-scale plantations, often in monocultures, exacerbate susceptibility to insect pests and pathogens (Sturrock et al., 2011; Pautasso et al., 2015; Desprez-Loustau et al., 2016). With globalization proceeding unabated, natural, and planted forests are increasingly attacked by invasive alien insect pests and pathogens (Eriksson et al., 2019). Natural resources in Canada and the U.S. are becoming endangered at alarming rates because hosts that have not evolved resistance (i.e., naïve hosts) to such non-native insect pests and pathogens are inherently at risk of functional, if not actual, extinction (Pautasso et al., 2012, 2015; Santini et al., 2013; Trumbore et al., 2015; Albrich et al., 2020; Bonello et al., 2020a). While recently

OPEN ACCESS

Edited by:
Ari Mikko Hietala, Norwegian Institute of Bioeconomy Research (NIBIO), Norway

Reviewed by:
Andrin Gross, Snow and Landscape Research (WSL), Switzerland
Paolo Gonthier, University of Turin, Italy

****Correspondence:***
Denita Hadziabdic
dhadziab@utk.edu

Specialty section:
This article was submitted to Pests, Pathogens and Invasions, a section of the journal Frontiers in Forests and Global Change

Received: *08 July 2021*
Accepted: *08 October 2021*
Published: *18 November 2021*

Citation:
Hadziabdic D, Bonello P, Hamelin R, Juzwik J, Moltzan B, Rizzo D, Stewart J and Villari C (2021) The Future of Forest Pathology in North America. Front. For. Glob. Change 4:737445. doi: 10.3389/ffgc.2021.737445

accelerating, this process has been ongoing since the onset of global commerce five centuries ago. In North America, some of the past non-native introductions, for example, *Cryphonectria parasitica* (chestnut blight) (Anagnostakis, 1987), *Cronartium ribicola* (white pine blister rust—WPBR) (Kinloch, 2003; Geils et al., 2010), and *Ophiostoma ulmi* and *novo-ulmi* (Dutch elm disease) (Gibbs, 1978), have caused irreversible changes to natural forest ecosystems. Examples of tree insect pests and pathogens that have changed forest ecosystems are not limited to the distant past: the last few decades have seen the appearance of damaging tree diseases such as sudden oak death (Rizzo and Garbelotto, 2003) and laurel wilt (Ploetz et al., 2017).

In some cases, invasive pathogens affect historically and culturally significant species, such as the ʻohiʻa tree in Hawaii that is threatened by the fungal disease known as rapid ʻohiʻa death [causal agents: *Ceratocystis lukuohia* and *Ceratocystis huliohia* (Mortenson et al., 2016; Barnes et al., 2018)]. These diseases can also have very broad ecosystem repercussions and affect species that are not directly attacked by the pathogens, but depend on the services provided by trees for their survival. For example, landscape-level mortality caused by the oak wilt agent: [causal agent: *Bretziella fagacearum* (Juzwik et al., 2011)], in both rural and urban forests in the U.S., negatively impacts endangered species that depend on oaks, such as the golden-cheeked warbler in Texas (Appel and Camilli, 2010). Similarly, WPBR threatens high-elevation pines such as whitebark pine (*Pinus albicaulis*), a keystone species that provides ecosystem services such as food for grizzly bears, erosion prevention, and microhabitat provisioning for plants and animals (Keane and Arno, 1993; Tomback and Achuff, 2010). By severely damaging the self-perpetuating properties of healthy forests, newly introduced insect pests and pathogens reduce the ecological resilience of our forest landscapes (Pautasso et al., 2015; Abrams et al., 2021).

CLIMATE CHANGE IS THE CHALLENGE OF THE FUTURE

Climate change is having a compounding impact on forest health (Kolb et al., 2016; Ramsfield et al., 2016) because it makes trees maladapted to their current environments. Yet, little is known of the potential outcomes of a changing climate on forest health (Seidl et al., 2017). More prolonged and extreme periods of drought, or increasing rainfall, will likely increase the frequency of abiotic stress events making tree hosts more vulnerable to both insect pest and pathogen attack. Some of the new and future climatic conditions will also provide novel niches for non-native invasive insect pests and pathogens as well as expanding the niches of native ones. For example, *Dothistroma pini* (Dothistroma needle blight), *Nothophaeocryptopus gaeumannii* (Swiss needle cast), and *Diplodia sapinea* (Diplodia tip blight and canker) have increased in frequency and intensity, creating large-scale defoliation and mortality that is driven by new climatic conditions, whether caused by more rainfall or drought conditions depending on areas where each of these occur (Woods et al., 2005; Stone et al., 2008; Brodde et al., 2019). Moreover, climate change also causes shifts in forest tree species composition. Well-known examples include changes from large trees in conifer-dominated European mountain landscapes to those dominated by smaller, mainly broadleaved trees (Albrich et al., 2020), which fundamentally alters the underlying forest health framework. Climate shifts are also expected to result in novel ecosystems, driven by migration and species distribution expansion of both hosts and pathogens (Pautasso et al., 2015). Ultimately, this will likely lead to further unforeseen forest health issues, spanning across wider geographical regions and affecting ecosystem services across continents.

FOREST PATHOLOGISTS ARE NEEDED TO FIND SOLUTIONS

The combined impact of invasive alien insect pests and pathogens and climate change can create enormous economic and environmental costs to our society, in the range of $4.3–20.2 trillion per year in ecosystem service losses (Costanza et al., 2014). Mitigating those losses is one of the most pressing challenges to ensure future healthy forests and continued provision of services. Forest health research can lead to innovative solutions and is central to both short- and long-term approaches. Predicting the outcome of host–pathogen–pest interactions in a changing climate will be a very important research avenue for future forest health (Desprez-Loustau et al., 2016). Highly trained forest pathologists are needed to mitigate this crisis. Forest tree pathogens attack long-lived organisms with highly differentiated woody tissue types, which requires a specialized understanding of tree–microbe–environment interactions. This skill set differs greatly from that required for agricultural crop plants, which are primarily annual, herbaceous, and confined to highly simplified agroecosystems. Forest pathology thus represents the necessary fusion of forest ecology and plant pathology required to understand the complexities of forest community structure and composition, pathogen-based biology, biogeography, forestry, genetics, and genomics within the context of host defense and resistance. By necessity, all of these diverse scientific domains pose challenges for the non-specialist, who is not adequately armed with the integrated knowledge necessary to formulate cogent management strategies.

The field of forest pathology is not new: it has developed over 130 years, stimulated by the severe impact of non-native, pathogen-caused epidemics during the first half of the twentieth century and with the purpose of preventing or controlling such events in the future (Boyce, 1961). Since the early 1980s, forest pathology positions in academia and the federal government in North America have undergone a steep decline, despite the significant increase in emerging pest issues (Martyn, 2009; Santini et al., 2013; Bonello et al., 2020b). Lack of trained personnel has occurred in tandem with reductions in organizationally visible forest pathology programs across forestry and plant pathology departments throughout the U.S. and Canada. The latter is a result of smaller departments being combined into larger units/divisions or simply being dissolved. This has resulted in the further erosion of forest pathology training (including faculty positions) in higher education, often

with forest pathology as a subject being relegated to a singular course or being combined into a forest protection/forest health course focused on diseases, insect pests, and/or fire.

The number of classically trained forest pathology faculty positions at U.S. universities has declined from over 40 positions in the 1980s to 22 positions in 2021. This includes 14 universities in which a forest pathologist faculty position was not replaced following retirement. In the federal government sector, there has also been a steep reduction in the total number of USDA-FS-Research and Development research scientist positions since 1985. Between 1985 and 2007, the number of all research scientists decreased by 44% (from 985 to 547) (USDA FS, 2007). The proportional change in position numbers, however, did vary by research series classification. Currently, the series with larger numbers of FS researchers include Research Ecologist, Research Forester, and Research Social Scientist. In comparison, there are currently nine Research Plant Pathologists employed (estimated 2.2% of the research scientist cadre) (NFC Insight data, USDA OCIO Enterprise Analytics Team). Between 1985 and 2007, the proportion of scientists in this series per total research scientists decreased from 5.1 to 2.9% (USDA FS, 2007). The USDA FS also employs Plant Pathologists (non-research positions) with responsibilities for detection and monitoring, oversight of federally funded disease suppression programs, and technical assistance. These plant pathologists (39 in 2021 per NFC Insight data, USDA OCIO Enterprise Analytics Team) may be considered the "first responders" while research plant pathologists are often the initial investigators of new and emerging tree disease.

SUCCESS STORIES IN FOREST PATHOLOGY

Forest-pathology-based research has generated some considerable successes in tree disease management. One important case is represented by Heterobasidion root disease (HRD), caused by the *Heterobasidion annosum* species complex. HRD is found throughout coniferous forests of the Northern Hemisphere (Garbelotto and Gonthier, 2013). *Heterobasidion irregulare*, one of the species in this complex, is considered a native species in North America and it has a very low impact in unmanaged or extensively managed forests but causes high mortality in intensively managed pine plantations (Otrosina and Garbelotto, 2010). An innovative solution was developed, based on the pathogen infection cycle (which occurs *via* freshly cut stumps with additional spread through root contacts) by treating stumps with borate compounds (e.g., disodium octaborate tetrahydrate or DOT) or by inoculating the stumps with saprobic wood decay fungi such as *Phlebiopsis gigantea* that outcompete the pathogen. These strategies are considered "among the most effective and sustainable in forestry" and are commercially available around the world, preventing the death of millions of trees (Garbelotto and Gonthier, 2013).

Tree breeding for disease resistance is another successful avenue for controlling tree diseases. Fusiform rust (*Cronartium quercuum* f. sp. *fusiforme*) is a very damaging pathogen that attacks the stems and branches of pines, causing high levels of mortality. Breeding for disease resistance has made it possible to control fusiform rust to maintain low disease levels in loblolly and slash pine plantations in the southern U.S. (Schmidt, 2003). Breeding for disease resistance can also help protect endangered tree species. Several white pine species, including high elevation white pines, have now been bred for resistance to WPBR, making it possible to restore white pines in areas where these pines were previously endangered (Sniezko et al., 2014). Breeding and developing resistant Port-Orford-cedar (POC) for resistance to the exotic root pathogen *Phytophthora lateralis* (Zobel et al., 1985) is another success story (Sniezko et al., 2012). Planting resistant POC and developing operational use of multiple disease management practices have been credited with the recent downgrade of POC status from "vulnerable" to "near threatened" by the IUNC (Pike et al., 2021).

Pathogen identification and detection have revolutionized how we diagnose tree diseases (Stewart et al., 2018). Plant health clinics now routinely use DNA-based methods (Martin et al., 2009; Wu et al., 2011; Lamarche et al., 2015; Yang and Juzwik, 2017; Oren et al., 2018; Parra et al., 2020; Rizzo et al., 2021; Stackhouse et al., 2021) that provide rapid and accurate diagnostics. Regulatory agencies have adopted the tools developed by forest pathologists for their day-to-day testing for invasive species. This has been instrumental in preventing the spread and tracking sources of pathogens such as *Phytophthora ramorum* (sudden oak death) (Grünwald et al., 2019). PCR tests targeting this pathogen have now been used millions of times around the world to provide rapid and reliable molecular identification and help contain this pathogen to western states and provinces of North America (Martin et al., 2009).

Ultimately, it is the integration of multiple approaches that offers the best long-term solutions. This is the case with oak wilt, initially recognized as a mysterious rapid wilting of black oaks (*Quercus velutina*) that was discovered in the early 1940s (Henry 1944), shortly after the discovery of chestnut blight and Dutch elm disease in North America. The fungus *B. fagacearum* spreads above-ground by insect vectors and below-ground through naturally grafted root systems and is known to occur only in the eastern U.S., where it is arguably considered non-native (Juzwik et al., 2008). Control tools and management approaches developed by forest pathologists over the past 75 years and implemented in both urban and rural forests have resulted in effective multi-pronged disease management. Above-ground pathogen transmission by sap beetles (Coleoptera: Nitidulidae) is minimized by timely removal of wilted red oaks, avoidance of oak wounding during high-risk season(s), and restricting movement of firewood and logs with bark from oak wilt-affected areas. Below-ground transmission is stopped by mechanical disruption of common or grafted root systems between diseased and nearby healthy oaks. These selected success stories demonstrate the need for increased research capacity for multidisciplinary approaches that range from basic research for knowledge acquisition to applied research to find solutions.

THE NEED FOR FOREST PATHOLOGISTS IN THE FUTURE

Forest pathology researchers and practitioners are our first *line of defense*, one that is constantly under pressure from a variety of stakeholders facing new and re-emerging forest health issues. Although there are a number of success stories related to mitigating forest diseases, new, unknown, and emerging pest issues are on the rise (Santini et al., 2013). The challenge of predicting outbreaks under future climates and the increasing global movement of invasive pathogens will require novel skills. The need for a traditional "forest specialist" worked well in the past because there were enough "unknown" disease etiologies to investigate and sustain the career of several forest pathologists to tackle a single disease system for decades. However, future generations of forest pathologists will require even more multidisciplinary training and approaches. They will need to acquire multidisciplinary knowledge to better characterize diverse pathosystems (Martyn, 2009). Furthermore, it is critical that resource opportunities sufficient to support the clear needs identified here be strategic, focused, and applied across the continuum of basic to applied research and solution implementation. An expanding cadre of research forest pathologists with the modern training necessary to tackle these problems is urgently needed.

The current forest health crisis brought about by climate change and globalization creates the need and opportunity to train the upcoming generation of forest pathologists. For example, multidisciplinary research consortia are increasingly necessary to tackle the societal grand challenges that forest decline syndromes represent. Such consortia must include forest pathologists, forest entomologists, forest ecologists, silviculturists, traditional forest geneticists, modelers, remote sensing specialists, as well as experts in artificial intelligence, microbial ecology, and novel genomics approaches such as CRISPR-Cas9, to name a few. This will require constant inputs and multiple resource providers and careful and intentional strategic planning to achieve defined forest health objectives. The past and current generations of forest pathologists have demonstrated the value of their work by providing innovative solutions to forest health challenges. The next generation of forest pathologists will have access to an extraordinary toolbox ranging from classical to cutting-edge tools to address and provide solutions to current and future forest health crises. They should be at the forefront of the fight against invasive tree pest and pathogen invasions in the era of climate change.

AUTHOR CONTRIBUTIONS

All authors listed have made a substantial, direct and intellectual contribution to the work, and approved it for publication.

FUNDING

Funding and salaries for this project were provided by state and federal funds appropriated to the University of Tennessee Institute of Agriculture, University of Tennessee; the Ohio Agricultural Research and Development Center, The Ohio State University; The University of British Columbia; United States Department of Agriculture-Forest Service; University of California; Colorado State University; and the D. B. Warnell School of Forestry and Natural Resources, University of Georgia.

REFERENCES

Abrams, J., Greiner, M., Schultz, C., Evans, A., and Huber-Stearns, H. (2021). Can forest managers plan for resilient landscapes? Lessons from the United States national forest plan revision process. *Environ. Manage.* 67, 574–588. doi: 10.1007/s00267-021-01451-4

Albrich, K., Rammer, W., and Seidl, R. (2020). Climate change causes critical transitions and irreversible alterations of mountain forests. *Glob. Chang. Biol.* 26, 4013–4027. doi: 10.1111/gcb.15118

Anagnostakis, S. L. (1987). Chestnut Blight: the classical problem of an introduced pathogen. *Mycologia* 79, 23–37. doi: 10.2307/3807741

Appel, D. N., and Camilli, K. S. (2010). "Assessment of oak wilt threat to habitat of the golden-cheeked warbler, an endangered species, in central Texas," in *Advances in threat assessment and their application to forest and rangeland management. Gen. Tech. Rep. PNW-GTR-802*, eds J. M. Pye, H. M. Rauscher, Y. Sands, D. C. Lee, and J. S. Beatty, (Portland, OR: US Department of Agriculture, Forest Service, Pacific Northwest and Southern Research Stations), 61–71.

Barnes, I., Fourie, A., Wingfield, M. J., Harrington, T., McNew, D., Sugiyama, L., et al. (2018). New *Ceratocystis* species associated with rapid death of *Metrosideros polymorpha* in Hawai'i. *Persoonia* 40, 154–181. doi: 10.3767/persoonia.2018.40.07

Bastin, J.-F., Finegold, Y., Garcia, C., Mollicone, D., Rezende, M., Routh, D., et al. (2019). The global tree restoration potential. *Science* 365, 76–79. doi: 10.1126/science.aax0848

Bastin, J.-F., Finegold, Y., Garcia, C., Mollicone, D., Rezende, M., Routh, D., et al. (2020). Erratum for the Report: "The global tree restoration potential" by J.-F. Bastin, Y. Finegold, C. Garcia, D. Mollicone, M. Rezende, D. Routh, C. M. Zohner, T. W. Crowther and for the Technical Response "Response to Comments on 'The global tree restoration potential'" by J.-F. Bastin, Y. Finegold, C. Garcia, N. Gellie, A. Lowe, D. Mollicone, M. Rezende, D. Routh, M. Sacande, B. Sparrow, C. M. Zohner, T. W. Crowther. *Science* 368, eabc8905. doi: 10.1126/science.abc8905

Bonello, P., Campbell, F. T., Cipollini, D., Conrad, A. O., Farinas, C., Gandhi, K. J. K., et al. (2020a). Invasive tree pests devastate ecosystems - a proposed new response framework. *Front For Glob Change* 3, 2. doi: 10.3389/ffgc.2020.00002

Bonello, P., Hadziabdic, D., Rizzo, D., Tomimatsu, G., and Beattie, G. (2020b). Bolstering forest pathology to ensure a robust forest health community for the future. *Phytopathol. News* 54.

Boyce, J. S. (1961). *Forest Pathology, 3rd Edn*. New York, NY: McGraw-Hill.

Brodde, L., Adamson, K., Julio Camarero, J., Castaño, C., Drenkhan, R., Lehtijärvi, A., et al. (2019). Diplodia tip blight on its way to the North: drivers of disease emergence in Northern Europe. *Front. Plant Sci.* 9:1818. doi: 10.3389/fpls.2018.01818

Costanza, R., de Groot, R., Sutton, P., van der Ploeg, S., Anderson, S., I, K, Kubiszewski I, et al. (2014). Changes in the global value of ecosystem services. *Glob. Environ. Change* 26, 152–158. doi: 10.1016/j.gloenvcha.2014.04.002

Desprez-Loustau, M.-L., Aguayo, J., Dutech, C., Hayden, K. J., Husson, C., Jakushkin, B., et al. (2016). An evolutionary ecology perspective to address forest pathology challenges of today and tomorrow. *Ann. For. Sci.* 73, 45–67. doi: 10.1007/s13595-015-0487-4

Di Sacco, A., Hardwick, K. A., Blakesley, D., Brancalion, P. H. S., Breman, E., Cecilio Rebola, L., et al. (2021). Ten golden rules for reforestation to optimize carbon sequestration, biodiversity recovery and livelihood benefits. *Glob. Chang. Biol.* 27, 1328–1348. doi: 10.1111/gcb.15498

Donovan, G. H., and Butry, D. T. (2009). The value of shade: estimating the effect of urban trees on summertime electricity use. *Energy Build.* 41, 662–668. doi: 10.1016/j.enbuild.2009.01.002

Donovan, G. H., Butry, D. T., Michael, Y. L., Prestemon, J. P., Liebhold, A. M., Gatziolis, D., et al. (2013). The relationship between trees and human health: evidence from the spread of the emerald ash borer. *Amer. J. Prevent. Med.* 44, 139–145. doi: 10.1016/j.amepre.2012.09.066

Eriksson, L., Boberg, J., Cech, T. L., Corcobado, T., Desprez-Loustau, M.-L., Hietala, A. M., et al. (2019). Invasive forest pathogens in Europe: cross-country variation in public awareness but consistency in policy acceptability. *Ambio* 48, 1–12. doi: 10.1007/s13280-018-1046-7

Garbelotto, M., and Gonthier, P. (2013). Biology, epidemiology, and control of *Heterobasidion* species worldwide. *Annu. Rev. Phytopathol.* 51, 39–59. doi: 10.1146/annurev-phyto-082712-102225

Geils, B. W., Hummer, K. E., and Hunt, R. S. (2010). White pines, *Ribes*, and blister rust: a review and synthesis. *For. Pathol.* 40, 147–185. doi: 10.1111/j.1439-0329.2010.00654.x

Gibbs, J. N. (1978). Intercontinental epidemiology of Dutch Elm disease. *Annu. Rev. Phytopathol.* 16, 287–307. doi: 10.1146/annurev.py.16.090178.001443

Grünwald, N. J., LeBoldus, J. M., and Hamelin, R. C. (2019). Ecology and evolution of the sudden oak death pathogen *Phytophthora ramorum*. *Annu. Rev. Phytopathol.* 57, 301–321. doi: 10.1146/annurev-phyto-082718-100117

Ideno, Y., Hayashi, K., Abe, Y., Ueda, K., Iso, H., Noda, M., et al. (2017). Blood pressure-lowering effect of Shinrin-yoku (Forest bathing): a systematic review and meta-analysis. *BMC Complement. Altern. Med.* 17, 409. doi: 10.1186/s12906-017-1912-z

Juzwik, J., Appel, D., MacDonald, W., and Burks, S. (2011). Challenges and successes in managing Oak Wilt in the United States. *Plant Dis.* 95, 888–900. doi: 10.1094/PDIS-12-10-0944

Juzwik, J., Harrington, T. C., MacDonald, W. L., and Appel, D. N. (2008). The origin of *Ceratocystis fagacearum*, the oak wilt fungus. *Annu. Rev. Phytopathol.* 46, 13–26. doi: 10.1146/annurev.phyto.45.062806.094406

Keane, R. E., and Arno, S. F. (1993). Rapid decline of whitebark pine in western Montana: evidence from 20-year remeasurements. *Western J. Appl. Forest* 8, 44–47. doi: 10.1093/wjaf/8.2.44

Kinloch, B. B. (2003). White pine blister rust in North America: past and prognosis. *Phytopathology* 93, 1044–1047. doi: 10.1094/PHYTO.2003.93.8.1044

Kolb, T. E., Fettig, C. J., Ayres, M. P., Bentz, B. J., Hicke, J. A., Mathiasen, R., et al. (2016). Observed and anticipated impacts of drought on forest insects and diseases in the United States. *For. Ecol. Manage.* 380, 321–334. doi: 10.1016/j.foreco.2016.04.051

Lamarche, J., Potvin, A., Pelletier, G., Stewart, D., Feau, N., Alayon, D. I. O., et al. (2015). Molecular detection of 10 of the most unwanted alien forest pathogens in Canada using real-time PCR. *PLoS ONE* 10, e0134265. doi: 10.1371/journal.pone.0134265

Martin, F. N., Coffey, M. D., Zeller, K., Hamelin, R. C., Tooley, P., Garbelotto, M., et al. (2009). Evaluation of molecular markers for *Phytophthora ramorum* detection and identification: testing for specificity using a standardized library of isolates. *Phytopathology* 99, 390–403. doi: 10.1094/PHYTO-99-4-0390

Martyn, R. D. (2009). Where will the next Norman Borlaug come from? A U.S. perspective of plant pathology education and research. *Plant Protect. Sci.* 45, 125–139. doi: 10.17221/22/2009-PPS

Mortenson, L. A., Flint Hughes, R., Friday, J. B., Keith, L. M., Barbosa, J. M., Friday, N. J., et al. (2016). Assessing spatial distribution, stand impacts and rate of *Ceratocystis fimbriata* induced 'ohi'a (*Metrosideros polymorpha*) mortality in a tropical wet forest, Hawai'i Island, USA. *For. Ecol. Manage.* 377, 83–92. doi: 10.1016/j.foreco.2016.06.026

Nowak, D. J., Crane, D. E., and Stevens, J. C. (2006). Air pollution removal by urban trees and shrubs in the United States. *Urb. Forest. Urb. Green.* 4, 115–123. doi: 10.1016/j.ufug.2006.01.007

Oren, E., Klingeman, W., Gazis, R., Moulton, J., Lambdin, P., Coggeshall, M., et al. (2018). A novel molecular toolkit for rapid detection of the pathogen and primary vector of thousand cankers disease. *PLoS ONE* 13, e0185087. doi: 10.1371/journal.pone.0185087

Otrosina, W. J., and Garbelotto, M. (2010). Heterobasidion occidentale sp nov and *Heterobasidion irregulare* nom. nov.: a disposition of North American Heterobasidion biological species. *Fung Biol.* 114, 16–25. doi: 10.1016/j.mycres.2009.09.001

Palmer, L. (2021). How trees and forests reduce risks from climate change. *Nat. Clim. Chang.* 11, 374–377. doi: 10.1038/s41558-021-01041-6

Parra, P. P., Dantes, W., Sandford, A., de la Torre, C., Pérez, J., Hadziabdic, D., et al. (2020). Rapid detection of the laurel wilt pathogen in sapwood of Lauraceae hosts. *Plant Health Prog.* 21, 356–364. doi: 10.1094/PHP-06-20-0049-RS

Pautasso, M., Döring, T. F., Garbelotto, M., Pellis, L., and Jeger, M. J. (2012). Impacts of climate change on plant diseases-opinions and trends. *Eur. J. Plant Pathol.* 133, 295–313. doi: 10.1007/s10658-012-9936-1

Pautasso, M., Schlegel, M., and Holdenrieder, O. (2015). Forest health in a changing world. *Microb. Ecol.* 69, 826–842. doi: 10.1007/s00248-014-0545-8

Pike, C. C., Koch, J., and Nelson, C. D. (2021). Breeding for resistance to tree pests: successes, challenges, and a guide to the future. *J. Forest.* 119, 96–105. doi: 10.1093/jofore/fvaa049

Ploetz, R. C., Kendra, P. E., Choudhury, R. A., Rollins, J. A., Campbell, A., Garrett, K., et al. (2017). Laurel Wilt in natural and agricultural ecosystems: understanding the drivers and scales of complex pathosystems. *Forests* 8, 48. doi: 10.3390/f8020048

Raffa, K. F., Aukema, B., Bentz, B. J., Carroll, A., Erbilgin, N., Herms, D. A., et al. (2009). A literal use of "forest health" safeguards against misuse and misapplication. *J. Forest.* 107, 276–277. Available online at: https://www.fs.usda.gov/treesearch/pubs/19615

Ramsfield, T., Bentz, B., Faccoli, M., Jactel, H., and Brockerhoff, E. (2016). Forest health in a changing world: effects of globalization and climate change on forest insect and pathogen impacts. *Forestry* 89, 245–252. doi: 10.1093/forestry/cpw018

Rizzo, D., and Garbelotto, M. (2003). Sudden oak death: endangering California and Oregon forest ecosystems. *Front. Ecol. Environ.* 1, 197–204. doi: 10.1890/1540-9295(2003)001[0197:SODECA]2.0.CO;2

Rizzo, D., Moricca, S., Bracalini, M., Benigno, A., Bernardo, U., Luchi, N., et al. (2021). Rapid detection of *Pityophthorus juglandis* (Blackman) (Coleoptera, Curculionidae) with the Loop-Mediated Isothermal Amplification (LAMP) method. *Plants* 10, 1048. doi: 10.3390/plants10061048

Santini, A., Ghelardini, L., De Pace, C., Desprez-Loustau, M. L., Capretti, P., Chandelier, A., et al. (2013). Biogeographical patterns and determinants of invasion by forest pathogens in Europe. *New Phytol.* 197, 238–250. doi: 10.1111/j.1469-8137.2012.04364.x

Schmidt, R. A. (2003). Fusiform rust of southern pines: a major success for forest disease management. *Phytopathology* 93, 1048–1051. doi: 10.1094/PHYTO.2003.93.8.1048

Seidl, R., Thom, D., Kautz, M., Martin-Benito, D., Peltoniemi, M., Vacchiano, G., et al. (2017). Forest disturbances under climate change. *Nat. Clim. Chang.* 7, 395–402. doi: 10.1038/nclimate3303

Sherwood, P., Villari, C., Capretti, P., and Bonello, P. (2015). Mechanisms of induced susceptibility to *Diplodia* tip blight in drought-stressed Austrian pine. *Tree Physiol.* 35, 549–562. doi: 10.1093/treephys/tpv026

Sniezko, R., Hamlin, J., and Hansen, E. (2012). "Operational program to develop *Phytophthora lateralis*-resistant populations of Port-Orford-cedar (*Chamaecyparis lawsoniana*)," in *Proceedings of the Fourth International Workshop on the Genetics of Host-Parasite Interactions in Forestry: Disease and Insect Resistance in Forest Trees. Gen. Tech. Rep. PSW-GTR-240*, Vol. 240 (Albany, CA: Pacific Southwest Research Station, Forest Service, US Department of Agriculture), 65–79.

Sniezko, R. A., Smith, J., Liu, J.-J., and Hamelin, R. C. (2014). Genetic resistance to Fusiform rust in southern pines and white pine blister rust in white pines - a contrasting tale of two rust pathosystems - current status and future prospects. *Forests* 5, 2050–2083. doi: 10.3390/f5092050

Stackhouse, T., Boggess, S., Hadziabdic, D., Trigiano, R. N., Ginzel, M., and Klingeman, W. (2021). Conventional gel electrophoresis and TaqMan probes enable rapid confirmation of Thousand Cankers Disease from diagnostic samples. *Plant Dis*. doi: 10.1094/PDIS-10-20-2258-RE. [Epub ahead of print].

Stewart, J. E., Kim, M.-S., and Klopfenstein, N. B. (2018). Molecular genetic approaches toward understanding forest-associated fungi and their interactive roles within forest ecosystems. *Curr. Forest. Rep.* 4, 72–84. doi: 10.1007/s40725-018-0076-5

Stone, J. K., Coop, L. B., and Manter, D. K. (2008). Predicting effects of climate change on Swiss needle cast disease severity in Pacific Northwest forests. *Canad. J. Plant Pathol.*30, 169–176. doi: 10.1080/07060661.2008.10540533

Sturrock, R. N., Frankel, S. J., Brown, A. V., Hennon, P. E., Kliejunas, J. T., Lewis, K. J., et al. (2011). Climate change and forest diseases. *Plant Pathol.* 60, 133–149. doi: 10.1111/j.1365-3059.2010.02406.x

Tomback, D. F., and Achuff, P. (2010). Blister rust and western forest biodiversity: ecology, values and outlook for white pines. *For. Pathol.* 40, 186–225. doi: 10.1111/j.1439-0329.2010.00655.x

Trumbore, S., Brando, P., and Hartmann, H. (2015). Forest health and global change. *Science* 349, 814–818. doi: 10.1126/science.aac6759

USDA Forest Service. (2007). USDA Forest Service Research & Development 2006 highlights. Report No. FS-890. *USDA Forest Service*. p 58. Available online at: https://www.frames.gov/catalog/8414

Woods, A., Coates, K. D., and Hamann, A. (2005). Is an unprecedented Dothistroma needle blight epidemic related to climate change? *Bioscience* 55, 761–769. doi: 10.1641/0006-3568(2005)055[0761:IAUDNB]2.0.CO;2

Wu, C. P., Chen, G. Y., Li, B., Su, H., An, Y. L., Zhen, S. Z., et al. (2011). Rapid and accurate detection of *Ceratocystis fagacearum* from stained wood and soil by nested and real-time PCR. *For. Pathol.* 41, 15–21. doi: 10.1111/j.1439-0329.2009.00628.x

Yang, A., and Juzwik, J. (2017). Use of nested and real-time PCR for the detection of *Ceratocystis fagacearum* in the sapwood of diseased oak species in Minnesota. *Plant Dis.* 101, 480–486. doi: 10.1094/PDIS-07-16-0990-RE

Zobel, D. B., Roth, L. F., and Hawk, G. M. (1985). *Ecology, Pathology, and Management of Port-Orford-cedar (Chamaecyparis lawsoniana)*. General Technical Report PNW- 184, Vol. 184. US Department of Agriculture, Forest Service, Pacific Northwest Forest and Range Experiment Station, p. 161.

Conflict of Interest: The authors declare that the research was conducted in the absence of any commercial or financial relationships that could be construed as a potential conflict of interest.

frontiers in Forests and Global Change

ORIGINAL RESEARCH
published: 13 December 2021
doi: 10.3389/ffgc.2021.740994

Predicting Present and Future Suitable Climate Spaces (Potential Distributions) for an Armillaria Root Disease Pathogen (*Armillaria solidipes*) and Its Host, Douglas-fir (*Pseudotsuga menziesii*), Under Changing Climates

Mee-Sook Kim[1]*†, John W. Hanna[2]†, Jane E. Stewart[3], Marcus V. Warwell[4], Geral I. McDonald[2] and Ned B. Klopfenstein[2]*

[1] USDA Forest Service, Pacific Northwest Research Station, Corvallis, OR, United States, [2] USDA Forest Service, Rocky Mountain Research Station, Moscow, ID, United States, [3] Department of Agricultural Biology, Colorado State University, Ft. Collins, CO, United States, [4] USDA Forest Service, Southern Region, Atlanta, GA, United States

Climate change and associated disturbances are expected to exacerbate forest root diseases because of altered distributions of existing and emerging forest pathogens and predisposition of trees due to climatic maladaptation and other disturbances. Predictions of suitable climate space (potential geographic distribution) for forest pathogens and host trees under contemporary and future climate scenarios will guide the selection of appropriate management practices by forest managers to minimize adverse impacts of forest disease within forest ecosystems. A native pathogen (*Armillaria solidipes*) that causes Armillaria root disease of conifers in North America is used to demonstrate bioclimatic models (maps) that predict suitable climate space for both pathogen and a primary host (*Pseudotsuga menziesii*, Douglas-fir) under contemporary and future climate scenarios. Armillaria root disease caused by *A. solidipes* is a primary cause of lost productivity and reduced carbon sequestration in coniferous forests of North America, and its impact is expected to increase under climate change due to tree maladaptation. Contemporary prediction models of suitable climate space were produced using Maximum Entropy algorithms that integrate climatic data with 382 georeferenced occurrence locations for DNA sequence-confirmed *A. solidipes*. A similar approach was used for visually identified *P. menziesii* from 11,826 georeferenced locations to predict its climatic requirements. From the contemporary models, data were extrapolated through future climate scenarios to forecast changes in geographic areas where native *A. solidipes* and *P. menziesii* will be climatically adapted. Armillaria

Edited by:
Alberto Santini, Institute for Sustainable Plant Protection, National Research Council, Consiglio Nazionale delle Ricerche (CNR), Italy

Reviewed by:
Angus J. Carnegie, New South Wales Department of Primary Industries, Australia
Simone Prospero, Swiss Federal Institute for Forest, Snow and Landscape Research (WSL), Switzerland

***Correspondence:**
Mee-Sook Kim
meesook.kim@usda.gov
Ned B. Klopfenstein
ned.klopfenstein@usda.gov

† These authors have contributed equally to this work and share first authorship

Specialty section:
This article was submitted to Pests, Pathogens and Invasions, a section of the journal Frontiers in Forests and Global Change

Received: *14 July 2021*
Accepted: *05 November 2021*
Published: *13 December 2021*

Citation:
Kim M-S, Hanna JW, Stewart JE, Warwell MV, McDonald GI and Klopfenstein NB (2021) Predicting Present and Future Suitable Climate Spaces (Potential Distributions) for an Armillaria Root Disease Pathogen (Armillaria solidipes) and Its Host, Douglas-fir (Pseudotsuga menziesii), Under Changing Climates. Front. For. Glob. Change 4:740994. doi: 10.3389/ffgc.2021.740994

root disease is expected to increase in geographic areas where predictions suggest *A. solidipes* is well adapted and *P. menziesii* is maladapted within its current range. By predicting areas at risk for Armillaria root disease, forest managers can deploy suitable strategies to reduce damage from the disease.

Keywords: climate change, drought, potential distribution, root disease, species distribution modeling, tree maladaptation

INTRODUCTION

Armillaria root disease, caused by *Armillaria* spp., is a leading cause of growth loss and mortality of a diverse range of horticultural and timber trees in many temperate regions around the world (e.g., Heinzelmann et al., 2019). In coniferous forests of North America, *Armillaria solidipes* (formerly North American *A. ostoyae*) is a native pathogen that causes Armillaria root disease that negatively impacts growth and survival of many conifer species (Ferguson et al., 2003; Lockman and Kearns, 2016) including *Pseudotsuga menziesii* (Douglas-fir), which is a dominant component of many forest stands in western North America and an important tree for ecological, sociological, and economic purposes.

Changing climate, extreme weather events (e.g., drought, high temperatures), and/or other disturbances (e.g., fire, insect attack, and forest management activities) are causing increased disease severity by *A. solidipes* on stressed *P. menziesii* (Morrison, 2011; Murray and Leslie, 2021). Armillaria root disease, in conjunction with the adverse impacts from climate and extreme weather events, can predispose trees to attack by other biotic agents including bark beetles (e.g., Hertert et al., 1975; Kulhavy et al., 1984; Tkacz and Schmitz, 1986), which can result in tree mortality and increased availability of nutritional substrates for inoculum of *Armillaria* species that can, in turn, contribute to future disease on the site. When characterizing the ecological role of *Armillaria* in western North America, it is crucial to consider that *Armillaria* also behaves as a saprophyte, colonizing trees that succumbed to other abiotic and biotic causes. Thus, careful observations are required to determine the interactive role of Armillaria root disease in relation to climate, extreme weather, and other interacting biotic/abiotic factors (Kubiak et al., 2017). While Armillaria root disease is well known for its negative impacts on tree health, causing economic impact and reduced carbon sequestration potential of forests, it is important to note that *Armillaria* can also contribute ecological benefits, which include nutrient cycling, habitat formation (e.g., nesting cavities), and food for wildlife, such as small birds and mammals (e.g., Steeger and Hitchcock, 1998; Parsons et al., 2003; Heinzelmann et al., 2019).

Although information is generally lacking on the incidence and spread of Armillaria root disease over time and space in association with climate and extreme weather events, the known spatial occurrence of *A. solidipes* from extensive sampling offers a unique opportunity to apply bioclimatic modeling to identify climatic components associated with its occurrence. Output from these models can be coupled with GIS to project maps that show the predicted suitable climate space (potential distribution or realized climate niche) across geographic areas, and when coupled with output from general circulation models (GCMs) show predicted future distributions of suitable climate spaces for *P. menziesii* and *A. solidipes*. Understanding the host-pathogen interaction under changing climates allows for predictions of the potential distributions of *P. menziesii* and *A. solidipes* across current and future landscapes to inform Armillaria root disease management.

Armillaria occurs primarily below ground, which represents a distinct environment that is relatively stable from minor weather fluctuations. Below-ground conditions (e.g., soil temperature and moisture) and microclimate can affect *A. solidipes*, soil microbial communities, and/or *P. menziesii*. These below-ground, climatic conditions are influenced by latitude/longitude, elevation, slope, aspect, topography, drainage, soil properties, crown cover, etc. The distribution of Armillaria root disease on a site is largely attributable to soil environments and microclimates that vary within and/or among stands. In addition, the occurrence of *A. solidipes* is associated with plant association groups or habitat types (i.e., well-defined associations of trees, shrubs, and herbaceous plants) that reflect soil temperature (e.g., represented by overstory trees) and moisture (e.g., represented understory plants) in conifer forests of western North America (e.g., McDonald et al., 2000; Kim et al., 2010). At the broadscale, bioclimatic models (e.g., MaxEnt: Maximum entropy species distribution modeling) can use presence-only survey data to project potential distribution of both pathogen and host tree species based on major climatic factors (e.g., 19 bioclimatic variables from the WorldClim) for contemporary or projected future time periods (Phillips et al., 2006). Furthermore, climate layers of projected future climates based on different greenhouse emission scenarios can be used to predict future potential distribution of both pathogen and host tree species under different projected climate scenarios.

In western North America, Armillaria root disease caused by *A. solidipes* is common on trees that are ecophysiologically maladapted (stressed by environmental factors), which can be attributed to climatic maladaptation and/or other disturbances (McDonald et al., 1987a; McDonald, 1990; Murray and Leslie, 2021). Projections of climate change in the northwestern United States predict an increase in the frequency and intensity of drought and higher temperatures that will result in more stressful environmental conditions for forest trees (Chmura et al., 2011). Thus, a reasonable approach toward predicting climate change impacts on Armillaria root disease at the broad scale is to use bioclimatic models to predict the realized climatic niche for the *P. menziesii* and *A. solidipes* pathosystem (e.g., Rehfeldt et al., 2006; Klopfenstein et al., 2009). Although *P. menziesii* spans a

wide geographic (19–44°N latitude and 100–118°W longitude; Hermann and Lavender, 1990) and climatic range in western North America, it is considered a specialist in terms of its climatic requirements for populations, making individual stands especially vulnerable to climate-induced stresses (e.g., Weiskittel et al., 2012; Rehfeldt et al., 2014b).

Our goals were to (1) predict suitable climate spaces (potential distributions) for *P. menziesii* and *A. solidipes* across western North America for contemporary climate and projected climate for the average of years 2081–2100; and (2) draw inferences from comparisons of the prediction models for the host (*P. menziesii*) and pathogen (*A. solidipes*) to predict geographic areas where *P. menziesii* will become maladapted due to climate change, which will likely exacerbate Armillaria root disease in areas where *A. solidipes* remains climatically adapted. We used georeferenced occurrence locations for visually identified *P. menziesii* and DNA sequence-confirmed *A. solidipes* in combination with location-specific climate data for bioclimatic modeling to predict where *A. solidipes* is likely to occur and cause increased disease pressure on maladapted and/or stressed *P. menziesii* under changing climatic conditions.

MATERIALS AND METHODS

Pseudotsuga menziesii Location Data

A total of 11,826 locations of *P. menziesii* were used from selected "fuzzy" coordinates obtained from Forest Inventory Analyses (FIA) data (Rehfeldt et al., 2014a) within the continental United States (locations from Canada and Mexico were not included because the FIA data are only available for the contiguous United States) (**Figure 1A**).

Armillaria solidipes Surveys, Identification, and Location Data

Briefly, surveys for Armillaria root disease pathogens require collection of *Armillaria* mycelia (e.g., mycelial fan, rhizomorph, or basidiocarp) for *Armillaria* identification via DNA sequences (e.g., Kim et al., 2000, 2006; Ross-Davis et al., 2012; Elías-Román et al., 2013; Klopfenstein et al., 2017). Careful examination of symptoms and signs can confirm that *Armillaria* is acting as a pathogen on the host. In addition, precise locations of identified *Armillaria* collections were recorded so that bioclimatic modeling can be applied to determine climatic influences on Armillaria root disease pathogens.

Armillaria solidipes point locations were collected from previous studies of distribution and ecology from the states/provinces of Washington, Oregon, Idaho, Montana, Utah, Wyoming, South Dakota, Arizona, Colorado, New Mexico, British Columbia (BC, Canada), and Chihuahua (Mexico) (McDonald et al., 1987b, 2011; Shaw, 1989; Omdal et al., 1995; McDonald, 1998, unpublished data; Kim et al., 2000; Ferguson et al., 2003; Van der Star et al., 2003; Worrall et al., 2004; Hanna et al., 2007, 2008, 2009, 2014; Blodgett and Lundquist, 2011; Klopfenstein et al., 2012; Berbee et al., 2014, 2015; Hoffman et al., 2014; Blodgett et al., 2015 and Hanna, unpublished data). For *Armillaria* surveys, the main lateral roots of diverse trees were excavated and inspected, and *Armillaria* samples were collected as mycelial fans under the bark, rhizomorphs, basidiocarps, and/or decayed wood. Isolates were established in culture and were confirmed as *A. solidipes* using basidiocarp morphology (e.g., some Canadian locations) and DNA-based species identification (e.g., Kim et al., 2000, 2006; Ross-Davis et al., 2012; Elías-Román et al., 2013; Klopfenstein et al., 2017). From these studies, *A. solidipes* isolates were recorded from 382 distinct locations throughout western North America (**Figure 1B**).

Climate Data and Bioclimatic Variables

Climate-based, species-distribution models using MaxEnt and 19 bioclimatic variables (**Table 1**) from Worldclim version 2.1 (Fick and Hijmans, 2017) were created for both host (*P. menziesii*) (**Figure 2**) and pathogen (*A. solidipes*) (**Figure 3**) for the contemporary (1970–2000) and future time periods (2081–2100) using Coupled Model Intercomparison Project phase 6 (CMIP6) (Eyring et al., 2016) data consisting of two different Shared Socioeconomic Pathways (SSPs) paired with The Canadian Earth System model version 5 (CanESM5) GCM (Swart et al., 2019) using 2.5-min data. In general, five SSPs narratives describe the broad socioeconomic trends that could shape future society and we chose to use two scenarios: SSP2-4.5 ("middle of the road" world where trends do not shift markedly from historical patterns) and SSP5-8.5 ("fossil-fueled development," which follows path of rapid and unconstrained growth in economic output and fossil fuel-based energy use). In addition, change in climate suitability for *P. menziesii* from the contemporary time period to the future time period for both SSPs (SSP2-4.5 and SSP5-8.5) were visually compared (**Figure 4**).

MaxEnt Modeling

To allow calculations in suitability models, input data for MaxEnt consisted of SWD (samples with data) files for each species that linked geographic coordinates (presence point locations) with climate variable values for each of the 19 bioclimatic variables. The models used 19 bioclimatic variables in three sets of 2.5-min, interpolation grids from worldclim.org (Fick and Hijmans, 2017). MaxEnt also uses SWD files of background locations or "pseudo-absences" to "train" the models. For the *P. menziesii* model, 292,639 actual absence point locations were used as background data. MaxEnt's logistic output (an index of probability from 0 to 1) was chosen for easier conceptualization compared to MaxEnt's raw exponential model. For the *A. solidipes* model, background points were created from 10,000 randomly selected geographical locations within the geographic range of the collected isolates.

MaxEnt parameters included cross-validation with 20 replicate runs to generate statistical data. Quantum GIS (QGIS)[1] was used to create the final outputs using MaxEnt's cumulative output. Each cumulative value is the sum of probabilities of cells less than or equal to the cell grid, times 100. MaxEnt's cumulative output was chosen for easier conceptualization compared to MaxEnt's logistic (an index of probability from 0 to 1) or raw exponential output. Totals of 11,826 and 382 locations were used for *P. menziesii* and *A. solidipes*, respectively.

[1] http://www.qgis.org/en/site/

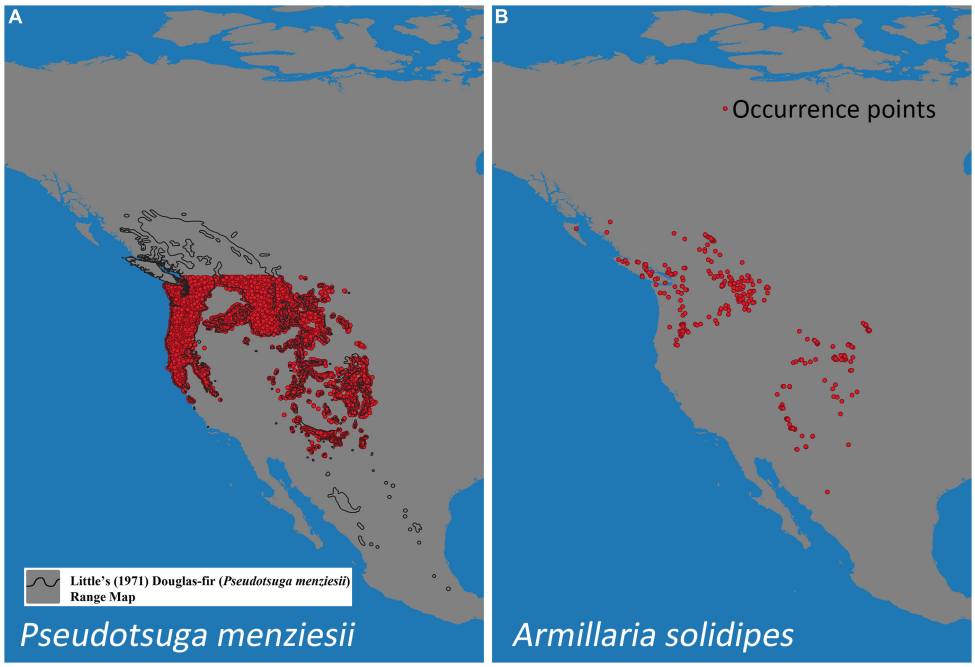

FIGURE 1 | Occurrence points of *Pseudotsuga menziesii* **(A)** and *Armillaria solidipes* **(B)** in North America. The black outline **(A)** designates Little's (1971) *P. menziesii* range map.

To evaluate the reliability of the model, the receiver operating characteristic (ROC) curve of the jackknife method was used (Dorfman et al., 1992). The areas under the ROC curve (AUC) values (ranging from 0 to 1) were generated to calculate model performance (e.g., prediction accuracy) based on true-positive, false-positive, true-negative, and false-negative rates. Higher AUC values (> 0.9) indicate higher reliability of the model (Wiley et al., 2003). Permutation importance (resulting from the values of each environmental variable on training presence and background data being randomly permuted, the model then re-evaluated on the permuted data; resulting drop in training AUC is normalized to percentages) of 19 bioclimatic variables derived from the WorldClim database used to model suitable climate space (potential distribution) based on known occurrence points for *P. menziesii* and *A. solidipes* (**Table 1**).

RESULTS

The MaxEnt bioclimatic model using all occurrence records of *P. menziesii* (N = 11,826) and *A. solidipes* (N = 382) (**Figures 1A,B**, respectively) shows a prediction where many geographic areas throughout the North America have some degree of probability of suitable climate (i.e., possesses a climate suitable for species survival) for both *P. menziesii* and *A. solidipes* (**Figures 2**, **3**, respectively). With 1.0 representing a perfect value and 0.5 representing presence by chance, the average test AUC ± standard deviation values, based on 20 replicate runs, were 0.953 ± 0.002 for *P. menziesii* and 0.960 ± 0.010 for *A. solidipes*.

For the *P. menziesii* model, the major bioclimatic variables (i.e., > 10%) of permutation importance were mean temperature of warmest quarter (Bio10), precipitation of coldest quarter (Bio19), and precipitation of driest quarter (Bio17). For the *A. solidipes* model, temperature annual range (Bio7), maximum temperature of warmest month (Bio5), annual mean temperature (Bio1), and minimum temperature of coldest month (Bio6) were the major bioclimatic variables (**Table 1**).

The predicted contemporary distribution of *P. menziesii* is consistent with the actual range of this tree species reported by Little (1971) (**Figure 2A**). The predicted contemporary distribution of *A. solidipes* shows a geographically wide distribution with more suitable habitat in the wetter forests of the Pacific Northwest and with pockets in the southwestern United States, which appear to be associated with areas that have monsoon seasons (**Figure 3A**). In general, the bioclimatic models predict that the contemporary suitable climatic space (potential distribution) of *A. solidipes* has considerable overlap with that of *P. menziesii* (e.g., northern Idaho, northern Cascade Mountains, Rocky Mountains, etc.).

The models predicted future suitable climate spaces for Year 2081–2100 under two climate scenarios, SSP2-4.5 and SSP5-8.5, are shown in **Figures 2B,C**, **3B,C** respectively. For both *P. menziesii* and *A. solidipes*, the suitable habitat shifts northwest toward more northern and coastal areas. Notably, for *P. menziesii*, the suitable climate space shifts considerably northward and is much smaller in size under the SSP5-8.5 model compared to the SSP2-4.5 model (**Figures 2B,C**). Predicted changes in climate suitability for *P. menziesii* in western North America from contemporary (1970–2000) to

TABLE 1 | Summary of MaxEnt's permutation importance value for each of the contemporary 19 bioclimatic variables (Bio1–Bio19) derived from the WorldClim (worldclim.org) database (1970–2000) used to model suitable climate space (potential distribution) based on occurrence points of *Pseudotsuga menziesii* and *Armillaria solidipes*.

Variable (Units)		*Pseudotsuga menziesii*	*Armillaria solidipes*
Bio1	Annual mean temperature (°C)	0.9	**12.7**
Bio2	Mean diurnal range [Mean of monthly (max temp - min temp)] (°C)	0.2	1
Bio3	Isothermality (Bio2/Bio7) (× 100)	0.5	0.7
Bio4	Temperature seasonality (SD × 100, Coefficient of variation) (°C)	9.7	1.2
Bio5	Maximum temperature of warmest month (°C)	0.8	**16.6**
Bio6	Minimum temperature of coldest month (°C)	4.4	**12.5**
Bio7	Temperature annual range (Bio5-Bio6) (°C)	3.8	**38.8**
Bio8	Mean temperature of wettest quarter (°C)	1.2	0.6
Bio9	Mean temperature of driest quarter (°C)	1.5	4.1
Bio10	Mean temperature of warmest quarter (°C)	**35**	0.2
Bio11	Mean temperature of coldest quarter (°C)	4	0
Bio12	Annual precipitation (mm)	2.8	0.5
Bio13	Precipitation of wettest month (mm)	2.2	0.3
Bio14	Precipitation of driest month (mm)	3.2	3.8
Bio15	Precipitation seasonality (Coefficient of variation) (-)	1.6	0.6
Bio16	Precipitation of wettest quarter (mm)	0.5	0.1
Bio17	Precipitation of driest quarter (mm)	**10.8**	0.7
Bio18	Precipitation of warmest quarter (mm)	4.8	4.9
Bio19	Precipitation of coldest quarter (mm)	**12**	0.8

Variables with the greatest permutation importance (> 10%) are in bold.

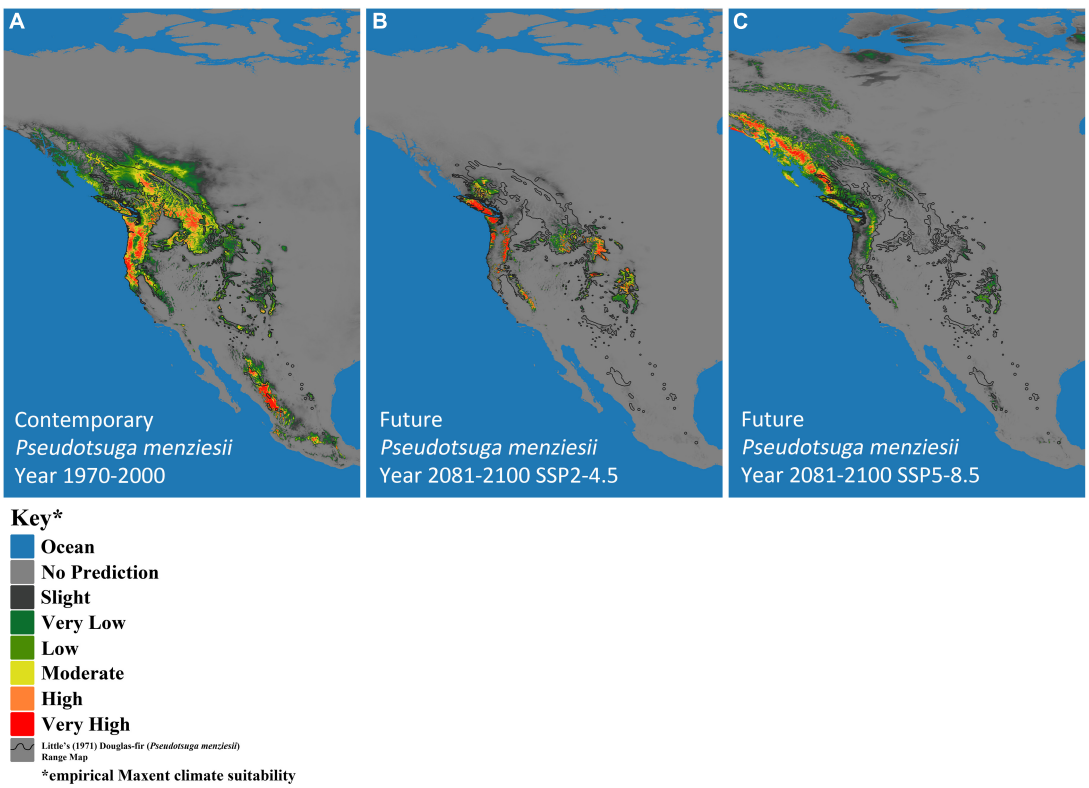

FIGURE 2 | MaxEnt-based, bioclimatic models for *Pseudotsuga menziesii* (Douglas-fir) in western North America. **(A)** Contemporary years (1970–2000), and two future models show two Shared Socioeconomic Pathway (SSP) scenarios (SSP2-4.5 and SSP5-8.5), **(B)** SSP2-4.5 and **(C)** SSP5-8.5. Darkest gray represents predicted empirical MaxEnt climate suitability, with dark green, light green, yellow, orange, and red indicating increased probability of climatic suitability, respectively. The black outline designates Little's (1971) *P. menziesii* range map.

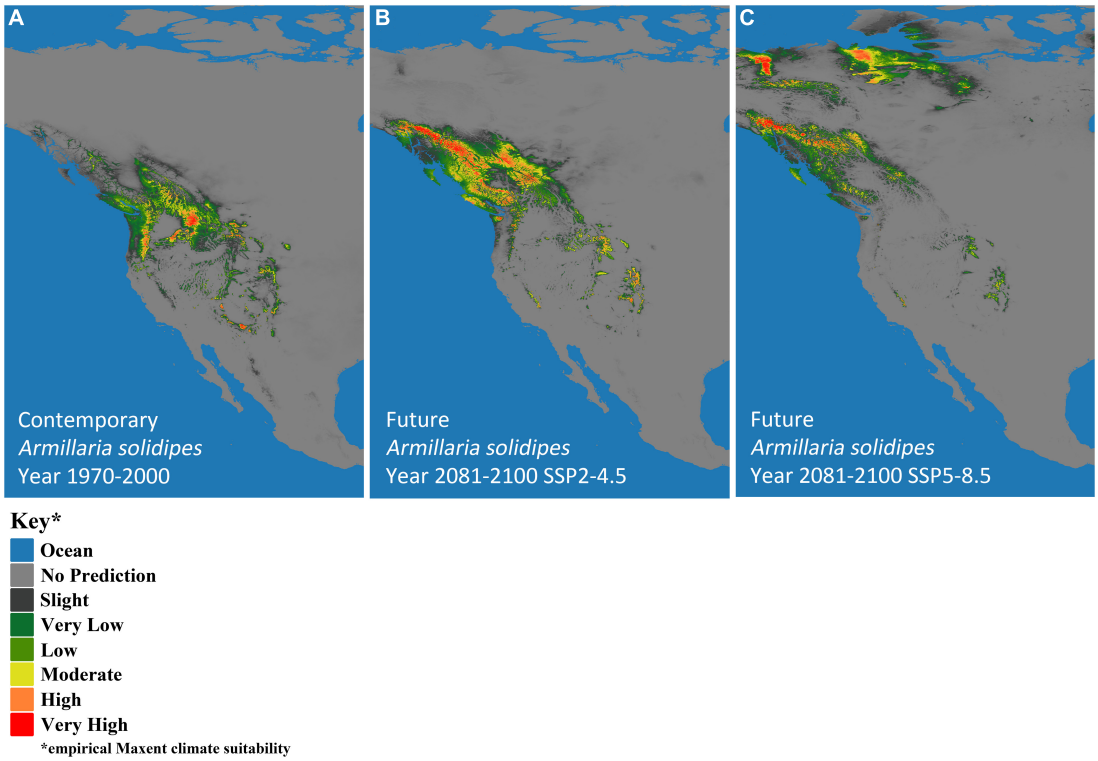

FIGURE 3 | MaxEnt-based, bioclimatic models for *Armillaria solidipes* in western North America. **(A)** Contemporary years (1970–2000) and two future models show two Shared Socioeconomic Pathway (SSP) scenarios (SSP2-4.5 and SSP5-8.5), **(B)** SSP2-4.5 and **(C)** SSP5-8.5. Darkest gray represents predicted empirical MaxEnt climate suitability, with dark green, light green, yellow, orange, and red indicating increased probability of climatic suitability, respectively.

future (2081–2100) models for both SSPs (SSP2-4.5 and SSP5-8.5) are shown in **Figures 4A,B**. Both future climate scenarios indicate increasing probability of disappearing climate suitability (i.e., ecophysiologically maladapted trees) for *P. menziesii* within its current range. Distributions of suitable climate space for *P. menziesii* in the Rocky Mountains that can be observed in **Figure 4A** are conspicuously absent under the more severe climate-change model of SSP5-8.5 (**Figure 4B**), though some climate suitability is observed in northern coastal regions.

When comparing the SSP2-4.5 and SSP5-8.5 models for *A. solidipes*, differences in suitable climate space are striking. In **Figure 3B** (SSP-4.5), the suitable climate space shifts northward and toward coastal areas, fairly similar to the *P. menziesii* suitable climate space predicted under the SSP2-4.5 model. However, the suitable climate space predicted under the SSP5-8.5 model highlights a new northern region of climatic suitability that coincides with newly identified areas with potential climatic suitability for *P. menziesii* under the same model (**Figure 3C**).

DISCUSSION

This study provides a sound approach for predicting potential forest disease incidence and potential severity under contemporary and changing climate scenarios. We used presence-only occurrence data for *A. solidipes* and both presence and absence (as background data) occurrence data for *P. menziesii* to produce predictions of potential contemporary and future distributions of these species using MaxEnt modeling. Predicted shifts in suitable climate space for both *P. menziesii* and *A. solidipes* are highly correlated as the predicted change in climate suitability moves dramatically northward for years 2081–2100 using both SSPs (SSP2-4.5 and SSP5-8.5). The results from this study strongly suggest that Armillaria root disease will be exacerbated in many areas where *P. menziesii* is predicted to become increasingly maladapted and extreme weather events will likely become more common. Predicting the potential distribution of both pathogen (*A. solidipes*) and a primary host (*P. menziesii*) under contemporary and future climate scenarios is critical to deploy suitable strategies to reduce damage from the disease.

In this study, the MaxEnt models performed remarkably well, based on the high AUC values (0.953 for *P. menziesii* and 0.960 for *A. solidipes*) that indicate high reliability and predictive accuracy. This approach seems to be quite reliable, especially given the relatively limited occurrence data for *A. solidipes*. In addition, MaxEnt is a robust predictor of collinearity in model training and highly correlated variables have little impact on the model output (Feng et al., 2019). This study predicts areas at risk for Armillaria root disease using the MaxEnt model, which works well with limited number of presence-only occurrence data (Phillips et al., 2006). Unlike *P. menziesii* (N = 11,826),

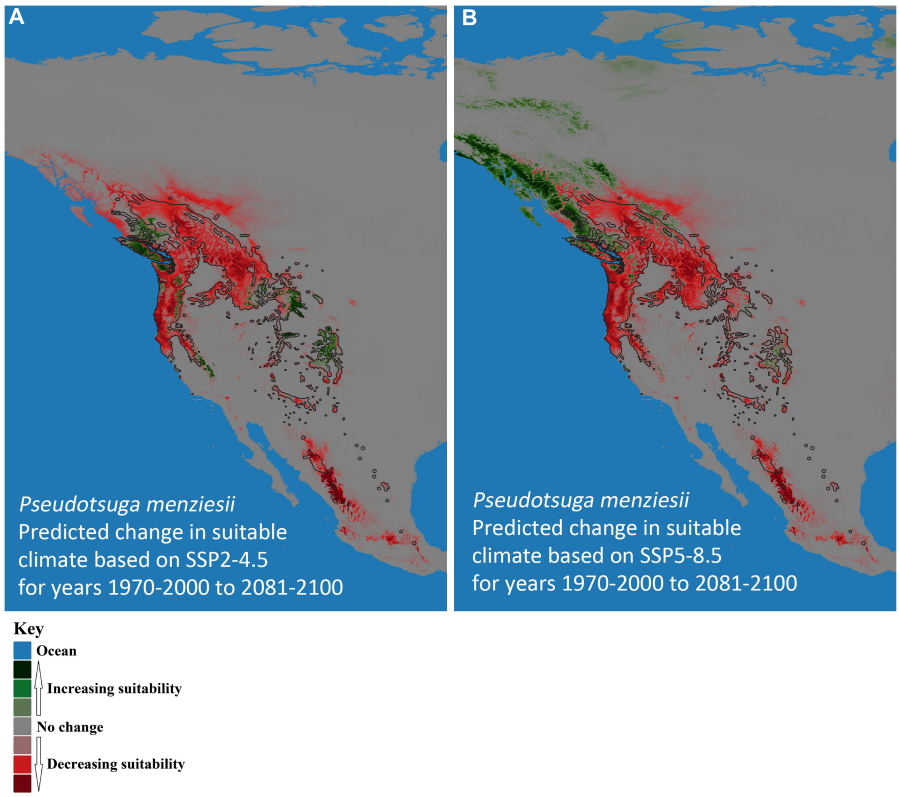

FIGURE 4 | Predicted change in climate suitability for *Pseudotsuga menziesii* (Douglas-fir) in western North America from contemporary (1970–2000) to future (2081–2100) models. **(A)** Shared Socioeconomic Pathway (SSP) SSP2-4.5 and **(B)** SSP5-8.5. Pink to dark red, respectively, indicates increasing probability of disappearing climate suitability (i.e., ecophysiologically maladapted trees), while light green to dark green, respectively, represents predictions of new climatically suitable areas. The black outline designates Little's (1971) *P. menziesii* range map.

the acquisition of occurrence data for *A. solidipes* (N = 382) required highly labor-intensive work including excavation of lateral roots, pathogen isolation, and DNA sequence-based identification to confirm occurrence (Klopfenstein et al., 2009). In addition, absence data for *Armillaria* are difficult to obtain and confirm with certainty. For these reasons, MaxEnt was applied to compare both host (*P. menziesii*) and pathogen (*A. solidipes*) using the same modeling parameters, although the model slightly overpredicts the suitable climate space compared to a presence/absence model (see Rehfeldt et al., 2014a for a climate niche model of *P. menziesii* based on a Random Forests classification algorithm). Overall, under the contemporary climate, the predicted potential distribution of *P. menziesii* using the MaxEnt is generally congruent with the established range map of *P. menziesii* within the continental United States (Little, 1971). Recently, MaxEnt bioclimatic models have been widely used to investigate the suitable climate space of other plants and plant pathogens, with high predictive performance (e.g., Kumar and Stohlgren, 2009; Khanum et al., 2013; Remya et al., 2015; Stewart et al., 2018, 2020; Tang et al., 2021).

Several other critical variables can be implemented to improve the precision of these prediction models for *P. menziesii* and *A. solidipes*. For *P. menziesii*, the MaxEnt models were based on presence and absence data at the species level. However, *P. menziesii* exhibits climatic adaptation at the intraspecies level where a given population within the species is genetically adapted to persist only over a portion of the climate range occupied by the species as a whole (e.g., Weiskittel et al., 2012; Rehfeldt et al., 2014a). Because our bioclimatic models do not explicitly include intraspecies adaptive structure (i.e., climate types), they likely underestimate the extent of climatic maladaptation within the species under predicted climate change. Of special note, *P. menziesii* with higher levels of drought tolerance were also associated with higher levels of resistance to Armillaria root disease, caused by *A. solidipes* (Cruickshank and Filipescu, 2017). Furthermore, summer droughts were associated with increased *A. solidipes*-caused mortality of *P. menziesii* in southern BC, Canada (Murray and Leslie, 2021). These findings further support that climatic maladaptation of *P. menziesii* will lead to increased infection by *A. solidipes*. Thus, predictions of *P. menziesii* maladaptation under future climate scenarios likely underestimate the extent of maladaptation and associated increased susceptibility to Armillaria root disease. However, east of the Cascade Range, *P. menziesii* is one of the most susceptible tree species to Armillaria root disease (Morrison, 1981; Robinson and Morrison, 2001), but the faster growing coastal variety of *P. menziesii* succumbs less often to *A. solidipes* infection (Johnson et al., 1972; Robinson and Morrison, 2001).

In addition, the population structure of *A. solidipes* is unknown; however, an individual *A. solidipes* genet (vegetative clone) can reside on a site up to ca. 1900–8650 years (Ferguson et al., 2003), suggesting that this root pathogen may possess a broad tolerance for changing climatic conditions. To address genetic differences within the species, population-level data are needed for both host and pathogen to refine climate-based models. Additional predictive variables (e.g., soil types, soil temperature and moisture, drainage properties/patterns, solar radiation, predictions of other *Armillaria* species, soil microbial communities, etc.) will affect the suitable climate distribution of *A. solidipes*, and this information could improve the resolution of predictive maps.

Reliable, long-term records are unavailable for quantifying Armillaria root disease levels because of difficulties associated with below-ground surveying, sampling, and identifying *Armillaria* spp. Long-term monitoring for Armillaria root disease in relation to weather/climate factors would provide an opportunity to directly determine climatic influences on the impact of the disease; however, such studies are complex because tree maturity and other stand conditions also change over time. Long-term monitoring is needed to further establish any climatic relationships with *P. menziesii* maladaptation, *A. solidipes* growth/survival, and Armillaria root disease of *P. menziesii*. Monitoring must also consider that the majority of *P. menziesii* associated with Armillaria root disease show no readily observable symptoms, except slower growth (Morrison et al., 2000; Cruickshank et al., 2011). In addition, evidence suggests complex interactions among *Armillaria* spp., in which some *Armillaria* sp. may serve as a biocontrol against more pathogenic *Armillaria* sp. under favorable site conditions (e.g., *A. altimontana* vs. *A. solidipes*) (Hanna, 2005; Warwell et al., 2019). For this reason, bioclimatic modeling of *Armillaria* spp. that are currently existing as saprophytes in a non-pathogenic mode is also warranted. Monitoring data need to include presence/absence of accurately identified *A. solidipes*, some measure of abundance (inoculum), and virulence of *Armillaria* to allow further refinements of climate-Armillaria root disease predictions. Continued surveys are also needed to further validate the relationship of Armillaria root disease with maladapted forest trees at diverse geographic locations.

Although the ranges of *P. menziesii* and *A. solidipes* show considerable overlap, *P. menziesii* extends further south into Mexico (Oaxaca) and it can exist in different regions with distinct climatic niches where *A. solidipes* does not occur (Cannon et al., 2008). Any differences in the ranges of *P. menziesii* and *A. solidipes* likely explain why the important climate variables (permutation importance > 10%) were different for *P. menziesii* and *A. solidipes* models. Mean temperature of warmest quarter (Bio10), precipitation of coldest quarter (Bio19), and precipitation of driest quarter (Bio17) are the significant variables to predict contemporary distribution for *P. menziesii*; whereas, temperature annual range (Bio7), maximum temperature of warmest month (Bio5), annual mean temperature (Bio1), and minimum temperature of coldest month (Bio6) were the major variables for *A. solidipes*. Among climate variables affecting *P. menziesii* distribution, the mean temperature of warmest quarter (Bio10) showed a greatest contribution (35%) followed by the precipitation of coldest (12%) and driest (10.8%) quarters. A previous study (Rehfeldt et al., 2014b) also found that temperature- and precipitation-related variables were important to predict species distribution of *P. menziesii*.

The climatic variables related to temperature demonstrated significant roles in the spatial distribution of *A. solidipes* in this study. Because *A. solidipes* can exhibit an extremely long-term occupancy of a site (e.g., Ferguson et al., 2003), this root pathogen apparently has the capacity of broad tolerance for changing climatic conditions. However, within a site, *A. solidipes* spreads predominately via vegetative growth of rhizomorphs, and the rate of *Armillaria* rhizomorph growth varies dependent on climatic factors, but warmer winters could extend the period for rhizomorph growth (e.g., Rishbeth, 1978; Van Der Kamp, 1993; Peet et al., 1996; Cruickshank et al., 1997). In situations where *Armillaria* spread via basidiospores, higher precipitation and temperatures in autumn will likely favor production of *Armillaria* basidiocarps, especially in Boreal regions (Ferguson et al., 2003; Heinzelmann et al., 2019). In general, growth and dispersal of *Armillaria* may specifically benefit from mild and moist seasons, while hot and dry seasons may increase host stress that allows *Armillaria* to overcome host defenses (Heinzelmann et al., 2019), which suggests that seasonal climates are important factors that contribute to Armillaria root disease.

Although predictions of future suitable climate space for *P. menziesii* and *A. solidipes* are dependent on the accuracy of the projected climate grids, the trends indicate that suitable climate space for both species will move northward and toward higher elevations under both SSP2-4.5 and SSP5-8.5 pathways. Under SSP2-4.5 and SSP5-8.5 conditions, while suitable climate for *A. solidipes* is predicted to decrease in many areas of the inland western United States and BC, Canada, *A. solidipes* will remain adapted to many areas of this region, where it will likely still persist and likely contribute significantly to decreased forest health and increased mortality where maladapted hosts remain. However, these models do not take adaptation into account, but it is presumed unlikely that either of these relatively long-lived species can dramatically adapt within such a short period time. A plausible hypothesis is that maladaptation (stress) caused by climate change can predispose host trees and result in increased susceptibility to root pathogens (e.g., Kliejunas et al., 2009; Sturrock et al., 2011).

The science-based information to predict potential distribution of Armillaria root disease pathogens and host trees under present and future climate scenarios will inform strategies to reduce Armillaria root disease. For example, predictive models will help identify tree populations at risk and prioritize species and seed source selection to address the objectives of adaptive management. In general, tree species/populations that are predicted to be adapted to future climates can be selected for or planted within sites that are expected to have suitable climate for the *Armillaria* pathogen. Many existing or naturally regenerated tree populations that exhibit a moderate-to-high degree of phenotypic plasticity for climatic adaptability

(i.e., generalists), such as *P. monticola*, will likely experience less stress from climatic maladaptation and should also exhibit higher resistance/tolerance to Armillaria root disease. Other forest management practices that reduce tree stress, such as increased spacing, may also reduce impacts of Armillaria root disease under a changing climate.

CONCLUSION

Contemporary and future predictions of suitable climate space of *P. menziesii* and *A. solidipes* generated by MaxEnt modeling is an informative tool that can be used to help reduce impacts from Armillaria root disease under changing climates. It is important to note, however, predicted suitable climate space for a species does not necessarily correspond to the future distribution of that species. Although the co-occurrence of suitable climate space for the pathogen and its host does not necessarily result in disease, it is a likely prerequisite for disease. As discussed above, future species distribution and the occurrence of disease will depend on many factors, such as population structure, migration, regeneration, competition, susceptibility to insect attack and diseases, and other interacting factors. The realized distribution of a species will be determined by the interactions among diverse biological, climatic, and environmental factors. Regardless, this study provides an approach to examine the influence of climate on the distribution of an Armillaria root disease pathogen (*A. solidipes*) and its host tree (*P. menziesii*). Such approaches are especially useful in determining areas with climate where *Armillaria* pathogens should not occur, and of course, Armillaria root disease will not occur in areas where the *Armillaria* pathogen does not occur. The climate-based modeling methods developed from this study can also be used to model other important forest pathogens and examine the potential for invasive species to occupy new geographic areas under contemporary and future climates.

DATA AVAILABILITY STATEMENT

The original contributions presented in the study are included in the article and further inquiries can be directed to the corresponding author.

AUTHOR CONTRIBUTIONS

NK, JH, JS, MW, GM, and M-SK designed the study and collected a partial *Armillaria solidipes* data. M-SK, NK, JS, and JH wrote the first draft of the manuscript. JH performed the data analyses. All authors contributed to manuscripts revision and approved the submitted version.

FUNDING

This project was partially funded by the Forest Health Protection, Special Technology Development Program (R1-2020-2, R4-2019-1, and R2-2018-1).

ACKNOWLEDGMENTS

We would like to thank A. L. Smith, H. Maffei, M. L. Fairweather, J. T. Blodgett, P. J. Zambino, J. Worrall, K. S. Burns, J. J. Jacobs, S. M. Ashiglar, J. E. Lundquist, A. L. Ross-Davis, C. Hoffman, R. Mathiasen, R. Hofstetter, J. D. Shaw, E. V. Nelson, M. R. Cleary, S. Brar, B. A. Richardson, and many other collaborators for their help with obtaining *Armillaria* collections and data.

REFERENCES

Berbee, M., Bazzicalupo, A., and Le Renard, L. (2014). *Direct GenBank Submission KJ146700: fungi of Capilano River Regional Park, North Vancouver BC Canada. Submitted (10-JAN-2014)*. Vancouver, British Columbia: University of British Columbia.

Berbee, M., Bazzicalupo, A., and Le Renard, L. (2015). *Direct GenBank Submission KP454026: fungi of Capilano River Regional Park, North Vancouver BC Canada. Submitted (09-JAN-2015)*. Vancouver, British Columbia: University of British Columbia.

Blodgett, J. T., Hanna, J. W., Pitman, E. W. I., Ashiglar, S. M., Lundquist, J. E., Kim, M.-S., et al. (2015). "Bioclimatic models estimate areas of suitable habitat for *Armillaria* spp. in Wyoming" in *Proceedings of the 62nd Western International Forest Disease Work Conference*. comps M. Murray and P. Palacios (Olympia, WA: Washington Department of Natural Resources). 29–33.

Blodgett, J. T., and Lundquist, J. E. (2011). "Distribution, species, and ecology of *Armillaria* in Wyoming," in *Proceedings of the 58th Western International Forest Work Conference*. comps M. L. Fairweather, and P. Palacios (Logan, UT: Utah State University). 58.

Cannon, P., Klopfenstein, N. B., Kim, M.-S., Hanna, J. W., Medel, R., and Alvarado-Rosales, D. (2008). "An *Armillaria* survey in Mexico: a basis for determining evolutionary relationships, assessing potentially invasive pathogens, evaluating future impacts of climate change, and developing international collaborations in forest pathology" in *Proceedings of the 55th Western International Forest Disease Work Conference*. comp M. G. Williams (Salem, OR: Oregon Department of Forestry). 29–39.

Chmura, D. J., Anderson, P. D., Howe, G. T., Harrington, C. A., Halofskyd, J. E., Peterson, D. L., et al. (2011). Forest responses to climate change in the northwestern United States: Ecophysiological foundations for adaptive management. *For. Ecol. Manag.* 261, 1121–1142. doi: 10.1016/j.foreco.2010.12.040

Cruickshank, M. G., and Filipescu, C. N. (2017). The interactive effect of root disease and climate on wood properties in halfsibling Douglas-fir families. *For. Ecol. Manag.* 392, 58–67. doi: 10.1016/j.foreco.2017.03.002

Cruickshank, M. G., Morrison, D. J., and Lalumière, A. (2011). Site, plot, and individual tree yield reduction of interior Douglas-fir associated with non-lethal infection by Armillaria root disease in southern British Columbia. *For. Ecol. Manag.* 261, 297–307. doi: 10.1016/j.foreco.2010.10.023

Cruickshank, M. G., Morrison, D. J., and Punja, Z. K. (1997). Incidence of *Armillaria* species in precommercial thinning stumps and spread of *Armillaria ostoyae* to adjacent Douglas-fir trees. *Can. J. For. Res.* 27, 481–490. doi: 10.1139/x96-185

Dorfman, D. D., Berbaum, K. S., and Metz, C. E. (1992). Receiver operating characteristic rating analysis: generalization to the population of readers and patients with the jackknife method. *Investig. Radiol.* 27, 723–731.

Elías-Román, R. D., Guzmán-Plazola, R. A., Klopfenstein, N. B., Alvarado-Rosales, D., Calderón-Zavala, G., Mora-Aguilera, J. A., et al. (2013). Incidence and phylogenetic analyses of *Armillaria* spp. associated with root disease in peach orchards in the State of Mexico, Mexico. *For. Pathol.* 43, 390–401. doi: 10.1111/efp.12043

Eyring, V., Bony, S., Meehl, G. A., Senior, C. A., Stevens, B., Stouffer, R. J., et al. (2016). Overview of the Coupled Model Intercomparison Project Phase 6 (CMIP6) experimental design and organization. *Geosci. Model Dev.* 9, 1937–1958. doi: 10.5194/gmd-9-1937-2016

Feng, X., Park, D. S., Liang, Y., Pandey, R., and Papeş, M. (2019). Collinearity in ecological niche modeling: confusions and challenges. *Ecol. Evol.* 9, 10365–10376. doi: 10.1002/ece3.5555

Ferguson, B. A., Dreisbach, T. A., Parks, C. G., Filip, G. M., and Schmitt, C. L. (2003). Coarse-scale population structure of pathogenic *Armillaria* species in a mixed-conifer forest in the Blue Mountains of northeast Oregon. *Can. J. For. Res.* 33, 612–623. doi: 10.1139/x03-065

Fick, S. E., and Hijmans, R. J. (2017). WorldClim 2: new 1-km spatial resolution climate surfaces for global land areas. *Int. J. Climatol.* 37, 4302–4315. doi: 10.1002/joc.5086

Hanna, J. W. (2005). *Armillaria ostoyae: genetic characterization and distribution in the western United States*. [master thesis]. Moscow, ID: University of Idaho, p. 116.

Hanna, J. W., Blodgett, J. T., Pitman, E. W. I., Ashiglar, S. M., Lundquist, J. E., Kim, M.-S., et al. (2014). "Climate-based species distribution models for *Armillaria solidipes* in Wyoming: a preliminary assessment" in *Proceedings of the 61st Annual Western International Forest Disease Work Conference*. comps K. Chadwick and P. Palacios (Logan, UT: Utah State University). 117–120.

Hanna, J. W., Kim, M.-S., Klopfenstein, N. B., Smith, A. L., and Maffei, H. M. (2008). "Determination of suitable climate space for *Armillaria ostoyae* in the Oregon East Cascades" in *Proceedings of the 55th Western International Forest Disease Work Conference*. comp M. G. McWilliams (Salem, OR: Oregon Department of Forestry). 92.

Hanna, J. W., Smith, A. L., Maffei, H. M., Kim, M.-S., and Klopfenstein, N. B. (2009). "Survey of *Armillaria* spp. in the Oregon East Cascades: baseline data for predicting climatic influences on Armillaria root disease," in *Proceedings of the 56th Annual Western International Forest Disease Work Conference*. comps F. Baker, C. Jamieson, and P. Palacios (Logan, UT: Utah State University). 53–59.

Hanna, J. W., Klopfenstein, N. B., Kim, M.-S., McDonald, G. I., and Moore, J. A. (2007). Phylogeographic patterns of *Armillaria ostoyae* in the western United States. *For. Pathol.* 37, 192–216. doi: 10.1111/j.1439-0329.2007.00497.x

Heinzelmann, R., Dutech, C., Tsykun, T., Labbé, F., Soularue, J.-P., and Prospero, S. (2019). Latest advances and future perspectives in *Armillaria* research. *Can. J. Plant Pathol.* 41, 1–23. doi: 10.1080/07060661.2018.1558284

Hermann, R. K., and Lavender, D. P. (1990). "*Pseudotsuga menziesii* (Mirb.) Franco" in *USDA Forest Service, Agriculture Handbook 654*. eds R. M. Burns and B. H. Honkala (Washington, DC: U.S. Department of Agriculture). 527–540.

Hertert, H. D., Miller, D. L., and Partridge, A. D. (1975). Interaction of bark beetles (Coleoptera: scolytidae) and root-rot pathogens in grand fir in northern Idaho. *Can. Entomol.* 107, 899–904.

Hoffman, C. W., Mathiasen, R. L., Hofstetter, R. W., Fairweather, M. L., Shaw, J. D., Hanna, J. W., et al. (2014). Survey for *Armillaria* by plant associations in northern Arizona. *J. Arizona-Nevada Acad. Sci.* 45, 76–86. doi: 10.2181/036.045.0204

Johnson, A. L. S., Wallis, G. W., and Foster, R. E. (1972). Impact of root rot and other diseases in young Douglas-fir plantations. *For. Chron.* 48, 316–319.

Khanum, R., Mumtaz, A., and Kumar, S. (2013). Predicting impacts of climate change on medicinal asclepiads of Pakistan using Maxent modeling. *Acta Oecol.* 49, 23–31. doi: 10.1016/j.actao.2013.02.007

Kim, M.-S., Klopfenstein, N. B., Hanna, J. W., and McDonald, G. I. (2006). Characterization of North American *Armillaria* species: genetic relationships determined by ribosomal DNA sequences and AFLP markers. *For. Pathol.* 36, 145–164. doi: 10.1111/j.1439-0329.2006.00441.x

Kim, M.-S., Klopfenstein, N. B., and McDonald, G. I. (2010). Effects of forest management practices and environment on occurrence of *Armillaria* species. *J. Korean For. Soc.* 99, 251–257.

Kim, M.-S., Klopfenstein, N. B., McDonald, G. I., Arumuganathan, K., and Vidaver, A. K. (2000). Characterization of North American *Armillaria* species by nuclear DNA content and RFLP analysis. *Mycologia* 92, 874–883. doi: 10.1080/00275514.2000.12061232

Kliejunas, J. T., Geils, B., Glaeser, J. M., Goheen, E. M., Hennon, P., Kim, M.-S., et al. (2009). *Climate and forest diseases of western North America: a literature review. Gen. Tech. Rep. PSW-GTR-225*. Albany, CA: USDA, Forest Service, Pacific Southwest Research Station, p. 54.

Klopfenstein, N. B., Hanna, J. W., Fairweather, M. L., Shaw, J. D., Mathiasen, R., Hoffman, C., et al. (2012). "Developing a prediction model for *Armillaria solidipes* in Arizona," in *Proceedings of the 59th Annual Western International Forest Disease Work Conference*. comps S. Zeglen and P. Palacios (Logan, UT: Utah State University). 149–152.

Klopfenstein, N. B., Kim, M.-S., Hanna, J. W., Richardson, B. A., and Lundquist, J. E. (2009). *Approaches to predicting potential impacts of climate change on forest disease: an example with Armillaria root disease. Res. Pap. RMRS-RP-76*. Fort Collins, CO: U.S. Department of Agriculture, Forest Service, Rocky Mountain Research Station, p. 10.

Klopfenstein, N. B., Stewart, J. E., Ota, Y., Hanna, J. W., Richardson, B. A., Ross-Davis, A. L., et al. (2017). Insights into the phylogeny of Northern Hemisphere *Armillaria*: neighbor-net and Bayesian analyses of translation elongation factor 1-α gene sequences. *Mycologia* 109, 75–91. doi: 10.1080/00275514.2017.1286572

Kubiak, K., Żółciak, A., Damszel, M., Lech, P., and Sierota, Z. (2017). *Armillaria* pathogenesis under climate changes. *Forests* 8:100. doi: 10.3390/f8040100

Kulhavy, D. L., Partridge, A. D., and Stark, A. W. (1984). Root diseases and blister rust associated with bark beetles (Coleoptera: scolytidae) in western white pine in Idaho. *Environ. Entomol.* 13, 813–817.

Kumar, S., and Stohlgren, T. J. (2009). Maxent modeling for predicting suitable habitat for threatened and endangered tree *Canacomyrica monticola* in New Caledonia. *J. Ecol. Natural Environ.* 1, 94–98.

Little, E. L. Jr. (1971). *Atlas of United States trees. Volume 1. Conifers and Important Hardwoods. Misc. Publ. no. 1146*. Washington, DC: U.S. Department of Agriculture, Forest Service.

Lockman, I. B., and Kearns, H. S. J. (2016). *Forest root diseases across the United States. Gen. Tech. Rep. RMRS-GTR-342*. Ogden, UT: U.S. Department of Agriculture, Forest Service, Rocky Mountain Research Station, p. 55.

McDonald, G. I. (1990). "Connecting forest productivity to behavior of soil-borne diseases" in *Proceedings-Management and Productivity of Western Montane Forest Soils*. comps A. E. Harvey and L. F. Neuenschwander (Ogden, UT: U.S. Department of Agriculture, Forest Service, Intermountain Research Station). 129–144.

McDonald, G. I. (1998). "Preliminary report on the ecology of *Armillaria* in Utah and the inland west" in *Proceedings of the 46th Annual Western International Forest Disease Work Conference*. comp L. Trummer (Anchorage, AK: U.S. Department of Agriculture, Forest Service). 85–92.

McDonald, G. I., Hanna, J. W., Smith, A. L., Maffei, H. M., Kim, M.-S., Ross-Davis, A. L., et al. (2011). "Preliminary report on the ecology and predicted suitable climate space of *Armillaria* in the East Cascades of Oregon" in *Proceedings of the 58th Annual Western International Forest Disease Work Conference*. comps M. L. Fairweather and P. Palacios (Logan, UT: Utah State University). 135–138.

McDonald, G. I., Harvey, A. E., and Tonn, J. R. (2000). "Fire, competition and forest pests: landscape treatment to sustain ecosystem function" in *Proceedings from the Joint Fire Science Conference and Workshop: crossing the Millennium: integrating Spatial Technologies and Ecological Principles for a New Age in Fire Management Volume 2*. tech eds L. F. Neuenschwander and K. C. Ryan. (Moscow, ID: University of Idaho and the International Association of Wildland Fire). 195–211.

McDonald, G. I., Martin, N. E., and Harvey, A. E. (1987a). *Armillaria in the Northern Rockies: pathogenicity and host susceptibility on pristine and disturbed sites. Res. Note INT-371*. Ogden, UT: U.S. Department of Agriculture, Forest Service, Intermountain Research Station, p. 5.

McDonald, G. I., Martin, N. E., and Harvey, A. E. (1987b). *Occurrence of Armillaria spp. in forests of the Northern Rocky Mountains. Res. Pap. INT-381*. Ogden, UT: U.S. Department of Agriculture, Forest Service, Intermountain Research Station, p. 7.

Morrison, D. J. (1981). "Armillaria root disease. A guide to disease diagnosis, development and management in British Columbia" in *Information Report. BC-X-203*. (Environment Canada: Canadian Forest Service).

Morrison, D. J. (2011). Epidemiology of Armillaria root disease in Douglas-fir plantations in the cedar-hemlock zone of the southern interior of British Columbia. *For. Pathol.* 41, 31–40. doi: 10.1111/j.1439-0329.2009.00630.x

Morrison, D. J., Pellow, K. W., Norris, D. J., and Nemec, A. F. L. (2000). Visible versus actual incidence of Armillaria root disease in juvenile coniferous stands

in the southern interior of British Columbia. *Can. J. For. Res.* 30, 405–414. doi: 10.1139/x99-222

Murray, M. P., and Leslie, A. (2021). Climate, radial growth, and mortality associated with conifer regeneration infected by root disease (*Armillaria ostoyae*). *For. Chron.* 97, 43–51. doi: 10.5558/tfc2021-006

Omdal, D. W., Shaw, C. G. III, Jacobi, W. R., and Wager, T. C. (1995). Variation in pathogenicity and virulence of isolates of *Armillaria ostoyae* on eight tree species. *Plant Dis.* 79, 939–944.

Parsons, S., Lewis, K. J., and Psyllakis, J. M. (2003). Relationships between roosting habitat and decay of aspen in the sub-boreal forests of British Columbia. *For. Ecol. Manag.* 177, 559–570. doi: 10.1016/S0378-1127(02)00448-6

Peet, F. G., Morrison, D. J., and Pellow, K. W. (1996). Rate of spread of *Armillaria ostoyae* in two Douglas-fir plantation in the southern interior of British Columbia. *Can. J. For. Res.* 26, 148–151.

Phillips, S. J., Anderson, R. P., and Schapire, R. E. (2006). Maximum entropy modeling of species geographic distributions. *Ecol. Modell.* 190, 231–259. doi: 10.1016/j.ecolmodel.2005.03.026

Rehfeldt, G. E., Crookston, N. L., Warwell, M. V., and Evans, J. S. (2006). Empirical analysis of plant-climate relationships for the western United States. *Int. J. Plant Sci.* 167, 1123–1150. doi: 10.1086/507711

Rehfeldt, G. E., Jaquish, B. C., López-Upton, J., Sáenz-Romero, C., St Clair, J. B., Leites, L. P., et al. (2014a). Comparative genetic responses to climate for the varieties of *Pinus ponderosa* and *Pseudotsuga menziesii*: realized climate niches. *For. Ecol. Manag.* 324, 126–137. doi: 10.1016/j.foreco.2014.02.035

Rehfeldt, G. E., Leites, L. P., St Clair, J. B., Jaquish, B. C., Sáenz-Romero, C., López-Upton, J., et al. (2014b). Comparative genetic responses to climate in the varieties of *Pinus ponderosa* and *Pseudotsuga menziesii*: clines in growth potential. *For. Ecol. Manag.* 324, 138–146. doi: 10.1016/j.foreco.2014.02.041

Remya, K., Ramachandran, A., and Jayakumar, S. (2015). Predicting the current and future suitable habitat distribution of *Myristica dactyloides* Gaertn. using MaxEnt model in the Eastern Ghats, India. *Ecol. Eng.* 82, 184–188.

Rishbeth, J. (1978). Effects of soil temperature and atmosphere on growth of *Armillaria* rhizomorphs. *Trans. Brit. Mycol. Soc.* 79, 213–220.

Robinson, R. M., and Morrison, D. J. (2001). Lesion formation and host response to infection by *Armillaria ostoyae* in the roots of western larch and Douglas-fir. *For. Pathol.* 31, 371–385. doi: 10.1046/j.1439-0329.2001.00260.x

Ross-Davis, A. L., Hanna, J. W., Kim, M.-S., and Klopfenstein, N. B. (2012). Advances toward DNA-based identification and phylogeny of North American *Armillaria* species using elongation factor-1 alpha gene. *Mycoscience* 53, 161–165. doi: 10.1007/S10267-011-0148-X

Shaw, C. G. III (1989). *Armillaria ostoyae* associated with mortality of new hosts in Chihuahua, Mexico. *Plant Dis.* 73, 775.

Steeger, C., and Hitchcock, C. L. (1998). Influence of forest structure and diseases on nest-site selection by sed-breasted nuthatches. *J. Wildl. Manag.* 62, 1349–1358.

Stewart, J. E., Kim, M.-S., Ota, Y., Sahashi, N., Hanna, J. W., Akiba, M., et al. (2020). Phylogenetic and population genetic analyses reveal three distinct lineages of the invasive brown root-rot pathogen, *Phellinus noxius*, and bioclimatic modeling predicts differences in associated climate niches. *Eur. J. Plant Pathol.* 156, 751–766. doi: 10.1007/s10658-019-01926-5

Stewart, J. E., Ross-Davis, A. L., Graça, R. N., Alfenas, A. C., Peever, T. L., Hanna, J. W., et al. (2018). Genetic diversity of *Puccinia psidii* in the Americas and Hawaii: Potential global implications. *For. Pathol.* 48:e12378. doi: 10.1111/efp.12378

Sturrock, R. N., Frankel, S. J., Brown, A. V., Hennon, P. E., Kliejunas, J. T., Lewis, K. J., et al. (2011). Climate change and forest diseases. *Plant Path.* 60, 133–149. doi: 10.1111/j.1365-3059.2010.02406.x

Swart, N. C., Cole, J. N. S., Kharin, V. V., Lazare, M., Scinocca, J. F., Gillett, N. P., et al. (2019). The Canadian Earth System Model version 5 (CanESM5.0.3). *Geosci. Model Dev.* 12, 4823–4873. doi: 10.5194/gmd-12-4823-2019

Tang, X., Yuan, Y., Li, X., and Zhang, J. (2021). Maximum entropy modeling to predict the impact of climate change on pine wilt disease in China. *Front. Plant Sci.* 12:652500. doi: 10.3389/fpls.2021.652500

Tkacz, B. M., and Schmitz, R. F. (1986). *Association of an Endemic Mountain Pine Beetle Population with Lodgepole Pine Infected by Armillaria Root Rot Disease in Utah. Res. Note INT-353*. Ogden, UT: U.S. Department of Agriculture, Forest Service, Intermountain Research Station, p. 7.

Van Der Kamp, B. J. (1993). Rate of spread of *Armillaria ostoyae* in the central interior of British Columbia. *Can. J. For. Res.* 23, 1239–1241. doi: 10.1139/x93-156

Van der Star, T., Berbee, M. L., Inderbitzin, P., and Fischer, A. L. (2003). *Direct GenBank Submission AY228342: sequencing performed as class project, Biology 323, University of British Columbia*. Vancouver, British Columbia: University of British Columbia.

Warwell, M. V., McDonald, G. I., Hanna, J. W., Kim, M.-S., Lalande, B. M., Stewart, J. E., et al. (2019). *Armillaria altimontana* is associated with healthy western white pine (*Pinus monticola*) planted in northern Idaho: evidence for *in situ* biological control of *A. solidipes*. *Forests* 10:294. doi: 10.3390/f10040294

Weiskittel, A. R., Crookston, N. L., and Rehfeldt, G. E. (2012). Projected future suitable habitat and productivity of Douglas-fir in western North America. *Schweiz. Z. Forstwes.* 163, 70–78. doi: 10.3188/szf.2012.0070

Wiley, E. O., Mcnyset, K. M., Peterson, A. T., Robins, C. R., and Stewart, A. M. (2003). Niche modeling perspective on geographic range predictions in the marine environment using a machine-learning algorithm. *Oceanography* 16, 120–127. doi: 10.5670/oceanog.2003.42

Worrall, J. J., Sullivan, K. F., Harrington, T. C., and Steimel, J. P. (2004). Incidence, host relations and population structure of *Armillaria ostoyae* in Colorado campgrounds. *For. Ecol. Manag.* 192, 191–206. doi: 10.1016/j.foreco.2004.01.009

Conflict of Interest: The authors declare that the research was conducted in the absence of any commercial or financial relationships that could be construed as a potential conflict of interest.

frontiers in Forests and Global Change

ORIGINAL RESEARCH
published: 25 February 2022
doi: 10.3389/ffgc.2021.756678

Genetic Lineage Distribution Modeling to Predict Epidemics of a Conifer Disease

Naomie Y. H. Herpin-Saunier[1,2], Kishan R. Sambaraju[1,2], Xue Yin[3], Nicolas Feau[3,4], Stefan Zeglen[5], Gabriela Ritokova[6], Daniel Omdal[7], Chantal Côté[2] and Richard C. Hamelin[1,3]*

[1] Department of Wood Sciences and Forestry, Laval University, Quebec, QC, Canada, [2] Laurentian Forestry Centre, Natural Resources Canada, Canadian Forest Service, Quebec, QC, Canada, [3] Department of Forest and Conservation Sciences, The University of British Columbia, Vancouver, BC, Canada, [4] Pacific Forestry Centre, Canadian Forest Service, Natural Resources Canada, Victoria, BC, Canada, [5] British Columbia Ministry of Forests, Lands, Natural Resource Operations and Rural Development, Nanaimo, BC, Canada, [6] Oregon Department of Forestry, Oregon State Hospital, Salem, OR, United States, [7] Department of Natural Resources, Washington State Government, Olympia, WA, United States

OPEN ACCESS

Edited by:
Ari Mikko Hietala, Norwegian Institute of Bioeconomy Research (NIBIO), Norway

Reviewed by:
Juha Honkaniemi, Natural Resources Institute Finland (Luke), Finland
Jeffrey Stone, Oregon State University, United States

***Correspondence:**
Naomie Y. H. Herpin-Saunier
naomie.herpin-saunier.1@ulaval.ca

Specialty section:
This article was submitted to Pests, Pathogens and Invasions, a section of the journal Frontiers in Forests and Global Change

Received: *10 August 2021*
Accepted: *23 December 2021*
Published: *25 February 2022*

Citation:
Herpin-Saunier NYH, Sambaraju KR, Yin X, Feau N, Zeglen S, Ritokova G, Omdal D, Côté C and Hamelin RC (2022) Genetic Lineage Distribution Modeling to Predict Epidemics of a Conifer Disease. Front. For. Glob. Change 4:756678. doi: 10.3389/ffgc.2021.756678

A growing body of evidence suggests that climate change is altering the epidemiology of many forest diseases. *Nothophaeocryptopus gaeumannii* (Rhode) Petrak, an ascomycete native to the Pacific Northwest and the causal agent of the Swiss needle cast (SNC) disease of Douglas-fir [*Pseudotsuga menziesii* (Mirbel) Franco], is no exception. In the past few decades, changing climatic conditions have coincided with periodic epidemics of SNC in coastal forests and plantations from Southwestern British Columbia (B.C.) to Southwestern Oregon, wherein an increase in the colonization of needles by *N. gaeumanii* causes carbon starvation, premature needle shedding and a decline in growth. Two major sympatric genetic lineages of *N. gaeumannii* have been identified in the coastal Pacific Northwest. Past research on these lineages suggests they have different environmental tolerance ranges and may be responsible for some variability in disease severity. In this study, we examined the complex dynamics between biologically pertinent short- and long-term climatic and environmental factors, phylogenetic lineages of *N. gaeumannii* and the severity patterns of the SNC disease. Firstly, using an ensemble species distribution modeling approach using genetic lineage presences as model inputs, we predicted the probability of occurrence of each lineage throughout the native range of Douglas-fir in the present as well as in 2050 under the "business as usual" (RCP8.5) emissions scenario. Subsequently, we combined these model outputs with short-term climatic and topographic variables and colonization index measurements from monitoring networks across the SNC epidemic area to infer the impacts of climate change on the SNC epidemic. Our results suggest that the current environmental tolerance range of lineage 1 exceeds that of lineage 2, and we expect lineage 1 to expand inland in Washington and Oregon, while we expect lineage 2 will remain relatively constrained to its current range with some slight increases in suitability,

particularly in coastal Washington and Oregon. We also found that disease colonization index is associated with the climatic suitability of lineage 1, and that the suitability of the different lineages could impact the vertical patterns of colonization within the crown. We conclude that unabated climate change could cause the SNC epidemic to intensify.

Keywords: climate change, epidemiology, Douglas-fir, Swiss needle cast, pathogen genetics

INTRODUCTION

Anthropogenic climate change threatens the health and resilience of forest trees and their ecosystems through a variety of direct and indirect effects (Shaw and Osborne, 2011; Sturrock et al., 2011; Desprez-Loustau et al., 2016). Conifers are believed to be particularly vulnerable to a warming climate (McDowell et al., 2016). Among these effects is the rising risk from biotic disturbance agents such as forest diseases (Drew Harvell et al., 2002; Sturrock et al., 2011). Fungal disease agents, due to their relatively short lifespans, are able to evolve adaptive traits more rapidly in response to environmental changes than their perennial hosts. Consequently, unprecedented epidemics can occur when favorable environmental conditions persist and exacerbate the effects of climate change on forest health, potentially resulting in severe ecological and economic impacts (Desprez-Loustau et al., 2016; Hessenauer et al., 2021).

One noteworthy example is *Nothophaeocryptopus gaeumannii* (Rhode) Petrak, an endophytic fungal associate of Douglas-fir [*Pseudotsuga menziesii* (Mirbel) Franco], an ecologically, economically and culturally important conifer native to the Pacific Northwest Coast in the United States and Canada. Though *N. gaeumannii* was previously only considered pathogenic in Douglas-fir's planted range, it has emerged as a threat in the tree's native range in western North America in recent decades (Hansen et al., 2000). The fungus is the causal agent of Swiss needle cast (SNC), a disease that results in premature defoliation of Douglas-fir, jeopardizing its health and productivity (Gaumann, 1928; Boyce, 1940; Hood and Kershaw, 1975; Maguire et al., 2002; Lavender and Hermann, 2014). Like most forest foliar pathogens, the presence and abundance of *N. gaeumannii* is linked to short and long-term climate patterns (Manter et al., 2003, 2005; Stone et al., 2007; Mildrexler et al., 2019). As outbreaks of SNC have become unprecedentedly frequent and severe, there have been considerable efforts to understand the factors driving its distribution and severity patterns (Shaw et al., 2021).

The emergence of SNC is inextricably tied to the reproductive cycle of *N. gaeumannii*, which in turn depends on local environmental conditions and the life cycle of its host. The fungus produces sexual fruiting bodies called pseudothecia that erupt through the stomata of Douglas-fir needles. With the right environmental conditions, these structures can increase in abundance and subsequently inhibit gas exchange and cause needle chlorosis and premature senescence, ultimately reducing vertical and radial growth by over 50% in the most severely affected stands (Manter et al., 2000; Maguire et al., 2011). The specific conditions leading to proliferation of *N. gaeumannii* are understood to be in large part linked to temperature and moisture fluctuations at relevant times in the life cycle of the fungus (Stone et al., 2008a). Mild fall and winter temperatures, concurrent with epiphytic and endophytic hyphae growth in Douglas-fir needles, are conducive to fungal development (Manter et al., 2005; Bennett and Stone, 2019). Wet conditions in the spring and summer, coincident with Douglas-fir bud burst and *N. gaeumannii* spore dispersal, increase spore-needle adherence and rainsplash dispersal, favoring *N. gaeumannii* abundance. Additionally, topographical features such as elevation, slope aspect and shading that moderate microclimate have also been identified as important predictors of disease severity (Rosso and Hansen, 2003; Manter et al., 2005; Lee et al., 2017). While the extent and severity of epidemics has varied over the last decades, coastal forests of Oregon and Washington states largely planted with young Douglas-fir have been the epicenter of SNC outbreaks. Hence, silvicultural factors such as tree age and species diversity, along with the Pacific Northwest coastal characteristics such as fog and oceanic climate are considered conducive to increased severity (Ritóková et al., 2016, 2021; Shaw et al., 2021).

Recent explorations into the phylogeography of *N. gaeumannii* in the Pacific Northwest suggest that the current crisis is not solely attributable to climatic changes (Winton et al., 2006; Bennett and Stone, 2016, 2019). The population structure and genetics of *N. gaeumannii* have also been investigated as a source of variability in disease severity. Two major non-interbreeding phylogenetic lineages of *N. gaeumannii* (named lineages 1 and 2) have been identified in the Pacific Northwest, and though they are sympatric, their spatial distributions suggest that they may be adapted to different environmental conditions and climates (Bennett and Stone, 2016, 2019). Whereas lineage 1 has been detected across the native range of Douglas-fir as well as in exotic plantations from Europe to New Zealand, lineage 2 has been detected almost exclusively in coastal areas west of the Coast mountains of Washington and Oregon in addition to a small number of sites in New Zealand (Bennett and Stone, 2016; Bennett et al., 2019). Prior observations have indicated that regions where both lineages are detected are generally more severely infected (Winton et al., 2006; Bennett and Stone, 2016), but thus far, the role of the lineages in disease patterns remains unclear (Bennett and Stone, 2019).

In this paper, we report the use of genetic lineage distribution modeling (LDM) to explore the epidemiology of SNC at different scales. Presence-only species distribution models (SDM), which predict the probability of occurrence of a species based on georeferenced presence points, true absence or pseudo-absence points and environmental predictors, are becoming essential tools in conservation biology and disease epidemiology, including for assessing the ecological and epidemiological implications of climate change

(Thuiller et al., 2005; Purse and Golding, 2015; Liu et al., 2020). In the context of a changing climate and increasingly accessible genomic tools, the integration of evolutionary information such as genetic clusters into SDMs can provide more accurate and informative predictions (Hoffmann and Sgrò, 2011; Gotelli and Stanton-Geddes, 2015; Desprez-Loustau et al., 2016; Nadeau and Urban, 2019). We believe that incorporating lineage-level distribution modeling with fine-scale severity data at monitoring sites may answer some important questions about the genetic and climatic characteristics underlying SNC epidemiology. The main questions we sought to address are: (i) What is the relationship between the climatic determinants of SNC and the distribution of lineages 1 and 2?; (ii) How will the potential distributions of the lineages change from the current climate to a future time period (2035–2065) under the "business as usual" climate scenario (RCP8.5)?; and (iii) can lineage climatic suitability be used to predict the average SNC severity at a site and to explain differences in within-tree severity patterns?

MATERIALS AND METHODS

Lineage Distribution Modeling Input Data

The study area chosen for the training and testing of our LDMs is the Marine West Coast Forests EPA Level I ecoregion, which covers the area of monitoring and provides a relatively ecologically homogeneous area for pseudo-absence selection (**Figure 1A**). The area of interest onto which we extrapolated our predictions is the entire Douglas-fir native range, which encompasses both the coastal (*P. menziesii* var. *menziesii*) and interior (*P. menziesii* var. *glauca*) varieties of Douglas-fir (Little, 1971) (**Figure 1A**).

Presence and absence points for the two phylogenetic lineages of *N. gaeumannii* in the PNW (**Supplementary Data Sheet S1**) were obtained from two sources: (i) lineage proportion data published by Bennett and Stone (2019) obtained using multilocus genotypes of a collection of isolates and (ii) lineage presence detection from samples of pseudothecia via real-time PCR using the methods described in **Supplementary Protocol S1**. The lineage identification from pseudothecia via real-time PCR used an established false positive signal to determine true presence with 99.5% accuracy if the targeted lineage constituted at least 5% of the pseudothecia in the sample using a statistical approach based on Geng et al. (1983). Therefore, to establish an equivalency in presence detection between these two sources of points, a lineage was considered absent in Bennett and Stone's (2019) collection of isolates wherever the proportion of the lineage was below 5%. The compilation of points from these two sources produced a dataset of 62 presence points and 9 absence points of lineage 1 (**Figure 1B**), and 42 presence points and 29 absence points of lineage 2 (**Figure 1C**). In order to reduce the spatial clustering of the data, the points were rarefied to a 5 km resolution using the SDMtoolbox 2.0 python package (Brown et al., 2017).

Nine pseudo-absence datasets were generated using several pseudo-absence selection methods and numbers of pseudo-absences to collectively maximize performance for all the selected algorithms while reducing the bias from each individual pseudo-absence generation method. These were (i) surface range envelope with the quantile value set at 0.025, (ii) a minimum buffer of 20 km between an absence and the nearest presence, and (iii) randomly selected points masked by an exhaustive collection of *N. gaeumannii* presence points from past published research and aerial surveys in Oregon, Washington and British Columbia (**Supplementary Data Sheet S2**). For each of the pseudo-absence methods, three datasets were generated containing different numbers of points. These were (i) the same number of pseudo-absence points as presence points (ii) one hundred pseudo-absence points, and (iii) one thousand pseudo-absence points. In total, this led to nine pseudo-absence datasets. The prevalence was set at 0.5, weighting the total presences and total absences and pseudo-absences equally. These methods are based on our interpretation of the results and

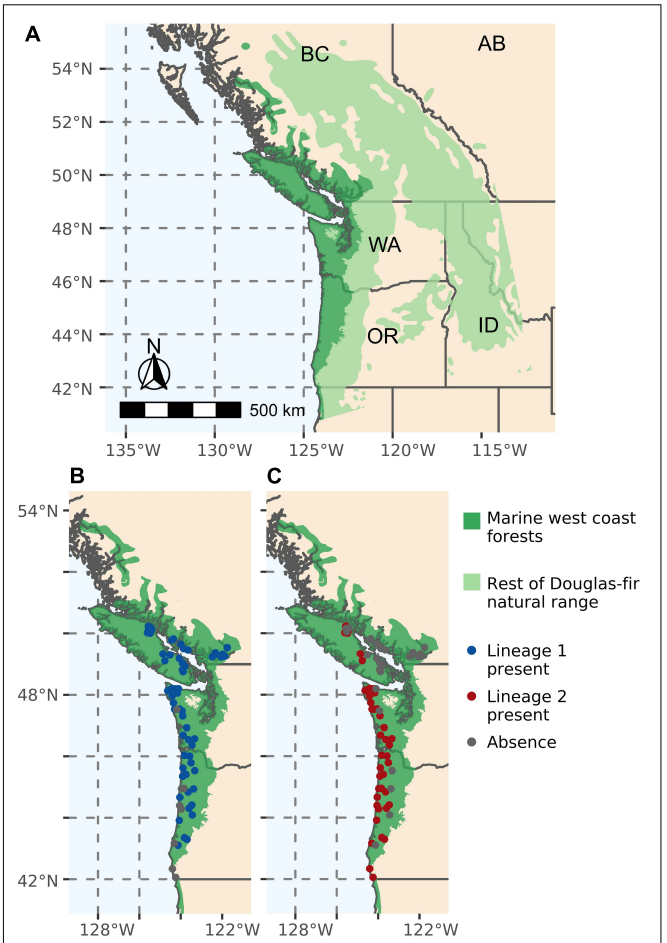

FIGURE 1 | (A) Douglas-fir native range in the Pacific Northwest (Little, 1971). The darker green shaded area is the Marine West Coast Forest EPA Level I Ecoregion, which is the study area used to train and test our lineage distribution modelings (LDMs). The lighter green shaded area is the rest of the Douglas-fir native range, the Area of Interest onto which we extrapolate our LDM predictions. **(B)** 62 presence and 9 absence points of lineage 1 of *Nothophaeocryptopus gaeumannii* across 71 sampled locations. **(C)** 42 presence and 29 absence points of lineage 2 of *N. gaeumannii* across 71 sampled locations.

recommendations of Barbet-Massin et al. (2012) and Liu et al. (2019).

Environmental Variables Selected for Lineage Distribution Modeling

The environmental variables incorporated in this analysis were average degree days above 5°C (DD5), Summer Heat Moisture Index (SHM) and annual Relative Humidity (RH) between 1980 and 2010 (henceforth the "current" climate), as well as distance from the nearest coastline (km).[1] DD5, SHM and RH were selected from a set of 28 bioclimatic variables produced by ClimateNA for different time periods (Wang et al., 2016). The variables were narrowed down based on their contribution to aforementioned temperature and wetness conditions conducive to *N. gaeumannii* proliferation, and then filtered based on their multicollinearity; only variables with a VIF below 0.5 were maintained. A short description of each variable and its rationale for inclusion in the LDM analysis is described in **Table 1**.

Rasters for future climate conditions were downloaded from ClimateNA for the period 2035-2065 (midpoint = 2050) under an ensemble of 13 Atmosphere-Ocean General Circulation Models (ACCESS-ESM1-5, BCC-CSM2-MR, CNRM-ESM2-1, CanESM5, EC-Earth3, GFDL-ESM4, GISS-E2-1-G, INM-CM5-0, IPSL-CM6A-LR, MIROC6, MPI-ESM1-2-HR, MRI-ESM2-0 and UKESM1-0-LL) of the Representative Concentration Pathway 8.5 climate change scenario (henceforth the "RCP8.5 2050 scenario"). This scenario, also known as the "business as usual" scenario, is intended to indicate the worst case scenario of climate change in the absence of mitigation policies, reflecting an increase in radiative forcing of 8.5 Watts/m^2 by the end of twenty-first century relative to pre-industrial levels (Moss et al., 2010). To provide an overview of how the values of the climate variables are forecast to change under the RCP8.5 2050 scenario, we extracted values from the climate variable rasters at the 71 lineage sampling locations and graphed box plots and probability densities comparing their current and future values.

[1]https://oceancolor.gsfc.nasa.gov/docs/distfromcoast/

Lineage Distribution Modeling Analysis

We used the SDM framework of the biomod2 R package (Thuiller et al., 2009). Four algorithms, Generalized Linear Models (GLM), Multiple Adaptive Regression Splines (MARS), Breiman and Cutler's Random Forests (RF) and Maximum Entropy (MAXENT) were used to construct an ensemble model for each lineage. This set of algorithms was selected to maximize both predictive performance and interpretability while minimizing bias by combining traditional regression methods with more flexible and computationally intensive machine learning algorithms. Three cross validation runs with a training:testing data split of 80:20 were computed for each pseudo-absence dataset. A total of 108 models were developed (nine pseudo-absence sets x four algorithms x three cross-validation runs) to predict the potential distributions of lineage 1 and lineage 2 in the study area.

Models were evaluated by examining the True Skill Statistic (TSS) scores, which are calculated by taking the sum of the True Positive Rate (sensitivity) and True Negative Rate (specificity) minus 1, for each combination of the algorithm, pseudo-absence set, and cross-validation run. To examine the relationship between *N. gaeumanii* lineage occurrence and the explanatory variables used in this analysis, variable importance values were computed as explained in Thuiller et al. (2009). In our study, this was calculated using three permutations (i.e., random rearrangements of data) of each variable and via comparison of the correlations between the predictions from the

TABLE 1 | Description, reason for inclusion and source of variables used in LDM.

Variable	Description	Reason for inclusion	Source
Annual degree days above 5°C (DD5)	The sum of the total number of accumulated degrees between 5°C and the mean daily temperature of each day in the year.	Mild winter conditions favour *N. gaeumannii* epiphytic and endophytic growth (Manter et al., 2005; Stone et al., 2008a; Bennett and Stone, 2019). Ascospore dispersal requires temperatures of 5°C to 28°C and growth is inhibited above 30°C, therefore mild summer temperatures are also favourable to *N. gaeumannii* (Michaels and Chastagner, 1984; Capitano, 1999; Rosso and Hansen, 2003). DD5 is also an important predictor of Douglas-fir productivity (Weiskittel et al., 2012).	ClimateNA/ Adaptwest
% Annual Relative Humidity (RH)	Proportion of absolute humidity in an air parcel out of the maximum humidity at that temperature.	Relative humidity favours ascospore germination (Wicklow and Zak, 1979; Beyer et al., 2005) and has been found to be a trigger of SNC epidemics (Watts et al., 2014).	ClimateNA/ Adaptwest
Summer Heat Moisture Index (SHM)	Ratio of the mean temperature of the warmest month to the mean May-September precipitation divided by 1000. Hot, dry summers have high SHM, while cool, wet years have low SHM.	Mild and wet spring and summer conditions are known to favour reproductive success and growth of *N. gaeumannii* (Michaels and Chastagner, 1984; Capitano, 1999; Rosso and Hansen, 2003; Mildrexler et al., 2016, 2019)	ClimateNA/ Adaptwest
Distance (km) to coast (dist)	Distance to the nearest coastline.	Distance from the coast is a proxy for a variety of environmental conditions strongly related to Swiss needle cast symptom presence and severity and is an important indicator of the relative proportion of Lineage 2 (Lee et al., 2017; Bennett and Stone, 2019; Mildrexler et al., 2019).	National Oceanic and Atmospheric Administration (NOAA)

re-arranged data versus the unshuffled data. Influential variables will have higher variable importance values (range: 0–1). Finally, to understand the relationships between the variables and the occurrence probability of the lineages, we graphed response plots for each variable developed based on the GLM models with a TSS score of 0.7 or above.

Ensemble modeling, where predictions from several different modeling techniques are combined, is applied to reduce bias and improve performance of SDMs (Araújo et al., 2005; Marmion et al., 2009). The predictions from the different modeling techniques were "ensembled" based on the average probabilities from high performing models (TSS > 0.7 for lineage 1 and TSS > 0.75 for lineage 2). Predictions from the ensembles were then projected to the entire range of Douglas-fir in the Pacific Northwest for current (1980–2010) and future conditions (2035–2065) under the RCP8.5 2050 scenario. Interpreting the probabilities of occurrence from this analysis as a measure of climatic suitability, we sought to explore associations between these outputs and disease severity.

Severity Modeling

Fine-scale severity data from across the epidemic zone sampled between 2015 and 2019 were acquired from researchers of monitoring networks in Washington, Oregon and B.C. The response variable used to signify *N. gaeumannii* abundance and therefore disease severity is the Colonization Index (CI), a heuristic approximation of the probability percentage that a given stoma is occluded by *N. gaeumannii* pseudothecia. This was assessed on 2-year old needles from the top, middle and bottom crown sections of trees. The number of trees and crown sections sampled per site varied in the different networks; only the upper crown was sampled in Washington, and mostly 5 trees were assessed in B.C. and 10 trees in Washington and Oregon. The CI (%) was obtained by multiplying the incidence (proportion of needles exhibiting occluded stomata) by the severity (proportion of pseudothecia occluded on the base, middle and tip of needles) on a subset of needles. The number of needles in these subsets also varied between the networks, with ten to 50 needles used for incidence assessment, and five to ten needles used for severity assessment.

To investigate the influence of lineage suitability on site-level average CI while controlling for sampling heterogeneity, local topography and short-term climate patterns, we utilized a binomial logistic regression with a logit link, incorporating only sites where data from all three crown sections were available (131 sites in total from Oregon and B.C.) (**Supplementary Data Sheet S3**). To account for sampling heterogeneity across the monitoring sites, we implemented a weighting system of observations with weights assigned as a function of the amount of sampling done at the site. To account for the effect of fine-scale topography and the degree of shading on a site, we chose to include hillshade pixel depth into the analysis, which is an indication of the level of shading at the site; high pixel depth signifies lighter color and hence a more illuminated site, while low pixel depth means a darker color and therefore a more shaded site. This variable was obtained by applying the hillshade function in QGIS 3.10.9 to a digital elevation model from ClimateNA with the azimuth set at 315° (NW). Additionally, the natural log of the average precipitation as snow in January (PAS01) from the two years preceding needle sampling was used to control for short-term winter conditions.

Model selection and inference in this study drew on an information theoretic approach proposed by Burnham and Anderson (2002) and implemented in the AICcmodavg package in R (Mazerolle, 2017). We built a global model along with a set of plausible nested candidate models (**Table 2**). Variables were scaled and centered on the mean prior to modeling. We assessed the evidence for each model based on the second-order Akaike Information Criterion for small sample sizes (AICc); the evidence ratios obtained are an indication of the number of times a given model is more parsimonious than a lower-ranked model (Burnham and Anderson, 2002; Mazerolle, 2017). Since more than one model carried a consequential proportion of the AICc weight, we employed multi-model averaging to compute model-averaged parameters and measures of uncertainty for the explanatory variables, with shrinkage applied based on the AICc weight of the different candidate models as suggested by Calin-Jageman and Cumming (2019). In accordance with Mazerolle (2017), model fit was evaluated based on the global model, which was designed as follows:

$$log(\frac{u_i(y\ =\ 1)}{u_i(y\ =\ 0)})\ =\ \beta_0\ +\ \beta_1 X_{1i}\ +\ \beta_2 X_{2i}\ +\ \beta_3 X_{3i}\ +\ \beta_4 X_{4i}$$

$$\frac{u_i(y\ =\ 1)}{u_i(y\ =\ 0)}\ =\ e^{\beta_0\ +\ \beta_1 X_{1i}\ +\ \beta_2 X_{2i}\ +\ \beta_3 X_{3i}\ +\ \beta_4 X_{4i}}$$

where $\frac{u_i(y=1)}{u_i(y=0)}$ is the odds ratio that a given stomata on a given needle is occluded *versus* unoccluded by pseudothecia at the i^{th} site. The weight of each observation is an estimation of the number of needles measured for pseudothecia occlusion at the site, calculated by taking the total of the product of the number of needles measured for prevalence and severity at the site. For instance, at a site where all three crown sections of ten trees are sampled, and at every crown section ten needles are used for severity estimation and 50 needles for prevalence estimation,

TABLE 2 | (A) Akaike's Information Criterion adjusted for small sample sizes (AICc) weight and AICc score of the highest ranked (AICc weight above 0) generalized linear models associating colonization index (CI) values with lineage suitability, climate and topography and **(B)** estimates of the mean and standard deviations of the response (CI probability) and explanatory variables [ln(PAS01), hillshade, L1 suitability, L2 suitability].

(A) Candidate model	AICc	AICc Weight
L1 suitability, ln(PAS01), hillshade	–260.52	0.74
L1 suitability, L2 suitability, ln(PAS01), Hillshade	–258.39	0.25
ln(PAS01), hillshade	–251.44	0.01

(B) Variable	Mean value ± SD	Model-averaged estimate ± SE
L1 suitability	0.56 ± 0.22	0.03 ± 0.01
L2 suitability	0.50 ± 0.32	0 ± 0
ln(PAS01)	2.26 ± 0.79	–0.03 ± 0.01
Hillshade	179.5 ± 10.70	0.02 ± 0.01
CI (probability)	0.16 ± 0.10	

the weight is equal to 3 × 10 × (10 × 50) = 15000. The weights range from 2,450 to 18,150. The intercept, β_0 is the value of the CI when the other variables are held at 0 (i.e., at their mean values). $\beta_1$is the coefficient for the effect of PAS01 on CI, $X_{1i}$is the millimeters of PAS01 at the i^{th} site. $\beta_2$is the coefficient for the effect of hillshade on CI, $X_{2i}$is the hillshade pixel depth at the i^{th} site. $\beta_3$is the coefficient for the effect of lineage 1 probability of occurrence on CI, $X_{3i}$is the probability of occurrence of lineage 1 at the i^{th} site. $\beta_4$is the coefficient for the effect of lineage 2 probability of occurrence on CI, $X_{4i}$is the probability of occurrence of lineage 2 at the i^{th} site. The probability of occurrence values for lineage 1 (X_{3i}) and lineage 2 (X_{4i}) for each site were extracted from the ensemble model-based lineage potential distribution maps for the current (1980-2010) time period.

Finally, we explored correlations between the two lineage suitability outcomes and average CI in the different crown sections using correlation plots and Pearson's correlation tests based on data from all the SNC monitoring networks (a total of 211 sites in Oregon, Washington and B.C.).

RESULTS

Environmental Variables Shaping Lineage Climatic Suitability

DD5 and SHM are the two most important predictors among the explanatory variables for both lineage 1 and lineage 2, though the importance of DD5 appears to be higher for lineage 1, while SHM is more important for lineage 2 (**Figure 2A**). Distance to coast and RH are also much more important predictors for presence of lineage 2 than for lineage 1 (**Figure 2A**). According to the averaged predictions of the best performing GLMs, the optimal conditions for presence differ significantly between the lineages. Lineage 1 has a much broader range of suitability for distances further from the coast and for hotter and drier summers than lineage 2 (**Figure 2B**). The tolerance range of lineage 1 for both low and high annual average RH values exceeds that of lineage 2 (**Figure 2B**). In contrast, lineage 2 has a slightly broader tolerance in terms of higher DD5 (a greater accumulation of daily degrees experienced above 5°C) (**Figure 2B**).

Evaluation scores for lineage 1 were generally lower than for lineage 2, which may be a reflection of its broader environmental tolerance throughout the study area (**Figure 3**). According to their TSS scores, the regression methods discriminated between presences and absences better for lineage 2 than for lineage 1 (L1 GLM = 0.72, L1 MARS = 0.7, L2 GLM = 0.6, L2 MARS = 0.64), while random forests performed similarly for both (L1 RF = 0.66, L2 RF = 0.65). Maxent had the weakest discrimination capacity for both lineages (L1 MAXENT.Phillips = 0.5, L2 MAXENT.Phillips = 0.61) (**Figure 3**). However, the TSS scores, which range from -1 (no points classified correctly) to 1 (all points classified correctly) were 0.74 and 0.78 for lineages 1 and 2 ensemble models, respectively (**Figure 3**). Such TSS values indicate "good" to "very good" model predictions (Préau et al., 2019).

Impact of Climate Change on the Distribution of the *Nothophaeocryptopus gaeumannii* Lineages

At the lineage presence points included in the LDMs, the climate variables are forecast to change between "current" climate conditions and those in the 2050 RCP8.5 scenario. The most remarkable change is DD5, which will increase across its entire range of values, with its mean increasing from 1996 to 2700 degree days (**Figure 4A**). The mean SHM will increase from 53 to 73, indicating hotter and drier summers overall (**Figure 4B**). The range of RH will remain relatively unchanged, with the mean decreasing from 71 to 69% (**Figure 4C**).

These changes are reflected in the patterns of probability of occurrence forecast for the two lineages, which can be interpreted as a measure of climatic suitability. Under the current climate, the coastal zone west of the Cascade and Coast ranges extending from the Lower Mainland of B.C. to central Oregon is highly suitable for both lineages. However, the areas of very high suitability for lineage 1 extend further inland into the B.C. Fraser valley and northeast out to the eastern coast of Vancouver Island, as well as inland to the western slopes of the Oregon Cascades (**Figure 5A**). Lineage 1 also has relatively higher suitability values throughout the interior Douglas-fir range than lineage 2, particularly in the interior (**Figures 5A** vs. **C**). In contrast, the areas of high suitability for lineage 2 under current conditions are constrained to a narrow strip of land along the coast of the study area along with a pocket on the eastern coast of Vancouver Island. However, its range of high suitability values extends further South than that of lineage 1, to the Southern limit of our study area (**Figure 5C**).

Under the climatic conditions forecast by the RCP8.5 2050 scenario, changes in the climatic suitability of lineage 1 are predicted to increase by a probability of up to 0.1 in large swathes of the Douglas-fir range (**Figure 5B**). The highest increase in suitability is predicted east of the coast in Washington and Oregon; for example, the Willamette Valley and Western slopes of the Oregon and Washington Cascades should become significantly more suitable areas for lineage 1 (**Figure 5B**). There are some areas where the suitability of lineage 1 is forecast to decrease; Vancouver Island, the Olympic Peninsula and Puget Sound (**Figure 5B**).

Under the RCP8.5 scenario, lineage 2 is likely to remain similarly geographically limited, with areas in the interior of the Douglas-fir range becoming generally even less suitable to Lineage 2 (**Figure 5D**). Some increases in suitability are forecast in Southeastern Vancouver Island and the Puget Sound (**Figure 5D**).

Lineage Suitability and Colonization Index

Out of our set of plausible candidate models for predicting CI, two models carried the highest proportion of the AICc weight. These were (i) the one including ln(PAS01), hillshade and lineage 1 suitability and the global model, carrying 74% and 25%, respectively (**Table 2**). Using model-averaging, we are able to obtain parameter estimates and their uncertainties as measured by standard error for each of our explanatory

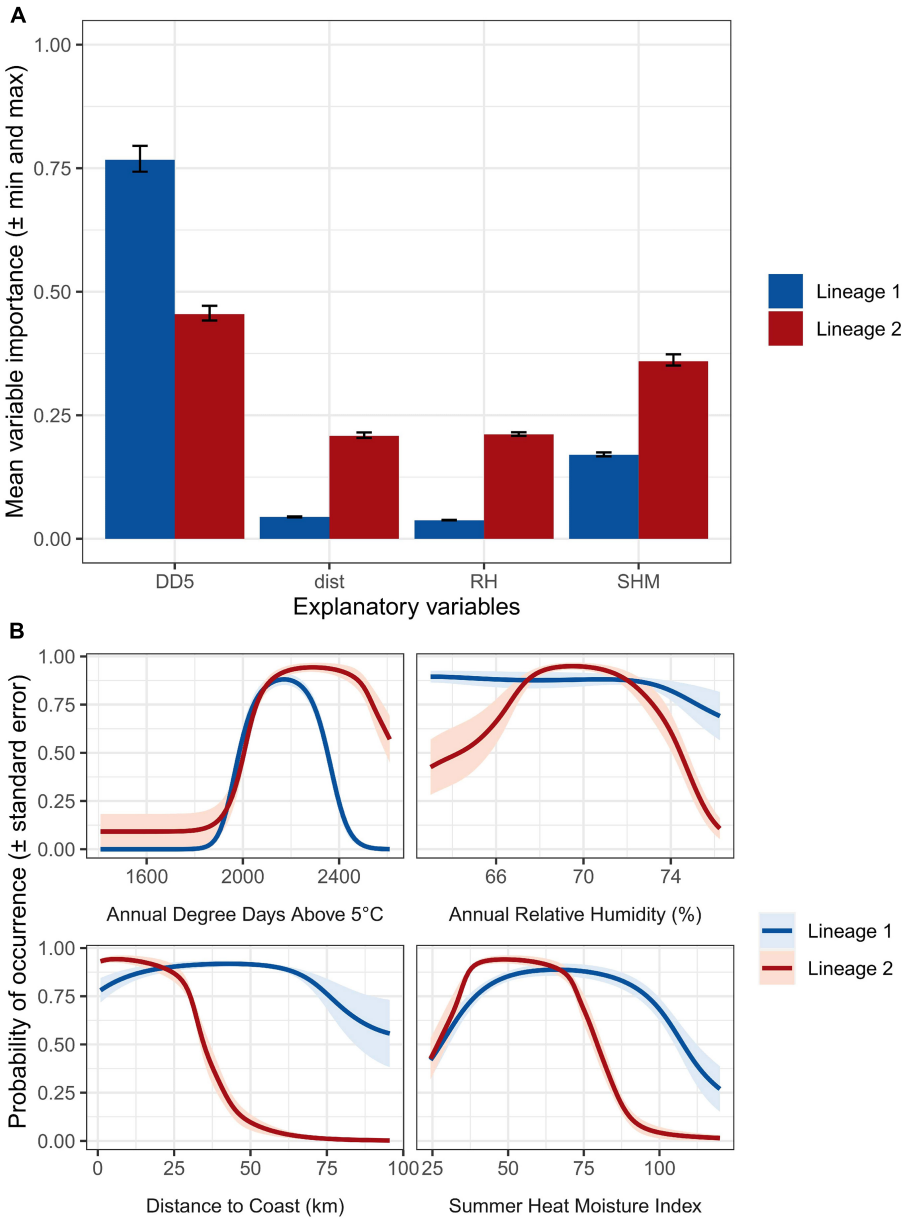

FIGURE 2 | (A) Importance of explanatory variables for lineage (blue bars) 1 and lineage 2 (red bars) of *Nothophaeocryptopus gaeumannii* for the ensemble models. Error bars indicate the maximum and minimum importance values calculated by permuting each variable three times and comparing the correlation between predictions when the variable is randomized *versus* not randomized. **(B)** Response plots of explanatory variables for the generalized linear models included in the ensembles of lineage 1 (blue lines and light blue shading) and lineage 2 (red lines and light red shading). Lines indicate the mean probability of occurrence prediction of the models. Shading indicates the standard error of the mean probability of occurrence estimates of the models.

variables. These are 0.03 (±0.01) for lineage 1, 0.0 for lineage 2, −0.03 (±0.01) for ln(PAS01), and 0.01 (±0.01) for hillshade (**Table 2**). This means that when ln(PAS01) and hillshade are held constant, the odds of a stomata being occluded by a pseudothecium are multiplied by 1.03 ($e^{0.03}$) with a 1 unit increase in lineage 1 suitability. In effect, this indicates a positive association between lineage 1 climatic suitability and CI, even when short-term winter conditions and local topography are taken into account. This association is supported by the evidence ratios between the models; the candidate model including lineage 1 suitability along with the log of PAS01 and hillshade was 93.966 times more parsimonious than the one including only the log of PAS01 and hillshade. We found no such association with lineage 2 climatic suitability. In terms of the effects of short-term winter climate patterns and topography, ln(PAS01) of the previous two years has a negative association with CI, while hillshade pixel value has a positive association with CI, implying that higher CI should

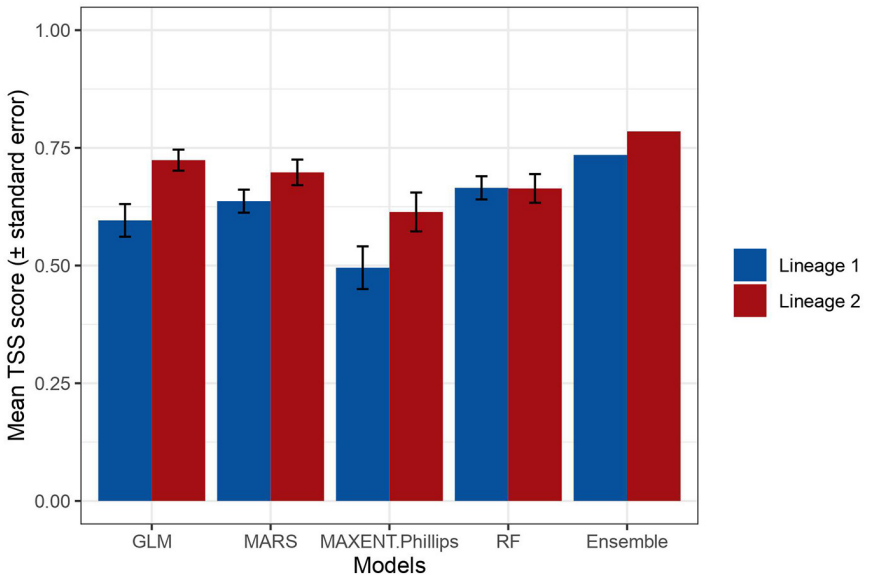

FIGURE 3 | Mean True Skill Statistic (TSS) scores of the individual and ensemble models for lineage 1 (blue bars) and lineage 2 (red bars) of *Nothophaeocryptopus gaeumannii*. Error bars represent the standard error around the mean TSS score. TSS scores range from -1 (none of the presences or absences classified correctly) to 1 (all presences and absences classified correctly).

be found where there is lower precipitation in January and on less shaded sites.

The logistic regression model fit of our global model was excellent, with a Hosmer Lemeshow test p-value of 0.99 and no concerning patterns in the residuals once a log-transformation was applied to PAS01 (**Supplementary Figure S1**).

Lineage Suitability and Within-Tree Vertical Infection Patterns

Significant positive correlations were observed between lineage 1 climatic suitability and CI in the middle (r = 0.17, P = 0.04) and lower (r = 0.29, P = 0.0004) crown sections (**Figure 6A**). A weak positive correlation was observed between lineage 2 climatic suitability and the upper crown section CI (r = 0.14, P = 0.05). Lineage 2 climatic suitability and the CI values in the lower crown section were negatively correlated (r = –0.39, $P < 0.0001$) (**Figure 6B**).

DISCUSSION

Climatic Niches of Two Genetic Lineages of Swiss Needle Cast

Our results indicate that the two genetic lineages described for *N. gaeumannii* have overlapping environmental distributions but different environmental tolerance ranges. Indeed, while there are areas where one lineage completely supplants the other, they are also often present in the same site, sometimes in very close proximity; in fact, both lineages have been identified on a single needle (Bennett and Stone, 2019). Our research adds support to a number of previous findings relating to *N. gaeumannii* and its lineages, while providing further insight into the niche optima of the lineages in terms of a few key variables.

Overall, both lineages 1 and 2 (and therefore the whole *N. gaeumannii* species in the Pacific Northwest) prefer coastal climate and warm temperatures, and favor mild and wet conditions, as opposed to hot and dry conditions, in the spring and summer, suggesting that geographic areas under these conditions should be more susceptible to SNC epidemics. This agrees with the conclusions of a wide range of other studies into the climatic determinants of SNC distribution and severity (Manter et al., 2005; Lee et al., 2017; Shaw et al., 2021).

The difference in niche in terms of DD5 corresponds with the dominance of lineage 2 and absence of lineage 1 at survey sites in southernmost Oregon sites. Similarly, the much broader tolerance for higher SHM and continentality of lineage 1 manifests in its complete supplantation of lineage 2 in hotter and drier conditions farther from the coast, a phenomenon also remarked by Bennett and Stone (2019). These differences in tolerance may be explained by the population structure of the lineages. *N. gaeumannii* is a homothallic species which appears to reproduce predominantly via selfing with occasional outcrossing events (Bennett and Stone, 2019). According to multilocus genotypes analyzed by Bennett and Stone (2016, 2019) lineage 1 has a higher genotypic diversity, genotypic richness and genetic diversity than lineage 2, which is considered relatively clonal. The diversity of genotypes in lineage 1 and the different phenotypes they can produce could be an explanation for its broad environmental tolerance. Conversely, the lack of genotypic diversity in lineage 2 may explain its limited environmental range. The phenotypes produced by these different genetic clusters may also hold insights into relationships between severity and lineage climatic suitability evoked by our CI modeling.

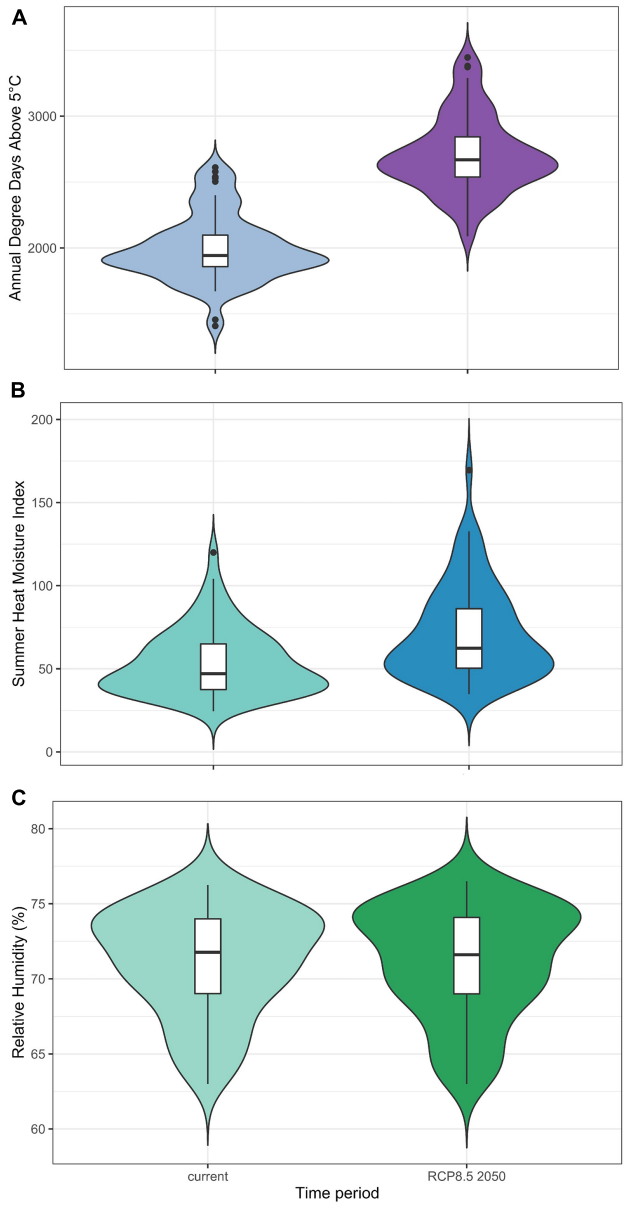

FIGURE 4 | Boxplots of median, interquartile range and outliers, with probability distributions of **(A)** degree days above 5°C, **(B)** summer heat moisture index and **(C)** relative humidity (%) at the 71 sampling sites used in the LDMs. The left side violin plot represents the current (1980–2010) distribution of values, while the right side violin plot represents distribution of values in 2035–2065 under the RCP8.5 emissions scenario (RCP8.5 2050).

Differences in Pathogenicity Between Lineage 1 and Lineage 2

The results of our severity modeling demonstrates the utility of LDMs for predicting forest disease severity, while also highlighting the importance of using both short-term winter climate along with topography data in improving prediction of colonization levels of *N. gaeumannii* when using down-scaled climate data.

While precipitation as snow was a strong predictor of CI, the inclusion of hillshade in models helped to explain the values of outliers such as several highly infected sites in the Chilliwack area of B.C. and the Tillamook area of Oregon, as well as relatively uninfected sites in the Florence and Coos Bay areas of Oregon that were not explained by PAS01 or lineage suitability. This is in agreement with previous research that noted the importance of shading, aspect and elevation in SNC epidemics (Rosso and Hansen, 2003; Lee et al., 2017). Our results also suggest that the distribution and suitability of the lineages may assist in predicting disease severity along with short-term climate.

Differences in pathogenicity between genetic lineages is not uncommon in forest pathogens. Some of the most notable examples include the lineages of *Phytophthora ramorum* Werres, De Cock, and Man in't Veld (Elliott et al., 2011) and *Ophiostoma ulmi* (Buisman) Melin and Nannf. (Hessenauer et al., 2020). In the case of SNC for which infection severity is dependent on abundance of pseudothecia, differences in pathogenicity between lineages should arise as the result of competitive advantages such as improved dispersal ability, higher growth rate, or an adaptation to the local environment. Initially, the clonal population structure of lineage 2 and the concentration of the most severe outbreaks in areas of Washington and Oregon where this lineage was abundant led to the proposition that this lineage had a competitive advantage over lineage 1 and is part of the etiology of the PNW's SNC epidemic (Winton et al., 2006; Bennett et al., 2019). Yet, lineage 2 is conspicuously absent from the B.C. Lower Mainland's most severely infected stands, while several sites in Southern Oregon almost exclusively populated with lineage 2 have little to no symptoms of SNC according to aerial surveys (Bennett and Stone, 2019). Indeed, though they do not allow us to infer causality, our results indicate a slight association between climatic suitability of lineage 1 and the site average levels of colonization by *N. gaeumannii*, even after accounting for short-term climatic and topographic effects. In contrast, our model averaging revealed no such association with lineage 2 climatic suitability. According to ecological niche theory, the climatic suitability values generated by our LDMs should approximate the local abundance of each lineage (Maguire, 1973; Guisan et al., 2017). As CI is a reflection of pathogen abundance, its association with lineage 1 suitability and lack thereof with lineage 2 suitability may be interpreted as evidence for a competitive advantage in favor of lineage 1. Our findings are supported by preliminary results from phenotyping experiments, which showed that isolates of lineage 1 most common on the coast have a higher phenotypic plasticity and grow faster than those of lineage 2 in three different temperature conditions and three drought conditions (Yin et al., 2020). Our findings also concur with those from Bennett and Stone (2019), who tested the hypothesis of higher pathogenicity of lineage 2, but found no association between the relative proportion of lineage 2 and SNC symptoms when distance from the coast was held constant.

The significant association between CI and lineage suitability, as well as the high evidence ratios of models that incorporated lineage 1 suitability over those that didn't, provides evidence that LDMs can be useful in estimating the severity patterns of the epidemic. This not only helps us to make inferences

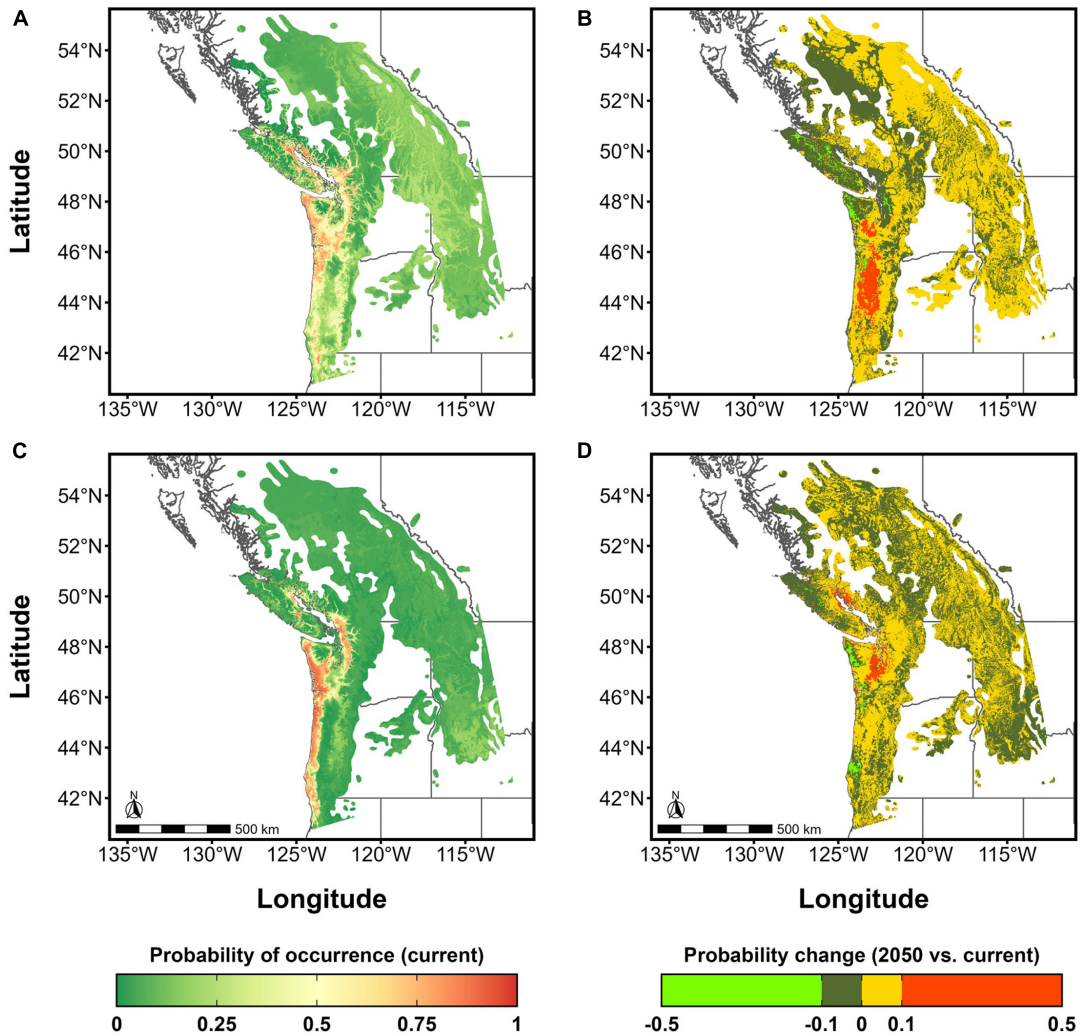

FIGURE 5 | Maps of climatic suitability of lineages 1 and 2 of *Nothophaeocryptopus gaeumannii* in the Pacific Northwest Douglas-fir range **(A)** Lineage 1 climatic suitability map under current (1980–2010) climate; **(B)** Change in lineage 1 climatic suitability under the RCP8.5 2050 climate; **(C)** Lineage 2 climatic suitability map under current (1980–2010) climate; **(D)** Change in lineage 2 climatic suitability under the RCP8.5 2050 climate.

to greater spatial scales, but also to much smaller scales such as within the tree. Differences in the relationships between CI and lineage suitability in the upper, middle and lower crown sections reveal some intriguing possibilities such as within-tree niche partitioning between the lineages, and may help to explain the differing patterns of vertical colonization in the monitoring networks. The occupation of the same host by different species or reproductively isolated lineages as is the case with *N. gaeumannii* poses a problem in ecology as it violates the competitive exclusion principle (Hardin, 1960). However, a possible answer to this conundrum has been found in fine-scale spatial or temporal niche partitioning between cryptic species or non-interbreeding subpopulations. Evidence of this in forest pathogens includes the complex of fungal species causing oak powdery mildew in Europe and fungal symbionts of the mountain pine beetle in western North-America (Feau et al., 2012; Hamelin et al., 2016; Ojeda Alayon et al., 2017). The correlation between lineage 1 suitability and lower and middle crown section CI and the weak correlation between lineage 2 suitability and the upper crown section CI suggests that the lineages may prefer different crown sections - lineage 1 the lower and middle sections, and lineage 2 the upper section. This would be consistent with the different colonization levels found in B.C., where lineage 1 is most prominent and the lower sections are most severely infected, as opposed to Oregon where the upper section of the crown is most infected in highly diseased sites and lineage 2 is more common (Shaw et al., 2014; Bennett and Stone, 2019).

It is important to note that although CI is the primary mechanistic sign of SNC, it is not always correlated with the ultimately damaging symptom of premature defoliation (Manter et al., 2003; Montwé et al., 2021). The host dynamics of this disease remain obscure; indeed, studies on silvicultural practices (Filip et al., 2000; El-Hajj et al., 2004; Lan et al., 2019a), as well as host age (Lan et al., 2019b), tree provenance and family

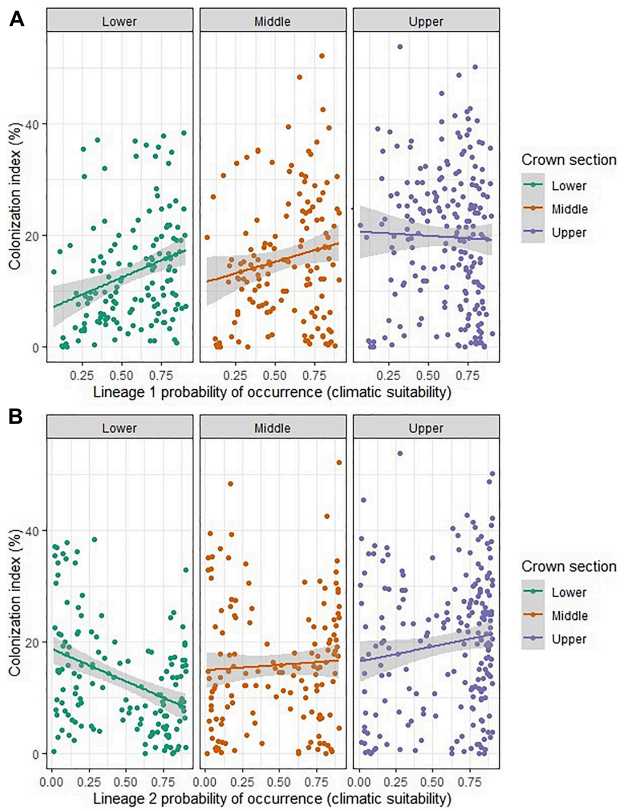

FIGURE 6 | Correlation plots between *Nothophaeocryptopus gaeumannii* lineage suitability and colonization index (CI) in different crown sections **(A)** Relationship between lineage 1 suitability and CI in the upper, middle and lower sections of the tree; **(B)** Relationship between lineage 2 suitability and CI in the upper, middle and lower sections of the tree.

(Johnson, 2002; Montwé et al., 2021) have reported different and even contradictory results on relationships of these factors with symptom severity and disease tolerance and resistance. Crucially, the interacting effect of climate change on both the host and pathogen is an important knowledge gap which should be addressed in further research. In addition, the importance of different climate variables on disease severity seems to vary spatially, according to differences in site biogeoclimatic characteristics (Stone et al., 2008a; Lee et al., 2013). Hitherto, distance from the coast has been widely used in SNC modeling as a proxy for this variability in site characteristics as it applies well to the relatively linear coastline of Oregon where the disease has been most studied, but the parameter is not as useful in Washington and Southwestern B.C, which have more complex coastlines. Modeling work such as ours on the full extent of the epidemic requires replacement of this proxy variable with more widely applicable variables such as ecosystem classification zones. The lack of compatibility between ecosystem classification systems across the national boundaries of the Pacific Northwest is a barrier to this effort. While many important challenges for understanding and managing the SNC epidemic remain, the combined use of genetic information along with climate data at different timescales and topographic data provides some useful insight that could aid forest management decision-making in the context of climate change.

Implications for Climate Change

The results of our study suggest that it is not lineage 2 but rather lineage 1 that may be the driver of disease severity currently in the coastal Pacific Northwest. Though it can be problematic to extrapolate results beyond the spatial and temporal scope of an observational dataset, we do so under the fundamental assumption that species conserve their niches (Peterson et al., 1999; Liu et al., 2020). This allows us to make some informed predictions about the trajectory of the SNC epidemic to the rest of the Douglas-fir range under the RCP8.5 2050 scenario. The increase in lineage 1 suitability observed in our predictions in this scenario indicate that the frequency of SNC epidemics may increase in coming years, particularly extending into the Willamette valley and Western slopes of the Cascades, which until now have been spared of the disease's impact (Ritóková et al., 2016; Shaw et al., 2021). The expansion to new suitable locations reflects the current tolerance of lineage 1 for a wide range of climate conditions. Considering the relatively high genetic diversity of this lineage, it is consistent with the general idea that a more diverse subpopulation of a fungus will have more chance to adapt successfully to a changing environment than a clonal subpopulation (Drenth et al., 2019). When taken together with our severity modeling results, the outputs of our lineage 1 LDMs can be interpreted as indicators of future disease severity, assuming that warmer climates will also lead to an increase in the frequency of optimal short-term winter conditions such as low PAS01. As such, the increase in the overall suitability values across much of the Douglas-fir range in the RCP8.5 2050 scenario suggests that the severity of epidemics can be expected to intensify throughout much of the lineage 1 distribution if greenhouse gas emissions continue unabated in the coming decades.

In contrast, the extent and suitability levels of lineage 2 are predicted to remain relatively similar according to our LDMs, with increases in probability over 0.1 in Northern Washington and Northeastern Vancouver Island. We believe this may be due to increases in suitability resulting from favorable DD5 being offset by rising SHM to which lineage 2 has a very limited tolerance (**Figure 4**). However, it is important to mention a number of caveats to this result. Firstly, clonal populations such as that of lineage 2 tend to expand spatially as they do not need to compete against other genotypes and are usually indicative of a highly successful individual, but they are more vulnerable to collapse due to their lack of adaptability; this population structure is epidemiologically important but difficult to factor into modeling. It is also noteworthy that various studies in the epidemic zone show a historical trend toward increasing spring and summer precipitation in the epidemic zone (Stone et al., 2008b; Mildrexler et al., 2019; Montwé et al., 2021), as opposed to the drying trend forecast in our RCP8.5 scenario. This and fluctuations in short-term weather patterns introduce additional uncertainties in our future

predictions under the RCP8.5 emission scenario, which call for caution in interpreting our maps. Future risk assessments will immensely benefit from rangewide determinations of SNC genetic lineages and accurate estimations of climate and host dynamics in this region.

CONCLUSION

Climate-driven SDMs have traditionally been used to assess habitat suitability for a given species including forest pathogens (Pandit et al., 2020; Pedlar et al., 2020). We are unaware of studies in forest pathology that have used genetic clusters as inputs into SDM, and outputs of these models for assessing the severity of forest pests or diseases. Our study addresses this knowledge gap by including results from predictive maps of the climatic suitability of the two *N. gaeumannii* lineages (lineage 1 and 2) into severity modeling. By considering the whole epidemic area this study provides the most geographically extensive investigation of the short and long-term climate dynamics of SNC. We believe that future research should focus on the phenotyping of the *N. gaeumannii* lineages, including the coastal and interior variants of lineage 1, as well as other evolutionary differences between the lineages, such as dispersal ability. This could be used to fine-tune our SDMs using mechanistic models which are known to perform better with native pathogens in their realized niches. Our results indicate that there is a sound theoretical and empirical underpinning for using LDMs as tools to not only predict the current and future climatic suitability of the SNC lineages, but also to attempt to identify high disease severity risk areas under current and future climate conditions.

DATA AVAILABILITY STATEMENT

The original contributions presented in the study are included in the article/**Supplementary Material**, further inquiries can be directed to the corresponding author.

AUTHOR CONTRIBUTIONS

NH-S conceptualized the research with help from KRS and RCH, did labwork for lineage qPCR identification, completed the data analysis, and wrote the manuscript. KRS contributed to conceptualization, co-supervision, and writing (review and editing). XY contributed by developing the methods used for lineage identification by qPCR in this research and by helping NH-S with labwork and data collection. NF contributed by supervising the development of the methods used for lineage identification by qPCR and writing (review and editing). SZ contributed to sample and data acquisition. DO and GR contributed to sample acquisition. CC contributed to data acquisition. RCH contributed to conceptualization. All authors contributed to the article and approved the submitted version.

FUNDING

This research was financially supported by the CoAdapTree Project (241REF), with funding from Genome Canada, Genome British Columbia, Genome Alberta, and Genome Québec (a full list of sponsors is available at https://coadaptree.forestry.ubc.ca/sponsors/). The Pest Risk Management Programme of Natural Resources Canada also provided funding for this project.

ACKNOWLEDGMENTS

We would like to thank the many researchers and assistants who helped provide us with samples and severity data from the different monitoring networks. From the B.C. monitoring network, Lucy Stad, Ann Wong, Jack Sweeten, B A Blackwell and Associates and Kerley and Associates Forestry Consulting. From the Oregon and Washington network, the members of the Swiss Needle Cast Cooperative, particularly Doug Mainwaring and Andrew Bluhm, plus John Browning and Anna Leon. From the Washington monitoring network, Rachel Brooks. We also owe a debt of gratitude to the student lab assistants involved in the quantification of disease severity, including Berni Van der Meer, Alanna Love and Yifan Yuan. Finally, we would like to thank Isabelle Giguère for her essential logistical work in receiving samples from the different networks and providing lab training and overall support throughout the completion of this project.

SUPPLEMENTARY MATERIAL

The Supplementary Material for this article can be found online at: https://www.frontiersin.org/articles/10.3389/ffgc.2021.756678/full#supplementary-material

Supplementary Figure S1 | Assumptions of logistic regression tested on our global model. **(A)** Parametric bootstrap of the deviance simulated on 5000 binomial models. **(B)** Kolmogorov-Smirnov tests for model adjustment and comparisons of standardized residuals with ranked model predictions to test for outliers and model fit, based on 250 simulations of binomial models. **(C)** Various plots to check for residual heterogeneity (residuals vs fitted), normality (QQ-plot), and outliers (Scale-location, residuals vs leverage), as well as to check for patterns in residuals for the different predictors.

Supplementary Data Sheet S1 | Data sheet of SNC presence points collected by Chantal Coté and Naomie Herpin-Saunier. Chantal Coté compiled a collection of points from published articles and online repositories of species occurrences (e.g. GBIF), while Naomie generated additional points by converting shapefiles of areas showing SNC symptoms from aerial surveys by the Swiss Needle Cast Cooperative, Washington Department of Natural Resources and British Columbia Ministry of Forests, Lands, Natural Resource Operations and Rural Development into points. All of these points were combined and rarefied to a 5 km distance between points. These were used as a mask for pseudo-absence data selection in the building of the SDM datasets.

Supplementary Data Sheet S2 | Data sheet of lineages 1 and 2 presence and absence points.

Supplementary Data Sheet S3 | Data sheet of colonization index measurements at Swiss needle cast monitoring sites used for severity modelling.

Supplementary Protocol S1 | Real-time PCR protocol used for lineage presence detection at monitoring sites using multiple pseudothecia per site.

REFERENCES

Araújo, M. B., Whittaker, R. J., Ladle, R. J., and Erhard, M. (2005). Reducing uncertainty in projections of extinction risk from climate change. *Glob. Ecol. Biogeogr.* 14, 529–538.

Barbet-Massin, M., Jiguet, F., Albert, C. H., and Thuiller, W. (2012). Selecting pseudo-absences for species distribution models: how, where and how many? *Methods Ecol. Evol.* 3, 327–338.

Bennett, P. I., Hood, I. A., and Stone, J. K. (2019). The genetic structure of populations of the Douglas-Fir Swiss needle cast fungus *Nothophaeocryptopus gaeumannii* in New Zealand. *Phytopathology* 109, 446–455. doi: 10.1094/PHYTO-06-18-0195-R

Bennett, P. I., and Stone, J. K. (2016). Assessments of population structure, diversity, and phylogeography of the Swiss needle cast fungus (*Phaeocryptopus gaeumannii*) in the U.S. *Pacif. Northwest. For. Trees Livelihoods* 7:14.

Bennett, P. I., and Stone, J. K. (2019). Environmental variables associated with *Nothophaeocryptopus gaeumannii* population structure and Swiss needle cast severity in Western Oregon and Washington. *Ecol. Evol.* 9, 11379–11394. doi: 10.1002/ece3.5639

Beyer, M., Verreet, J.-A., and Ragab, W. S. M. (2005). Effect of relative humidity on germination of ascospores and macroconidia of *Gibberella zeae* and deoxynivalenol production. *Int. J. Food Microbiol.* 98, 233–240. doi: 10.1016/j.ijfoodmicro.2004.07.005

Boyce, J. S. (1940). A needle cast of douglas-fir associated with *Adelopus gaeumannii*. *Phytopathol* 30, 649–659.

Brown, J. L., Bennett, J. R., and French, C. M. (2017). SDMtoolbox 2.0: the next generation Python-based GIS toolkit for landscape genetic, biogeographic and species distribution model analyses. *PeerJ* 5:e4095. doi: 10.7717/peerj.4095

Burnham, K. P., and Anderson, D. R. (Eds.) (2002). *Model Selection and Multimodel Inference: A Practical Information–Theoretic Approach*. New York, NY: Springer.

Calin-Jageman, R. J., and Cumming, G. (2019). The New statistics for better science: ask how much, how uncertain, and what else is known. *Am. Stat.* 73(Supp 1), 271–280. doi: 10.1080/00031305.2018.1518266

Capitano, B. R. (1999). *The Infection and Colonization of Douglas-fir Needles by the Swiss Needle Cast Pathogen, Phaeocryptopus gaeumannii* (Rhode) Petrak (MS Thesis). Corvallis, OR: Oregon State University.

Desprez-Loustau, M.-L., Aguayo, J., Dutech, C., Hayden, K. J., Husson, C., Jakushkin, B., et al. (2016). An evolutionary ecology perspective to address forest pathology challenges of today and tomorrow. *Ann. For. Sci.* 73, 45–67. doi: 10.1007/s13595-015-0487-4

Drenth, A., McTaggart, A. R., and Wingfield, B. D. (2019). Fungal clones win the battle, but recombination wins the war. *IMA Fungus* 10:18.

Drew Harvell, C., Mitchell, C. E., Ward, J. R., Altizer, S., Dobson, A. P., Ostfeld, R. S., et al. (2002). Climate warming and disease risks for terrestrial and marine Biota. *Science* 296, 2158–2162. doi: 10.1126/science.1063699

El-Hajj, Z., Kavanagh, K., Rose, C., and Kanaan-Atallah, Z. (2004). Nitrogen and carbon dynamics of a foliar biotrophic fungal parasite in fertilized Douglas-fir. *New Phytol.* 163, 139–147. doi: 10.1111/j.1469-8137.2004.01102.x

Elliott, M., Sumampong, G., Varga, A., Shamoun, S. F., James, D., Masri, S., et al. (2011). Phenotypic differences among three clonal lineages of *Phytophthora ramorum*. *For. Pathol.* 41, 7–14. doi: 10.1111/j.1439-0329.2009.00627.x

Feau, N., Lauron-Moreau, A., Piou, D., Marçais, B., Dutech, C., and Desprez-Loustau, M.-L. (2012). Niche partitioning of the genetic lineages of the oak powdery mildew complex. *Fungal Ecol.* 5, 154–162. doi: 10.1016/j.funeco.2011.12.003

Filip, G. M., Kanaskie, A., Kavanagh, K. L., Johnson, G., Johnson, R., and Maguire, D. A. (2000). *Silviculture and Swiss Needle Cast: Research and Recommendations.* Corvallis, OR: Forest Research Laboratory, Oregon State University.

Gaumann. (1928). Eine neue krankheit der douglastanne. *Zeitschrift Fur Pflanzenkrankheiten Pflanzenschutz* 38, 70–78.

Geng, S., Campbell, R. N., Carter, M., and Hills, F. J. (1983). Quality control programs for seedborne pathogens. *Plant Dis.* 67, 236–242. doi: 10.1094/pd-67-236

Gotelli, N. J., and Stanton-Geddes, J. (2015). Climate change, genetic markers and species distribution modelling. *J. Biogeogr.* 42, 1577–1585. doi: 10.1111/jbi.12562

Guisan, A., Thuiller, W., and Zimmermann, N. E. (2017). *Habitat Suitability and Distribution Models: With Applications in R*. Cambridge: Cambridge University Press.

Hamelin, F. M., Bisson, A., Desprez-Loustau, M.-L., Fabre, F., and Mailleret, L. (2016). Temporal niche differentiation of parasites sharing the same plant host: oak powdery mildew as a case study. *Ecosphere* 7:e01517.

Hansen, E. M., Stone, J. K., Capitano, B. R., Rosso, P., Sutton, W., Winton, L., et al. (2000). Incidence and impact of Swiss needle cast in forest plantations of Douglas-fir in Coastal Oregon. *Plant Dis.* 84, 773–778. doi: 10.1094/PDIS.2000.84.7.773

Hardin, G. (1960). The competitive exclusion principle. *Science* 131, 1292–1297.

Hessenauer, P., Feau, N., Gill, U., Schwessinger, B., Brar, G. S., and Hamelin, R. C. (2021). Evolution and adaptation of forest and crop pathogens in the *Anthropocene*. *Phytopathology* 111, 49–67. doi: 10.1094/PHYTO-08-20-0358-FI

Hessenauer, P., Fijarczyk, A., Martin, H., Prunier, J., Charron, G., Chapuis, J., et al. (2020). Hybridization and introgression drive genome evolution of Dutch elm disease pathogens. *Nat. Ecol. Evol.* 4, 626–638. doi: 10.1038/s41559-020-1133-6

Hoffmann, A. A., and Sgrò, C. M. (2011). Climate change and evolutionary adaptation. *Nature* 470, 479–485.

Hood, I. A., and Kershaw, J. D. (1975). *Distribution and Infection Period of Phaeocryptopus gaeumannii in New Zealand*. Available online at: https://www.scionresearch.com/__data/assets/pdf_file/0006/58848/NZJFS51975HOOD201_208.pdf (accessed October 30, 1974).

Johnson, G. R. (2002). Genetic variation in tolerance of Douglas-fir to Swiss needle cast as assessed by symptom expression. *Silvae Genet.* 51, 80–88.

Lan, Y.-H., Shaw, D. C., Ritóková, G., and Hatten, J. A. (2019a). Associations between Swiss needle cast severity and foliar nutrients in young-growth Douglas-fir in Coastal Western Oregon and Southwest Washington, USA. *For. Sci.* 65, 537–542. doi: 10.1093/forsci/fxz022

Lan, Y. H., Shaw, D. C., Beedlow, P. A., Lee, E. H., and Waschmann, R. S. (2019b). Severity of Swiss needle cast in young and mature Douglas-fir forests in western Oregon, USA. *For. Ecol. Manag.* 442, 79–95. doi: 10.1016/j.foreco.2019.03.063

Lavender, D. P., and Hermann, R. K. (2014). *The Genus Pseudotsuga*. Available online at: https://www.for.gov.bc.ca/ftp/rsi/external/!publish/Dry%20Fir%20Committee/Literature%20Review/Baseline%20Literature/Lavender_Hermann_2014_Douglasfir.pdf (accessed June 25, 2021).

Lee, E. H., Beedlow, P. A., Waschmann, R. S., Burdick, C. A., and Shaw, D. C. (2013). Tree-ring analysis of the fungal disease Swiss needle cast in western Oregon coastal forests. *Can. J. For. Res.* 43, 677–690. doi: 10.1139/cjfr-2013-0062

Lee, E. H., Beedlow, P. A., Waschmann, R. S., Tingey, D. T., Cline, S., Bollman, M., et al. (2017). Regional patterns of increasing Swiss needle cast impacts on Douglas-fir growth with warming temperatures. *Ecol. Evol.* 7, 11167–11196. doi: 10.1002/ece3.3573

Little, E. L. (1971). *Atlas of United States trees. Volume 1. Conifers and Important Hardwoods. Miscellaneous Publication 1146.* Washington, DC: U.S. Department of Agriculture, Forest Service, 320.

Liu, C., Newell, G., and White, M. (2019). The effect of sample size on the accuracy of species distribution models: considering both presences and pseudo-absences or background sites. *Ecography* 42, 535–548. doi: 10.1111/ecog.03188

Liu, C., Wolter, C., Xian, W., and Jeschke, J. M. (2020). Most invasive species largely conserve their climatic niche. *Proc. Natl. Acad. Sci. U.S.A.* 117, 23643–23651. doi: 10.1073/pnas.2004289117

Maguire, B. (1973). Niche response structure and the analytical potentials of its relationship to the habitat. *Am. Natural.* 107, 213–246.

Maguire, D. A., Kanaskie, A., and Voelker, W. (2002). Growth of young Douglas-fir plantations across a gradient in Swiss needle cast severity. *West. J. Appl. For.* 17, 86–95. doi: 10.1093/wjaf/17.2.86

Maguire, D. A., Mainwaring, D. B., and Kanaskie, A. (2011). Ten-year growth and mortality in young Douglas-fir stands experiencing a range in Swiss needle cast severity. *Can. J. For. Res.* 41, 2064–2076. doi: 10.1139/x11-114

Manter, D. K., Bond, B. J., Kavanagh, K. L., Rosso, P. H., and Filip, G. M. (2000). *Pseudothecia* of Swiss needle cast fungus, *Phaeocryptopus gaeumannii*, physically block stomata of Douglas fir, reducing CO2 assimilation. *New Phytol.* 148, 481–491. doi: 10.1046/j.1469-8137.2000.00779.x

Manter, D. K., Reeser, P. W., and Stone, J. K. (2005). A climate-based model for predicting geographic variation in swiss needle cast severity in the Oregon Coast range. *Phytopathology* 95, 1256–1265. doi: 10.1094/PHYTO-95-1256

Manter, D. K., Winton, L. M., Filip, G. M., and Stone, J. K. (2003). Assessment of Swiss needle cast disease: temporal and spatial investigations of fungal colonization and symptom severity. Phytopathologische Zeitschrift. *J. Phytopathol.* 151, 344–351. doi: 10.1046/j.1439-0434.2003.00730.x

Marmion, M., Parviainen, M., Luoto, M., Heikkinen, R. K., and Thuiller, W. (2009). Evaluation of consensus methods in predictive species distribution modelling. *Divers. Distrib.* 15, 59–69. doi: 10.1111/j.1472-4642.2008.00491.x

Mazerolle, M. J. (2017). *Package "AICcmodavg." R Package*. 281. Available online at: https://cran.uib.no/web/packages/AICcmodavg/AICcmodavg.pdf (accessed August 21, 2020).

McDowell, N. G., Williams, A. P., Xu, C., Pockman, W. T., Dickman, L. T., Sevanto, S., et al. (2016). Multi-scale predictions of massive conifer mortality due to chronic temperature rise. *Nat. Clim. Chang.* 6, 295–300. doi: 10.1038/nclimate2873

Michaels, E., and Chastagner, G. A. (1984). Seasonal availability of *Phaeocryptopus gaeumannii* ascospores and conditions that influence their release. *Plant Dis.* 68, 942–944. doi: 10.1094/pd-69-942

Mildrexler, D. J., Shaw, D. C., and Cohen, W. B. (2019). Short-term climate trends and the Swiss needle cast epidemic in Oregon's public and private coastal forestlands. *For. Ecol. Manag.* 432, 501–513. doi: 10.1016/j.foreco.2018.09.025

Mildrexler, D. J., Yang, Z., Cohen, W. B., and Bell, D. M. (2016). A forest vulnerability index based on drought and high temperatures. *Remote Sens. Environ.* 173, 314–325.

Montwé, D., Elder, B., Socha, P., Wyatt, J., Noshad, D., Feau, N., et al. (2021). Swiss needle cast tolerance in British Columbia's coastal Douglas-fir breeding population. *Forestry* 94, 193–203. doi: 10.1093/forestry/cpaa024

Moss, R. H., Edmonds, J. A., Hibbard, K. A., Manning, M. R., Rose, S. K., van Vuuren, D. P., et al. (2010). The next generation of scenarios for climate change research and assessment. *Nature* 463, 747–756. doi: 10.1038/nature08823

Nadeau, C. P., and Urban, M. C. (2019). Eco-evolution on the edge during climate change. *Ecography* 42, 1280–1297. doi: 10.1086/704780

Ojeda Alayon, D. I., Tsui, C. K. M., Feau, N., Capron, A., Dhillon, B., Zhang, Y., et al. (2017). Genetic and genomic evidence of niche partitioning and adaptive radiation in mountain pine beetle fungal symbionts. *Mol. Ecol.* 26, 2077–2091. doi: 10.1111/mec.14074

Pandit, K., Smith, J., Quesada, T., Villari, C., and Johnson, D. J. (2020). Association of recent incidence of foliar disease in pine species in the Southeastern United States with Tree and Climate Variables. *Forests* 11:1155. doi: 10.3390/f11111155

Pedlar, J. H., McKenney, D. W., Hope, E., Reed, S., and Sweeney, J. (2020). Assessing the climate suitability and potential economic impacts of Oak wilt in Canada. *Sci. Rep.* 10:19391. doi: 10.1038/s41598-020-75549-w

Peterson, A. T., Soberón, J., and Sánchez-Cordero, V. (1999). Conservatism of ecological niches in evolutionary time. *Science* 285, 1265–1267. doi: 10.1126/science.285.5431.1265

Préau, C., Isselin-Nondedeu, F., Sellier, Y., Bertrand, R., and Grandjean, F. (2019). Predicting suitable habitats of four range margin amphibians under climate and land-use changes in southwestern France. *Reg. Environ. Chang.* 19, 27–38. doi: 10.1007/s10113-018-1381-z

Purse, B. V., and Golding, N. (2015). Tracking the distribution and impacts of diseases with biological records and distribution modelling. *Biol. J. Linn. Soc.* 115, 664–677. doi: 10.1186/s12868-016-0283-6

Ritóková, G., Mainwaring, D. B., Shaw, D. C., and Lan, Y.-H. (2021). Douglas-fir foliage retention dynamics across a gradient of Swiss needle cast in coastal Oregon and Washington. *Can. J. For. Res.* 51, 573–582. doi: 10.1139/cjfr-2020-0318

Ritóková, G., Shaw, D. C., Filip, G., Kanaskie, A., and Norlander, D. (2016). Swiss needle cast in western oregon douglas-fir plantations: 20-year monitoring results. *For. Trees Livelihoods* 7:155.

Rosso, P. H., and Hansen, E. M. (2003). Predicting swiss needle cast disease distribution and severity in young douglas-fir plantations in coastal Oregon. *Phytopathology* 93, 790–798. doi: 10.1094/PHYTO.2003.93.7.790

Shaw, D. C., Ritóková, G., Lan, Y.-H., Mainwaring, D. B., Russo, A., Comeleo, R., et al. (2021). Persistence of the Swiss needle cast outbreak in Oregon Coastal Douglas-fir and new insights from research and monitoring. *J. For.* 119, 407–421.

Shaw, D. C., Woolley, T., and Kanaskie, A. (2014). Vertical foliage retention in Douglas-fFir across environmental gradients of the Western Oregon Coast range influenced by Swiss needle cast. *Northwest Sci.* 88, 23–32. doi: 10.3955/046.088.0105

Shaw, M. W., and Osborne, T. M. (2011). Geographic distribution of plant pathogens in response to climate change. *Plant Pathol.* 60, 31–43. doi: 10.1111/j.1365-3059.2010.02407.x

Stone, J. K., Capitano, B. R., and Kerrigan, J. L. (2008a). The histopathology of *Phaeocryptopus gaeumannii* on Douglas-fir needles. *Mycologia* 100, 431–444. doi: 10.3852/07-170r1

Stone, J. K., Coop, L. B., and Manter, D. K. (2008b). Predicting effects of climate change on Swiss needle cast disease severity in Pacific Northwest forests. *Can. J. Plant Pathol.* 30, 169–176.

Stone, J. K., Hood, I. A., Watt, M. S., and Kerrigan, J. L. (2007). Distribution of Swiss needle cast in New Zealand in relation to winter temperature. *Australas. Plant Pathol. APP* 36, 445–454.

Sturrock, R. N., Frankel, S. J., Brown, A. V., Hennon, P. E., Kliejunas, J. T., Lewis, K. J., et al. (2011). Climate change and forest diseases. *Plant Pathol.* 60, 133–149. doi: 10.1016/j.actatropica.2021.106123

Thuiller, W., Lafourcade, B., Engler, R., and Araújo, M. B. (2009). BIOMOD - a platform for ensemble forecasting of species distributions. *Ecography* 32, 369–373. doi: 10.1111/j.1600-0587.2008.05742.x

Thuiller, W., Lavorel, S., Araújo, M. B., Sykes, M. T., and Colin Prentice, I. (2005). Climate change threats to plant diversity in Europe. *Proc. Natl. Acad. Sci. U.S.A.* 102, 8245–8250. doi: 10.1073/pnas.0409902102

Wang, T., Hamann, A., Spittlehouse, D., and Carroll, C. (2016). Locally downscaled and spatially customizable climate data for historical and future periods for North America. *PLoS One* 11:e0156720. doi: 10.1371/journal.pone.0156720

Watts, A., Meinzer, F., and Saffell, B. J. (2014). *Fingerprints of a Forest Fungus: Swiss Needle Cast, Carbon Isotopes, Carbohydrates, and Growth in Douglas-fir. Science Findings 167*. Portland, OR: US Department of Agriculture, Forest Service, Pacific Northwest Research Station, 167.

Weiskittel, A. R., Crookston, N. L., and Rehfeldt, G. E. (2012). Projected future suitable habitat and productivity of Douglas-fir in western North America. *Schweiz. Z. For.* 163, 70–78.

Wicklow, D. T., and Zak, J. C. (1979). Ascospore germination of carbonicolous ascomycetes in fungistatic soils: an ecological interpretation. *Mycologia* 71, 238–242.

Wilhelmi, N. P., Shaw, D. C., Harrington, C. A., St. Clair, J. B., and Ganio, L. M. (2017). Climate of seed source affects susceptibility of coastal Douglas-fir to foliage diseases. *Ecosphere* 8:e02011.

Winton, L. M., Hansen, E. M., and Stone, J. K. (2006). Population structure suggests reproductively isolated lineages of *Phaeocryptopus gaeumannii*. *Mycologia* 98, 781–791. doi: 10.3852/mycologia.98.5.781

Yin, X., Feau, N., Tanney, J. B., and Hamelin, R. C. (2020). Mining herbarium samples to study adaptation to climate change in a tree pathogen. [Conference Presentation Abstract]. British Columbia regional meeting, 2020/Réunion régionale de la Colombie-Britannique, 2020. *Can. J. Plant Pathol.* 43, 332–338. doi: 10.1080/07060661.2021.1889804

Conflict of Interest: The authors declare that the research was conducted in the absence of any commercial or financial relationships that could be construed as a potential conflict of interest.

Publisher's Note: All claims expressed in this article are solely those of the authors and do not necessarily represent those of their affiliated organizations, or those of the publisher, the editors and the reviewers. Any product that may be evaluated in this article, or claim that may be made by its manufacturer, is not guaranteed or endorsed by the publisher.

frontiers in Forests and Global Change

ORIGINAL RESEARCH
published: 31 March 2022
doi: 10.3389/ffgc.2022.726388

Differential Virulence Among *Geosmithia morbida* Isolates Collected Across the United States Occurrence Range of Thousand Cankers Disease

Karandeep Chahal[1†], *Romina Gazis*[2], *William Klingeman*[3], *Paris Lambdin*[1], *Jerome Grant*[1], *Mark Windham*[1] *and Denita Hadziabdic*[1*]

[1] Department of Entomology and Plant Pathology, University of Tennessee, Knoxville, TN, United States, [2] Department of Plant Pathology, Tropical Research and Education Center, University of Florida, Homestead, FL, United States, [3] Department of Plant Sciences, University of Tennessee, Knoxville, TN, United States

OPEN ACCESS

Edited by:
Kimberly Wallin,
North Dakota State University,
United States

Reviewed by:
Braham Dhillon,
University of Florida, United States
Isabel Alvarez Munck,
United States Forest Service (USDA),
United States
Pierluigi Bonello,
The Ohio State University,
United States

***Correspondence:**
Denita Hadziabdic
dhadziab@utk.edu

†Present address:
Karandeep Chahal,
Department of Plant, Soil, and Microbial Sciences, Michigan State University, East Lansing, MI,
United States

Specialty section:
This article was submitted to Pests, Pathogens and Invasions, a section of the journal Frontiers in Forests and Global Change

Received: 16 June 2021
Accepted: 02 March 2022
Published: 31 March 2022

Citation:
Chahal K, Gazis R, Klingeman W, Lambdin P, Grant J, Windham M and Hadziabdic D (2022) Differential Virulence Among Geosmithia morbida Isolates Collected Across the United States Occurrence Range of Thousand Cankers Disease. Front. For. Glob. Change 5:726388. doi: 10.3389/ffgc.2022.726388

Thousand cankers disease (TCD), first documented in the western United States in the early 2000s, has spread into nine western and seven eastern states in the United States and northern Italy. TCD incidence and severity differ between eastern and western United States outbreak localities. Black walnut (*Juglans nigra*) trees, introduced into both urban and plantation settings in the western United States, have been severely impacted as evident by the documented high disease incidence and mortality. However, in eastern United States localities, where *J. nigra* is native, host-pathogen-vector interactions resulted in two different outcomes: trees either die or partly recover followed by infection. Recent genetic studies on the TCD causal agent, *Geosmithia morbida*, indicate the spatial genetic structure and high levels of genetic diversity among United States populations. Using detached branch inoculation assays, we reported differential virulence among 25 *G. morbida* isolates collected across the current distribution range of the disease. As a proxy for virulence, the canker area was measured to 7 days after inoculation. Varying degrees of virulence were observed among tested *G. morbida* isolates, which was partly explained by their genetic provenance (genetic clusters). Isolates that grouped within genetic cluster 2 ($n = 7$ from the eastern United States and $n = 6$ from the western United States; mean = 210.34 mm^2) induced significantly larger cankers than isolates that grouped within genetic cluster 1 ($n = 12$; all western United States isolates; mean = 153.76 mm^2). Canker sizes varied among isolates within each genetic cluster and were not correlated with a geographic region (eastern vs. western United States) but rather to the isolated state of origin. Mean canker size also differed in response to isolates that originated from different tree host species. *G. morbida* isolates collected from *Juglans major* induced statistically smaller cankers when compared to isolates recovered from undetermined *Juglans* species but not from *J. nigra*. In sum, the increased mortality reported for western United States walnut tree populations cannot be explained by a higher virulence of local *G. morbida*. Plausible explanations for the observed disparity include environmental conditions, such

as prolonged drought, greater population densities of walnut twig beetle causing a higher number of inoculation events to individual trees, and multiple introductions of *G. morbida* originating from multiple locations. Future experimental evaluation should be undertaken to quantify the influence of these factors on the local epidemics.

Keywords: cankers, *Geosmithia morbida*, pathogenicity, thousand cankers disease, virulence, *Pityophthorus juglandis*, walnut twig beetle, *Juglans nigra*

INTRODUCTION

Thousand cankers disease (TCD) is a disease complex that involves interactions between walnut twig beetle (WTB), *Pityophthorus juglandis* Blackman (Coleoptera: Curculionidae: Scolytinae), a canker-causing fungal pathogen, *Geosmithia morbida* Kolarik, Freeland, Utley, and Tisserat (Ascomycota: Hypocreales: Bionectriaceae), and susceptible host plants, walnut (*Juglans* spp. L.) and wing nut (*Pterocarya* spp.) Kunth (Tisserat et al., 2009, 2011; Kolarik et al., 2011; Hishinuma et al., 2016). Although most *Juglans* and *Pterocarya* species are susceptible, symptoms are more severe in *Juglans nigra* L., the eastern United States native black walnut (Utley et al., 2013; Rugman-Jones et al., 2015; Hishinuma et al., 2016; Hefty et al., 2018). External symptoms of TCD include wilting, flagging, crown thinning, and branch dieback followed by the emergence of epicormic shoots (Tisserat et al., 2009). Internal symptoms include numerous localized small cankers within the phloem that can coalesce and girdle the tree (Kolarik et al., 2011; Tisserat et al., 2011). Vertical and horizontal phloem-restricted galleries beneath the bark provide evidence of beetle feeding and reproduction (Tisserat et al., 2011; Seybold et al., 2019).

Fungal members of the genus *Geosmithia* Pitt are ubiquitous and have been reported from North and South America, Europe, Asia, and Australia (Kolarík et al., 2008, 2017; Chahal et al., 2017). The majority of *Geosmithia* spp. are associated with bark and ambrosia beetles infesting diverse host plants, including coniferous and hardwoods (Chahal et al., 2017; Kolarík et al., 2017; Schuelke et al., 2017; Huang et al., 2019). Although most *Geosmithia* spp. are saprophytes, a few species can act as weak pathogens (Schuelke et al., 2017), including *G. morbida* (Kolarik et al., 2011; Kolarík et al., 2017), which was the first pathogenic species described in this genus. The second one was *Geosmithia* sp. 41 (initially identified as *Geosmithia pallida* by Lynch et al., 2014), the causal agent of foamy bark disease on *Quercus agrifolia* Nee. (California live oak) and other oak species (Huang et al., 2019). Although the associations of *Geosmithia* spp. with bark and ambrosia beetles are documented (Huang et al., 2017; Jankowiak and Bilański, 2018), the details of the ecological interactions among *Geosmithia* spp., its beetle vector(s), and host plant(s) are not fully understood (Huang et al., 2019). This is true for the TCD pathosystem, in which the nutritional role of *G. morbida* is still largely unknown. *G. morbida* has only been reported to colonize hosts in the *Juglandaceae* family (Tisserat et al., 2009). However, the fungus has been recently recovered from other subcortically active beetles besides WTB (Chahal et al., 2019; Moore et al., 2019), suggesting that the fidelity of *G. morbida* to WTB as the most functional beetle associate may have been overestimated. Additional work is needed to elucidate the potential role of other insect species in the efficient transmission of the pathogen and on the development of disease on susceptible hosts (Chahal et al., 2019).

Although, by 2009, TCD was documented in most of the states of western United States (Tisserat et al., 2009, 2011), the first detection in the eastern United States (Knoxville, Tennessee) was recorded in 2010, representing an imminent threat to *J. nigra* in urban and forest settings (Grant et al., 2011). The initial occurrence of TCD in the western United States is spatially pertinent since it overlaps with the native range of the TCD vector, WTB (Kolarik et al., 2011; Sitz et al., 2021). Following the initial discovery of TCD in Tennessee, members of this disease complex were subsequently reported in Indiana, Maryland, North Carolina, Ohio, Pennsylvania, and Virginia (Hansen et al., 2011; Hadziabdic et al., 2014; Daniels et al., 2016), as well as in Italy (Montecchio and Faccoli, 2014; Moricca et al., 2019). Forest Inventory and Analysis (FIA) projections estimated that TCD could have been present in the eastern United States at least 10 years before the first report was made (Randolph et al., 2013). In the eastern United States, *J. nigra* mortality attributed to TCD has been very low (<5%) in comparison with mortality rates in western states where ∼60% of *J. nigra* populations have been removed (Newton et al., 2009; Tisserat et al., 2011; Randolph et al., 2013; Seybold et al., 2019). Furthermore, recovery of some *J. nigra* trees following TCD infection has been documented in the eastern United States (Griffin, 2015; Seybold et al., 2019). Slow TCD progression and partial recovery have also been observed in affected populations distributed in the western United States (Seybold et al., 2019) but at lower rates compared to the eastern United States. In the western United States, the high tree mortality of *Juglans* spp. has been observed in diverse habitats, including agricultural plantations, urban forests, and wildland settings (Seybold et al., 2019). These patterns were not observed in the eastern United States, where the majority of affected trees are distributed in the urban landscape, along roads, and in recreational parks, suggesting that resistance to *G. morbida* may be naturally present in native, *J. nigra* trees (Griffin, 2015; Seybold et al., 2019; Sitz et al., 2021). We hypothesized that differences in TCD outcome observed between eastern and western United States are due to differential virulence present in *G. morbida* populations.

Population studies have revealed high genetic diversity and spatial structure among *G. morbida* populations distributed across the United States (Hadziabdic et al., 2014; Zerillo et al., 2014). *G. morbida* populations collected across the entire

geographic distribution of TCD can be grouped into two distinct genetic clusters (Hadziabdic et al., 2014; Hadziabdic et al., unpublished). This grouping not only indicates the complexity of the pathogen inoculum but also supports earlier suggestions that *G. morbida*, such as WTB, is likely native to North America (Sitz et al., 2021). The current working hypothesis states that *G. morbida* evolved in close association with at least one native *Juglans* species within the western United States range of WTB and that *G. morbida* was present, but undetected, in the eastern United States for a long time before it was first documented (Hadziabdic et al., 2014; Zerillo et al., 2014; Sitz et al., 2021). The study by Sitz et al. (2021) supported this hypothesis by reporting regional resistance and variation in host responses to *G. morbida* infestations in *J. nigra* trees. Their results indicated higher resistance in *J. nigra* populations in the western and central ranges of the native distribution, where TCD has not been documented (Sitz et al., 2021).

The objective of this study was to determine whether isolates collected from different localities have different virulence profiles. We hypothesized that differences in *G. morbida* virulence are correlated to their genetic cluster assignment and that their genetic grouping can explain the difference in TCD incidence and severity observed between eastern and western states. Using canker size as a proxy for virulence, our specific objectives were a) to measure canker size resulting from *G. morbida* inoculation into *J. nigra* host branches and b) to compare canker size variation as a function of genetic clustering and geographic and host origin.

MATERIALS AND METHODS

Selection of *G. morbida* Isolates

Preliminary genetic profiling from early examinations of this data set led to the selection of the 25 *G. morbida* isolates that were used in this study. Isolates were chosen based on their genetic diversity and assignment probability to belong to one of the assigned genetic clusters (Hadziabdic et al., unpublished data; **Supplementary Figure S1**). More specifically, these isolates were chosen as representatives of five putative genetic clusters and were used to initiate the experiments. Subsequent addition of *G. morbida* isolates from additional states led to a reanalysis of the data and reorganization of genetic variability across the United States into two genetic clusters (Hadziabdic et al., unpublished data; **Supplementary Figure S1**) that are consistent with the previous study (Zerillo et al., 2014). Thus, experiments reported here were conducted with 12 isolates from genetic cluster 1 (all western United States isolates) and 13 isolates representing genetic cluster 2 ($n = 7$ from the eastern United States and $n = 6$ from the western United States) (**Table 1**).

TABLE 1 | *Geosmithia morbida* isolates selected for inoculation experiment per genetic groupings of Hadziabdic et al. unpublished.

Genetic cluster[a]	Isolate number[b]	Geographic origin[c]	Collection location[d]	Host[e]	Genbank accession[f]
Cluster 1	GM101	Western	AZ	*J. major*	MG008832
Cl. 1	GM104	Western	AZ	*J. major*	MG008838
Cl. 1	GM106	Western	AZ	*J. major*	MG008840
Cl. 1	GM133	Western	AZ	*J. major*	MG008842
Cl. 1	GM140	Western	AZ	*J. major*	MG008845
Cl. 1	GM156	Western	CO	*J. microcarpa*	MG008830
Cl. 1	GM158	Western	CO	*J. nigra*	MG008844
Cl. 1	GM170	Western	CO	*J. nigra*	MG008836
Cl. 1	GM186	Western	CO	*J. nigra*	MG008834
Cl. 1	GM216	Western	NM	*J. major*	MG008839
Cl. 1	GM236	Western	NM	*J. major*	MG008837
Cl. 1	GM269	Western	UT	*J. nigra*	MG008831
Cluster 2	GM188	Western	CO	*J. nigra*	MG008841
Cl. 2	GM301	Western	OR	*Juglans* sp.	MG008826
Cl. 2	GM250	Western	OR	*Juglans* sp.	MG008827
Cl. 2	GM252	Western	OR	*Juglans* sp.	MG008829
Cl. 2	GM259	Western	UT	*J. nigra*	MG008823
Cl. 2	GM277	Western	UT	*J. nigra*	MG008825
Cl. 2	GM66	Eastern	IN	*J. nigra*	MG008828
Cl. 2	GM67	Eastern	IN	*J. nigra*	MG008833
Cl. 2	GM59	Eastern	NC	*J. nigra*	MG008843
Cl. 2	GM293	Eastern	OH	*J. nigra*	MG008824
Cl. 2	GM50	Eastern	PA	*J. nigra*	MG008822
Cl. 2	GM11	Eastern	TN	*J. nigra*	MG008846
Cl. 2	GM25	Eastern	TN	*J. nigra*	MG008835
Negative_ Control	Neg_Cntrl	-	-	-	
Positive_ Control	GM17	Eastern	TN	*J. nigra*	MG008849

[a] *Genetic cluster association of Geosmithia morbida isolates were characterized using our unpublished data and combining eastern and western isolates (294 samples); Hadziabdic et al., unpublished.*
[b] *Alphanumeric laboratory identification code for Geosmithia morbida isolates.*
[c] *Source of isolate origin from either eastern or western United States.*
[d] *State in which the G. morbida isolate was collected.*
[e] *Juglans host species (where known) from which the G. morbida isolate was collected.*
[f] *GenBank accession number.*

Molecular Confirmation of Selected Axenic Isolates

Axenic single-spore cultures were obtained from all the 25 *G. morbida* isolates following established protocols (Hadziabdic et al., 2014). All isolates were confirmed as *G. morbida* through morphological (prior to this study) and molecular identification. In brief, mycelial plugs from each isolate were grown in Difco™ Potato Dextrose Broth at room temperature (25°C) for 3 weeks following established protocols (Gazis et al., 2018). DNA was extracted from harvested mycelium as described previously (Gazis et al., 2018; Chahal et al., 2019). The Internal Transcribed Spacer (ITS) region was amplified using the primers ITS1F (Gardes and Bruns, 1993) and ITS4R (White et al., 1990). Each PCR reaction-mix (final volume 25 μl) contained 12.5 μl GoTaq®G2 Hot Start Master Mix (Promega Corp., Madison, WI, USA), 1.25 μl 10 mM reverse primer, 1.25 μl 10 mM forward primer, 1 μl dimethyl sulfoxide (DMSO, Sigma–Aldrich, St Louis, MO, USA), 1 μl of genomic DNA (∼25 ng/μl), and double-distilled water to complete the total volume of 25 μl. The PCR thermal cycle started with an initial denaturation step of 2 min

at 94°C followed by 15 cycles of denaturation for 30 s at 94°C, annealing for 30 s at 65°C, and primer extension for 1 min at 72°C; followed by 30 cycles of 30 s at 94°C, 30 s at 48°C, and 1 min at 72°C; and followed by a final elongation for 10 min at 72°C. The amplifications of PCR products were confirmed with gel electrophoresis. PCR products were sent to MCLAB laboratories (www.mclab.com) for cleaning and sequencing. Sequencher TM 4.9 (Gene Codes Corp., Ann Arbor, MI, USA) was used to assess the quality of the chromatograms and assemble the strands into contigs. Basic Local Alignment Search Tool (BLAST) was used to compare the ITS sequences deposited in the NCBI nucleotide database. Generated ITS sequences were deposited to GenBank (**Table 1**).

Preparation of *J. nigra* Branch Sections

Detached branch assays were used to limit the potential confounding effects inherent in using field trees, such as differences in host genotype and microclimates. Two mature (>35-year-old) *J. nigra* trees located at Middle Tennessee Research & Education Center, Spring Hill, Tennessee, USA (latitude/longitude 35°43'01.3" N, 86°57'19.3" W; 35°43'03.0" N, 86°57'18.7" W) were selected as a source of branch sections for each of the two inoculation experiments that were repeated. For each inoculation treatment, each of two replicates was completed using branch sections taken from a single tree. None of the TCD complex members have been reported in Spring Hill, or from Maury and Williamson counties in Tennessee where Spring Hill is located. Symptoms of TCD were not observed on trees at the Spring Hill site. Once branches were detached, 10 cut branch sections (∼1 m length) from each tree were visually inspected for the presence of TCD signs and symptoms. During the examination, a portion of the outer bark layer from branch sections was peeled to verify that cankers, phloem discoloration, lesions, or necrotic areas nor galleries of other wood-boring beetles were present. Collected tree branches were also verified to be free of *G. morbida* using the molecular protocol described by Oren et al. (2018). In brief, three individual samples each containing approximately 150 mg of drilled inner wood shavings were collected from portions of 10 different branches that were harvested from each tree (**Supplementary Figure S2**). Samples were stored at −20°C until processed. DNA extractions, PCR amplifications, and amplicons were conducted as described by Oren et al. (2018). Molecular detection of *G. morbida* from source branches was negative for pathogen DNA, indicating that prior to this experiment, selected branch sections were free from *G. morbida* infection. The cut branches were stored at 4°C (∼5 days) prior to inoculation. Branches were cut into branch sections (length = 8 cm, diameter = 2–3 cm) using a handsaw and surface-sterilized with 70% ethanol (**Supplementary Figure S3**). Cut ends of inoculated branch sections were then dipped into paraffin wax and wrapped with aluminum foil to prevent evaporation and preserve moisture.

Inoculations of *J. nigra* Branch Sections With *G. morbida* Isolates

Fungal isolates were grown in Petri dishes (10 cm diameter, 1.5 cm depth) containing 20 ml of half-strength PDA at 25°C for 4 weeks. *G. morbida* isolates GM17, which is a well-characterized strain used in multiple previous studies (e.g., host-plant inoculations, development of molecular detection protocols, and comparative genetics and genomics experiments) was used as a positive control. Agar-only plugs were inserted into wounds as a negative control. Once branch pieces had dried following surface sterilization, sections were chosen randomly for *G. morbida* inoculation experiments (**Supplementary Figure S3**). Using a cordless drill with a 3.175-mm diameter bit, two ∼2-mm-deep wounds were offset on opposing sides of six separate branch sections per fungal isolate. Branch sections were inoculated by using a sterile, 4-mm diameter (o.d.) Humboldt Brass Cork Borer (Fisher Scientific, Pittsburgh, PA, USA) to remove a piece of fungal agar plug, which was then picked using a sterile scalpel, inverted, and inserted completely into each of the two opposing wounds per branch section. Colonized agar plugs were obtained from the edge of the growing colonies, and all plugs were completely covered by the fungus. Wounded branch sections were wrapped with Parafilm (M Laboratory Film, Bemis, Neenah, WI, USA), and the diameter of each inoculated branch section was recorded using a digital caliper (Lyman Products Corp., Middletown, CT, USA). Inoculated branch sections were incubated at 25°C in darkness for 7 days.

Canker Measurements

To visualize cankers in the phloem of cut branches before extensive tissue oxidation occurred, lesions were assessed to 7 days after inoculation (7 DAI). A sterile scalpel was used to shave the outer bark from around the wounding site exposing the cankers (**Supplementary Figure S3**), and the digital images of exposed cankers beside a reference scale were taken immediately. Image processing and analysis software, ImageJ (https://imagej.nih.gov/ij/) (Schneider et al., 2012), was used to measure canker area from digital photographs. The software was calibrated to standardize each photograph to the reference scale included in each photograph.

Confirmation of Pathogenicity *via* Modified Koch's Postulates

To confirm *G. morbida* as the causal agent of the observed cankers, a modified version of Koch's postulates was conducted using the rapid molecular detection method described by Oren et al. (2018). Three of six replicated branch sections used in each isolate inoculation were randomly selected, and one of the inoculation sites was selected for molecular screening. Under sterile conditions, drill shavings of phloem and wood tissues were collected only from the margins of the cankers, excluding the inoculation wound site. Sample collection, DNA extraction, and PCR amplification for pathogen detection were performed as described by Oren et al. (2018).

Statistical Analysis

The effects of the genetic cluster, isolates, *Juglans* host, location (state), and region (eastern vs. western United States) (**Table 1**) on canker size were each analyzed using the mixed model analysis for split-plot design with the individual *J. nigra* trees as the experiment unit for the whole plot effects. Diagnostic

analysis was conducted to assess model assumptions. The rank transformation was applied if diagnostic analysis exhibited violation of normality and equal variance assumptions. *Post-hoc* multiple comparisons were performed with Tukey's adjustment. Statistical significance was identified at $P < 0.05$. Analyses were conducted in SAS 9.4 TS1M7 for Windows 64x (SAS Institute Inc., Cary, NC, USA).

RESULTS

Confirmation of Koch's Postulates

From 150 samples tested (25 *G. morbida* isolates across six replicates), 147 were positive for the presence of *G. morbida* DNA in tissues collected from the margins of cankers (98% *G. morbida* detection rate). Phloem margins from darkened damage-response areas of six agar-only control samples were also tested, and *G. morbida* DNA was not detected from any of these samples.

Effect of the Variation in Branch Section Diameter on Canker Area

Branch sections of 2–3 cm diameter (average of 2.5 cm) were used for inoculations. The potential effect of variation in branch section diameter on the canker area was analyzed. Canker area did not differ in response to branch diameter ($P = 0.569$); therefore, branch diameters were pooled for further analyses.

Effect of Genetic Cluster, State, and Host Origin of Fungal Isolate on Canker Size

Overall, *G. morbida* isolates from genetic cluster 2 induced significantly larger cankers than the ones from cluster 1, yielding a mean canker area of 210.34 mm^2 and 153.76 mm^2, respectively

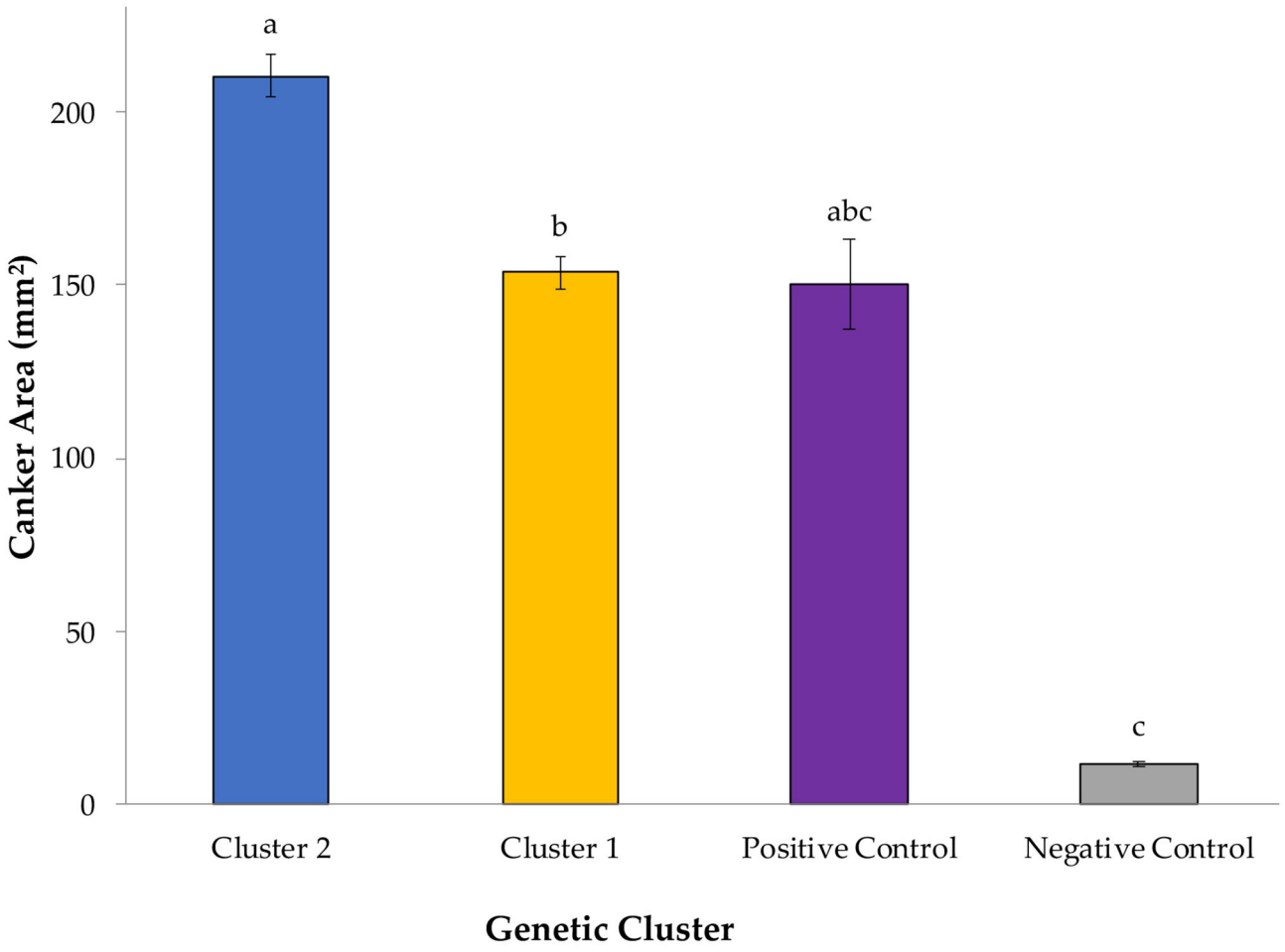

FIGURE 1 | Mean canker sizes were observed at 7 days after inoculation (DAI) with *Geosmithia morbida* isolates representing 2 genetic clusters, as were characterized in the studies by Hadziabdic et al. (2014) and Hadziabdic et al. (unpublished data, **Supplementary Figure S1**). In this study, 12 *G. morbida* isolates represented genetic cluster 1 and 13 *G. morbida* isolates represented genetic cluster 2. Within cluster or control group, treatment mean separations were made using least square mean estimates calculated from rank-transformed canker areas and differ significantly ($P < 0.05$; Tukey's honestly significant difference) when indicated with different letters. Mean canker areas and standard errors of genetic clusters and controls depicted here reflect non-transformed data measured across assays performed on both assayed trees.

($P = 0.034$; **Figure 1**). Canker sizes did not differ significantly among isolates within cluster 1 ($P = 0.080$), but canker sizes differed among isolates within cluster 2 ($P = 0.0003$). All *G. morbida* isolates resulted in the formation of cankers with areas that were significantly larger than responses observed in the negative control (effect of wound in isolation), except for isolates GM140 ($P = 0.184$) and GM158 ($P = 0.196$) (affiliated with cluster 1) and GM11 ($P = 0.623$) and GM59 ($P = 0.063$) (affiliated with cluster 2) (**Figure 2**). These isolates induced cankers; however, their smaller lesion areas were not statistically different from lesions produced by the wounding alone (**Figure 2**). Irrespective of genetic cluster association, all *G. morbida* isolates were variable in the mean canker sizes observed 7 DAI ($P < 0.001$). Despite variability observed across mean canker sizes from all isolates (Figure 2), differences were observed in mean canker sizes when analyzed according to the states in which the *G. morbida* isolates were collected ($P < 0.001$). At 7 DAI, the largest mean canker areas were induced by isolates GM 293 (OH), GM 277 (UT), GM 50 (PA), GM 259 (UT), and GM 301 (OR) (**Figure 2**). The largest canker sizes were observed across a mixture of western (OR and UT) with eastern (IN, OH, and PA) states. Similar variability was also evident in the state origins of isolates that induced smaller canker areas. However, we caution that for several states (OH, PA, and NC), only a single isolate could be obtained for assays, which restricts the validity of predictions that may be inferred regarding isolates from these states. When the results from these three state isolates were removed from data analysis, the effect of canker size on collection location (AZ, CO, IN, NM, OR, TN, and UT) was significant ($P = 0.0019$). To address this limitation to the experimental design, a comparison of canker areas was analyzed according to the eastern vs. western geographic region from which isolates originated and canker sizes among *G. morbida* isolates did not statistically differ ($P = 0.927$). Thus, our results indicate that the geographic origin of isolates is not a good predictor of expected virulence. Mean canker areas observed between geographic groups were 188 ± 8.6 mm^2 for eastern and 181 ± 4.4 mm^2 for western isolates (data not shown).

Finally, the observed mean canker areas differed when isolates were grouped by origin from different *Juglans* sp. hosts ($P = 0.048$). Mean canker area of isolates collected from *Juglans major* induced statistically smaller cankers when compared to isolates recovered from undetermined *Juglans* spp. ($P = 0.045$) but not from *J. nigra* ($P = 0.134$) (**Figure 3**). Cankers induced by the isolate recovered from *Juglans microcarpa*, which were excluded

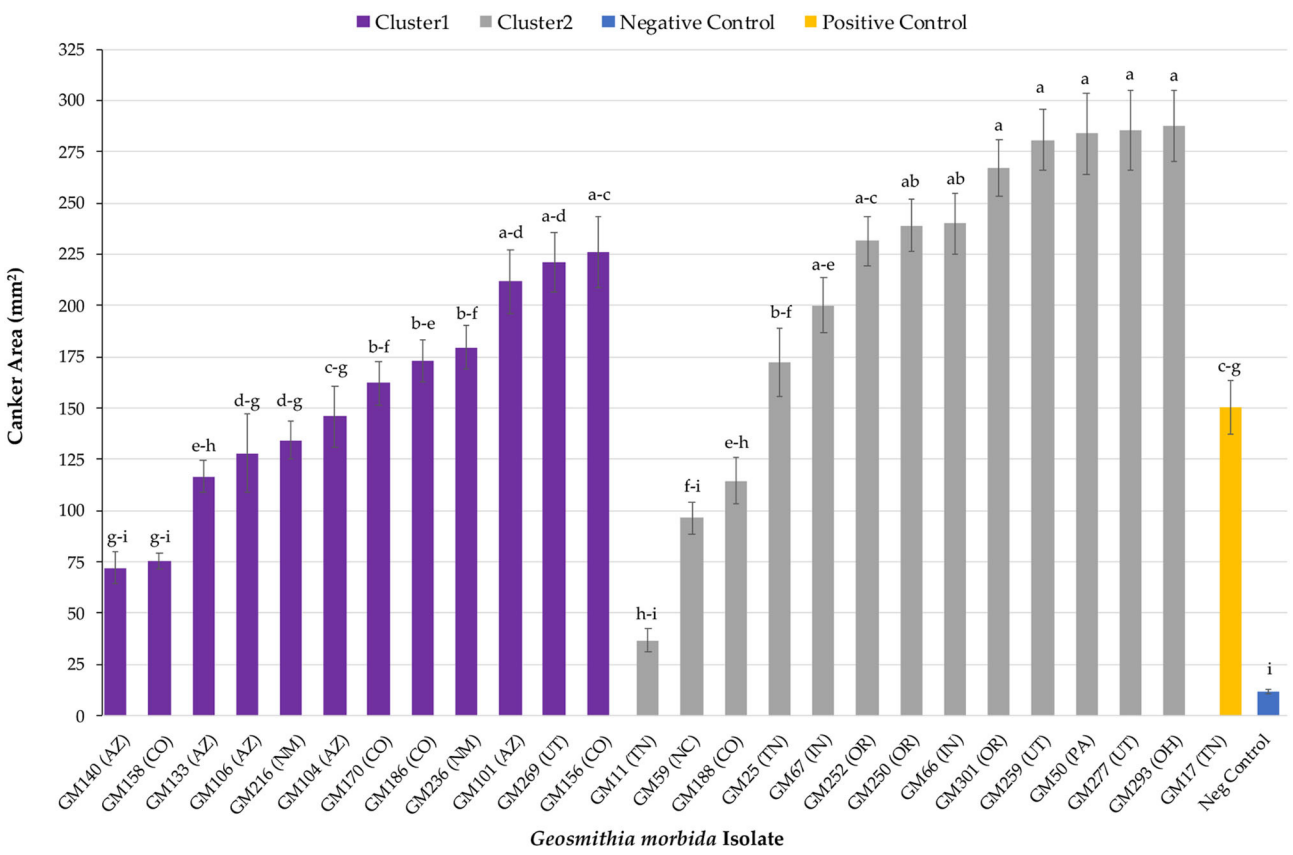

FIGURE 2 | Mean canker area observed across all *G. morbida* isolates. For each isolate, treatment mean separations were made using least square mean estimates calculated from rank-transformed canker areas and differ significantly ($P < 0.05$; Tukey's honestly significant difference) when indicated with different letters. Mean canker areas and standard errors depicted here reflect non-transformed data measured across both assayed trees.

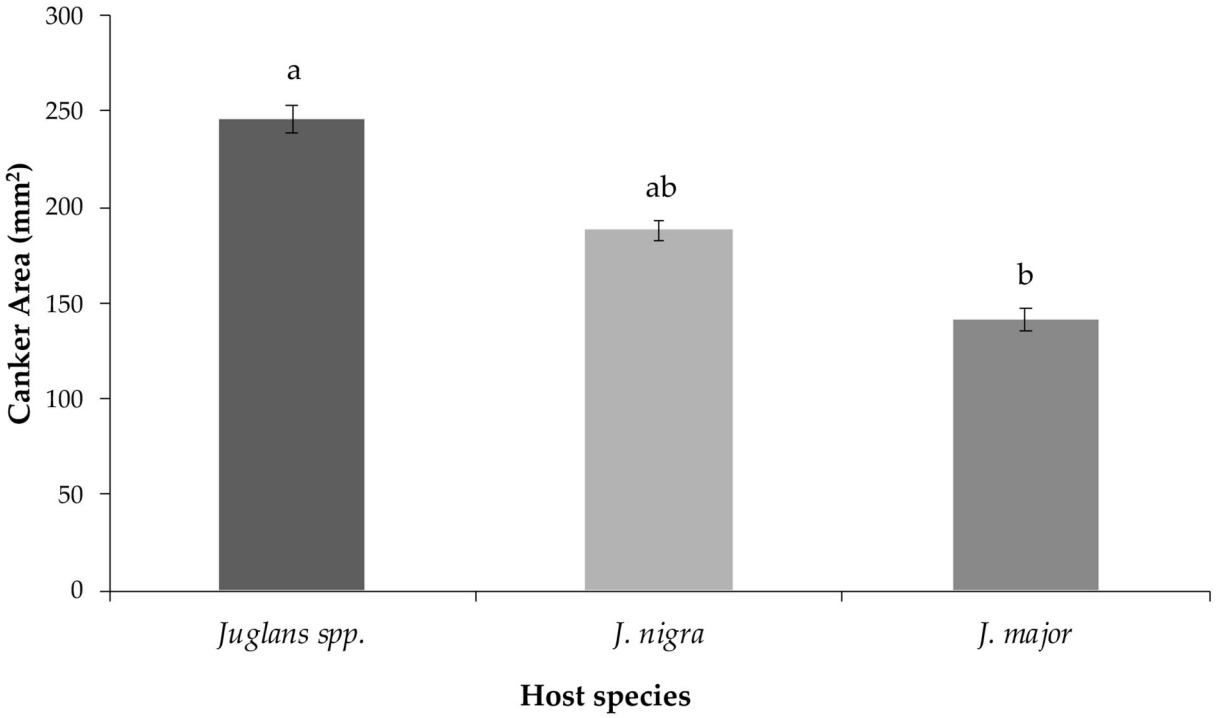

FIGURE 3 | Mean canker area measured for lesions induced by *G. morbida* isolates that were grouped based on *Juglans* species host source as follows: undetermined *Juglans* spp., *Juglans major*, and *Juglans nigra*. Within species, treatment mean separations were made using least square mean estimates calculated from rank-transformed canker areas and differ significantly ($P < 0.05$; Tukey's honestly significant difference) when indicated with different letters. Non-transformed data and standard errors are presented.

from statistical comparisons due to limited sample size, yielded intermediate-sized cankers averaging 225.81 ± 17.28 mm^2.

DISCUSSION

All tested *G. morbida* isolates induced canker formation. However, the geographic origin of the isolates (eastern vs. western origin) was not correlated to their virulence and could not be used to provide meaningful insights into the different disease outcomes observed between the two regions. While our data indicate that *G. morbida* isolates assigned to genetic cluster 2 (mixture of eastern and western isolates) yielded cankers with a larger mean size than isolates in cluster 1 (western isolates only), the virulence of *G. morbida* may only be partially explained by their genetic grouping into distinct clusters (clustering herein was based on *G. morbida* microsatellites, Hadziabdic et al., 2014, unpublished data). Isolates belonging to the same cluster induced a wide range of canker sizes. After 7 days, canker areas induced by *G. morbida* isolates in cluster 2 ranged in size from 36 to 287 mm^2 (from isolates GM11 and GM293, respectively) compared with canker areas from 72 to 225 mm^2 (isolates GM140 and GM156, respectively) induced by *G. morbida* isolates from cluster 1. Overall, *G. morbida* isolates from genetic cluster 2 yielded cankers that were more variable in size than isolates from genetic cluster 1. Significant differences were observed among mean canker sizes according to the states from which the *G. morbida* isolates were collected. Given the variability observed in canker sizes at 7 DAT, however, state provenance of the isolates was not a reliable predictor of potential virulence. This observation is further evidence in support of the hypothesis that multiple introductions of *G. morbida* have occurred across time and which have originated from multiple locations (Hadziabdic et al., 2014; Zerillo et al., 2014). Given the lack of statistical significance observed when comparing canker sizes induced by western vs. eastern isolates, our hypothesis for explaining the greater TCD severity seen in the western localities was not supported by these laboratory assays. Similarly, results do not support anecdotal observations that *G. morbida* has been less virulent in the eastern United States. Factors, including environmental conditions, host-plant genetics, and interactions with other fungi and microorganisms, are likely to contribute to virulence across the distributed range of *G. morbida*. We also acknowledged that the lack of resolution could be partly due to the low number of isolates from eastern ($n = 7$) in comparison with western ($n = 18$) states.

Detached branch and stem assays are often used in pathogenicity assays for fungi affecting shrubs (Wagner et al., 2006), woody ornamentals (Guo et al., 2015), and forest trees (Amponsah et al., 2011; Sessa et al., 2017) as rapid alternatives to *in planta* inoculations. Detached branch assays can be as reliable as *in vivo* assays for pathogenicity, virulence, and germplasm screening experiments (Smith, 1996; Kohpina et al.,

2000; Dodd et al., 2005; Stewart et al., 2005; Baskarathevan et al., 2012). These assays are also particularly appropriate when regulated or quarantined organisms, such as *G. morbida*, are being studied. In addition, detached tissue assays are easier to handle and offer greater reproducibility by enabling the use of branch sections with uniform diameters allowing appropriate replication, consistent inoculum delivery, and greater accuracy in the quantification of disease symptoms (Kohpina et al., 2000; Hüberli et al., 2002). However, this system is not without its flaws or biological shortcomings. Disadvantages of detached tissue assays are that host-defense mechanisms may be compromised and detached branches may not adequately reflect the whole plant response (Sessa et al., 2017). For example, larger cankers were observed on detached branches of necrotic grapevine tissue compared to results from *in vivo* branch inoculations, which shows the importance of host-plant defense response in mitigating disease severity (Amponsah et al., 2011).

Virulence can play an important role in pathogen emergence and reemergence, potential host switches, and range expansion, thus making it very challenging to control and contain further spread (Sacristán and García-Arenal, 2008). Our study demonstrated variable virulence outcomes for isolates from both of our genetic clusters. This mixed result is consistent with the variable virulence that was observed by Tran et al. (2020), in which the virulence of the fungal pathogens *Monilinia fructicola* and *Monilinia laxa* on Japanese plum, *Prunus salicina* cv. "Fortune," did not correlate to pathogen genotypes. Similar results have been reported in other studies using *in planta* and detached branch assays, wherein differences in virulence were not correlated with genetic diversity of canker-causing fungal pathogens (Baskarathevan et al., 2012; Billones-Baaijens et al., 2013; Elena et al., 2015). The geographic origin of fungal isolates also was not associated with the virulence of canker-forming *Neonectria ditissima* fungus in apple trees (Campos et al., 2017) nor for various canker-forming Botryosphaeriaceae fungal pathogens that infect multiple host plants, including softwood and hardwood tree species (Mohali et al., 2007; Piškur et al., 2011; Félix et al., 2017).

Zerillo et al. (2014) used both single nucleotide polymorphisms and microsatellite markers to genotype *G. morbida* isolates across 17 geographic regions distributed across eastern and western United States with results that revealed the presence of four genetically distinct groups that were clustered into three different geographic regions. Based on this information, Sitz et al. (2017) conducted an *in planta* pathogen virulence field study using isolates from three genetic clusters. In their study, the virulence of *G. morbida* (using canker size as proxy) isolates was evaluated when inoculated into branches of standing trees. The authors also assessed canker formation when branches were co-inoculated with *Fusarium solani* species complex (FSSC). This latter step was undertaken because FSSC members have been recovered with *G. morbida* and might be associated with disease severity in the late stages of the disease (Tisserat et al., 2009; Montecchio et al., 2015).

Similar to our study, canker sizes induced by *G. morbida* (only) isolates from Colorado were not significantly correlated within the genetic cluster of the isolate (Sitz et al., 2017). Unlike our study, however, no significant difference in canker size was observed between genetic clusters (Sitz et al., 2017). The 183 mm^2 canker area that was averaged among all *G. morbida* isolates used in our study was much larger than the 87 mm^2 mean canker area reported by Sitz et al. (2017). From the co-inoculation efforts of Sitz et al. (2017) with *G. morbida* and FSSC members, the authors found that these pathogens do not yield a synergistic response. In our own preliminary studies on co-inoculation of juvenile *J. nigra* trees with *F. solani* and with eastern United States (TN), the isolates of *G. morbida* yielded contradictory results (data not shown). We caution that the specific role of FSSC members in tree mortality remains under-examined and should be a focus of future pathogenicity efforts. In sum, other factors including differences in environmental conditions, inoculation method, incubation period, host-plant age and condition, and *in planta* vs. detached branch assays all are likely to have contributed to different results found between Sitz et al.'s (2017) study and our study. Ideally, our ability to resolve these questions would require in-field, *in planta* assays using isolates from across the distributed range of *G. morbida* and inoculated into clonal *Juglans* germplasm.

Forest pathosystems are complex, especially when an insect vector is involved or more than one pathogen species contribute to the disease, as occurs in Ceratocystis wilt of 'ohi'a (Hughes et al., 2020), beech leaf disease (Burke et al., 2020; Ewing et al., 2021), black pod of cocoa (Guest, 2007), and TCD on walnuts and wing nuts (Tisserat et al., 2009; Montecchio et al., 2015). The potential for multiple pathogen interactions makes it difficult to identify and document the role of each organism in tree decline. Interestingly, the *F. solani* isolate that was originally recovered from Colorado (Tisserat et al., 2009) did not yield a synergistic response in terms of canker size when co-inoculated with *G. morbida* on *J. nigra* branches (Sitz et al., 2017). Sitz et al. (2017) found that cankers induced by *Fusarium* alone were not different from the cankers induced by negative control inoculations. Members of FSSC have also been found in diseased *J. nigra* and *Juglans regia* trees in Italy where TCD has been recently introduced (Montecchio et al., 2015). Montecchio et al. (2015) observed that cankers induced by a *Fusarium* isolate from FSSC-25 alone were similar to cankers induced by *Fusarium* and *G. morbida* co-inoculations and were significantly larger than negative control inoculations. Hence, their results suggest *Fusarium* as a contributing pathogen to early stages of TCD in Italy (Montecchio et al., 2015). Differences in virulence results of *Fusarium* isolates in both studies (Montecchio et al., 2015; Sitz et al., 2017) are similar to our observed differences in *G. morbida* inoculation trails. These inconsistencies may be explained by the differences in *F. solani*/*G. morbida* strains used in testing trials, genotype, and age of host, environmental conditions, type of propagules used as inoculum, and incubation period. In future, a large-scale study that involves the inoculations of multiple strains of *Fusarium* from different TCD-associated FSSC groups on diverse *J. nigra* genotypes could help articulate the functional role of *Fusarium* in TCD etiology and epidemiology.

We also examined if virulence was correlated to the tree host species. If TCD members (host, pathogen, and vector) exist in isolation, pathogen populations could have adapted to particular hosts and, therefore, respond differently when inoculated into *J. nigra*. The isolates used in this study were recovered from cankers

on *J. major*, *J. microcarpa*, *J. nigra*, and unidentified *Juglans* spp. Canker sizes were significantly different when isolates were analyzed by host. Isolates collected from *J. major* induced significantly smaller cankers compared to isolates collected from other *Juglans* spp. but not from *J. nigra*. This finding is not surprising since the TCD vector, i.e., WTB, is native to the southwestern United States, and it has been hypothesized that both *G. morbida* and WTB have coevolved in a native host, Arizona walnut (*J. major*) (Zerillo et al., 2014; Rugman-Jones et al., 2015; Seybold et al., 2019). One plausible explanation is that *G. morbida* isolates from *J. major* might have reduced virulence on that particular host due to a coevolutionary relationship, and the concept of host-jumping into other *Juglans* spp. could provide further clues into the current virulence and migration patterns of *G. morbida*. This idea was further elaborated in a recent study by Sitz et al. (2021) that included 640 trees from wild and selected *J. nigra* families and found that improved seedlings (improved selections for enhanced growth and timber quality) exhibited larger canker sizes when compared to wild trees from the same provenance. Unfortunately, breeding efforts (Beineke, 1989; McKenna and Coggeshall, 2018; Sitz et al., 2021) may have resulted in nontargeted selection for reduced defense response against *G. morbida* infection. The authors further proposed that differences in TCD dynamics between *J. nigra* tree populations distributed in the western range of the species natural distribution vs. populations distributed in the central region (wild trees in the regions without TCD) reflect enhanced genetic resistance as a result of coevolution with *G. morbida* (Sitz et al., 2021).

CONCLUSION

Our results indicated varying degrees of virulence among tested *G. morbida* isolates, which was partly explained by their genetic provenance (state-of-origin). From the variables we tested here, genetic clustering (*G. morbida* isolates from genetic cluster 2 induced significantly larger cankers), state of origin, and *Juglans* host species could provide some explanation regarding the differences observed in *G. morbida* canker sizes. Although significant differences in canker size were noted when results from isolates were pooled within genetic cluster, host, geographic, and state-of-origin factors, a high level of variability was observed across most of these tested variables. Differential TCD severity and incidence between the western and eastern regions of the United States might instead result from other biotic (Gazis et al., 2018; Chahal et al., 2019) and abiotic factors (Griffin, 2015), or a combination of both (Seybold et al., 2019). The infestation level of WTB is likely a critical factor in determining tree mortality, as tree decline and death occur due to cambium-girdling caused by the coalescence of *G. morbida* cankers formed as a consequence of numerous beetle inoculations and WTB gallery formations (Tisserat et al., 2011). Hence, the lower levels of WTB infestation will result in less *G. morbida* inoculations and less likelihood of lesion coalescence to occur. In the eastern United States, WTB populations have been declining (Chahal et al., 2019), which in turn may be limiting the impact of TCD where *J. nigra* is native (Seybold et al., 2019).

DATA AVAILABILITY STATEMENT

The raw data supporting the conclusions of this article will be made available by the authors upon request, without undue reservation.

AUTHOR CONTRIBUTIONS

DH, RG, WK, and MW conceived and designed the experiments including the major conceptual ideas and proof outline. KC and MW collected samples. KC carried out the experiments. RG contributed to the processes. All authors contributed to the interpretation of the results, manuscript writing, editing, and provided critical feedback to shape the experiments, analyses, and finally produce the manuscript.

FUNDING

This research was conducted in partial fulfillment of an MS degree for K.C. from The University of Tennessee and was funded by the Woodtiger Foundation as part of the *Evaluating Impact of Thousand Cankers Disease on Black Walnut: Risk Assessment, Biological Control, and Development of Novel Assessment Tools* project. Additional support was provided by the USDA National Institute of Food and Agriculture Hatch Project #1009630: TEN00495.

ACKNOWLEDGMENTS

We thank Mr. Kevin Thompson (Director, Middle Tennessee Research & Education Center, Spring Hill, TN) for his help in collecting *J. nigra* branches. We are thankful to Sara Collins (University of Tennessee, Knoxville, TN, USA) for her assistance in laboratory work and to Sun Xiaocun (University of Tennessee, Knoxville, TN, USA) for statistical consulting and analyses.

SUPPLEMENTARY MATERIAL

The Supplementary Material for this article can be found online at: https://www.frontiersin.org/articles/10.3389/ffgc.2022.726388/full#supplementary-material

REFERENCES

Amponsah, N. T., Jones, E. E., Ridgway, H. J., and Jaspers, M. V. (2011). Identification, potential inoculum sources and pathogenicity of botryosphaeriaceous species associated with grapevine dieback disease in New Zealand. *Eur. J. Plant Pathol. 131*, 467. doi: 10.1007/s10658-011-9823-1

Baskarathevan, J., Jaspers, M. V., Jones, E. E., Cruickshank, R. H., and Ridgway, H. J. (2012). Genetic and pathogenic diversity of *Neofusicoccum parvum* in New Zealand vineyards. *Fungal Biol.* 116, 276–288. doi: 10.1016/j.funbio.2011.11.010

Beineke, W. F. (1989). Twenty years of black walnut genetic improvement at Purdue University. *North. J. Appl. For.* 6, 68–71. doi: 10.1093/njaf/6.2.68

Billones-Baaijens, R., Jones, E. E., Ridgway, H. J., and Jaspers, M. V. (2013). Virulence affected by assay parameters during grapevine pathogenicity studies with Botryosphaeriaceae nursery isolates. *Plant Pathol.* 62, 1214–1225. doi: 10.1111/ppa.12051

Burke, D. J., Hoke, A. J., and Koch, J. (2020). The emergence of beech leaf disease in Ohio: Probing the plant microbiome in search of the cause. *For. Pathol.* 50, e12579. doi: 10.1111/efp.12579

Campos, J. D. S., Bogo, A., Sanhueza, R. M. V., Casa, R. T., Silva, F. N. D., Cunha, I. C. D., et al. (2017). European apple canker: morphophysiological variability and pathogenicity in isolates of *Neonectria ditissima* in southern Brazil. *Ciência Rural*. 47. doi: 10.1590/0103-8478cr20160288

Chahal, K., Gazis, R., Klingeman, W., Hadziabdic, D., Lambdin, P., Grant, J., et al. (2019). Assessment of alternative candidate subcortical insect vectors from walnut crowns in habitats quarantined for thousand cankers disease. *Environ. Entomol*. 48, 882–893. doi: 10.1093/ee/nvz064

Chahal, K., Gazis, R. O., Grant, J., Hadziabdic, D., Lambdin, P., Klingeman, W., et al. (2017). Preliminary assessment of insect-associated *Geosmithia* species in Tennessee. *Phytopathology.* 107, 113.

Daniels, D., Nix, K., Wadl, P., Vito, L., Wiggins, G., Windham, M., et al. (2016). Thousand cankers disease complex: a forest health issue that threatens *Juglans* species across the US. *Forests*. 7, 260. doi: 10.3390/f7110260

Dodd, R. S., Hüberli, D., Douhovnikoff, V., Harnik, T. Y., Afzal-Rafii, Z., and Garbelotto, M. (2005). Is variation in susceptibility to *Phytophthora ramorum* correlated with population genetic structure in coast live oak (*Quercus agrifolia*)? *New Phytologist.* 165, 203–214. doi: 10.1111/j.1469-8137.2004.01200.x

Elena, G., Garcia-Figueres, F., Reigada, S., and Luque, J. (2015). Intraspecific variation in *Diplodia seriata* isolates occurring on grapevines in Spain. *Plant Pathol.* 64, 680–689. doi: 10.1111/ppa.12296

Ewing, C. J., Slot, J., Benítez, M. S., Rosa, C., Malacrin,ò, A., Bennett, A., et al. (2021). The foliar microbiome suggests that fungal and bacterial agents may be involved in the Beech Leaf Disease Pathosystem. *Phytobiomes J.* 5, 335–349. doi: 10.1094/PBIOMES-12-20-0088-R

Félix, C., Pinto, G., Amaral, J., Fernandes, I., Alves, A., and Esteves, A. C. (2017). Strain-related pathogenicity in *Diplodia corticola*. *For. Pathol.* 47, e12366. doi: 10.1111/efp.12366

Gardes, M., and Bruns, T. D. (1993). ITS primers with enhanced specificity for basidiomycetes: application to the identification of mycorrhizae and rusts. *Mol. Ecol.* 2, 113–118. doi: 10.1111/j.1365-294X.1993.tb00005.x

Gazis, R., Poplawski, L., Klingeman, W., Boggess, S. L., Trigiano, R. N., Graves, A. D., et al. (2018). Mycobiota associated with insect galleries in walnut with thousand cankers disease reveals a potential natural enemy against *Geosmithia morbida*. *Fungal Biology* 122, 241–253. doi: 10.1016/j.funbio.2018.01.005

Grant, J. F., Windham, M. T., Haun, W. G., Wiggins, G. J., and Lambdin, P. L. (2011). Initial assessment of thousand cankers disease on black walnut, *Juglans nigra*, in eastern Tennessee. *Forests.* 2, 741–748. doi: 10.3390/f2030741

Griffin, G. J. (2015). Status of thousand cankers disease on eastern black walnut in the eastern United States at two locations over 3 years. *For. Pathol.* 45, 203–214. doi: 10.1111/efp.12154

Guest, D. (2007). Black pod: diverse pathogens with a global impact on cocoa yield. *Phytopathology.* 97, 1650–1653. doi: 10.1094/PHYTO-97-12-1650

Guo, Y., Olsen, R. T., Kramer, M., and Pooler, M. (2015). Effective bioassays for evaluating boxwood blight susceptibility using detached stem inoculations. *HortScience.* 50, 268–271. doi: 10.21273/HORTSCI.50.2.268

Hadziabdic, D., Vito, L. M., Windham, M. T., Pscheidt, J. W., Trigiano, R. N., and Kolarik, M. (2014). Genetic differentiation and spatial structure of *Geosmithia morbida*, the causal agent of thousand cankers disease in black walnut (*Juglans nigra*). *Curr. Genet.* 60, 75–87. doi: 10.1007/s00294-013-0414-x

Hansen, M. A., Bush, E., Day, E., Griffin, G., and Dart, N. (2011). *Walnut Thousand Cankers Disease Alert*. Blacksburg, Virginia: Virginia Cooperative Extension. Available online at: https://www.vdacs.virginia.gov/pdf/techpestalert.pdf.

Hefty, A. R., Aukema, B. H., Venette, R. C., Coggeshall, M. V., McKenna, J. R., and Seybold, S. J. (2018). Reproduction and potential range expansion of walnut twig beetle across the Juglandaceae. *Biol. Invasions.* 20, 2141–2155. doi: 10.1007/s10530-018-1692-5

Hishinuma, S. M., Dallara, P. L., Yaghmour, M. A., Zerillo, M. M., Parker, C. M., Roubtsova, T. V., et al. (2016). Wingnut (Juglandaceae) as a new generic host for *Pityophthorus juglandis* (Coleoptera: Curculionidae) and the thousand cankers disease pathogen, *Geosmithia morbida* (Ascomycota: Hypocreales). *Can. Entomol*. 148, 83–91. doi: 10.4039/tce.2015.37

Huang, Y. T., Kolaník, M., Kasson, M. T., and Hulcr, J. (2017). Two new *Geosmithia* species in *G. pallida* species complex from bark beetles in eastern USA. *Mycologia.* 109, 790–803. doi: 10.1080/00275514.2017.1410422

Huang, Y. T., Skelton, J., Johnson, A. J., Kolaník, M., and Hulcr, J. (2019). *Geosmithia* species in southeastern USA and their affinity to beetle vectors and tree hosts. *Fungal Ecol.* 39, 168–183. doi: 10.1016/j.funeco.2019.02.005

Hüberli, D., Tommerup, I. C., Colver, M. C., Colquhoun,C, I. J., and Hardy, G. E. S. J. (2002). Temperature and inoculation method influence disease phenotypes and mortality of *Eucalyptus marginata* clonal lines inoculated with *Phytophthora cinnamomi*. *Australas. Plant Pathol.* 31, 107–118. doi: 10.1071/AP01078

Hughes, M. A., Juzwik, J., Harrington, T., and Keith, L. (2020). Pathogenicity, symptom development and colonization of *Metrosideros polymorpha* by *Ceratocystis lukuohia. Plant Dis.* 104, 2233–2241. doi: 10.1094/PDIS-09-19-1905-RE

Jankowiak, R., and Bilański, P. (2018). *Geosmithia* species associated with fir-infesting beetles in Poland. *Acta Mycologica*. *53*, 1115. doi: 10.5586/am.1115

Kohpina, S., Knight, R., and Stoddard, F. L. (2000). Evaluating faba beans for resistance to ascochyta blight using detached organs. *Aust. J. Exp. Agric.* 40, 707–713. doi: 10.1071/EA99168

Kolarik, M., Freeland, E., Utley, C., and Tisserat, N. (2011). *Geosmithia morbida* sp. nov., a new phytopathogenic species living in symbiosis with the walnut twig beetle (*Pityophthorus juglandis*) on *Juglans* in USA. *Mycologia.* 103, 325–332. doi: 10.3852/10-124

Kolaník, M., Hulcr, J., Tisserat, N., De Beer, W., Kostovčík, M., Kolaníkov,á, Z., et al. (2017). *Geosmithia* associated with bark beetles and woodborers in the western USA: taxonomic diversity and vector specificity. *Mycologia.* 109, 185–199. doi: 10.1080/00275514.2017.1303861

Kolaník, M., Kubátová, A., Hulcr, J., and PaŽoutová, S. (2008). *Geosmithia* fungi are highly diverse and consistent bark beetle associates: evidence from their community structure in temperate Europe. *Microbial Ecol.* 55, 65–80. doi: 10.1007/s00248-007-9251-0

Lynch, S. C., Wang, D. H., Mayorquin, J. S., Rugman-Jones, P. F., Stouthamer, R., and Eskalen, A. (2014). First report of *Geosmithia pallida* causing foamy bark canker, a new disease on coast live oak (*Quercus agrifolia*), in association with *Pseudopityophthorus pubipennis* in California. *Plant Dis.* 98, 1276–1276. doi: 10.1094/PDIS-03-14-0273-PDN

McKenna, J. R., and Coggeshall, M. V. (2018). *The genetic improvement of black walnut for timber production. in Plant Breeding Reviews*. Goldman, I. (ed). New Jersey: John Wiley and Sons, Inc. 41, 263–290. doi: 10.1002/9781119414735.ch6

Mohali, S., Slippers, B., and Wingfield, M. J. (2007). Identification of Botryosphaeriaceae from *Eucalyptus*, *Acacia* and *Pinus* in Venezuela. *Fungal Div.* 25, 103–125. Available online at: https://www.fungaldiversity.org/fdp/sfdp/25-7.pdf

Montecchio, L., and Faccoli, M. (2014). First record of thousand cankers disease *Geosmithia morbida* and walnut twig beetle *Pityophthorus juglandis* on *Juglans nigra* in Europe. *Plant Dis.* 98, 696. doi: 10.1094/PDIS-10-13-1027-PDN

Montecchio, L., Faccoli, M., Short, D. P. G., Fanchin, G., Geiser, D. M., and Kasson, M. T. (2015). First report of *Fusarium solani* phylogenetic species 25 associated with early stages of thousand cankers disease on *Juglans nigra* and *Juglans regia* in Italy. *Plant Dis.* 99, 1183–1183. doi: 10.1094/PDIS-01-15-0103-PDN

Moore, M., Juzwik, J., Miller, F., Roberts, L., and Ginzel, M. D. (2019). Detection of *Geosmithia morbida* on numerous insect species in four eastern states. *Plant Health Prog.* 20, 133–139. doi: 10.1094/PHP-02-19-0016-RS

Moricca, S., Bracalini, M., Benigno, A., Ginetti, B., Pelleri, F., and Panzavolta, T. (2019). Thousand cankers disease caused by *Geosmithia morbida* and its insect vector *Pityophthorus juglandis* first reported on *Juglans nigra* in Tuscany, Central Italy. *Plant Dis.* 103, 369–369. doi: 10.1094/PDIS-07-18-1256-PDN

Newton, L., Fowler, G., Neeley, A. D., Schall, R. A., and Takeuchi, Y. (2009). *Pathway assessment: Geosmithia sp. and Pityophthorus juglandis Blackman movement from the western into the eastern United States*. US Department of Agriculture, Animal and Plant Health Inspection Service. Available online at: http://thousandcankers.com/wp-content/uploads/2018/08/APHIS_Geosmithia_10_2009.pdf.

Oren, E., Klingeman, W., Gazis, R., Moulton, J., Lambdin, P., Coggeshall, M., et al. (2018). A novel molecular toolkit for rapid detection of the pathogen and primary vector of thousand cankers disease. *PloS ONE.* 13, e0185087. doi: 10.1371/journal.pone.0185087

Piškur, B., Pavlic, D., Slippers, B., Ogris, N., Maresi, G., Wingfield, M. J., et al. (2011). Diversity and pathogenicity of Botryosphaeriaceae on declining *Ostrya carpinifolia* in Slovenia and Italy following extreme weather conditions. *Eur. J. For. Res.* 130, 235–249. doi: 10.1007/s10342-010-0424-x

Randolph, K. C., Rose, A. K., Oswalt, C. M., and Brown, M. J. (2013). Status of black walnut (*Juglans nigra* L.) in the eastern United States in light of the discovery of thousand cankers disease. *Castanea.* 78, 2–14. doi: 10.2179/12-024

Rugman-Jones, P. F., Seybold, S. J., Graves, A. D., and Stouthamer, R. (2015). Phylogeography of the walnut twig beetle, *Pityophthorus juglandis*, the vector of thousand cankers disease in North American walnut trees. *PLoS ONE.* 10, e0118264. doi: 10.1371/journal.pone.0118264

Sacristán, S., and García-Arenal, F. (2008). The evolution of virulence and pathogenicity in plant pathogen populations. *Mol. Plant Pathol.* 9, 369–384. doi: 10.1111/j.1364-3703.2007.00460.x

Schneider, C. A., Rasband, W. S., and Eliceiri, K. W. (2012). NIH Image to ImageJ: 25 years of image analysis. *Nat. Methods.* 9, 671–675. doi: 10.1038/nmeth.2089

Schuelke, T. A., Wu, G., Westbrook, A., Woeste, K., Plachetzki, D. C., Broders, K., et al. (2017). Comparative genomics of pathogenic and nonpathogenic beetle-vectored fungi in the genus *Geosmithia*. *Genome Biol. Evol.* 9, 3312–3327. doi: 10.1093/gbe/evx242

Sessa, L., Abreo, E., Bettucci, L., and Lupo, S. (2017). Diversity and virulence of *Diaporthe* species associated with wood disease symptoms in deciduous fruit trees in Uruguay. *Phytopathol. Mediterr.* 56, 431–444.

Seybold, S. J., Klingeman, I. I. I., W. E., Hishinuma, S. M., Coleman, T. W., and Graves, A. D. (2019). Status and impact of walnut twig beetle in urban forest, orchard, and native forest ecosystems. *J. For.* 117, 152–163. doi: 10.1093/jofore/fvy081

Sitz, R. A., Luna, E. K., Caballero, J. I., Tisserat, N. A., Cranshaw, W. S., McKenna, J. R., et al. (2021). Eastern black walnut (*Juglans nigra* L.) originating from native range varies in their response to inoculation with *Geosmithia morbida*. *Front. For. Glob. Change.* 4, 627911. doi: 10.3389/ffgc.2021.627911

Sitz, R. A., Luna, E. K., Caballero, J. I., Tisserat, N. A., Cranshaw, W. S., and Stewart, J. E. (2017). Virulence of genetically distinct *Geosmithia morbida* isolates to black walnut and their response to coinoculation with *Fusarium solani*. *Plant Dis.* 101, 116–120. doi: 10.1094/PDIS-04-16-0535-RE

Smith, B. J. (1996). Detached stem assay to evaluate the severity of stem blight of rabbiteye blueberry (*Vaccinium ashei*). *In VI International Symposium on Vaccinium Culture.* 446, 457–464. doi: 10.17660/ActaHortic.1997.446.66

Stewart, P. J., Clark, J. R., and Fenn, P. (2005). Detached cane assay of resistance to botryosphaeria cane canker (*Botryosphaeria dothidea*) in eastern US blackberry genotypes. *Int. J. Fruit Sci.* 5, 57–64. doi: 10.1300/J492v05n04_07

Tisserat, N., Cranshaw, W., Leatherman, D., Utley, C., and Alexander, K. (2009). Black walnut mortality in Colorado caused by the walnut twig beetle and thousand cankers disease. *Plant Health Prog.* 1–10. doi: 10.1094/PHP-2009-0811-01-RS

Tisserat, N., Cranshaw, W., Putnam, M. L., Pscheidt, J., Leslie, C. A., Murray, M., et al. (2011). Thousand cankers disease is widespread in black walnut in the western United States. *Plant Health Prog.* 1–4. doi: 10.1094/PHP-2011-0630-01-BR

Tran, T. T., Li, H., Nguyen, D. Q., Sivasithamparam, K., Jones, M. G. K., and Wylie, S. J. (2020). Comparisons between genetic diversity, virulence and colony morphology of *Monilinia fructicola* and *Monilinia laxa* isolates. *J Plant Pathol.* 1–9. doi: 10.1007/s42161-020-00498-2

Utley, C., Nguyen, T., Roubtsova, T., Coggeshall, M., Ford, T. M., Grauke, L. J., et al. (2013). Susceptibility of walnut and hickory species to *Geosmithia morbida*. *Plant Dis.* 97, 601–607. doi: 10.1094/PDIS-07-12-0636-RE

Wagner, S., Kaminski, K., and Werres, S. (2006). "Inoculation trials with *Phytophthora ramorum* on Moorland species", in *Second Science Symposium: The State of Our Knowledge* (p. 520). Gen. Tech. Rep. PSW-GTR-196. Albany, CA: Pacific Southwest Research Station, Forest Service, U.S. Department of Agriculture. doi: 10.2737/PSW-GTR-196

White, T. J., Bruns, T., Lee, S. J. W. T., and Taylor, J. (1990). Amplification and direct sequencing of fungal ribosomal RNA genes for phylogenetics. *PCR Protocols: A Guide to Methods and Applications.* 18, 315–322. doi: 10.1016/B978-0-12-372180-8.50042-1

Zerillo, M. M., Caballero, J. I., Woeste, K., Graves, A. D., Hartel, C., Pscheidt, J. W., et al. (2014). Population structure of *Geosmithia morbida*, the causal agent of thousand cankers disease of walnut trees in the United States. *PloS ONE.* 9, e112847. doi: 10.1371/journal.pone.0112847

Conflict of Interest: The authors declare that the research was conducted in the absence of any commercial or financial relationships that could be construed as a potential conflict of interest.

The reviewer PB declared a past collaboration with the author DH to the handling editor at the time of review.

The reviewer BD declared a shared affiliation with the author RG to the handling editor at the time of review.

frontiers | Frontiers in Forests and Global Change

ORIGINAL RESEARCH
published: 20 June 2022
doi: 10.3389/ffgc.2022.872584

Mechanisms of Pine Disease Susceptibility Under Experimental Climate Change

Soumya K. Ghosh[1], Jason C. Slot[1], Erik A. Visser[2], Sanushka Naidoo[2], Michael G. Sovic[3], Anna O. Conrad[1†], Bethany Kyre[1†], Vinod Vijayakumar[1†] and Pierluigi Bonello[1]*

[1] Department of Plant Pathology, The Ohio State University, Columbus, OH, United States, [2] Department of Biochemistry, Genetics and Microbiology, Forestry and Agricultural Biotechnology Institute (FABI), University of Pretoria, Pretoria, South Africa, [3] Center for Applied Plant Sciences, The Ohio State University, Columbus, OH, United States

OPEN ACCESS

Edited by:
Jane E. Stewart,
Colorado State University,
United States

Reviewed by:
Eeva Terhonen,
Natural Resources Institute Finland (Luke), Finland
Nicolas Feau,
Natural Resources Canada, Canada

***Correspondence:**
Soumya K. Ghosh
ghosh.188@osu.edu

†Present addresses:
Anna O. Conrad,
USDA Forest Service, Northern Research Station, Hardwood, Tree Improvement and Regeneration Center, West Lafayette, IN, United States

Bethany Kyre,
Department of Entomology, University of Kentucky, Lexington, KY, United States

Vinod Vijayakumar,
Charles River Laboratories, Columbus, OH, United States

Specialty section:
This article was submitted to Pests, Pathogens and Invasions, a section of the journal Frontiers in Forests and Global Change

Received: 09 February 2022
Accepted: 16 May 2022
Published: 20 June 2022

Citation:
Ghosh SK, Slot JC, Visser EA, Naidoo S, Sovic MG, Conrad AO, Kyre B, Vijayakumar V and Bonello P (2022) Mechanisms of Pine Disease Susceptibility Under Experimental Climate Change. Front. For. Glob. Change 5:872584. doi: 10.3389/ffgc.2022.872584

Climate change (CC) conditions projected for many temperate areas of the world, expressed by way of excessive temperatures and low water availability, will impact forest health directly by means of abiotic stress but also by predisposing trees to pathogenic attack. However, we do not yet know how such environmental conditions alter the physiology and metabolism of trees to render them more susceptible to pathogens. To explore these mechanisms, we conditioned 3-year-old Austrian pine saplings to a simulated CC environment (combined drought and elevated temperatures), followed by pathogenic inoculation with two sister fungal species characterized by contrasting aggressiveness, *Diplodia sapinea* (aggressive) and *D. scrobiculata* (less aggressive). Lesion lengths resulting from infection were measured after 3 weeks to determine phenotypes, while dual transcriptomics analysis was conducted on tissues collected from the margins of developing lesions on separate branches 72 h post inoculation. As expected, climate change conditions enhanced host susceptibility to the less aggressive pathogen, *D. scrobiculata*, to a level that was not statistically different from the more aggressive *D. sapinea*. Under controlled climate conditions, *D. sapinea* induced suppression of critical pathways associated with host nitrogen and carbon metabolism, while enhancing its own carbon assimilation. This was accompanied by suppression of host defense-associated pathways. In contrast, *D. scrobiculata* infection induced host nitrogen and fatty acid metabolism as well as host defense response. The CC treatment, on the other hand, was associated with suppression of critical host carbon and nitrogen metabolic pathways, alongside defense associated pathways, in response to either pathogen. We propose a new working model integrating concurrent host and pathogen responses, connecting the weakened host phenotype under CC treatment with specific metabolic compartments. Our results contribute to a richer understanding of the mechanisms underlying the oft-observed increased susceptibility to fungal infection in trees under conditions of low water availability and open new areas of investigation to further integrate our knowledge in this critical aspect of tree physiology and ecology.

Keywords: climate change, *Pinus nigra*, tree defense, host metabolism, necrotrophic, *Diplodia sapinea*, *Diplodia scrobiculata*, fungal metabolism

INTRODUCTION

The elevated temperatures predicted under climate change scenarios can directly impact plant physiology. The effects are expressed mostly through exacerbation of water limitation due to elevated vapor pressure deficits, which impose extra demands on the water relation capabilities of trees (Adams et al., 2009; Williams et al., 2013). Under sub-lethal drought conditions, physiological processes other than carbon starvation or interruption of water conduction can render droughted plants more susceptible to mortality from pathogen attack. For example, plants often respond by reducing photosynthesis and growth, accumulating compatible solutes (osmoprotectants) such as the amino acid proline (Pro), producing reactive oxygen species (ROS), and altering specialized metabolism, among other processes (Chaves et al., 2003; Bhargava and Sawant, 2013).

One system-level question emerges from this conceptual framework: "How does climate change-associated stress affect the internal environment of a tree to predispose it to fungal infection?" This is currently one of the top 10 unanswered questions in plant-pathogen interactions (Harris et al., 2020).

Tree pathosystems, such as those involving *Diplodia* spp. and other Botryosphaeriaceae, represent a large class of emerging diseases caused by opportunistic fungi that mostly 'sit-and-wait' as asymptomatic endophytes, becoming highly destructive necrotrophs only under certain host and environmental conditions (Herre et al., 2007; Slippers and Wingfield, 2007), such as low water availability, that predispose the tree to infection (Blodgett et al., 1997a,b). However, the molecular and metabolic mechanisms underlying stress-induced tree susceptibility to pathogens remain poorly understood. This inhibits predictions of how tree pathosystems will behave and evolve under projected climate change scenarios. System-level studies of the main players will address this deficiency (Bostock et al., 2014). Our work to date using the Austrian pine (*Pinus nigra*) – *D. sapinea* pathosystem has addressed basic mechanisms underlying host susceptibility under normal growth (Blodgett and Bonello, 2003; Luchi et al., 2005; Wang et al., 2006; Eyles et al., 2007; Barto et al., 2008; Wallis et al., 2008, 2011; Sherwood and Bonello, 2013, 2016) as well as under drought conditions. Under relatively severe drought, we have observed alterations in (1) levels of some free phenolics, lignin, and terpenoids; (2) Pro metabolism; (3) ROS homeostasis; and (4) possible alteration in programmed cell death (PCD), and fungal capacity to neutralize/take advantage of host responses (Sherwood et al., 2015).

Our aim in this study was to investigate how climate change affects the interactions between host and opportunistic pathogens like *Diplodia* spp. To do so, we subjected 3-year-old Austrian pine saplings to simulated climate change conditions of combined reduced water availability and elevated temperatures. After a period of conditioning, we inoculated the saplings and monitored infection processes using two closely related species of contrasting aggressiveness: *D. sapinea* (aggressive) and *D. scrobiculata* (non-aggressive) (Blodgett and Bonello, 2003; De Wet et al., 2003). To gain insight into system-level processes, we conducted transcriptomic analyses of simultaneous host and pathogen responses. We hypothesized that any shifts in aggressiveness (or, conversely, host susceptibility) due to climate change conditions would be more evident with *D. scrobiculata* and be explained by differential dual (host and pathogen) gene expression in the preliminary stages of infection.

MATERIALS AND METHODS

Plant Material

Open pollinated, 3-year-old potted Austrian pine saplings were received from Willoway Nurseries (Madison, OH, United States). Trees were maintained in an ornamental nursery yard in the Dept. of Horticulture and Crop Sciences at The Ohio State University (Columbus, OH, United States). After repotting trees into a potting mix consisting of equal parts of Com-Til compost (provided by Department of Public Utilities, city of Columbus, OH, United States), pine bark, and organic matter (the latter primarily comprised of composted yard waste) trees were transferred to the greenhouse for several months of growth.

Growth Chamber Conditions

Three weeks before inoculation, trees were transferred to two growth chambers for acclimation. We imposed the following conditions (more details in **Supplementary Information SI1**):

Control treatment (CT): daily minimum of 15°C and maximum of 28°C (corresponding to a 16/8 h light/dark cycle), and RH of 60% throughout, to generate a VPD of 0.7 and 1.5 kPa[1] during dark and light, respectively.

CC treatment (CCT): daily minimum of 20°C and maximum of 33°C (corresponding to a 16/8 h light/dark cycle), and RH of 60% throughout, to generate a VPD of 0.9 and 2.0 kPa during dark and light, respectively. Pre-dawn needle water potentials were measured with a Scholander pressure bomb (PMS Instrument Co., Corvallis, OR, United States).

Inoculation Treatments

Our experimental design was constrained by logistical limitations imposed by the availability of growth chambers: one for the CT and one for the CCT. To account for variation between growth compartments (Potvin, 2000), we used a split-plot design with combined heat/drought treatment (the CCT) as the main plot factor (represented by individual growth chambers) and inoculation state (i.e., mock-inoculated and plants inoculated with *D. sapinea* or *D. scrobiculata*) and sampling time (i.e., 12 and 72 h, and 3 weeks post-inoculation) as the subplot factors (Potvin, 2000). Each inoculation treatment was replicated six times, for a total of 18 trees in each chamber.

On February 17, 2017, trees were inoculated with *D. sapinea* or *D. scrobiculata*, or mock inoculated. Isolates of *D. sapinea* (Sherwood and Bonello, 2013) and *D. scrobiculata* (Santamaria et al., 2011) were obtained from Dr. Glenn Stanosz of University of Wisconsin Madison and grown and maintained on potato dextrose agar (PDA) in the dark at room temperature. Each treated shoot was lightly wounded by removing a small (<5 mm × 5 mm) area of epidermis, using a razor blade, 3–4 cm

[1] http://cronklab.wikidot.com/calculation-of-vapour-pressure-deficit

distal to the transition point between previous and current year growth. Inoculum (or just PDA growth medium in the case of mocks) was placed on the wound, mycelium side down, and the inoculation court was then wrapped with parafilm. Each tree was randomly assigned to a single inoculation treatment (mock, *D. sapinea* or *D. scrobiculata*) and randomly treated on six different branches (two branches per time point). The whole inoculation process was conducted over the course of 5 h. No uninoculated controls were used due to growth chamber space availability imposing limitations on numbers of usable plants.

Shoots were sampled at 12, 72 h (3 days), and 3 weeks for transcriptomics and dissected at 3 weeks for determination of relative susceptibility (phenotype) based on lesion lengths. All mock inoculations resulted in no lesions and were excluded from determination of relative susceptibility. Lesions from *D. sapinea* and *D. scrobiculata*-infected branches on each tree were averaged and the means used as a single data point for that tree. Differences in lesion length between *D. sapinea* and *D. scrobiculata* were analyzed separately for CT and CCT trees using two-tailed *t*-tests assuming unequal variances, as the number of available biological replicates was $n = 3–6$.

We did not have the resources to conduct RNA-seq analysis at all time points, so we decided to analyze host and fungal responses at 72 h, which we deemed the best compromise to uncover significant genes in the interactions. Based on all our work for the past 18 years on this system, we did not expect any detectable systemic effects of multiple, concurrent inoculations on different shoots of the same tree over the local host responses expressed in each shoot.

Tissue Sampling

At sampling time, shoots were removed with pruners, placed individually into paper coin envelopes, and immediately flash frozen in liquid N before transfer to −80°C until processing. Subsequently, tissues were harvested to contain either the whole lesion on CT saplings, or the margin of the much longer lesions on CCT saplings, by collecting shavings obtained with a liquid N-chilled razor blade and liquid N-chilled tweezers. Shavings were first dropped into a 50 ml Falcon tube containing liquid N, and then transferred to pre-weighed 2-ml screw-capped Eppendorf tubes, which were then dropped into liquid N. The tubes were transferred to cardboard freezer boxes and stored at −80°C.

RNA Extraction and Gene Expression Analysis

Tissue collected 72 h post-inoculation was ground in liquid nitrogen using a mortar and pestle that were pre-chilled in liquid N. Ground tissue was returned to the sampling tube and weight determined before storage at −80°C. RNA extraction was carried out following a standard protocol (Chang et al., 1993) modified for pine samples (500 ul extraction buffer preheated at 65°C, sample in buffer incubated at 65°C for an hour), from approximately three biological replicates of each treatment combination. RNA extracts were then treated with DNaseI, amplification grade per the manufacturer's instructions (Invitrogen, Thermo Fisher Scientific, Waltham, MA, United States) and cleaned-up with the RNeasy Plant Mini Kit per manufacturer's instructions (Qiagen, Germantown, MD, United States). Samples were quantified spectrophotometrically using a NanoDrop (Thermo Fisher Scientific, Wilmington, DE, United States) and quality and concentration were assessed using TapeStation (Agilent Technologies, Inc., Santa Clara, CA, United States). Samples with 260/280 nm and 260/230 nm ratios between 1.8–2.2 and 1.6–2.2, respectively, were considered of sufficient purity. RNA library preparation for dual transcriptome analyses of host and pathogen was carried out and paired-end sequences were generated *via* Illumina NextSeq500 platform at the Molecular and Cellular Imaging Center, The Ohio State University, Wooster, OH, United States.

Sequence Quality Control, Assembly, and Annotation

The workflow used here is shown in **Supplementary Figure 2** (**Supplementary Information SI1**). Briefly, all samples were multiplexed and sequenced across four lanes. To exclude lane biases, sequenced reads were mapped to the *Pinus tecunumanii* transcriptome (Visser et al., 2018) using kallisto v0.44.0 (Bray et al., 2016) and expression data were clustered. Subsequently, reads from all lanes were concatenated for each sample. Concatenated reads were trimmed for adaptors and low-quality bases with Trimmomatic v0.36 (Bolger et al., 2014) and those with a trimmed length >40 were retained. Concatenated and filtered read quality was assessed using FastQC[2]. To generate a *P. nigra* reference transcriptome, a series of preliminary transcriptomes was assembled with transABYSS v2.0.1 (Robertson et al., 2010), using trimmed read data with a *k*-mer range of 21 to 51 with a step of 2 and 55 to 75 with a step of 4, and Trinity v2.4.0 (Grabherr et al., 2011), with a *k*-mer range of 21 to 31 with a step of 2 using trimmed data as well as *in silico* normalized trimmed reads both *de novo* and genome guided against the *P. taeda* v2.01 genome assembly[3]. The preliminary assemblies were combined, and the resulting superset of transcripts was run through the Evidential genes pipeline (Gilbert, 2016) to reduce redundancy and select for optimally assembled transcripts, producing a set of putative host unigenes.

As an unannotated *D. sapinea* reference genome was available, pathogen unigenes were predicted using AUGUSTUS v3.3.3 (Stanke et al., 2008) on the *Diplodia sapinea* genome (Van Der Nest et al., 2014) using the *Aspergillus fumigatus* training annotation as well as *Diplodia corticola* cDNA (ENA accession PRJNA325745) to improve the prediction. Both pine and fungal unigenes were annotated using EnTAP v0.8.2 (Hart et al., 2020) with GeneMarkS-T v5.1 (Tang et al., 2015), diamond v0.8.31 (Buchfink et al., 2014) and eggnog v0.12.7 (Huerta-Cepas et al., 2016). Annotation parameters used were minimum query coverage = 80, minimum target coverage = 60, and minimum e-value = $1.0e^{-05}$. BLASTp similarity search alignments were performed against the RefSeq complete protein (release 87), UniProt/SwissProt-KB (2018-04) and NCBI non-redundant (nr,

[2]http://www.bioinformatics.babraham.ac.uk/projects/fastqc/

[3]https://treegenesdb.org/

2018-04) databases for both species, as well as the TAIR10 proteome for pine. For the host, the final reference unigenes were produced by removing sequences with best BLASTp hits from the following taxa as contaminants: Fungi, Bacteria, Insecta, Opisthokonta, Archaea, Viruses and Alveolata. The pine and *Diplodia* proteomes were further annotated using GhostKOALA (Kanehisa et al., 2016) to add KEGG orthology (KO) numbers and Mercator (Lohse et al., 2014) was used to annotate the Austrian pine proteome for analysis with MapMan (Thimm et al., 2004).

Analysis of Differentially Expressed Genes

Read Mapping and Expression Quantification

Host (from the final reference transcriptome assembly) and pathogen (predicted from the *D. sapinea* reference genome) unigenes were concatenated to produce a combined reference transcriptome. Kallisto v0.44.0 (Bray et al., 2016) was used to map the concatenated sequenced reads and quantify expression against the combined reference for each sample. Kallisto output was imported into R v4.0.4 (R Core Team, 2021) using tximport v1.22.0 (Soneson et al., 2015) to separate host and pathogen mapped read sets and perform expression analysis. Transcripts that were only represented in mock samples were removed and only those transcripts, which had at least 20 reads in 3 or more samples in each dataset, were retained.

For the Host

Host expression was analyzed using DESeq2 v1.34.0 (Love et al., 2014). Filtered count data were read into a differential expression (DE) object and library sizes were estimated by treatment type. A Poisson distance matrix was generated for the normalized host reads to determine possible clustering of samples by treatment type. A multi-dimensional scaling (MDS) plot was generated to investigate possible correlation by treatment or condition. Analyses of differentially expressed genes (DEGs) were then performed for the following pairwise comparisons of interest: (1) host responses to *D. sapinea* vs. mock inoculation under CT, (2) host responses to *D. scrobiculata* vs. mock inoculation under CT, (3) dual responses of host and pathogen following *D. sapinea* attack vs. *D. scrobiculata* attack under CT, (4) dual responses of host and pathogen following *D. scrobiculata* attack under CCT vs. CT (**Figure 1**).

For the Pathogen

Both DESeq2 v1.34.0 (Love et al., 2014) and edgeR v3.36.0 (Robinson et al., 2010) were used to identify differentially expressed genes for the pathogen comparisons. Filtered counts were read into a DE object and effective library sizes were estimated for each treatment type. An MDS plot was generated to visualize the profile differences between different treatment types (climate conditions and inoculation type) and a mean-variance plot was generated to determine the overall fitness of the model.

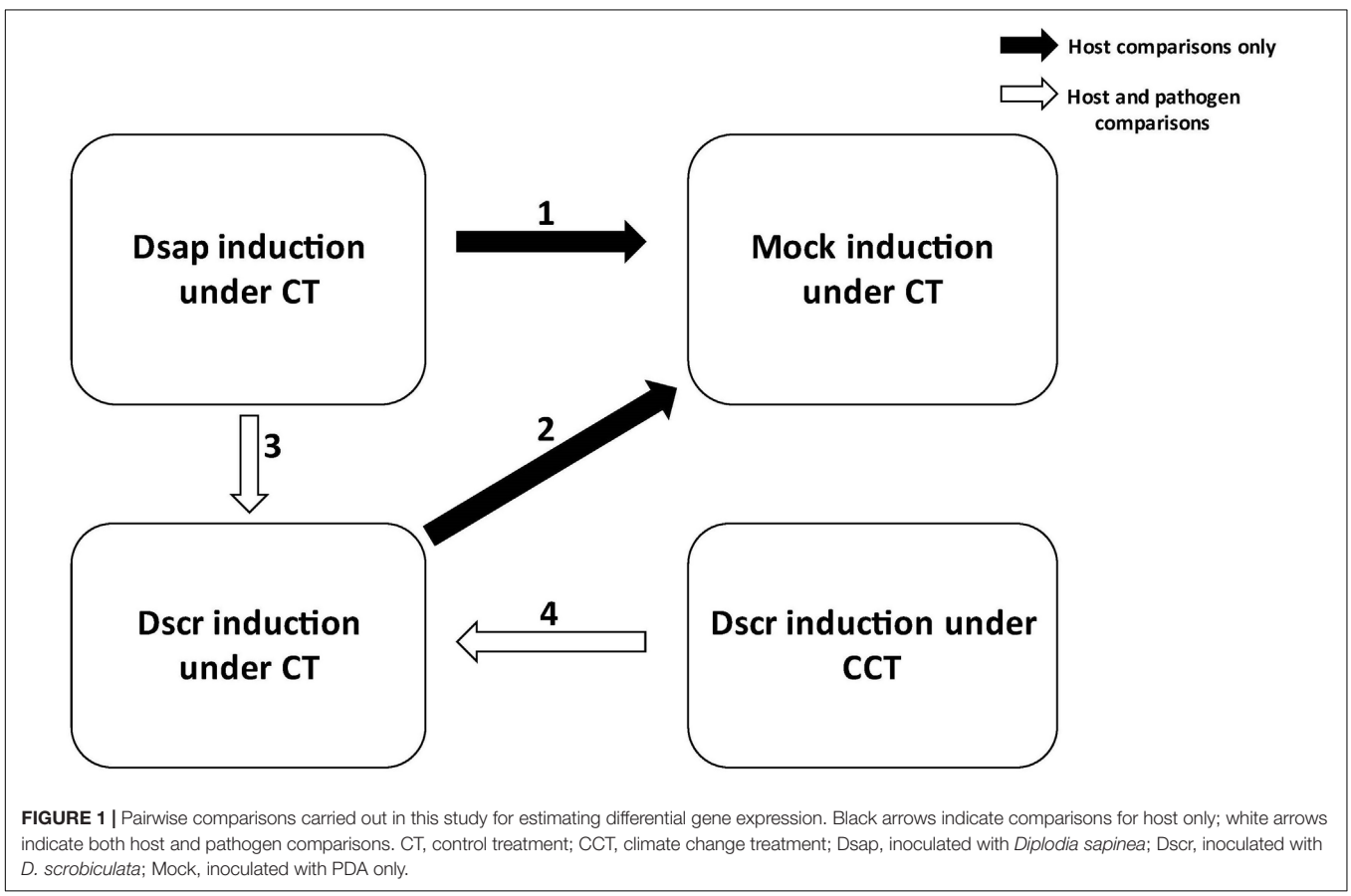

FIGURE 1 | Pairwise comparisons carried out in this study for estimating differential gene expression. Black arrows indicate comparisons for host only; white arrows indicate both host and pathogen comparisons. CT, control treatment; CCT, climate change treatment; Dsap, inoculated with *Diplodia sapinea*; Dscr, inoculated with *D. scrobiculata*; Mock, inoculated with PDA only.

Pairwise comparisons for DEGs were established as follows: (3) *D. sapinea* vs. *D. scrobiculata* during infection of pines under CT, (4) *D. scrobiculata* during infection of CCT pines vs. CT pines (**Figure 1**).

To perform GO functional enrichment analysis of DEGs we used a false discovery rate (FDR) $p < 0.05$ and a threshold of $\log_2$ fold change ratio of ± 0.5 ($\sim 1\times$ fold change in expression). These filtered DEGs were sorted by EGGNOG annotations and KEGG pathways reconstructed to visualize what genes were affected in global metabolic pathways. However, to investigate biological relevance of the most significant and highly expressed genes for a given comparison we applied a more stringent threshold of $\log_2$ fold change ratio of ± 2.3 ($\sim 5\times$ fold change in expression).

RESULTS

Abiotic Stress

On February 14, March 1, March 3, and March 8, 2017, needle water potentials averaged −0.1 and −1.3 kPa, −0.3 and −2.0 kPa, −0.3 and −2.0 kPa, and −0.1 and −2.4 kPa, ($N = 6$ for each mean), for the pines in the CT and CCT chambers, respectively. Differences in water potential were reflected in needle appearance (**Figure 2A**).

Diplodia scrobiculata Is as Aggressive as *D. sapinea* Under Climate Change Conditions

Three weeks post-inoculation, all pines in the CT chamber were alive and had developed lesions in all pathogen inoculated pines. On the other hand, trees in the CCT chamber appeared close to dying with at least half (greater than 50%) of them having at least 1/3 of the crown still green but chlorotic (**Figure 2A**). In all cases, lesions on CCT saplings were significantly longer than those on CT plants (**Figure 2B**). Notably, lesions produced by *D. scrobiculata* in the CCT chamber (Figure 1 in **Supplementary Information SI1**) were as long as those produced by *D. sapinea*, i.e., *D. scrobiculata* became as aggressive as *D. sapinea* or, conversely, the host became equally susceptible to both pathogens (**Figure 2B**).

Metatranscriptome Assemblies

FastQC was used to obtain an overview of general read quality (Bray et al., 2016). Trimmed and filtered reads generated using Trimmomatic (Bolger et al., 2014) retained 539,379,336 of the original 857,867,066 reads (∼63%), ranging between 40 and 150 nucleotides in length. Preliminary k-mer assemblies were produced *de novo* ($n = 33$) and genome guided against the *P. taeda* v2.01 genome ($n = 6$), followed by concatenation to produce a superset containing 5,246,838 transcripts (**Table 1**). This superset was further reduced, using the Evidential genes pipeline, to 315,357 transcripts for 30,632 Austrian pine unigenes, while 13,863 *D. sapinea* unigenes were extracted from the *D. sapinea* genome using the Augustus gene prediction pipeline (**Table 1**).

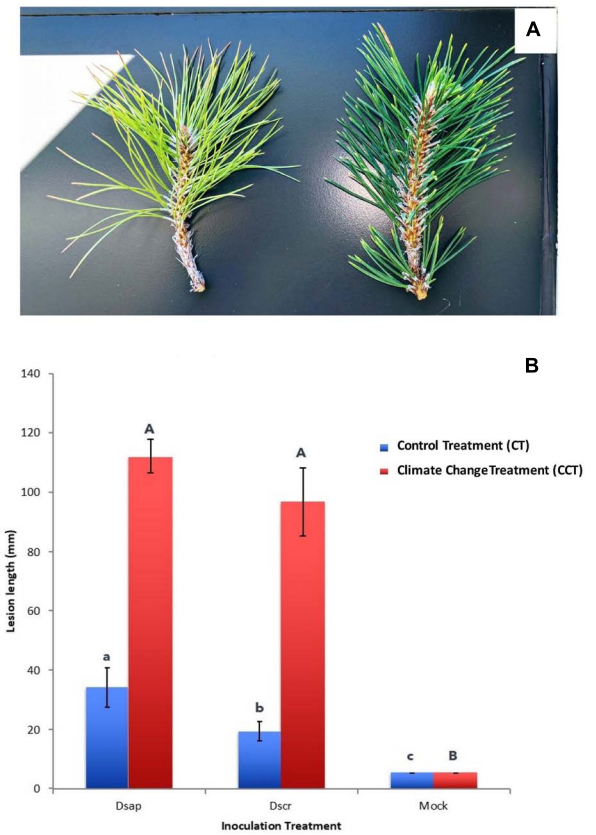

FIGURE 2 | (A) Chlorotic and partly desiccated appearance of pine needles subjected to climate change treatment (left) vs. deep green and turgid needles in the control treatment (right). **(B)** Lesion lengths (mm) measured 3 weeks post inoculation. *X*-axis: Dsap, inoculation with *D. sapinea*; Dscr, inoculation with *D. scrobiculata*. Blue bars represent the control climate treatment (CT), red bars the climate change treatment (CCT). Error bars: standard error of the mean. Different letters represent significant differences within climate treatment (lower case letters for CT, upper case letters for CCT). CCT: $t_6 = 3.078$, $p = 0.015$; CT: $t_8 = 1.189$, $p = 0.279$.

Functional Annotation of Host and Pathogen Transcriptome

The Austrian pine and *D. sapinea* unigenes were annotated using EnTAP (Hart et al., 2020). Non-pine sequences as well as unannotated sequences were discarded (**Table 1**). Annotation resulted in *P. nigra* v1.0 assembly (Pini_v1.0) containing 19,882 unigenes (8,196 with KEGG Orthology – KO – numbers) and 10,612 *D. sapinea* unigenes (4,021 with KO numbers). [All raw sequence reads are publicly available in NCBI, and accession information is provided in **Supplementary Information SI4**.]

Differentially Expressed Genes Analyses

Mapping and filtering produced a subset of 17,443 expressed genes for Austrian pine and 2,303 expressed genes for *Diplodia* spp. The similarity of the host reads was assessed using a Poisson matrix (Figure 3, **Supplementary Information SI1**); identical treatment types generally showed the closest relationships. Library size ranges were 15–20 million and 0.004–0.3 million

reads per sample for the host and pathogen datasets, respectively (**Figure 3**). The mean-variance plot indicated that the Poisson model was likely inappropriate for the fungi due to higher-than-expected dispersion over the mean (Figure 4, **Supplementary Information SI1**). Therefore, we generated respective MDS plots for host RNA-seq data and filtered pathogen RNA-seq data, to evaluate clustering based on treatment/species types (Figure 5, **Supplementary Information SI1**).

A series of comparisons enabled us to dissect the changes in gene expression patterns associated with key metabolic responses in the host and pathogens under the two climate conditions (Figure 1, **Supplementary Information SI2**). Specifically, comparisons 1 and 2 in **Figure 1** focus on host gene expression resulting from pathogen inoculation under CT, comparison 3 focuses on dual responses of host and pathogen following *D. sapinea* vs. *D. scrobiculata* inoculation under CT, while comparison 4 centers on dual responses of host and pathogen following *D. scrobiculata* inoculation under CCT vs. CT. The volcano plots in **Figure 4** provide an overview of the numbers of highly significant DEGs for the four comparisons, which were then investigated by their EGGNOG annotations (Huerta-Cepas et al., 2016), followed by mapping to KEGG (Kanehisa and Sato, 2020) pathways and biological processes through Gene Ontology (GO).

TABLE 1 | Summary of assembly statistics.

Parameters[1]	Concatenated assemblies	Evigene (*P. nigra*)	Pini_v1.0[2]	Non-pine	Unannotated	Augustus Evigene (*D. sapinea*)
N	5,246,838	30,632	19,882	3,677	7,073	13,863
N50	1,210	1,762	2,022	801	718	5,670
Smallest	350	351	351	351	351	297
Largest	10,917	10,561	10,561	6,147	5,321	22,668
N bases	4,870,308,207	40,263,498	32,680,629	2,704,062	4,878,807	61,522,400
Mean length	948.91	1314.43	1643.73	735.4	689.78	4437.00
N > 1 k	1,406,126	15,207	13,633	641	933	9,347
N > 10 k	14	2	2	0	0	3
N with ORF	2,254,456	23,281	18,122	2,458	2,701	8,381
Mean ORF%	63.21	78.25	78.91	82.52	71.45	60.46

[1]*N = total number of contigs; N50 = statistically weighted average such that 50% of the entire assembly is formed by contigs of equal size or larger than this value; N with ORF = number of contigs with Open Reading Frames.*
[2]*Pini_v1.0: Pinus nigra v1.0 transcriptome assembly.*

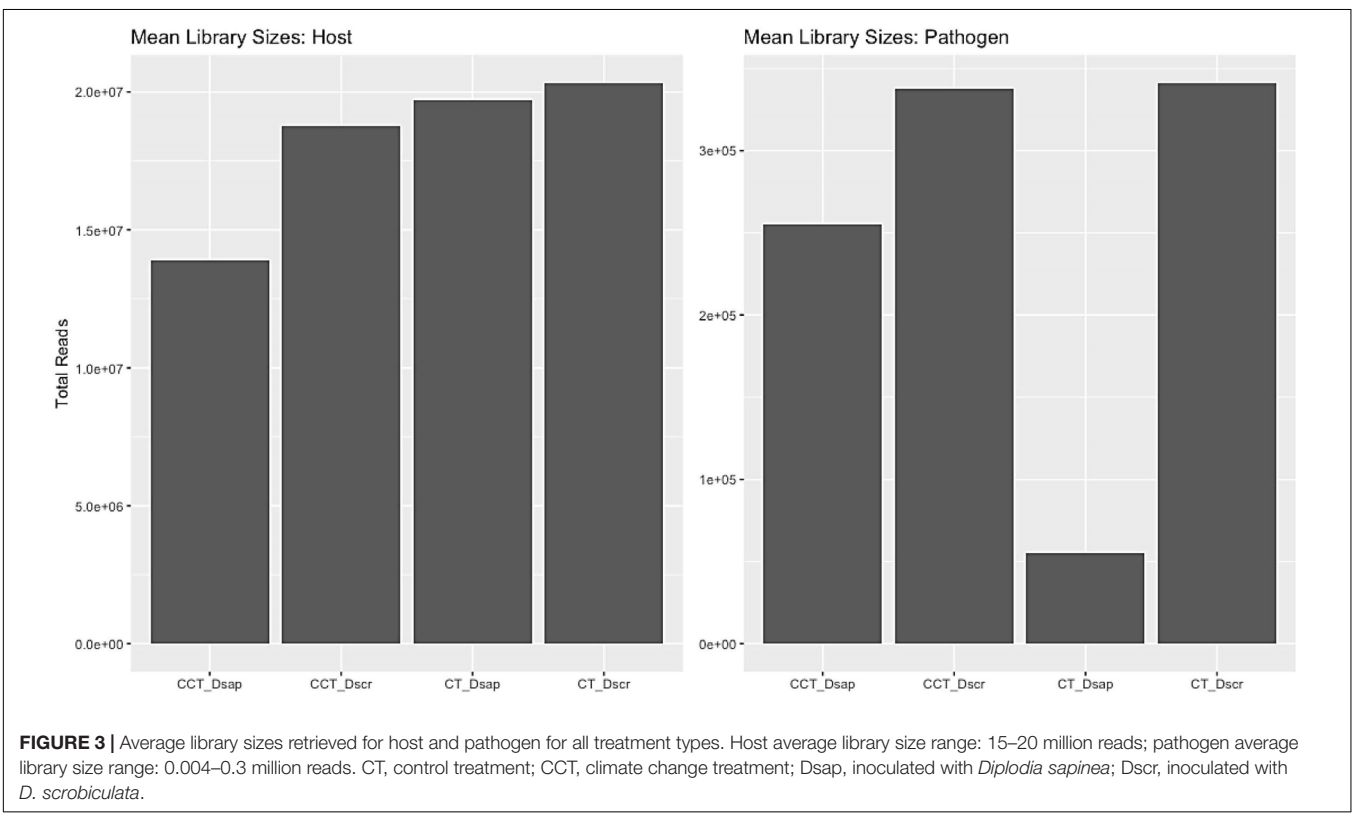

FIGURE 3 | Average library sizes retrieved for host and pathogen for all treatment types. Host average library size range: 15–20 million reads; pathogen average library size range: 0.004–0.3 million reads. CT, control treatment; CCT, climate change treatment; Dsap, inoculated with *Diplodia sapinea*; Dscr, inoculated with *D. scrobiculata*.

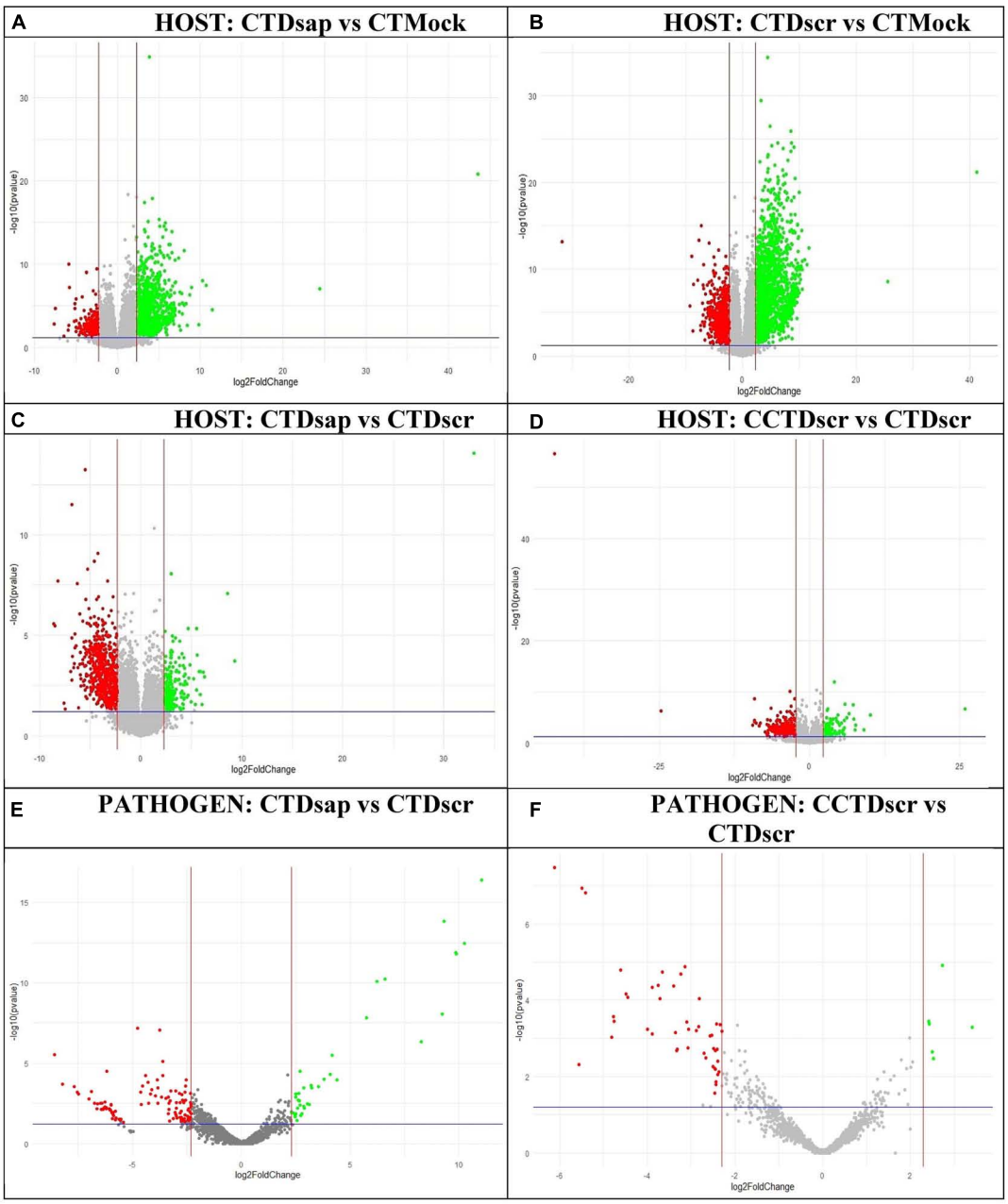

FIGURE 4 | Volcano plots of DEGs for individual host and pathogen comparisons. Upregulated and downregulated genes marked in green and red, respectively, based on actual fold-change >5 (upregulated) or <–5 (downregulated) [i.e., $\log_2$ (fold-change) >2.3 (up) or <–2.3 (down)] and $p < 0.05$. Labels: **(A)** host comparison 1, **(B)** host comparison 2, **(C)** host comparison 3, **(D)** host comparison 4, **(E)** pathogen comparison 3, **(F)** pathogen comparison 4 (**Figure 1**). CT, control treatment; CCT, climate change treatment; Dsap, *Diplodia sapinea*; Dscr, *D. scrobiculata*; Mock, mock inoculated.

We also looked at gene expression overlaps between different host and pathogen comparisons, respectively. We found 2,526 (31%) overlapping DEGs between comparisons 1 and 2, while 405 (5%) DEGs were exclusive to CTDsap vs. CTMock and 2,910 (35%) DEGs were exclusive to CTDscr vs. CTMock (**Figure 4**). At the same time, 437 (5%) DEGs overlapped between comparisons 2 and 4, with 1,099 (13%) DEGs exclusive to CCTDscr vs. CTDscr (**Figure 5**). Similarly for pathogen comparisons, we found 12 (6%) DEGs overlapping between comparisons 3 and 4. Comparison 3 produced 40 (21%) DEGs and 135 (72%) DEGs were mapped to CCTDscr vs. CTDscr, respectively (**Figure 5**). The complete sets of DEGs and their corresponding GO: Biological processes, for individual comparisons of host and pathogen were tested for enrichment using the TopGO package (Alexa and Rahnenfuhrer, 2021). The classic Fisher method was selected for running the enrichment analysis based

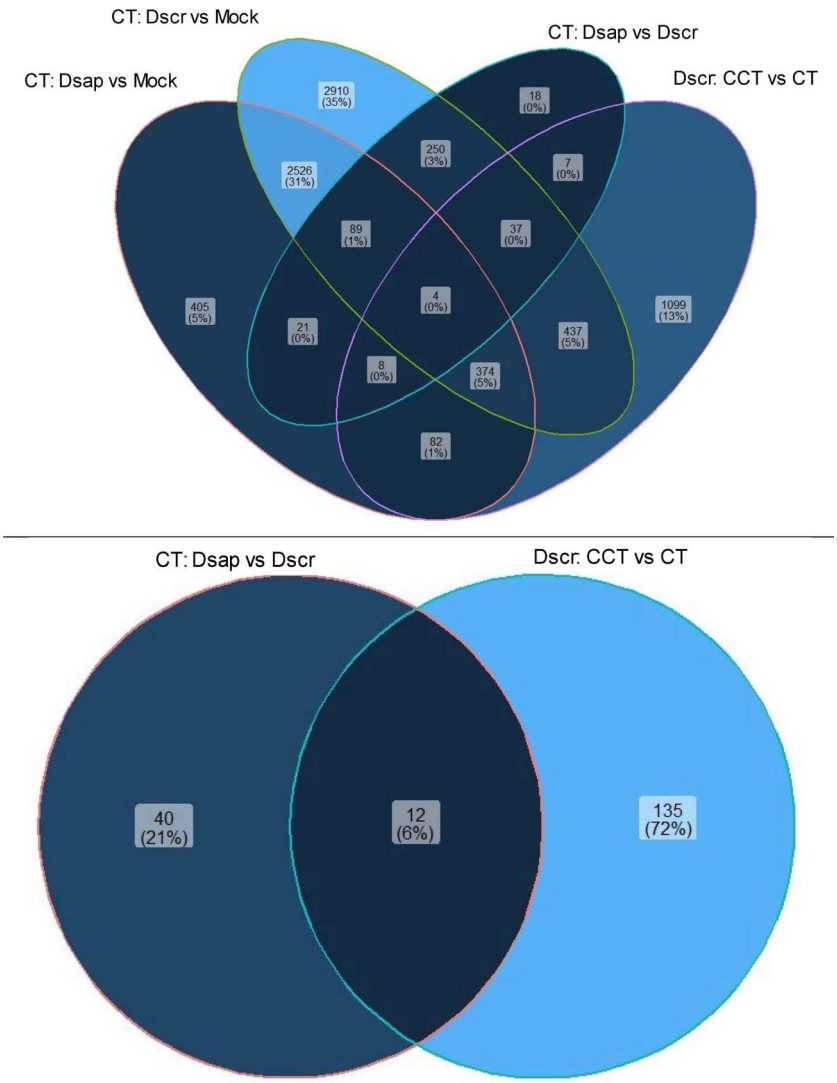

FIGURE 5 | Venn diagram showing unique and overlapping sets of DEGs for host (top) and pathogen (bottom). CT, control treatment; CCT, climate change treatment; Dsap, *Diplodia sapinea*; Dscr, *D. scrobiculata*; Mock, mock inoculated.

on quality comparisons with the elimKS method (Figure 6, **Supplementary Information SI1**). Enriched GO terms are listed in **Supplementary Information SI3**.

Host Responses

Comparison 1: *D. sapinea* Infection vs. Mock Under Control Treatment

In this comparison, a total of 3,509 genes were differentially expressed (adj. p-value < 0.05). 2,661 of these were assigned KEGG orthologs and were mapped to various general pathways, while 1,221 were annotated to various GO terms. Out of all 3,509 DEGs, 781 were annotated *via* all three platforms (i.e., EGGNOG, KEGG, and GO) and were assigned to various metabolic functions/pathways. DEGs were annotated to 32 different GO terms, including response to stimulus (646 DEGs), response to stress (381 DEGs), response to oxygen containing compounds (425 DEGs), response to endogenous stimulus (236 DEGs), response to biotic stimulus (292 DEGs), and defense response (298 DEGs), among other responses (**Figure 6A**). Our stringent filtering threshold (actual fold-change ±5) produced a list of 512 DEGs, with 308 upregulated genes and 204 downregulated genes that had KEGG and GO annotations (spreadsheet Host-comparison1 in **Supplementary Information SI2**).

Primary Metabolic Responses

Among 28 DEGs with photosynthetic GO terms, only two were assigned to both KEGG and GO (**Figure 7A**). Six different transcripts were mapped to fatty acid biosynthesis on KEGG and assigned to fatty acid or lipid metabolism GO terms (**Figure 7A**).

Defense Associated Responses

Gene ontology terms associated with defense responses, such as oxygen containing compounds (646 DEGs), defense response

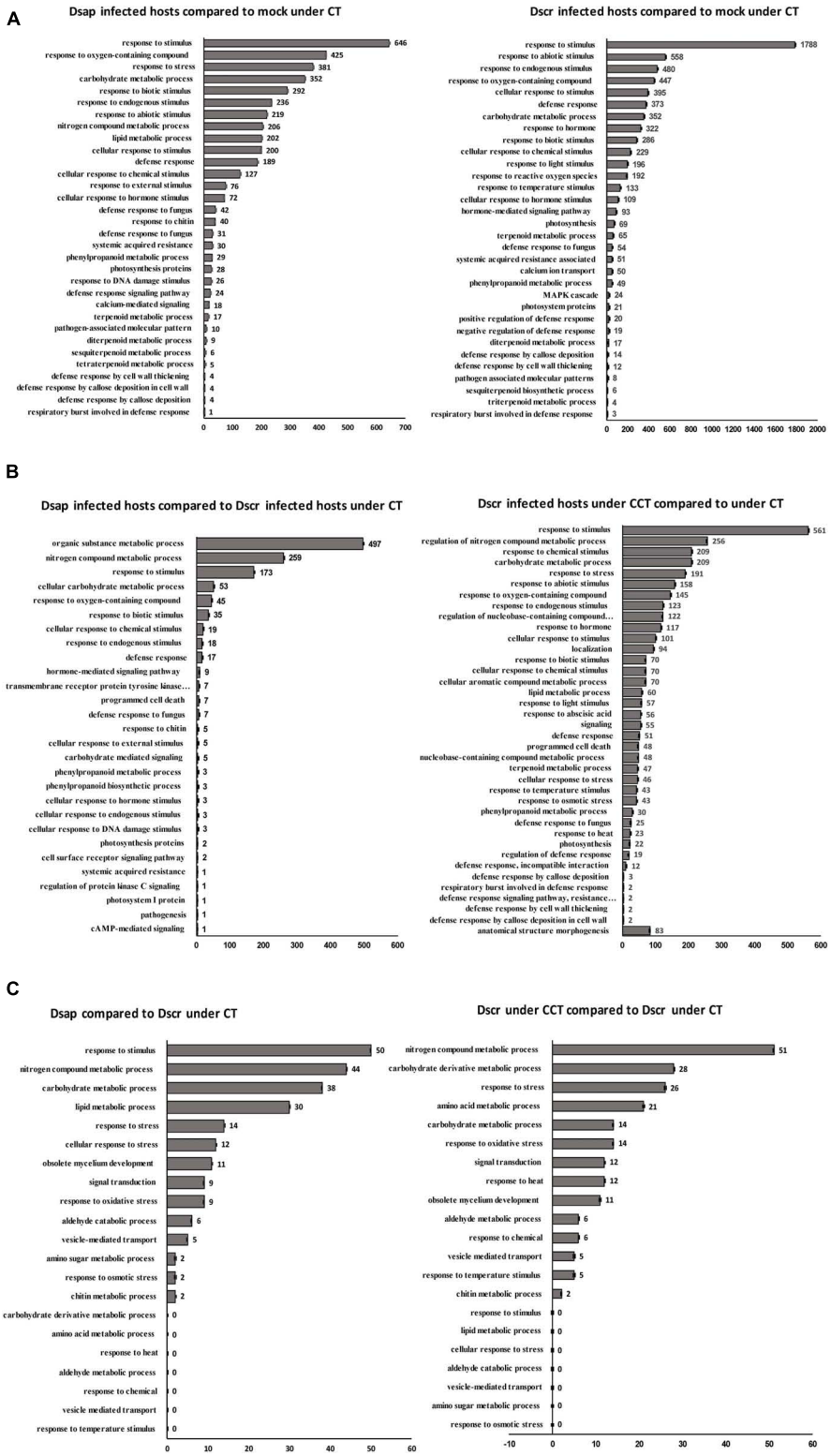

FIGURE 6 | (A) Significant host gene functions annotated using Blast2GO. *X*-axis: number of differentially expressed genes; *y*-axis: ontology associated functions. Left: comparison 1; right: comparison 2 (**Figure 1**). **(B)** Significant host gene functions annotated using Blast2GO. *X*-axis: number of differentially expressed genes; *y*-axis: ontology associated functions. Left: comparison 3; right: comparison 4 (**Figure 1**). **(C)** Significant pathogen gene functions annotated using Blast2GO. *X*-axis: number of differentially expressed genes; *y*-axis: ontology associated functions. Left: comparison 3; right: comparison 4 (**Figure 1**). CT, control treatment; CCT, climate change treatment; Dsap, *Diplodia sapinea*; Dscr, *D. scrobiculata*; Mock, mock inoculated.

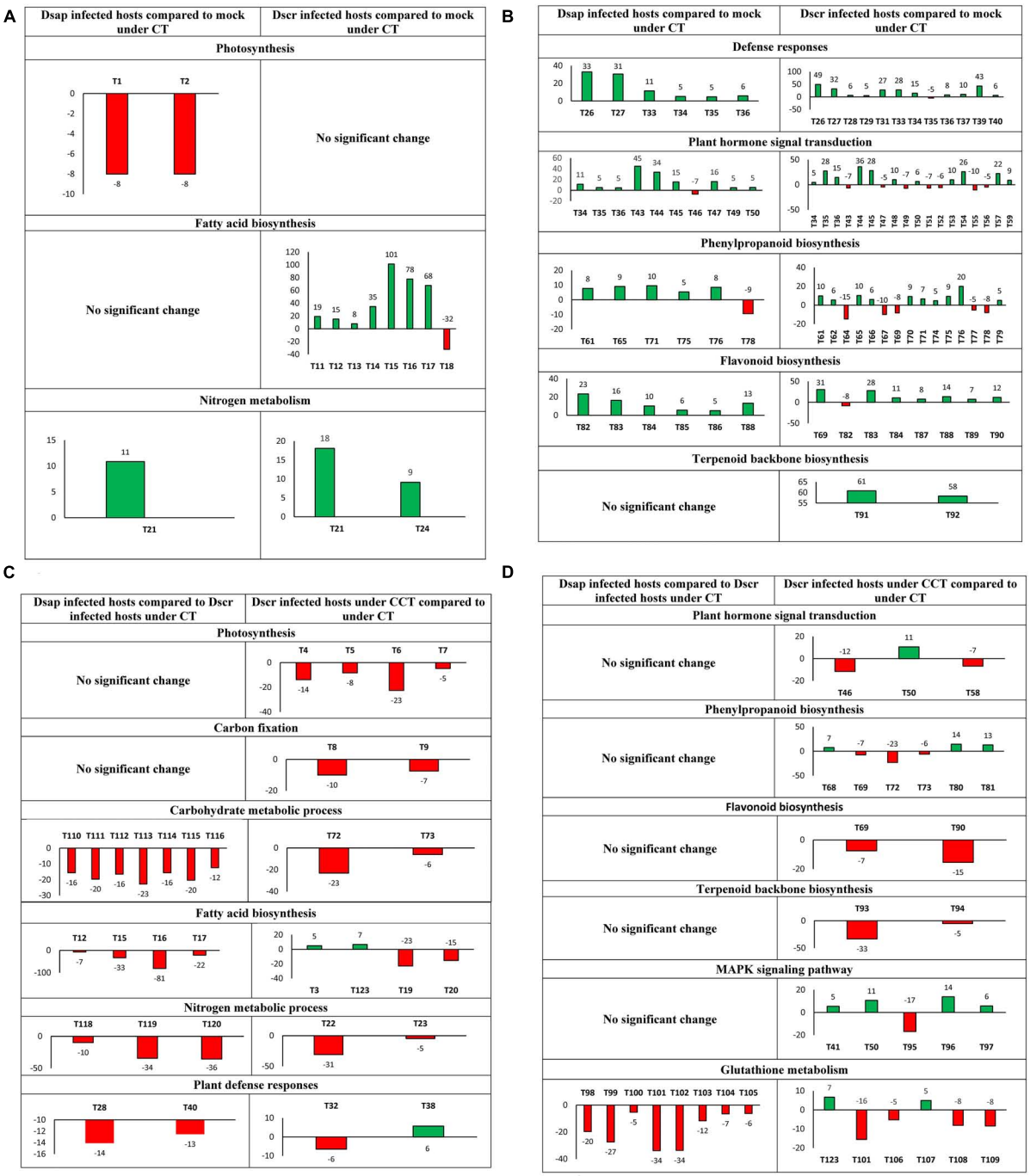

FIGURE 7 | (A) Most significant DEGs by actual fold-change (*Y*-axis) >5 (up) or <–5 (down) and $p < 0.05$, in host metabolic pathways (T = transcript): T1 – ATP synthase delta chain, T2 – photosystem II, T11–T14 – 3-oxoacyl-[acyl-carrier-protein] reductase (fabG), T15 – fatty acid synthase (FAS1), T16 – FAS2, T17–T18 – Stearoyl-[acyl-carrier-protein] 9-desaturase 7, chloroplastic (FAB2), T21 – carbonic anhydrase, T24 – Glutamate dehydrogenase A (gdhA) (Spreadsheet Host-comparison2 in **Supplementary Information SI2**). **(B)** T26–T29-calmodulin-like proteins (CML), T31-calmodulin (CALM), T33–T35- pathogenesis related 1 (PR1), T36-WRKY, T37–39-enhanced disease susceptibility (EDS1), T40-elongation factor (efTu), T43–T45-jasmonate domain protein (JAZ), T46–T47-auxin responsive protein, T49-Gibberellin Insensitive 1 (GID1), T50–T52 protein phosphatase 2C (PP2C), T53-coronatine insensitive protein (COI1), T54-age-related resistance-A (ARR-A) protein, T55-serine threonine protein kinase, T56–T57-xyloglucan endotransglycosylase (TCH4), T59-cyclin D3, T61–T62-cinnamoyl alcohol dehydrogenase (CAD), T64–T67-peroxidase, T69-caffeoyl CoA o-methyltransferase, T70–T71-beta glucosidase, T74–T77-4-coumarate CoA ligase, T78-cinnamoyl CoA reductase, T79-putative lysophospholipase, T82–T87-chalcone synthase, T88–T89-flavonoid 3′-monoxygenase, T90-anthocyanidin reductase, T91-acetyl CoA-acetyltransferase, T92-farnesyl pyrophosphate synthetase (Spreadsheet Host-comparison2 in **Supplementary Information SI2**). **(C)** T3-a/bccP, T4-ferredoxin, T5–T7-chlorophyll a-b binding protein, T8-fructose-1,6-bisphosphatase, T9-glyceraldehyde-3-phosphate dehydrogenase (GAPD), T12-3-oxoacyl-[acyl-carrier-protein] reductase (fabG), T15-fatty acid synthase (FAS1), T16-FAS2, T17-adaptor protein (fadD), T19–T20-myristoyl-acyl carrier

(Continued)

FIGURE 7 | protein thioesterase, T22, T23-carbonic anhydrase, T28, T32-CML, T38-WRKY, T40-efTu, T72, T73-beta-glucosidase, T110, T111-isocitrate dehydrogenase, T112-dihydrolipoyl dehydrogenase, T113-citrate synthase, T114-ATP-citrate synthase subunit, T115-fumarate hydratase, T116-aconitase hydratase, T118-gdhA, T119-alanine aminotransferase, T120-PyrABCN, T123-alcohol dehydrogenase. **(D)** T41-ROS burst protein, T46-auxin responsive protein, T50-PP2C, T58-TCH4, T68-peroxidase, T69-caffeoyl-CoA o-methyl transferase, T72, T73-beta glucosidase, T80, T81-reductase, T90-anthocyanidin reductase, T93, T94-geranylgeranyl pyrophosphate synthase (GGPPS), T95-Cu transporting ATPase, T96-chitinase, T97-1-aminocyclopropane-1-carboxylate synthase, T98-isocitrate dehydrogenase, T99-T106-glutathione reductase, T107-glutathione peroxidase, T108-Ribonucleotide Reductase Catalytic Subunit M1 (RRM1), T109-ribonucleotide diphosphate (RNDP) reductase, T123-alcohol dehydrogenase (Spreadsheet Host-comparison4 in **Supplementary Information SI2**). Numeric bar labels indicate actual fold-change of respective transcripts.

to fungus (73 DEGs), response to chitin (40 DEGs), cell wall thickening (4 DEGs), and callose deposition (8 DEGs) were identified (**Figure 6A**). 12 DEGs were mapped to the KEGG pathway for plant-pathogen interactions. Two calcium binding (CML – calmodulin like) proteins associated with cell morphogenesis involved in differentiation and 18 DEGs assigned to GO: calcium-mediated signaling were identified (**Figure 6A**). Three transcripts were annotated to pathogenesis-related protein 1 (PR1) on KEGG and EGGNOG and assigned GO: defense response, along with a WRKY transcription factor and another transcript annotated to disease resistance (RPS2) (**Figure 7B**) (Spreadsheet Host-comparison1 in **Supplementary Information SI2**).

Phytohormone Responses

A total of 15 transcripts were mapped to the plant hormone transduction pathway on KEGG, including significant responses for jasmonate ZIM domain-containing (JAZ) proteins, gibberellin receptor (GID1), and auxin responsive GH3 gene (**Figure 7B**).

Specialized Metabolic Responses

The biosynthesis and metabolism of terpenoids were represented in various GO terms such as terpenoid metabolic process (17 DEGs), tetraterpenoid biosynthetic process (5 DEGs), sesquiterpenoid metabolic process (6 DEGs), and diterpenoid metabolic process (9 DEGs) (**Figure 6A**). We found 7 DEGs mapped to terpenoid backbone biosynthesis on KEGG, 29 DEGs associated with GO: phenylpropanoid metabolic process (**Figure 6A**), and 11 DEGs mapped to phenylpropanoid biosynthesis pathway on KEGG. These included beta-glucosidase, cinnamyl alcohol dehydrogenase, peroxidase, 4-coumarate-CoA ligase, cinnamoyl-CoA reductase, chalcone synthase, and flavonoid 3′-monooxygenase (**Figure 7B**) (Spreadsheet Host-comparison1 in **Supplementary Information SI2**).

The enrichment analysis produced a list of 10 most significant GO terms with respect to both classic Fisher and Kolmogorov-Smirnov elimination tests (Spreadsheet Host-comparison1 in **Supplementary Information SI3**). The most enriched terms included obsolete oxidation-reduction process, carbohydrate metabolic process, cellular amino acid metabolic process, fatty acid metabolic process, and response to chitin (Figure 7 in **Supplementary Figures 7–10**).

Comparison 2: *D. scrobiculata* Infection vs. Mock Under Control Treatment

In this comparison, a total of 6,628 genes were differentially expressed. 2,935 of these were assigned KEGG orthologs and were mapped to various general pathways, while 2,384 were annotated to various GO terms. Out of all 6,628 DEGs, 1,576 were filtered *via* annotation on all three platforms and mapped to 32 different GO terms including response to stimulus (1,788 DEGs), response to biotic stimulus (286 DEGs), defense response (373 DEGs), carbohydrate metabolic process (352 DEGs), among others (**Figure 6A**). Our 5-fold threshold produced a filtered list of 2,434 DEGs, with 1,537 upregulated genes and 897 downregulated genes (Spreadsheet Host-comparison2 in **Supplementary Information SI2**).

Primary Metabolic Responses

A total of 90 DEGs were represented by photosynthesis through GO annotation (**Figure 6A**), and further identified on KEGG, including ATP synthase (ATPF1D), photosystem II (psb27) protein, and a chlorophyll a-b binding (LHCB7) protein (Spreadsheet Host-comparison2 in **Supplementary Information SI2**) (**Figure 7A**). 21 DEGs were mapped to fatty acid biosynthesis process on KEGG, including fatty acid synthase genes, short-chain type dehydrogenase (fabG), and acyl-CoA-synthetase (Spreadsheet Host-comparison2 in **Supplementary Information SI2**). Under nitrogen metabolism, carbonic anhydrase (CAH) protein and another glutamate dehydrogenase (gdhA) transcript were higher in *D. scrobiculata* infected pines as compared to mock infected pines (**Figure 7A**).

Defense Associated Responses

A total of 495 DEGs were mapped to various GO terms associated with defense responses by the host, including defense response (373 DEGs), defense response to fungus (54 DEGs), defense response by cell wall thickening (12 DEGs), and callose deposition (14 DEGs) (**Figure 6A**). 25 DEGs were assigned to the plant-pathogen interaction pathway (**Figure 6A**), including calcium binding (CML) protein, calmodulin (CALM) protein, elongation factor Tu, heat shock (HSP90A) protein, and WRKY proteins (**Figure 7B**).

Phytohormone and Associated Responses

A total of 415 DEGs were assigned to hormone related GO terms, including GO: response to hormone (322 DEGs) and hormone mediated signaling pathway (93 DEGs) and 43 DEGs were mapped to the plant hormone signal transduction pathway (**Figure 6A**). Most significant DEGs included JAZ proteins, auxin responsive GH3 gene, xyloglucan endotransglucosylase hydrolase (TCH4) protein, gibberellin receptor (GID1) protein, coronatine-insensitive (COI-1) protein, ubiquitin dependent protein catabolic process, two-component response regulator

(ARR-A) protein, protein phosphatase 2C, cyclin D3 (CYCD3) protein (**Figure 7B**).

Specialized Metabolic Responses

A total of 32 DEGs were mapped to terpenoid backbone biosynthesis pathway on KEGG (**Figure 6A**). Most significant DEGs included, acetyl-CoA acetyltransferase and farnesyl pyrophosphate synthetase (FPPS) protein (**Figure 7B**). We also found 22 transcripts mapped to the phenylpropanoid biosynthesis pathway on KEGG, including cinnamyl alcohol dehydrogenase, peroxidase, reductase, and 4-coumarate-CoA ligase (4CL) (**Figure 7B**). Further, there were 11 transcripts mapped to flavonoid biosynthesis pathway on KEGG, including chalcone synthase (CHS), flavonoid 3′-monooxygenase (CYP75B1) (**Figure 7B**).

The enrichment analysis produced a list of 19 most significant GO terms with respect to both classic Fisher and Kolmogorov-Smirnov elimination tests (Spreadsheet Host-comparison2 in **Supplementary Information SI3**). The most enriched terms included ribosome biogenesis, rRNA metabolic process, response to chitin, and cytosolic transport (Figure 8 in **Supplementary Figures 7–10**).

Comparison 3: Effects of *D. sapinea* vs. *D. scrobiculata* Infections Under Control Treatment

In this comparison, a total of 434 genes were differentially expressed. All 434 DEGs were assigned KEGG orthologs and were mapped to various general pathways, but only 172 were annotated to various GO terms. 130 host DEGs were annotated to different metabolic pathways on all three platforms, with higher number of annotations for pathways like response to stimulus (50 DEGs), lipid metabolic process (30 DEGs), nitrogen compound metabolic process (44 DEGs), and carbohydrate metabolic process (38 DEGs) (**Figure 6B**). Our 5-fold threshold produced a filtered list of 233 genes that were less expressed in hosts infected by *D. sapinea* relative to *D. scrobiculata* infected hosts (Spreadsheet Host-comparison3 in **Supplementary Information SI2**).

Primary Metabolic Responses

Under the citric acid cycle pathway on KEGG and assigned GO: carbohydrate metabolic process, significant DEGs were reported for isocitrate dehydrogenase genes, citrate synthase genes, dihydrolipoyl dehydrogenase, fumarate hydratase, aconitate hydratase (**Figure 7C**). Under nitrogen metabolism, significant DEGs were annotated as alanine aminotransferase and glutamate dehydrogenase (**Figure 7C**). Four transcripts mapped to fatty acid biosynthesis pathway on KEGG were also downregulated, including fatty acid synthase, acyl-CoA-synthase, and short chain dehydrogenase (**Figure 7C**).

Defense Associated Responses

Three genes mapped to the plant-pathogen interactions and MAPK signaling pathway on KEGG and assigned GO: receptor mediated endocytosis, nucleotide metabolic process, mitochondrial translation, were downregulated. Of them, calmodulin, serine-threonine protein kinase, elongation factor efTu protein were the most significant DEGs (**Figure 7D**).

Phytohormone and Associated Responses

Under plant hormone signal transduction pathway on KEGG, significant DE included xyloglucan endotransglucosylase hydrolase protein (TCH4) and assigned GO: response to external stimulus, plant-type cell wall organization (**Figure 7D**). Additionally, 9 DEGs were mapped to the glutathione metabolism pathway on KEGG and assigned GO: response to oxidative stress, glutamate metabolic process, NADP metabolic process, including glutathione S-transferase and glutathione reductase (**Figure 7D**). Others cAMP signaling pathway associated genes such as cell division control protein RAC1, RAS homolog gene family protein RHOA, and a serine threonine protein phosphatase were lower (**Figure 7D**).

The cinnamoyl alcohol dehydrogenase, mapped to phenylpropanoid and lignin biosynthesis pathways was also lower in *D. sapinea* infected hosts relative to *D. scrobiculata* infected hosts (**Figure 7D**).

The enrichment analysis produced a list of 10 most significant GO terms with respect to both classic Fisher and Kolmogorov-Smirnov elimination tests (Spreadsheet Host-comparison3 in **Supplementary Information SI3**). The most enriched terms included DNA metabolic process, DNA methylation, DNA duplex unwinding, leaf vascular tissue pattern formation, and phloem or xylem histogenesis (Figure 9 in **Supplementary Figures 7–10**).

Comparison 4: Host Response to *D. scrobiculata* Infection Under Climate Change Treatment

In this comparison, a total of 2,048 genes were differentially expressed. 732 of these were mapped to various KEGG pathways and 679 DEGs assigned to various GO terms and the most represented GO functions included response to stress (561 DEGs), response to nitrogen metabolic process (256 DEGs), carbohydrate metabolic process (209 DEGs), response to oxygen-containing compound (145 DEGs), response to abiotic stimulus (158 DEGs), and defense response (51 DEGs) (**Figure 6B**). Our 5-fold threshold produced a filtered list of 936 DEGs, with 162 upregulated genes and 674 downregulated genes (Spreadsheet Host-comparison4 in **Supplementary Information SI2**).

Primary Metabolic Responses

We found that 7 transcripts mapped to KEGG pathways associated with photosynthesis and carbon fixation, including chlorophyll A-B binding protein, ferredoxin protein, phosphoenolpyruvate carboxykinase, fructose-1,6-bisphosphatase, and glyceraldehyde-3-dehydrogenase (**Figure 7C**). We also found two beta-glucosidase genes downregulated 23-fold and 6-fold, respectively in pines infected with *D. scrobiculata* under CCT as compared to CT (**Figure 7C**). We also found 60 genes mapped to GO terms associated with lipid metabolic process, including myristoyl-acyl carrier protein thioesterase, and fatty acyl-CoA reductase (**Figure 7C**). An alcohol dehydrogenase gene assigned to GO: response to hypoxia, response to abiotic stimulus, was also upregulated (**Figure 7C**).

Defense Associated Responses

Among the key GO terms related to defense, 51 DEGs were assigned to defense response, 101 DEGs assigned to cellular

response to stimulus, 158 DEGs for response to abiotic stress, 25 DEGs for defense response to fungus, 70 DEGs for response to biotic stress (**Figure 6B**). Other important defense associated GO functions included respiratory burst involved in defense, resistance gene-related defense response signaling pathway, defense response by cell wall thickening, and defense response by callose deposition (**Figure 6B**). We further found 9 DEGs mapped to the plant-pathogen interactions pathway on KEGG. Significant DEGs included 3-ketoacyl-coa synthase, respiratory burst oxidase, calcium binding protein, and WRKY transcription factor (**Figures 7C,D**).

Phytohormone Responses

We also found 117 DEGs assigned GO: response to hormone, 56 DEGs assigned GO: response to abscisic acid (**Figure 6B**), and 9 DEGs mapped to the plant hormone signal transduction process on KEGG. Significant DEGs included auxin-responsive protein, phosphatase 2C, xyloglucan endotransglucosylase hydrolase, copper-transporting ATPase protein (**Figure 7D**). Other DEGs mapped under the host mitogen associated protein kinase (MAPK) signaling included respiratory burst oxidase, chitinase and 1-aminocyclopropane -1-carboxylate synthase (ACS6) (**Figure 7D**). Interestingly, we also found 14 DEGs mapped to the glutathione metabolism pathway, besides 145 DEGs assigned GO: response to oxygen-containing compound and 2 DEGs assigned GO: respiratory burst involved in defense (**Figure 6B**). Significant DEGs included glutathione S-transferase, and glutathione peroxidase (**Figure 7D**) (Spreadsheet Host-comparison4 in **Supplementary Information SI2**).

Specialized Metabolic Responses

We also observed 47 DEGs assigned to GO: terpenoid metabolic process (**Figure 6B**), and 7 transcripts that were mapped to the terpenoid backbone biosynthesis pathway, including geranylgeranyl pyrophosphate synthase (**Figure 7C**). 30 DEGs were assigned to phenylpropanoid metabolic process (**Figure 6B**), and 7 DEGs were mapped to the phenylpropanoid and flavonoid biosynthesis pathway on KEGG, including reductase, caffeoyl-CoA o-methyltransferase, peroxidase, and flavonoid 3′-monooxygenase (**Figure 7D**) (Spreadsheet Host-comparison4 in **Supplementary Information SI2**).

The enrichment analysis produced a list of 13 most significant GO terms with respect to both classic Fisher and Kolmogorov-Smirnov elimination tests (Spreadsheet Host-comparison4 in **Supplementary Information SI3**). The most enriched terms included cotyledon vascular tissue pattern formation, alpha-amino acid biosynthetic process, mRNA metabolic process, fatty acid beta-oxidation, and establishment of localization in cell (Figure 10 in **Supplementary Figures 7–10**).

Pathogen Responses

Comparison 3: *D. sapinea* vs. *D. scrobiculata* Infections Under Control Treatment

In this comparison, a total of 211 genes were differentially expressed. Out of these, 156 DEGs were assigned KEGG orthologs and were mapped to various general pathways, and 172 DEGs were annotated to various GO terms. Our 5-fold threshold produced a filtered list of 58 DEGs, with 27 genes more highly expressed, and 21 genes expressed lower in *D. sapinea* relative to *D. scrobiculata* (Spreadsheet Pathogen-comparison3 in **Supplementary Information SI2**). We also found 30 DEGs that were assigned to various GO terms and the most represented GO functions included response to stimulus (50 DEGs), response to nitrogen metabolic process (44 DEGs), carbohydrate metabolic process (38 DEGs), and lipid metabolic process (30 DEGs) (**Figure 6C**).

Primary Metabolic Responses

We found two transcripts mapped to KEGG pathways for carbon metabolism and biosynthesis of amino acids. Significant DEGs included glyceraldehde-3-phosphate dehydrogenase, and triose phosphate isomerase under various carbon-associated pathways (**Table 2**). Additionally, a thiamine biosynthesis protein (NMT1) that was assigned GO: nitrogen metabolic process, aromatic compound metabolic process, was also higher (**Table 2**). Under various lipid associated pathways, a sterol 24-c-methyltransferase transcript, and RING finger transcript were also reported (**Table 2**).

Specialized Metabolism and Signaling

We also found a gamma-glutamyl transpeptidase transcript annotated to glutathione metabolism pathway on KEGG and assigned GO: response to nitrogen starvation, and elongation factor 2 transcript to be lower in *D. sapinea* as compared to *D. scrobiculata* under CT (**Table 2**).

The enrichment analysis produced a list of 8 most significant GO terms with respect to both classic Fisher and Kolmogorov-Smirnov elimination tests (Spreadsheet Pathogen-comparison3 in **Supplementary Information SI3**). The most enriched terms included nuclear chromosome segregation, ascospore-type prospore assembly, protein deubiquitination, polyol metabolic process, and response to stress (Figure 11 in **Supplementary Figures 11–12**).

Comparison 4: *D. scrobiculata* Under Climate Change Treatment vs. Control Treatment

We documented a total of 147 DEGs significantly affected by the climate treatment. Out of these 147 DEGs, 56 were assigned KEGG orthologs and were mapped to various general pathways, and all were annotated with GO terms. Thereafter, our 5-fold threshold produced a filtered list of 30 DEGs, with 6 upregulated and 24 downregulated by climate change conditions (Spreadsheet Pathogen-comparison4 in **Supplementary Information SI2**). The same 56 DEGs that had KEGG orthologs were also assigned various GO terms, including nitrogen compound metabolic process (51 DEGs), carbohydrate and its derivative metabolic process (42 DEGs), response to stress (26 DEGs), response to heat (12 DEGs) (**Figure 6C**).

Primary Metabolic Responses

Various carbon metabolizing enzyme genes such as triose phosphate isomerase, beta-glucosidase, L-iditol 2-dehydrogenase, and cardiolipin synthase were among the most significant (**Table 3**). We also found 21 DEGs assigned GO: amino acid metabolic process (**Figure 6C**), including

TABLE 2 | Significant DE genes under various metabolic pathways for pathogen comparison 3 (**Figure 1**): CTDsap vs. CTDscr.

Transcript ID	EGGNOG	logFC	Actual FC	Adj. *p*-value	KEGG Orthology
Carbon metabolic process					
tig00000024.g11826.t1	glyceraldehyde-3-phosphate dehydrogenase	6.3	39.7	3.09E-11	K00134
tig00000027.g13503.t1	Triose-phosphate isomerase	3.2	10.2	0.002	K01803
AMPK signaling pathway					
tig00000005.g4874.t1	elongation factor 2	2.9	8.2	0.002	K03234
Necroptosis					
tig00000005.g4528.t1	Heat shock protein	2.7	7.3	7.83E-06	K04079
tig00000002.g2373.t1	Histone H2A	9.9	97.6	4.54E-11	K11251
Plant-pathogen interaction					
tig00000005.g4528.t1	Heat shock protein	2.7	7.3	4.54E-11	K04079
Steroid biosynthesis					
tig00000010.g9170.t1	Sterol 24-c-methyltransferase	−2.6	−6.7	0.00088	K00559
Thiamine metabolism					
tig00000021.g11454.t1	Thiamine biosynthesis protein (Nmt1)	2.6	6.9	0.01510	K18278
tig00000003.g3794.t1	RING finger	−5.4	−29.3	0.00180	K01061
Glutathione metabolism					
tig00000006.g5533.t1	gamma-glutamyl transpeptidase	−4.5	−20.7	5.47E-05	K00681

TABLE 3 | Significant DE genes under various metabolic pathways for pathogen comparison 4 (**Figure 1**): CCTDscr vs. CTDscr.

Transcript ID	EGGNOG	logFC	Actual FC	Adj. *p*-value	KEGG Orthology
Sucrose and starch metabolism					
tig00000002.g1573.t1	beta-glucosidase	−2.8	−8	0.048378	K05349
tig00000001.g1035.t1	L-iditol 2-dehydrogeanse	2.5	6.4	0.003366	K00008
Biosynthesis of amino acids					
tig00000027.g13503.t1	Triose-phosphate isomerase	3.8	14.1	0.022454	K01803
tig00000001.g1232.t1	glutamine synthetase	−2.4	−5.5	0.038446	K01915
Nitrogen metabolic process					
tig00000006.g5807.t1	cyanide hydratase	3.4	11.9	0.009250	K10675
tig00000021.g11454.t1	Thiamine biosynthesis protein (Nmt1)	2.4	5.9	0.000427	K18278
Plant-pathogen interactions					
tig00000003.g3121.t1	cardiolipin synthase	−2.3	−5.1	0.042621	K08744
tig00000007.g6441.t1	heat shock HSP1	−2.9	−8.3	0.000627	K03283
Necroptosis					
tig00000001.g1232.t1	glutamine synthetase	−2.4	−5.5	0.038446	K01915
Translation					
tig00000007.g6659.t1	large subunit ribosomal protein L7Ae	−4.8	−23.2	0.000942	K02936
tig00000011.g9633.t1	small subunit of the ribosomal protein S15e	−4.8	−22.6	0.000356	K02958
tig00000011.g9947.t1	Aspartyl-tRNA synthetase	2.3	5.1	0.000431	K01876

thiamine biosynthesis protein (NMT1), cyanide hydratase, aspartyl-tRNA-synthetase, heat shock protein (HSPA1), large subunit of ribosomal protein L7Ae and small subunit of the ribosomal protein (**Table 3**). The large subunit was assigned GO: cytoplasmic translation, obsolete mycelium development and the small subunit was assigned GO: RNA export from nucleus, cytoplasmic translation (**Table 3**), although both subunits are constituents of the EF-Tu protein domain.

The enrichment analysis produced a list of 11 most significant GO terms with respect to both classic Fisher and Kolmogorov-Smirnov elimination tests (Spreadsheet Pathogen-comparison4 in **Supplementary Information SI3**). The most enriched terms included ATP metabolic process, cellular amino acid catabolic process, alpha-amino acid catabolic process, electron transport chain, and respiratory electron transport chain (Figure 12 in **Supplementary Figures 11–12**).

DISCUSSION

Climate change poses major physiological challenges that can shift the dynamics of tree-pathogen interactions (Desprez-Loustau et al., 2006). The CCT used in this study mimicked possible climate change scenarios that allowed the investigation of how host and pathogens may be impacted by such adverse conditions. While we found clear indications of abiotic stress

responses in both host and pathogen, we acknowledge that the responses we documented are on a noticeably short time scale, one that does not consider longer term adaptive responses, both physiological/ecological (habituation) and evolutionary. Even so, we found that a simulated CCT shifted the outcome of the interactions between Austrian pine and the normally non-aggressive fungus *D. scrobiculata*, resulting in lesions on par with *D. sapinea*. We speculate either enhanced aggressiveness of the pathogen, increased susceptibility of the host, or both, support the phenotypic findings of past studies (reviewed in Desprez-Loustau et al., 2006).

We dissected the underlying molecular features of this phenomenon *via* a dual transcriptomics approach. One challenge with this approach is that read recovery rates vary widely between host and pathogen due to substantially lower absolute amounts of pathogen RNA relative to host RNA in infected tissues (Naidoo et al., 2018). We mitigated this challenge in our recovery method for host and pathogen reads by filtering out transcripts that were only represented in mock samples but had no reads in infected samples. We further only retained transcripts that were represented at least 20 times in at least three sample types irrespective of treatment combination (Visser et al., 2019; Hernandez-Escribano et al., 2020).

Within these limits we asked several key questions through different comparisons, considering the host response to the two pathogens separately, the host response under climate change conditions and the pathogen responses under both climate change and control climate. The most significant DEGs were then analyzed under two major categories, primary and specialized metabolism, the latter associated with defense. This eventually resulted in the cellular models presented in **Figure 8**, one for the host and one for the pathogens. We infer the following conclusions from the main comparisons in the study.

Reduced Host Photosynthetic Rate Contributes to *D. sapinea* Pathogenesis

Host photosynthetic pathways were suppressed, specifically in *D. sapinea* infection vs. mock inoculation under CT (comparison 1). The ATP synthase delta chain protein and photosystem II proteins are localized in the chloroplast and are involved in ATP proton pump assembly and PSII (photosystem II) light harvesting complex, respectively. Meanwhile, carbonic anhydrase (CAH) is involved in important cellular functions such as mesophyll carbon dioxide conductance, oxidative stress protection, lipid biosynthesis, and phytohormone mediated signaling (Polishchuk, 2021) but, perhaps more importantly, with ABA-independent stomatal closure (Kolbe et al., 2018). Taken together, this evidence suggests that attack by *D. sapinea* suppresses photosynthesis, leading to host carbon starvation.

Suppressed Host Defense Responses Contribute to *D. sapinea* Pathogenesis

Under CT, and compared directly to *D. scrobiculata* infection, critical defense responses were suppressed by *D. sapinea* infection, including calmodulin-like (CML) protein genes that have been associated with HR expression (Chiasson et al., 2005), enhanced resistance to insect pests (Ma et al., 2008), and biotrophic and hemi-biotrophic lifestyles (Leba et al., 2012). Similarly, PR proteins, an inducible and diverse group that accumulate in response to stress and have been demonstrated to be significantly associated with necrotrophic pathogens (Boccardo et al., 2019), were suppressed, as were WRKY transcription factors, which reportedly mediate the cross-talk between salicylic acid and jasmonic mediated defense signaling (Li et al., 2004; Zheng et al., 2006). Finally, pathways associated with biosynthesis of specialized metabolites like phenolics and flavonoids, which have been associated with resistance in this system (Sherwood and Bonello, 2013), were also suppressed. Thus, compared to *D. scrobiculata* infection, the elicitation of host defense responses by *D. sapinea* is severely impaired under CT, which explains, at least in part, the baseline difference in aggressiveness between the two pathogens.

Necrotrophic Host Interactions With *D. sapinea* Trigger Phytohormone Crosstalk

Plant defense responses are regulated by the crosstalk between phytohormone pathways. Under CT and upon *D. sapinea* infection, Austrian pine responded by ramping up crosstalk of various phytohormones, leading primarily to jasmonate-mediated defense signaling, consistent with the basic necrotrophic aspects of this association. Such response was concomitant with a downregulation of auxin and gibberellic acid-responsive genes and an upregulation of PP2C type proteins. Jasmonate ZIM-domain (JAZ) containing proteins have been associated with regulation of jasmonate accumulation *via* suppression of MYC2 proteins (Chini et al. 2007), while auxin responsive genes are linked to reductions of host defense by suppression of the salicylic acid pathway (Djami-Tchatchou et al., 2020). Gibberellin receptors such as GID1 are crucial for GA signal transduction and have been associated with enhanced susceptibility in host plants *via* antagonistic crosstalk with jasmonate pathways (Song et al., 2014). Finally, PP2C type proteins have been linked to modulation of defense responses by possible suppression of various target PR proteins and ROS-scavenging enzymes (Zhu et al., 2018).

D. scrobiculata-Induced Host Nitrogen and Fatty Acid Metabolism Contributes to Host Defense

Our data suggest that *D. scrobiculata* infection increases metabolism and transport of amino acids and lipids but does not affect photosynthesis, unlike *D. sapinea* under CT. However, one glutamate dehydrogenase (GDH) transcript was upregulated, suggesting that infection results in enhanced reversible transamination of 2-oxoglutarate to form glutamate (Labboun et al., 2009), which contributes to leaf glutamate homeostasis along with the NADH-GOGAT cycle. The fatty acid biosynthesis pathway was also overall highly induced. Among induced fatty acid enzymes, acyl-CoA dehydrogenase and various short chain fatty acid dehydrogenases catalyze the initial step in respective cycles of fatty acid beta oxidation. Similarly,

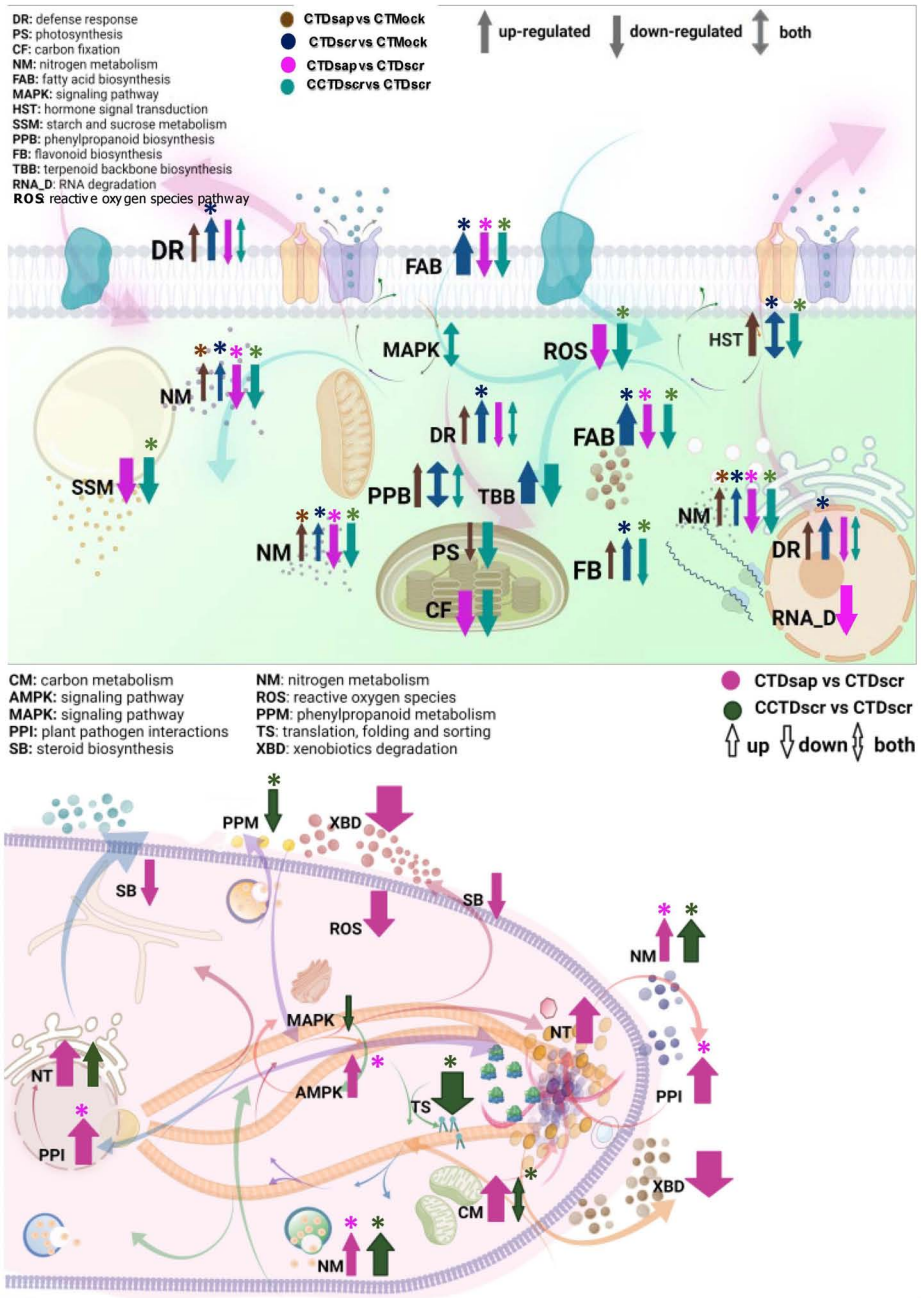

FIGURE 8 | Working models of host (top) and pathogen (bottom) cellular networks of various primary and specialized metabolic pathways. Abbreviations represent GO function and colored arrows indicate respective host and pathogen comparisons. Arrow widths represent arbitrary relative magnitude of changes in significantly expressed DEGs mapped under each pathway for a given host/pathogen comparison. Enriched pathways are marked with asterisks.

fatty acid synthases (FAS) catalyze the biosynthesis of various long chain fatty acids from respective precursor acyl-CoAs. Furthermore, xyloglucan endotransglucosylase hydrolase (XTH) activity was enhanced. XTH induces cell growth and extension (Miedes et al., 2014) *via* increased short chain xyloglucan synthesis (Niraula et al., 2021). Taken together, this evidence suggests that Austrian pine enhances homeostasis and growth processes in response to *D. scrobiculata* infection under CT, contributing to a positive outcome for the host against this less aggressive pathogen.

D. scrobiculata Elicits a Stronger Defense Response

Under CT, *D. scrobiculata* infection elicited a much stronger host defense response compared to *D. sapinea* infection and the

mock treatment *via* enhancement of PR protein biosynthesis, as well as calcium and jasmonate-mediated defense signaling. This was especially evident by enhanced biosynthesis of coronatine insensitive1 (COI1) proteins, which are critical in almost every step of jasmonate signaling (Katsir et al., 2008). There are further indications of phytohormone cross-talk from enhanced ARR-A proteins that are involved in age-related defense response in coordination with phytohormones such as salicylates, jasmonates, and ethylene (Shah and Zeier, 2013). At the same time, enhanced CALM proteins, along with CMLs, a calcium dependent protein kinase, and calcineurin B-like proteins suggests active regulation of the calcium-calmodulin signaling pathway (Cheval et al., 2013), which has been associated with responses to both biotic and abiotic stress.

Diplodia scrobiculata also induced host defense-associated phenylpropanoid pathways, demonstrated by several significant DEGs. Cinnamoyl alcohol dehydrogenases (CAD) are involved in lignin biosynthesis and have been associated with defense-induced phenylpropanoid metabolism (Logemann et al., 1997; Tronchet et al., 2010). Furthermore, the peroxidase-generated apoplastic oxidative burst contributes to damage associated molecular pattern (DAMP)-elicited immunity (Survila et al., 2016). We also documented an induction in flavonoid and terpenoid biosynthesis. Strong induction of host defenses is likely a key contributor to the less aggressive baseline phenotype exhibited by *D. scrobiculata* infection under CT.

Impaired Host Primary Metabolism and Defense Responses Further Aid *D. sapinea* Pathogenesis

Diplodia sapinea had more profound effects than *D. scrobiculata* on host primary metabolism. What appears to be a rapid depletion of carbon, nitrogen, and lipid resources might explain why the host is less able to counter a *D. sapinea* infection than a *D. scrobiculata* infection under CT. We observed some overlap in DEGs between biological comparisons 1 and 2, where we investigated host responses to *D. sapinea* vs. mock and host responses to *D. scrobiculata* vs. mock inoculation, respectively, under CT. We then used comparison 3 to further dissect differences in dual host and pathogen responses following *D. sapinea* and *D. scrobiculata* attacks under CT. While we observed no significant differences in host photosynthetic and carbon fixation pathways, the carbohydrate metabolic process was heavily suppressed in *D. sapinea* infected hosts compared to *D. scrobiculata* infected hosts. Specifically, key genes of the Krebs cycle, such as citrate synthase, aconitase hydratase (which catalyzes isomerization of citrate to isocitrate), isocitrate dehydrogenase (which catalyzes conversion of isocitrate to alpha-ketoglutarate and release of carbon dioxide), and fumarate hydratase (which catalyzes conversion of fumarate into malate) were significantly suppressed. Dihydrolipoyl dehydrogenase, which is part of the pyruvate dehydrogenase multienzyme complex that connects cytosolic glycolysis with mitochondrial citrate cycle and acts as an ROS neutralizer (Babady et al., 2007), was also suppressed.

Fatty acid biosynthesis and nitrogen metabolism were also inhibited in Austrian pine inoculated with *D. sapinea,* compared to *D. scrobiculata*. Suppressed activity of critical enzymes such as gdhA, alanine aminotransferase, and glutamine aminotransferase (pyrABCN) indicate reduced nitrogen assimilation, possibly as a result of cellular hypoxia (Diab and Limami, 2016). Such processes may be the consequence of stomatal closure induced by *D. sapinea* and subsequent reduction in photosynthesis and nitrogen assimilation, which ultimately leads to depletion of carbon and nitrogen, and respiratory oxygen.

Finally, we observed reduced host defense responses, as indicated by suppression of CML, efTu, and glutathione reductase. Thus, it appears that reduced assimilation/metabolism of carbon, nitrogen, and fatty acids in Austrian pine, coupled with various suppressed defense responses, contribute to the accelerated baseline pathogenesis observed with *D. sapinea* vs. *D. scrobiculata* under CT.

Carbon Metabolism and Nitrogen Assimilation Are Crucial for *D. sapinea* Information Processing and Pathogenesis

In line with suppression of host carbon and nitrogen assimilation, fungal nitrogen assimilation and carbon metabolism were higher in *D. sapinea* compared to *D. scrobiculata* under CT. Specifically, glycolytic enzyme genes such as glyceraldehyde 3-phosphate dehydrogenase (GAPD) and another triose phosphate isomerase were enhanced in *D. sapinea* compared to *D. scrobiculata* under CT. At the same time, enhanced nitrogen metabolism (Nmt1 and elongation factor 2) is also indicative of higher activity of *D. sapinea* compared to *D. scrobiculata* under CT. In addition, we found enhanced environmental information processing in *D. sapinea,* as indicated by signaling pathways involved in necrotopsis, AMPK, and plant-pathogen interactions. For instance, a gamma-glutamyltranspeptidase (GGT) is involved in glutathione metabolism and is associated with enhanced transport of amino acids and detoxification of free oxygen radicals (Mehdi et al., 2001). Heat shock proteins also aid in fungal morphogenesis and environmental processing, including hyphal formation and pathogenicity (Tiwari et al., 2015).

Climate Change Induces Host Starvation *via* Suppression of Primary Metabolism

Host trees subjected to CCT and further challenged with *D. scrobiculata* displayed depletion of carbon resources, an outcome (if not a process) similar to the situation with *D. sapinea* under CT. This was evident from suppression of pigments involved in photoexcitation of chlorophyll, to enzymatic genes involved in the Calvin cycle, as well as starch and sucrose metabolism. Additionally, we also documented suppressed carbonic anhydrase activity, similar to *D. sapinea* infected hosts in comparison 3. Furthermore, enhanced upstream enzymes of host fatty acid metabolism, such as biotin carboxyl carrier protein (a/bccp) and an alcohol dehydrogenase, indicated synthesis of short chain fatty acids; however, fatty acid elongation and branching was affected as indicated by suppressed myristoyl-acyl

carrier protein thioesterases. Suppressed fatty acid biosynthesis suggests impairment of membrane integrity and lipid transport, which contribute to stress responses (Michaud and Jouhet, 2019). Thus, climate change conditions, as implemented here, cause suppression of carbon fixation and metabolism leading to carbon starvation, compounding the effects of *D. scrobiculata* infection and resulting in enhanced pathogenesis.

Climate Change Weakens the Host by Suppressing Defense Associated Metabolic Pathways

In *D. scrobiculata* infected hosts under CCT, reduced defense responses were indicated by suppression of CML and WRKY, in addition to enzymes in the phenylpropanoid biosynthesis pathway, such as caffeoyl-CoA-o-methyl transferase and beta glucosidases, and geranylgeranyl pyrophosphate synthases (GGPS) in the terpenoid biosynthesis pathway. Additionally, we report enhanced MAPK signaling and oxidative burst, as implied by reduced glutathione metabolism, all indicative of host responses to abiotic stress. Similarly to *D. sapinea* infected hosts under CT, the PP2C family proteins were also induced in *D. scrobiculata* infected hosts under CCT, indicating direct host defense suppression. Reduced glutathione metabolism, by means of suppressed glutathione and ribonucleotide diphosphate reductase (RNDP) activities, further indicates reduced ROS detoxification and lowered nitrogen transport in Austrian pine under CCT. Thus, climate change conditions, as implemented here, result in suppression of host defense responses.

Carbon and Nitrogen Assimilation Are Crucial for *D. scrobiculata* Survival Under Climate Change

Comparison 4, in which we investigated dual responses of host and pathogen following *D. scrobiculata* attack under CCT vs. CT, also revealed important patterns in gene expression in *D. scrobiculata* itself. For example, we found evidence of enhanced carbon metabolism by way of triose phosphate isomerase and enolase gene upregulation. Amino acid metabolism was enhanced as indicated by upregulation of a glutamine synthetase gene, in addition to the triose phosphate isomerase gene. Interestingly, the glutamine synthetase transcript was also mapped to the necroptosis pathway and has been reported to induce susceptibility *via* nitrogen competition between host and pathogen (Huang et al., 2017). We also documented enhanced protein processing and stress responses, as indicated by upregulation of heat shock (HSP) proteins and an aminoacyl-tRNA synthase gene. Taken together, this evidence suggests that the focus of pathogen metabolism is to acquire carbon and nitrogen, while lowered lipid metabolism could be a response to the climate change conditions as implemented in this study.

Integrated Model

All in all, our work highlights some major themes that facilitate a deeper understanding of pine-pathogen interactions under variable climate. We synthesize our results in two cellular models, one for the host and one for the two pathogens (**Figure 8**). The comparisons arranged in panels of **Figures 6A–C**, **7A–D** highlight host responses to the two pathogens vs. the mock and, more importantly, two different scenarios of host susceptibility, one including the baseline response to *D. sapinea* infection under CT, the other host responses to *D. scrobiculata* infection under CCT. The first observation is that maintaining primary metabolism homeostasis is key for survival of both the host and the pathogens. Infection by *D. sapinea* induces suppression of host carbon fixation and metabolism, fatty acid biosynthesis, and nitrogen metabolism, thereby leading to primary nutrient starvation (**Figure 8**). This is further supported by enhanced carbon and nitrogen metabolism in *D. sapinea* itself (**Figure 8**), which likely further contributes to host starvation. Moreover, suppressed host fatty acid metabolic pathways likely affect membrane integrity and vesicular trafficking, thereby influencing host response to stress (Michaud and Jouhet, 2019). On the other hand, suppressed lipid metabolism and steroid biosynthesis in *D. sapinea* perhaps suggests reduced activity of lipid transporters as well as reduced membrane trafficking (Rizzo et al., 2019). In contrast, infection by the less aggressive *D. scrobiculata* did not alter host carbon fixation, while nitrogen metabolism and fatty acid biosynthesis were enhanced (**Figure 8**) along with indications of active growth and homeostasis in hosts. Thus, the impaired state of host carbon fixation and metabolism is one of the primary explanations for the higher aggressiveness of *D. sapinea*, while primary metabolism of carbon, nitrogen, and fatty acids either remain unaffected or are enhanced.

Suppressed primary metabolism in *P. nigra* also likely contributes to the limitation of carbon-based defenses (phenolics, terpenoids), as well as ROS signaling. Indeed, host defense activation against *D. sapinea* was on a much lesser scale, relative to *D. scrobiculata,* under the baseline conditions of CT (**Figure 8**). For example, phenylpropanoid biosynthesis, which is at the core of defense-associated phenolics and flavonoids (Sherwood and Bonello, 2013), was much more pronounced in hosts under attack by *D. scrobiculata* than *D. sapinea* (**Figure 8**). Furthermore, terpenoid biosynthesis in *D. scrobiculata*-infected hosts was enhanced, whereas *D. sapinea* infection did not induce any changes (**Figure 8**). Interestingly, on the pathogen side, the plant pathogen interactions pathway was more enhanced and GO enriched in *D. sapinea* than in *D. scrobiculata* (**Figure 8**). Thus, the state of specialized metabolism on both sides of the interaction supports a view in which *D. sapinea* elicits global impairment of host metabolism affecting assimilation, growth and defense response *via* carbon and nitrogen starvation, explaining the occurrence of longer lesions under CT.

The picture changed dramatically under the climate change regimen for *D. scrobiculata*-infected hosts, which clearly experienced suppression of carbon fixation, starch and sucrose metabolism, nitrogen metabolism, and fatty acid biosynthesis, in a manner similar to that of hosts attacked by *D. sapinea* under control climate. These pathways were also GO enriched, further highlighting how CCT led to depletion of host resources and increased *D. scrobiculata* aggressiveness (**Figure 8**).

Likewise, CCT induced suppression of phenylpropanoid biosynthesis, terpenoid biosynthesis, and defense response pathways in the host (**Figure 8**). This was accompanied by suppression of ROS and hormone signaling pathways. On the pathogen side, while carbon metabolism and nitrogen metabolism were both GO enriched and enhanced, activity of phenylpropanoid metabolism was lower under CCT (**Figure 8**), possibly due to feedback from low production of phenylpropanoids in the starving host. Concurrently, we recorded a glutamine synthetase transcript mapped to the necroptosis pathway in *D. scrobiculata* under CCT, like *D. sapinea* infected hosts under CT. Also, CCT appears to affect *D. scrobiculata via* reduced MAPK signaling and post-translational protein processing, suggesting some impairment of host immune signaling (**Figure 8**). This suggests that CCT causes genome-wide suppression of various critical host secondary metabolic pathways either directly or *via* suppression of primary metabolism, thereby predisposing hosts to pathogenic infections.

Taken together, our evidence shows how critical carbon and nitrogen are for sustenance of cellular integrity and operation in plant pathogen interactions, no matter what the environmental conditions. Nitrogen and carbon mobilization and transport are highly responsive to both biotic and abiotic stress, and the cumulative stress from the climate change regime and pathogenic infection further aggravates host resource depletion and thus the ability to fight off infection. This appears to ultimately explain the altered lesion phenotypes under CCT. While informative, a study like ours points to metabolic pathways being affected; however, direct measurements of metabolites are necessary to determine how CC-associated stress affects the internal environment of the tree host at a system level to predispose trees to fungal infection.

DATA AVAILABILITY STATEMENT

The data presented in this study are deposited in the NCBI repository with Bioproject accession number PRJNA825834.

AUTHOR CONTRIBUTIONS

PB and JS ideated, designed, and planned the project. PB secured the funding. AC, BK, and VV contributed to experimental execution. SG, EV, SN, and MS conducted the gene expression analyses. SG and PB wrote the first drafts. AC, JS, EV, SN, and MS contributed to the editing, revisions, and final draft. All authors contributed to the article and approved the submitted version.

FUNDING

This work was funded by Ohio Agricultural Research Development Center SEED grant No. 2016-007 to PB and by other state and federal funds appropriated to The Ohio State University, College of Food, Agricultural, and Environmental Sciences, Ohio Agricultural Research and Development Center. This work was supported in part by the United States Department of Agriculture Forest Service. JS was supported by the National Science Foundation DEB-1638999.

ACKNOWLEDGMENTS

The authors wish to thank Caterina Villari for help with initial set up, Michael Kelly for providing the in-chamber CO_2 system, and Katie D'Amico-Willman and Carrie Fearer for their assistance with RNA extraction.

SUPPLEMENTARY MATERIAL

The Supplementary Material for this article can be found online at: https://www.frontiersin.org/articles/10.3389/ffgc.2022.872584/full#supplementary-material

REFERENCES

Adams, H. D., Guardiola-Claramonte, M., Barron-Gafford, G. A., Villegas, J. C., Breshears, D. D., Zou, C. B., et al. (2009). Temperature sensitivity of drought-induced tree mortality portends increased regional die-off under global-change-type drought. *Proc. Natl. Acad. Sci. U S A* 106, 7063–7066. doi: 10.1073/pnas.0901438106

Alexa, A., and Rahnenfuhrer, J. (2021). *topGO: Enrichment Analysis for Gene Ontology. R Package Version 2.46.0*. Available online at: https://bioconductor.org/packages/release/bioc/html/topGO.html

Babady, N. E., Pang, Y.-P., Elpeleg, O., and Isaya, G. (2007). Cryptic proteolytic activity of dihydrolipoamide dehydrogenase. *Proc. Natl. Acad. Sci.* 104, 6158–6163. doi: 10.1073/pnas.0610618104

Barto, E. K., Enright, S., Eyles, A., Wallis, C. M., Chorbadjian, R., Hansen, R., et al. (2008). Effects of soil fertility on systemic protein defense responses of Austrian pine to attack by a fungal pathogen and an insect defoliator. *J. Chem. Ecol.* 34, 1392–1400.

Bhargava, S., and Sawant, K. (2013). Drought stress adaptation: metabolic adjustment and regulation of gene expression. *Plant Breed.* 132, 21–32.

Blodgett, J. T., and Bonello, P. (2003). The aggressiveness of Sphaeropsis sapinea on Austrian pine varies with isolate group and site of infection. *Forest Pathol.* 33, 15–19.

Blodgett, J. T., Kruger, E. L., and Stanosz, G. R. (1997a). Effects of moderate water stress on disease development by Sphaeropsis sapinea on red pine. *Phytopathology* 87, 422–428. doi: 10.1094/PHYTO.1997.87.4.422

Blodgett, J. T., Kruger, E. L., and Stanosz, G. R. (1997b). Sphaeropsis sapinea and water stress in a red pine plantation in central Wisconsin. *Phytopathology* 87, 429–434. doi: 10.1094/PHYTO.1997.87.4.429

Boccardo, N. A., Segretin, M. E., Hernandez, I., Mirkin, F. G., Chacón, O., Lopez, Y., et al. (2019). Expression of pathogenesis-related proteins in transplastomic tobacco plants confers resistance to filamentous pathogens under field trials. *Sci. Rep.* 9:2791.

Bolger, A. M., Lohse, M., and Usadel, B. (2014). Trimmomatic: a flexible trimmer for Illumina sequence data. *Bioinformatics* 30, 2114–2120. doi: 10.1093/bioinformatics/btu170

Bostock, R. M., Pye, M. F., and Roubtsova, T. V. (2014). Predisposition in plant disease: exploiting the nexus in abiotic and biotic stress perception and

response. *Ann. Rev. Phytopathol.* 52, 517–549. doi: 10.1146/annurev-phyto-081211-172902

Bray, N. L., Pimentel, H., Melsted, P., and Pachter, L. (2016). Near-optimal probabilistic RNA-seq quantification. *Nat. Biotechnol.* 34, 525–527.

Buchfink, B., Xie, C., and Huson, D. H. (2014). Fast and sensitive protein alignment using DIAMOND. *Nat. Methods* 12, 59–60. doi: 10.1038/nmeth.3176

Chang, S., Puryear, J., and Cairney, J. (1993). A simple and efficient method for isolating RNA from pine trees. *Plant Mol. Biol. Reporter* 11, 113–116. doi: 10.1385/MB:19:2:201

Chaves, M. M., Maroco, J. P., and Pereira, J. S. (2003). Understanding plant responses to drought - from genes to the whole plant. *Funct. Plant Biol.* 30, 239–264. doi: 10.1071/FP02076

Cheval, C., Aldon, D., Galaud, J.-P., and Ranty, B. (2013). Calcium/calmodulin-mediated regulation of plant immunity. *Mol. Cell Res.* 1833, 1766–1771. doi: 10.1016/j.bbamcr.2013.01.031

Chiasson, D., Ekengren, S. K., Martin, G. B., Dobney, S. L., and Snedden, W. A. (2005). Calmodulin-like proteins from Arabidopsis and tomato are involved in host defense against *Pseudomonas* syringae pv. tomato. *Plant Mol. Biol.* 58, 887–897. doi: 10.1007/s11103-005-8395-x

Clifford, M. J., Royer, P. D., Cobb, N. S., Breshears, D. D., and Ford, P. L. (2013). Precipitation thresholds and drought-induced tree die-off: insights from patterns of Pinus edulis mortality along an environmental stress gradient. *N. Phytol.* 200, 413–421. doi: 10.1111/nph.12362

De Wet, J., Burgess, T., Slippers, B., Preisig, O., Wingfield, B. D., and Wingfield, M. J. (2003). Multiple gene genealogies and microsatellite markers reflect relationships between morphotypes of Sphaeropsis sapinea and distinguish a new species of Diplodia. *Mycol. Res.* 107, 557–566. doi: 10.1017/s0953756203007706

Desprez-Loustau, M. L., Marcais, B., Nageleisen, L. M., Piou, D., and Vannini, A. (2006). Interactive effects of drought and pathogens in forest trees. *Ann. Forest Sci.* 63, 597–612.

Diab, H., and Limami, A. M. (2016). Reconfiguration of N Metabolism upon Hypoxia Stress and Recovery: roles of Alanine Aminotransferase (AlaAT) and Glutamate Dehydrogenase (GDH). *Plants* 5, 2–25. doi: 10.3390/plants5020025

Djami-Tchatchou, A. T., Harrison, G. A., Harper, C. P., Wang, R., Prigge, M. J., Estelle, M., et al. (2020). Dual role of auxin in regulating plant defense and bacterial virulence gene expression during *Pseudomonas* syringae PtoDC3000 pathogenesis. *Mol. Plant-Microb. Interact.* 33, 1059–1071. doi: 10.1094/MPMI-02-20-0047-R

Eyles, A., Chorbadjian, R., Wallis, C. M., Hansen, R. C., Cipollini, D. F., Herms, D. A., et al. (2007). Cross-induction of systemic induced resistance between an insect and a fungal pathogen in Austrian pine over a fertility gradient. *Oecologia* 153, 365–374. doi: 10.1007/s00442-007-0741-z

Gilbert, D. (2016). Gene-omes built from mRNA seq not genome DNA. *F1000Research* 5:1695.

Grabherr, M. G., Haas, B. J., Yassour, M., Levin, J. Z., Thompson, D. A., and Amit, I. (2011). Full-length transcriptome assembly from RNA-Seq data without a reference genome. *Nat. Biotechnol.* 29, 644–652. doi: 10.1038/nbt.1883

Harris, J. M., Balint-Kurti, P., Bede, J. C., Day, B., Gold, S., Goss, E. M., et al. (2020). What are the top 10 unanswered questions in molecular plant-microbe interactions? *Mol. Plant-Microb. Interact.* 33, 1354–1365. doi: 10.1094/MPMI-08-20-0229-CR

Hart, A. J., Ginzburg, S., Xu, M., Fisher, C. R., Rahmatpour, N., Mitton, J. B., et al. (2020). EnTAP: bringing faster and smarter functional annotation to non-model eukaryotic transcriptomes. *Mol. Ecol. Resour.* 20, 591–604. doi: 10.1111/1755-0998.13106

Hernandez-Escribano, L., Visser, E. A., Iturritxa, E., Raposo, R., and Naidoo, S. (2020). The transcriptome of Pinus pinaster under Fusarium circinatum challenge. *BMC Genom.* 21:28. doi: 10.1186/s12864-019-6444-0

Herre, E. A., Mejia, L. C., Kyllo, D. A., Rojas, E., Maynard, Z., Butler, A., et al. (2007). Ecological implications of anti-pathogen effects of tropical fungal endophytes and mycorrhizae. *Ecology* 88, 550–558. doi: 10.1890/05-1606

Huang, H., Nguyen Thi, Thu, T., He, X., Gravot, A., Bernillon, S., et al. (2017). Increase of fungal pathogenicity and role of plant glutamine in nitrogen-induced susceptibility (NIS) to rice blast. *Front. Plant Sci.* 8:265. doi: 10.3389/fpls.2017.00265

Huerta-Cepas, J., Szklarczyk, D., Forslund, K., Cook, H., Heller, D., Walter, M. C., et al. (2016). EGGNOG 4.5: a hierarchical orthology framework with improved functional annotations for eukaryotic, prokaryotic and viral sequences. *Nucleic Acids Res.* 44, D286–D293. doi: 10.1093/nar/gkv1248

Kanehisa, M., and Sato, Y. (2020). KEGG Mapper for inferring cellular functions from protein sequences. *Protein Sci.* 29, 28–35. doi: 10.1002/pro.3711

Kanehisa, M., Sato, Y., and Morishima, K. (2016). BlastKOALA and GhostKOALA: KEGG tools for functional characterization of genome and metagenome sequences. *J. Mol. Biol.* 428, 726–731. doi: 10.1016/j.jmb.2015.11.006

Katsir, L., Schilmiller, A. L., Staswick, P. E., He, S. Y., and Howe, G. A. (2008). COI1 is a critical component of a receptor for jasmonate and the bacterial virulence factor coronatine. *Proc. Natl. Acad. Sci.* 105, 7100–7105. doi: 10.1073/pnas.0802332105

Kolbe, A. R., Brutnell, T. P., Cousins, A. B., and Studer, A. J. (2018). Carbonic anhydrase mutants in Zea mays have altered stomatal responses to environmental signals. *Plant Physiol.* 177, 980–989. doi: 10.1104/pp.18.00176

Labboun, S., Tercé-Laforgue, T., Roscher, A., Bedu, M., Restivo, F. M., Velanis, C. N., et al. (2009). Resolving the role of plant glutamate dehydrogenase. I. In vivo real time nuclear magnetic resonance spectroscopy experiments. *Plant Cell Physiol.* 50, 1761–1773. doi: 10.1093/pcp/pcp118

Leba, L.-J., Cheval, C., Ortiz-Martín, I., Ranty, B., Beuzón, C. R., Galaud, J.-P., et al. (2012). CML9, an Arabidopsis calmodulin-like protein, contributes to plant innate immunity through a flagellin-dependent signalling pathway. *Plant J.* 71, 976–989. doi: 10.1111/j.1365-313X.2012.05045.x

Li, J., Brader, G. N., and Palva, E. T. (2004). The WRKY70 transcription factor: a node of convergence for jasmonate-mediated and salicylate-mediated signals in plant defense. *Plant Cell* 16, 319–331. doi: 10.1105/tpc.016980

Logemann, E., Reinold, S., Somssich, I. E., and Hahlbrock, K. (1997). A novel type of pathogen defense-related cinnamyl alcohol dehydrogenase. *Biol. Chem.* 378, 909–914. doi: 10.1515/bchm.1997.378.8.909

Lohse, M., Nagel, A., Herter, T., May, P., Schroda, M., Zrenner, R., et al. (2014). Mercator: a fast and simple web server for genome scale functional annotation of plant sequence data. *Plant Cell Environ.* 37, 1250–1258. doi: 10.1111/pce.12231

Love, M. I., Huber, W., and Anders, S. (2014). Moderated estimation of fold change and dispersion for RNA-seq data with DESeq2. *Genom. Biol.* 15:550. doi: 10.1186/s13059-014-0550-8

Luchi, N., Ma, R., Capretti, P., and Bonello, P. (2005). Systemic induction of traumatic resin ducts and resin flow in Austrian pine by wounding and inoculation with Sphaeropsis sapinea and Diplodia scrobiculata. *Planta* 221, 75–84. doi: 10.1007/s00425-004-1414-3

Ma, W., Smigel, A., Tsai, Y.-C., Braam, J., and Berkowitz, G. A. (2008). Innate immunity signaling: cytosolic Ca2+ elevation is linked to downstream nitric oxide generation through the action of calmodulin or a calmodulin-like protein. *Plant Physiol.* 148, 818–828. doi: 10.1104/pp.108.125104

Mehdi, K., Thierie, J., and Penninckx, M. J. (2001). γ-Glutamyl transpeptidase in the yeast Saccharomyces cerevisiae and its role in the vacuolar transport and metabolism of glutathione. *Biochem. J.* 359, 631–637. doi: 10.1042/0264-6021:3590631

Michaud, M., and Jouhet, J. (2019). Lipid trafficking at membrane contact sites during plant development and stress response. *Front. Plant Sci.* 10:2. doi: 10.3389/fpls.2019.00002

Miedes, E., Vanholme, R., Boerjan, W., and Molina, A. (2014). The role of the secondary cell wall in plant resistance to pathogens. *Front. Plant Sci.* 5:358. doi: 10.3389/fpls.2014.00358

Naidoo, S., Visser, E. A., Zwart, L., Toit, Y. D., Bhadauria, V., and Shuey, L. S. (2018). Dual RNA-sequencing to elucidate the plant-pathogen duel. *Curr. Iss. Mol. Biol.* 27, 127–142. doi: 10.21775/cimb.027.127

Niraula, P. M., Zhang, X., Jeremic, D., Lawrence, K. S., and Klink, V. P. (2021). Xyloglucan endotransglycosylase/hydrolase increases tightly-bound xyloglucan and chain number but decreases chain length contributing to the defense response that Glycine max has to Heterodera glycines. *PLoS One* 16:e0244305. doi: 10.1371/journal.pone.0244305

Polishchuk, O. V. (2021). Stress-related changes in the expression and activity of plant carbonic anhydrases. *Planta* 253:58.

Potvin, C. (2000). ""ANOVA: Experimental Layout and Analysis"," in *Design and analysis of ecological experiments*, 2nd Edn, eds S. M. Scheiner and J. Gurevitch (New York: Oxford University Press), 415.

R Core Team (2021). *R: A Language and Environment for Statistical Computing*. Vienna, Austria: R Foundation for Statistical Computing.

Rizzo, J., Stanchev, L. D., Da Silva, V. K. A., Nimrichter, L., Pomorski, T. G., and Rodrigues, M. L. (2019). Role of lipid transporters in fungal physiology and pathogenicity. *Comput. Struct. Biotechnol. J.* 17, 1278–1289. doi: 10.1016/j.csbj.2019.09.001

Robertson, G., Schein, J., Chiu, R., Corbett, R., Field, M., Jackman, S. D., et al. (2010). De novo assembly and analysis of RNA-seq data. *Nat. Methods* 7, 909–912. doi: 10.1038/nmeth.1517

Robinson, M. D., Mccarthy, D. J., and Smyth, G. K. (2010). edgeR: a Bioconductor package for differential expression analysis of digital gene expression data. *Bioinformatics* 6, 139–140. doi: 10.1093/bioinformatics/btp616

Santamaria, O., Smith, D. R., and Stanosz, G. R. (2011). Interaction between Diplodia pinea and D. scrobiculata in red and jack pine seedlings. *Phytopathology* 101, 334–339. doi: 10.1094/PHYTO-07-10-0180

Shah, J., and Zeier, J. (2013). Long-distance communication and signal amplification in systemic acquired resistance. *Front. Plant Sci.* 4:30. doi: 10.3389/fpls.2013.00030

Sherwood, P., and Bonello, P. (2013). Austrian pine phenolics are likely contributors to systemic induced resistance against Diplodia pinea. *Tree Physiol.* 33, 845–854. doi: 10.1093/treephys/tpt063

Sherwood, P., and Bonello, P. (2016). Testing the systemic induced resistance hypothesis with Austrian pine and Diplodia sapinea. *Physiol. Mol. Plant Pathol.* 94, 118–125.

Sherwood, P., Villari, C., Capretti, P., and Bonello, P. (2015). Mechanisms of induced susceptibility to Diplodia tip blight in drought-stressed Austrian pine. *Tree Physiol.* 35, 549–562. doi: 10.1093/treephys/tpv026

Slippers, B., and Wingfield, M. J. (2007). Botryosphaeriaceae as endophytes and latent pathogens of woody plants: diversity, ecology and impact. *Fungal Biol. Rev.* 21, 90–106.

Soneson, C., Love, M. I., and Robinson, M. D. (2015). Differential analyses for RNA-seq: transcript-level estimates improve gene-level inferences. *F1000Research* 4:1521. doi: 10.12688/f1000research.7563.2

Stanke, M., Diekhans, M., Baertsch, R., and Haussler, D. (2008). Using native and syntenically mapped cDNA alignments to improve de novo gene finding. *Bioinformatics* 24, 637–644. doi: 10.1093/bioinformatics/btn013

Survila, M., Davidsson, P. R., Pennanen, V., Kariola, T., Broberg, M., Sipari, N., et al. (2016). Peroxidase-generated apoplastic ROS impair cuticle integrity and contribute to DAMP-elicited defenses. *Front. Plant Sci.* 7:1945. doi: 10.3389/fpls.2016.01945

Tang, S., Lomsadze, A., and Borodovsky, M. (2015). Identification of protein coding regions in RNA transcripts. *Nucleic Acids Res.* 43, 1–10. doi: 10.1093/nar/gkv227

Thimm, O., Bläsing, O., Gibon, Y., Nagel, A., Meyer, S., Krüger, P., et al. (2004). MAPMAN: a user-driven tool to display genomics data sets onto diagrams of metabolic pathways and other biological processes. *Plant J.* 37, 914–939. doi: 10.1111/j.1365-313x.2004.02016.x

Tiwari, S., Thakur, R., and Shankar, J. (2015). Role of Heat-Shock Proteins in Cellular Function and in the Biology of Fungi. *Biotechnol. Res. Int.* 2015, 1–11. doi: 10.1155/2015/132635

Tronchet, M., Balagué, C., Kroj, T., Jouanin, L., and Roby, D. (2010). Cinnamyl alcohol dehydrogenases-C and D, key enzymes in lignin biosynthesis, play an essential role in disease resistance in Arabidopsis. *Mol. Plant Pathol.* 11, 83–92. doi: 10.1111/j.1364-3703.2009.00578.x

Van Der Nest, M. A., Bihon, W., De Vos, L., Naidoo, K., Roodt, D., Rubagotti, E., et al. (2014). Draft genome sequences of Diplodia sapinea, Ceratocystis manginecans, and Ceratocystis moniliformis. *IMA Fungus* 5, 135–140. doi: 10.5598/imafungus.2014.05.01.13

Visser, E. A., Wegrzyn, J. L., Myburg, A. A., and Naidoo, S. (2018). Defence transcriptome assembly and pathogenesis related gene family analysis in Pinus tecunumanii (low elevation). *BMC Genom.* 19:1–13. doi: 10.1186/s12864-018-5015-0

Visser, E. A., Wegrzyn, J. L., Steenkamp, E. T., Myburg, A. A., and Naidoo, S. (2019). Dual RNA-seq analysis of the pine-Fusarium circinatum interaction in resistant (Pinus tecunumanii) and susceptible (Pinus patula) hosts. *Microorganisms* 7:315. doi: 10.3390/microorganisms7090315

Wallis, C., Eyles, A., Chorbadjian, R. A., Riedl, K., Schwartz, S., Hansen, R., et al. (2011). Differential effects of nutrient availability on the secondary metabolism of Austrian pine (Pinus nigra) phloem and resistance to Diplodia pinea. *Forest Pathol.* 41, 52–58.

Wallis, C. M., Eyles, A., Chorbadjian, R., Mcspadden-Gardner, B. B., Hansen, R., Cipollini, D. F., et al. (2008). Systemic induction of phloem secondary metabolism and its relationship to resistance to a canker pathogen in Austrian pine. *N Phytol.* 177, 767–778. doi: 10.1111/j.1469-8137.2007.02307.x

Wang, D., Eyles, A., Mandich, D., and Bonello, P. (2006). Systemic aspects of host-pathogen interactions in Austrian pine (Pinus nigra): a proteomics approach. *Physiol. Mol. Plant Pathol.* 68, 149–157.

Williams, A. P., Allen, C. D., Macalady, A. K., Griffin, D., Woodhouse, C. A., Meko, D. M., et al. (2013). Temperature as a potent driver of regional forest drought stress and tree mortality. *Nat. Clim. Change* 3, 292–297.

Zheng, Z., Qamar, S. A., Chen, Z., and Mengiste, T. (2006). Arabidopsis WRKY33 transcription factor is required for resistance to necrotrophic fungal pathogens. *Plant J.* 48, 592–605. doi: 10.1111/j.1365-313X.2006.02901.x

Zhu, X., Wang, Y., Su, Z., Lv, L., and Zhang, Z. (2018). Silencing of the Wheat Protein Phosphatase 2A Catalytic Subunit TaPP2Ac Enhances Host Resistance to the Necrotrophic Pathogen Rhizoctonia cerealis. *Front. Plant Sci.* 9:1437. doi: 10.3389/fpls.2018.01437

Author Disclaimer: The use of trade names is for the information and convenience of the reader and does not imply official endorsement or approval by the USDA or the Forest Service of any product to the exclusion of others that may be suitable.

Conflict of Interest: The authors declare that the research was conducted in the absence of any commercial or financial relationships that could be construed as a potential conflict of interest.

Publisher's Note: All claims expressed in this article are solely those of the authors and do not necessarily represent those of their affiliated organizations, or those of the publisher, the editors and the reviewers. Any product that may be evaluated in this article, or claim that may be made by its manufacturer, is not guaranteed or endorsed by the publisher.

Advantages of publishing in Frontiers

OPEN ACCESS
Articles are free to read for greatest visibility and readership

FAST PUBLICATION
Around 90 days from submission to decision

HIGH QUALITY PEER-REVIEW
Rigorous, collaborative, and constructive peer-review

TRANSPARENT PEER-REVIEW
Editors and reviewers acknowledged by name on published articles

Frontiers
Avenue du Tribunal-Fédéral 34
1005 Lausanne | Switzerland

Visit us: www.frontiersin.org
Contact us: frontiersin.org/about/contact

REPRODUCIBILITY OF RESEARCH
Support open data and methods to enhance research reproducibility

DIGITAL PUBLISHING
Articles designed for optimal readership across devices

FOLLOW US
@frontiersin

IMPACT METRICS
Advanced article metrics track visibility across digital media

EXTENSIVE PROMOTION
Marketing and promotion of impactful research

LOOP RESEARCH NETWORK
Our network increases your article's readership